IGM 86-101-307
Etude n° 307
Dossier 8355-101

PHYSICOCHEMICAL CHARACTERIZATION OF HIGH-PERFORMANCE FIBRE-REINFORCED ORGANIC-MATRIX COMPOSITES

PART 1. GENERAL DISCUSSION AND LITERATURE REVIEW

by

K. C. Cole and D. Noël

Industrial Materials Research Institute
National Research Council Canada
75, boul. de Mortagne
Boucherville, Québec, Canada
J4B 6Y4

May 1986

CNRC 25839

TABLE OF CONTENTS

List of figures iii
List of tables iii
Preface iv
Acknowledgement v
Summary vi
Résumé vi

1. INTRODUCTION 1

2. PRODUCTION AND TESTING OF COMPOSITE MATERIALS 6

- 2.1 The Fabrication Process 6
- 2.2 Matrix Chemistry 11
- 2.3 Physicochemical Characterization Methods 12
  - 2.3.1 Liquid Chromatography (LC) 12
  - 2.3.2 Infrared Spectroscopy (IR) 20
  - 2.3.3 Thermal Analysis 21
  - 2.3.4 Gas Chromatography (GC) 22
  - 2.3.5 Nuclear Magnetic Resonance (NMR) 22
  - 2.3.6 Dynamic Mechanical Analysis (DMA) 23
  - 2.3.7 Dynamic Dielectric Analysis (DDA) 23
  - 2.3.8 Ultraviolet-Visible Spectroscopy (UV-VIS) 24
  - 2.3.9 Other Techniques 24

3. LITERATURE REVIEW: SYSTEMS BASED ON TGDDM AND DDS 25

- 3.1 Analysis of Chemical Composition 25
  - 3.1.1 Analysis of TGDDM Epoxy Resins 25
  - 3.1.2 Analysis of TGDDM-DDS Mixtures 28
  - 3.1.3 Analysis of Narmco Rigidite 5208 29
  - 3.1.4 Analysis of Hercules Magnamite 3501 30
  - 3.1.5 Analysis of Fiberite Resin System 934 30
  - 3.1.6 Other Analytical Work 30
- 3.2 Effects of Altering Composition 31
- 3.3 Effects of Prepreg Aging 32
- 3.4 Effects of Adverse Environment on Cured Composite 35
- 3.5 Cure Kinetics and Matrix Morphology 37
  - 3.5.1 Matrix Morphology 37
  - 3.5.2 The Curing Reaction 38
  - 3.5.3 Cure Kinetics 40
  - 3.5.4 Rheological Studies 43

4. LITERATURE REVIEW: SYSTEMS OTHER THAN TGDDM-DDS 45

GLOSSARY 50

BIBLIOGRAPHY 51

LIST OF FIGURES

Figure	Description	Page
1	Current use of composite materials in the Challenger	4
2	Steps involved in the manufacture of a graphite-epoxy composite part based on Narmco 5208	7
3	Typical autoclave vacuum-bag setup for moulding composite parts	9
4	Some typical epoxy resins	13
5	Some typical amine hardeners	16
6	Some typical anhydride hardeners	18
7	Some typical catalysts and accelerators for epoxy cure	19

LIST OF TABLES

Table	Description	Page
1	Reported compositions of some commercial TGDDM-DDS systems	26
2	References concerning epoxy systems other than TGDDM-DDS	45
3	References concerning polyimide systems	49
4	References concerning thermoplastic matrix systems	49

PREFACE

This report is the first of a series resulting from a cooperative effort involving the Industrial Materials Research Institute (IMRI) of the National Research Council Canada (NRCC) (Boucherville, Québec) and Canadair Limited (Montréal, Québec). The subject is one of growing importance in high-technology manufacturing, namely the physicochemical characterization of high-performance fibre-reinforced organic-matrix composites. This first report begins with a general discussion which is meant as an introduction to the subject for those who are relatively unfamiliar with it. This is followed by a review of the recent literature which we hope will serve as a useful reference source for those who have some knowledge of the field but would like to acquire further information. Subsequent reports in the series will describe the results of original research involving the application of various chromatographic and spectroscopic techniques to typical commercial composite systems, with particular attention given to the graphite-epoxy system Narmco 5208/WC3000. The titles of the complete series are as follows:

Part 1. General Discussion and Literature Review
Part 2. Applications of Infrared Spectroscopy
Part 3. Applications of Liquid Chromatography
Part 4. Applications of Pyrolysis Gas Chromatography and Thermal Analysis
Part 5. A Study of the Room-Temperature Aging of Narmco 5208/WC3000 Prepreg
Part 6. Methods for Quality Control of Matrix Chemistry

ACKNOWLEDGEMENT

Apart from the authors, the following people directly contributed to the research described in this series of reports:

H. Roberge	NRCC-IMRI
A. Pilon	NRCC-IMRI
J.-J. Hechler	NRCC-IMRI
J. Boulanger	NRCC-IMRI
K. C. Overbury	Canadair Ltd.
A. Chouliotis	Canadair Ltd.
S. Toy	Canadair Ltd.

SUMMARY

The report deals with high-performance composite materials based on reinforcing fibres (graphite, Kevlar®, fibreglass) embedded in an organic matrix (epoxy, polyimide, thermoplastic). A brief introduction to the subject is followed by a discussion of the importance of the matrix chemistry and a description of analytical methods currently used to study and characterize it, such as Fourier transform infrared spectroscopy and high performance liquid chromatography. The recent literature concerning the applications of physicochemical methods to composite materials is reviewed, with particular emphasis on the widely used epoxy system TGDDM-DDS (tetraglycidyldiaminodiphenylmethane and diaminodiphenylsulphone).

RESUME

Le rapport a pour sujet les matériaux composites "haute performance" à base de matrices organiques (époxyde, polyimide, thermoplastique) et renforts fibreux (graphite, Kevlar®, fibres de verre). Une brève introduction est suivie d'une discussion sur l'importance de la composition chimique de la matrice, et d'une description des méthodes analytiques couramment utilisées pour l'étudier, telles la spectroscopie infrarouge à transformée de Fourier et la chromatographie liquide haute performance. Par la suite, un compte rendu de la littérature récente concernant l'application des méthodes physicochimiques aux matériaux composites est présenté en accordant une importance particulière au système époxy TGDDM-DDS (tétraglycidyldiaminodiphénylméthane et diaminodiphénylsulfone).

1. INTRODUCTION

The use of composite materials based on high-strength fibres embedded in an organic polymer matrix is growing at a rapid pace. The impetus for this growth comes from two important advantages, namely high mechanical strength combined with light weight. The strength is due primarily to the fibres, which are usually made of glass, carbon, graphite, or aromatic polyamide (aramid, Kevlar®). The shape, rigidity, and durability of the manufactured part are largely determined by the organic matrix, which holds the reinforcing fibres in place and distributes the stress among them. It also contributes to the light weight. Commonly used matrices are based on polyester, epoxy, and polyimide resins.

The properties and uses of advanced composites are discussed in numerous publications [1-7]. Their mechanical behaviour has been widely studied and the literature is vast. However, only recently has the matrix chemistry begun to receive a significant degree of attention from manufacturers of composite parts. Unlike metal alloys or thermoplastics, the thermosetting resins used in most fibre-reinforced composites are based on mixtures of chemicals which undergo complex reactions during formulation, storage, and processing. Variations in chemical composition can have significant effects on the processing behaviour (especially the rheology) and the final properties (both short- and long-term) of such materials. Good manufacturing procedure therefore requires an appreciation of the chemistry involved and a knowledge of how to analyze and control it. Over the past ten years an increasing amount of research has been devoted to this aspect, mainly involving physicochemical methods of characterization. Most of the work has involved "high-performance" composites based on epoxies and polyimides with carbon, graphite, and Kevlar fibres. Composites based on polyester and fibreglass are usually used in less critical applications which do not justify the added cost of extensive chemical characterization.

The principal consumer of high-performance advanced polymer composites is the aerospace industry, where lighter weight is a major factor in improving fuel economy. Recent figures [8,9] show that the world produced 22 million pounds of advanced polymer composites in 1984, with the price of fabricated parts ranging from $40 to $100 per pound. The total market value was 1.3 billion dollars (US). The market is projected to grow 16% per year over the next decade (22% in aerospace, 10% in other applications), with the following predicted distribution: aerospace 67%, sporting goods 16%, industrial applications 14%, automobiles 1%. By the year 2000, the market is expected to reach over 12 billion dollars. At present, epoxies account for 80% of the resins used in these high-performance applications, with other thermosets taking 12% and thermoplastics 8%.

Epoxies will remain the major matrix material for some time, but growth is predicted for such high-performance thermoplastics as polyetheretherketone (PEEK), polyphenylenesulphide (PPS), polysulphones, and oriented liquid crystal polymers.

Initially, the use of such composites in aircraft was limited to secondary structures such as interior panels, whose performance is not critical to the flight of the aircraft. In such cases, adequate performance can be assured by simple physical and mechanical testing of the raw materials used. As knowledge of composites grows and their properties improve, their use is being extended to primary structures, whose failure would interfere with the flight of the aircraft and therefore have grave consequences. Obviously such applications require much more rigourous quality assurance methods. Before using composites for primary structures in civil aircraft, the manufacturers must obtain approval from government regulatory agencies such as the Canadian Ministry of Transport and the U. S. Federal Aviation Administration (FAA), who require submission of detailed testing methods. There is growing interest in the use of physicochemical characterization techniques in conjunction with traditional mechanical methods. The FAA has expressed a preference [10] for high performance liquid chromatography (HPLC) and Fourier transform infrared spectroscopy (FTIR). The aviation industry, long accustomed to working mainly with metals, is in the process of adapting to the different approach which must be taken with these radically different composite materials.

In the forefront of the use of advanced polymer composites in aircraft structures are the U. S. defence agencies. For example, in its Advanced Composite Airframe Program (ACAP) [11], the U. S. Army hopes to achieve savings of 22% in weight and 17% in cost through the use of composites. Military aircraft like the FA-18A currently contain about 10% by weight of advanced composites, and an ultimate goal of 50% has been proposed for future aircraft. In commercial aeroplanes, the use of composite structures is lower but growing. Examples include the Boeing 757 and 767 (4% composite by weight, or over 1250 lb., including a 34-foot-long graphite-epoxy rudder) [12,13], the Lockheed L-1011 (2500 lb. of Kevlar/epoxy) [14], Bell and Sikorsky helicopters [15-17], McDonnell-Douglas aircraft [18], and an all-composite (graphite/epoxy) ten-place executive aircraft, the Lear Fan 2100 [9,10]. Applications in space include communications satellites [19] and the Space Shuttle, with its remote manipulator system (the "Canadarm") [20]. Details on the use of physicochemical methods to determine material acceptability for military applications are confidential. The first civil aircraft manufacturer to introduce such methods into its specifications was Boeing [22]. In Europe, acceptance control is still based on mechanical tests, but steps are being taken to develop standard physicochemical methods [23]. Recently, Technical Panel PTP3 of the Technical Cooperation Programme (a joint American, Australian, Canadian, United Kingdom organization) completed an exhaustive study [24] of a commonly-used epoxy resin (Epon 828). Samples manufactured in all four countries were analyzed using a wide range of techniques by several laboratories. Canada was represented in the programme by the National Aeronautical Establishment, but did not play an active role in the testing. The study led to the conclusion that the most valuable characterization techniques are liquid chromatography, Fourier transform infrared spectroscopy, and differential scanning calorimetry.

The work to be discussed in the present series of reports was undertaken at the suggestion of, and in collaboration with, Canadair Ltd. of Montréal. Like the above manufacturers, Canadair is incorporating composite components into its products [21]. The Challenger currently contains over 40 such components accounting for over 6% of the basic structural weight (Figure 1). These are all secondary structures. However, a program is underway to obtain approval for a primary structure, an outboard flap vane, which will probably be the first advanced composite primary structure to be approved for manufacture in Canada. This will require, among other things, the submission of quality assurance methods, including physicochemical testing. Since much of the U. S. technology is not available to Canadian industry, a joint project was undertaken between Canadair and the Industrial Materials Research Institute of the National Research Council Canada with the aim of extending Canadian competence in this field. This involved the following tasks:

(1) A survey of the recent published literature concerning the physicochemical characterization of high-performance organic-matrix composites.

(2) Experimental confirmation of published data pertinent to the particular systems of interest.

(3) Improvement of existing methods of physicochemical characterization.

(4) Investigation of new methods.

The first item is covered in this report. The object is firstly to provide a general overview of the subject for those not directly involved, and secondly to provide a source of references for those who are familiar with the subject but would like to obtain more specific information.

Subsequent reports will describe the results of the research performed. The area of prime concern is the characterization of the epoxy resin matrix, and one particular system

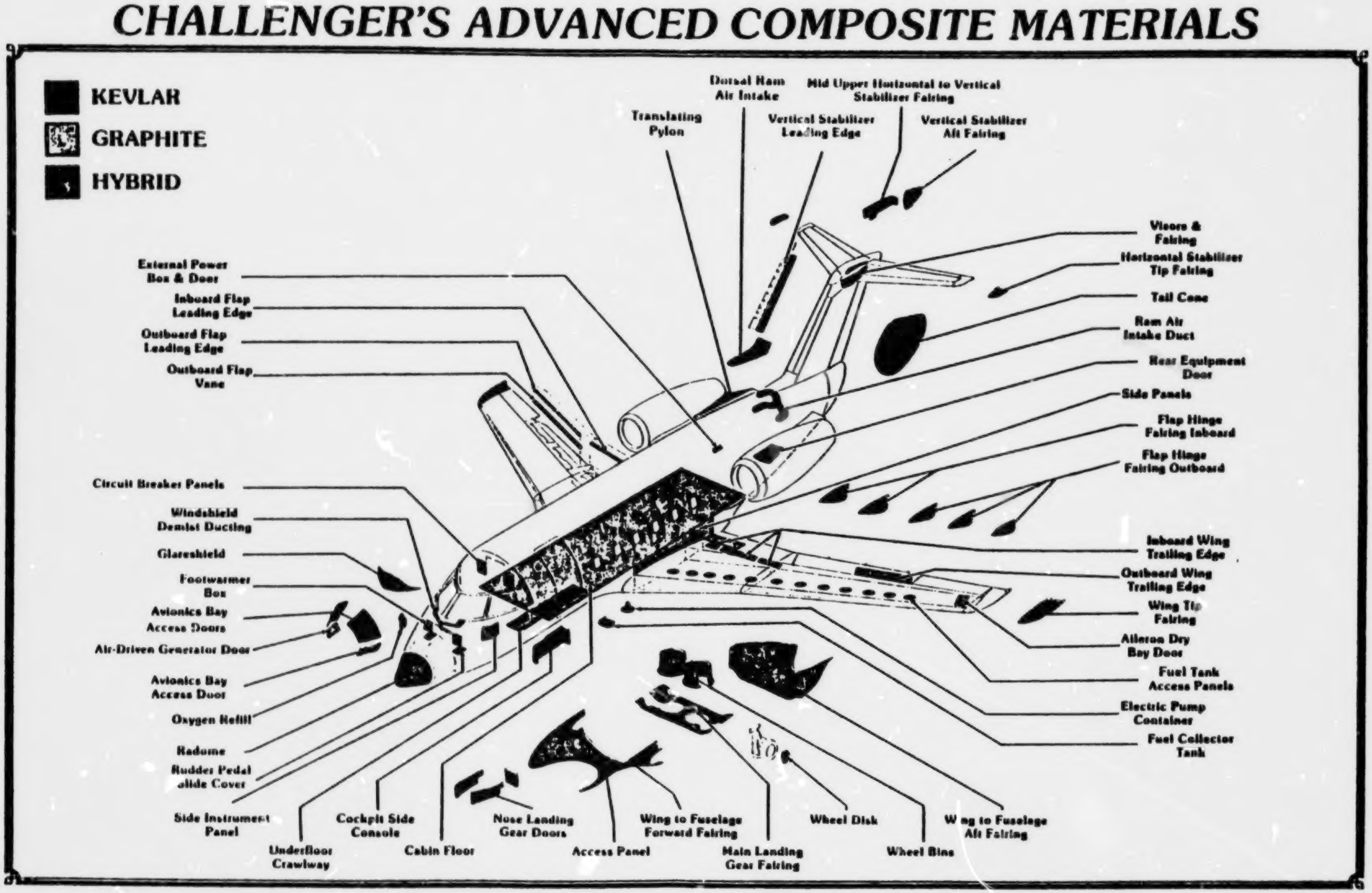

CHALLENGER'S ADVANCED COMPOSITE MATERIALS

KEVLAR
GRAPHITE
HYBRID
Translating Pylon
Dorsal Ram Air Intake
Vertical Stabilizer Leading Edge
Mid Upper Horizontal to Vertical Stabilizer Fairing
Vertical Stabilizer Aft Fairing
External Power Box & Door
Inboard Flap Leading Edge
Outboard Flap Leading Edge
Outboard Flap Vane
Circuit Breaker Panels
Windshield Demist Ducting
Glareshield
Footwarmer Box
Avionics Bay Access Doors
Air-Driven Generator Door
Avionics Bay Access Door
Oxygen Refill
Radome
Rudder Pedal Slide Cover
Side Instrument Panel
Underfloor Crawlway
Cockpit Side Console
Cabin Floor
Nose Landing Gear Doors
Access Panel
Wing to Fuselage Forward Fairing
Main Landing Gear Fairing
Wheel Disk
Wheel Bins
Wing to Fuselage Aft Fairing
Visors & Fairing
Horizontal Stabilizer Tip Fairing
Tail Cone
Ram Air Intake Duct
Rear Equipment Door
Side Panels
Flap Hinge Fairing Inboard
Flap Hinge Fairing Outboard
Inboard Wing Trailing Edge
Outboard Wing Trailing Edge
Wing Tip Fairing
Aileron Dry Bay Door
Fuel Tank Access Panels
Electric Pump Container
Fuel Collector Tank

Figure 1. Current use of composite materials in the Challenger.

has been studied in depth (Rigidite 5208 from Narmco, Inc.). The techniques used include liquid chromatography, infrared spectroscopy, thermal analysis, and pyrolysis gas chromatography. Although the methods were developed using Narmco 5208, they are of more general application and could be extended, with appropriate modifications, to other systems. These need not be restricted to the aerospace field. For example, other high-performance applications where such methods are valuable include the manufacture of printed circuit boards and structural adhesives.

2. PRODUCTION AND TESTING OF COMPOSITE MATERIALS

2.1 The Fabrication Process

Composite parts are made from a great number of different systems by a variety of processing methods [2,3]. One of the more versatile techniques is vacuum-bag moulding, with or without the use of an autoclave. The general procedure will be briefly outlined here using as an example the fabrication of test panels from Narmco Rigidite 5208/WC3000, the graphite-epoxy system used for most of the work to be described in subsequent reports in this series. The "5208" designates the epoxy resin system (discussed in more detail in Chapter 3), whereas the "WC3000" refers to the reinforcement (woven "Celion" graphite cloth, 3000 fibres per yarn). Figure 2 summarizes the procedure. Many of the principles involved also apply to other processing techniques.

The first step involves formulation of the resin system. In the case of Narmco 5208, there are three main components, two epoxy resins and an amine hardener, which may come from three different suppliers. These must be blended in the correct proportions; an imbalance can result in a matrix with less than optimum properties. Since the hardener is a solid and the epoxies are very viscous or semi-solid, heat is usually applied to facilitate the mixing. At this point the resin mixture is said to be at the "A-stage".

The resin is then used to impregnate the fibre reinforcement, which may take the form of unidirectional tape or woven cloth. Various types of Kevlar, graphite, and carbon fibres are available with different mechanical properties. (Although the terms "graphite" and "carbon" are often used indiscriminately, there is a difference [3]. Graphite fibres are produced at a higher temperature, are of higher purity (>99% carbon), have a more ordered microstructure, and generally have a higher tensile modulus but lower ultimate strength.) In the case of woven cloth, different yarn sizes and weave styles are available to suit different fabrication methods. Graphite fibres are usually treated with an organic coupling agent to improve fibre-matrix adhesion. Two methods are used for fibre impregnation: hot-melt and solution. In the first the resin is simply heated to reduce its viscosity for application to the fibre reinforcement; this method is used by Narmco for Rigidite 5208 unitape. In the second, the resin is dissolved in an organic solvent which is removed by evaporation after impregnation; this method is used by Narmco for woven cloth. The resin-impregnated fibre reinforcement is known as "prepreg". Heating the resin during mixing and/or impregnation causes partial reaction between epoxy and hardener, so in the prepreg the resin is said to be at the "B-stage". Even if solvent impregnation is used, heat may be applied at some point to "advance" the resin to give it the desired viscosity. The

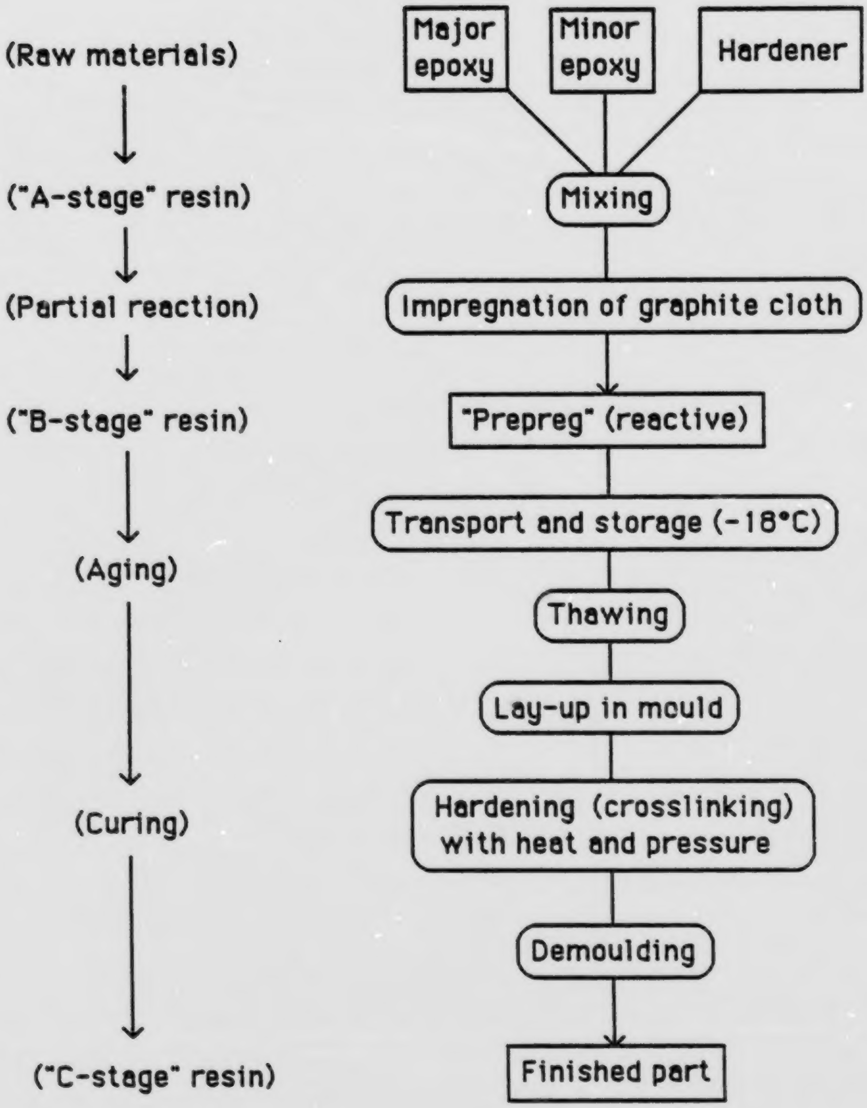
(Raw materials)
("A-stage" resin)
(Partial reaction)
("B-stage" resin)
(Aging)
(Curing)
("C-stage" resin)
Major epoxy
Minor epoxy
Hardener
Mixing
Impregnation of graphite cloth
"Prepreg" (reactive)
Transport and storage (-18°C)
Thawing
Lay-up in mould
Hardening (crosslinking) with heat and pressure
Demoulding
Finished part

Figure 2. Steps involved in the manufacture of a composite part based on Narmco 5208.

extent of the reaction between epoxy and hardener at this point is very important and must be carefully controlled, since it affects the physical properties and subsequent processing of the prepreg. To avoid further reaction, from this point on the prepreg must be kept at freezer temperature (about -18°C or 0°F) until it is used. This applies during shipping as well as storage.

A typical autoclave vacuum bag setup used to mould a panel is shown in Figure 3. The first step is to apply a release film to the mould surface. The thawed prepreg is then cut into pieces of the desired shape and these are "laid up" on the mould, the number of layers, or plies, being determined by the desired final thickness. Two important properties of the prepreg at this point are "tack", or the degree of adhesion between the different plies, and "drape", the ability of the prepreg to take the shape of the mould and to remain in this position without restraint. During lay-up, the different plies are laid down with specific fibre orientations chosen to control the directionality of the mechanical properties. When the required number of plies have been laid, a dam is built around the lay-up and it is covered with a sheet of porous peel-ply (e.g. Teflon-coated glass fabric). This is then covered with several plies of bleeder cloth (e.g. glass fabric), a sheet of plastic film, an optional pressure plate, and an air-bleeder pack. Finally, the whole assembly is completely enclosed in a nylon vacuum bag and sealed with vacuum sealing tape.

The system is now ready for cure, which consists of two distinct stages. First a vacuum is applied to the whole assembly, it is inserted in an autoclave, and a low positive pressure (about 70 kPa or 10 psi) is applied to the outside. It is then heated gradually to 135°C (275°F) and kept there for one hour. The heating lowers the resin viscosity, and the vacuum, together with the positive external pressure, removes entrapped volatiles and consolidates the different plies. Complete removal of volatiles (air, water, solvent, etc.) is critical in order to eliminate voids in the cured part, which would reduce the mechanical properties.

For the second stage of cure, the external pressure is increased to 590 kPa (85 psi) and the vacuum bag is vented to atmosphere. The temperature is increased gradually to 177°C (350°F) and held there for two hours. This step completes the crosslinking reaction between the epoxy and the hardener and produces a rigid part, which is then allowed to cool and removed from the mould. The resin is now said to be at the "C-stage".

During the cure, a certain amount of resin is squeezed from the lay-up into the bleeder cloth. As a consequence, the final part has a higher fibre-to-resin ratio than the initial prepreg. A "flow" test has been developed to measure the amount of resin lost when the prepreg is heated under pressure. Another test measures the "gel time", the time required for the resin to harden when heated to a certain temperature. A short gel time indicates that the resin in the prepreg is too advanced. In this case, hardening may start to

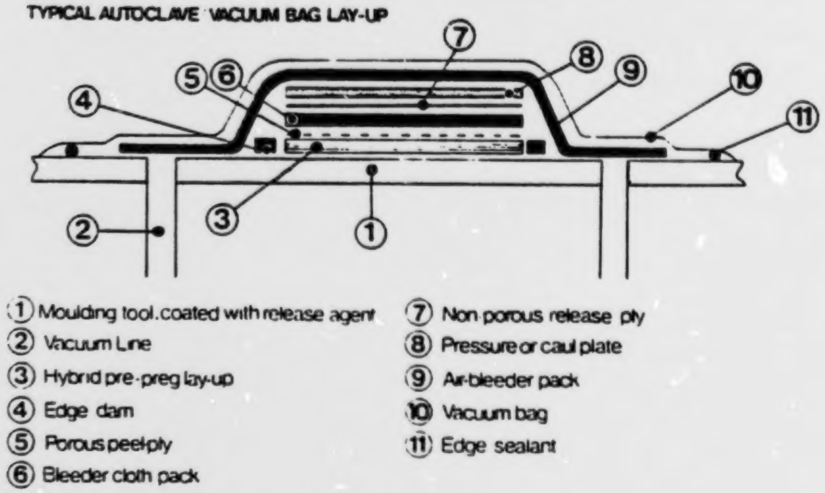
TYPICAL AUTOCLAVE VACUUM BAG LAY-UP
①
②
③
④
⑤
⑥
⑦
⑧
⑨
⑩
⑪
① Moulding tool.coated with release agent
② Vacuum Line
③ Hybrid pre-preg lay-up
④ Edge dam
⑤ Porous peel-ply
⑥ Bleeder cloth pack
⑦ Non porous release ply
⑧ Pressure or caul plate
⑨ Air-bleeder pack
⑩ Vacuum bag
⑪ Edge sealant

Figure 3. Typical autoclave vacuum-bag setup for moulding composite parts. (Ref. 4)

occur in the first stage of cure before all the volatiles have been removed and the layers properly consolidated. The incoming prepreg is usually tested for resin content, volatiles content, graphite areal weight, and tack. Test methods applied to the cured panel include void content, fibre content (% by volume), ply thickness, and of course, mechanical properties. The latter generally include tensile properties (ultimate strength, ultimate strain, and modulus), compressive properties (strength, strain, and modulus), and short beam shear strength.

Following is a brief general description of the more common tests, with references to methods published by the American Society for Testing and Materials (Annual Book of ASTM Standards, Volume 15.03). The specific conditions used in these tests depend on the type of material being tested and may vary from one manufacturer to another.

(1) Resin content and graphite areal weight (ASTM C613):

A square of prepreg is weighed and the area measured. The resin is extracted with a suitable solvent. The fibres are recovered, dried, and weighed. The results are used to calculate the resin content as % by weight and the graphite content in weight per unit area.

(2) Volatile content (ASTM D3530):

This is taken to be equal to the % weight lost when a square of prepreg is subjected to a specified temperature (usually between 100 and 200°C) for a specified time.

(3) Resin flow (ASTM D3531):

Two or more plies of prepreg are sandwiched together, weighed, and pressed under specified conditions of temperature, pressure, and time. The resin squeezed out is separated and its weight determined. This is expressed as a % of the total weight.

(4) Gel time (ASTM D3532):

Resin is squeezed from a sample of prepreg at a specified temperature and manipulated with a probe. The time at which the resin passes from a "stringy" state to a rubbery state is taken as the gel time.

(5) Tack:

A strip of prepreg is applied to a clean steel plate, a second strip is applied to the first, and the plate is placed in a vertical position. If the strips remain in position for the specified time, the test is considered positive.

(6) Ply thickness:

The thickness of a cured laminate panel is measured with a micrometre caliper and divided by the number of plies.

(7) Fibre volume and void content (ASTM D2734 and D3171):

The density of a sample of cured laminate is determined (ASTM D792). A weighed sample of the same laminate is digested in concentrated nitric acid to destroy the epoxy matrix. The fibres are recovered, dried, and weighed. Using the known densities of the fibres and the resin matrix, it is possible to calculate the fibre volume (%), the resin volume (%), and the void content (%).

(8) Tensile properties (ASTM D3039):

Tensile specimens are moulded or cut from laminate and strained to rupture. The following properties are evaluated: ultimate tensile stress, ultimate tensile strain, tensile modulus of elasticity.

(9) Compressive properties (ASTM D3410):

A sample of specified geometry is prepared and subjected to compression until it ruptures. The following properties are evaluated: ultimate compressive stress, ultimate compressive strain, compressive modulus of elasticity.

(10) Short-beam shear strength (ASTM D2344):

Suitable specimens are prepared and subjected to shear stress until breakage occurs. The apparent shear strength is calculated.

2.2 Matrix Chemistry

The physical properties and processing behaviour of the prepreg system are determined to a large extent by the matrix chemistry. The initial mechanical properties of a cured part are determined mainly by the fibres, and studies have shown that they are surprisingly insensitive to significant variations in the resin chemistry [25,26]. Over the longer term, however, this is not the case, since the behaviour of the composite with respect to high temperature, moisture, and other environmental factors is highly dependent on the nature of the matrix. Very little specific information is available concerning the relationship between matrix chemistry and long-term durability, and much work needs to be done. In the meantime, it is clear that if such composites are to be used in primary aircraft structures, one can not rely exclusively on simple mechanical testing to detect batch variations which may be disastrous in the long term. Physicochemical methods are being developed as a more sensitive means of assuring consistent performance [28-35].

Matrix chemistry can be quite complex. Figures 4 to 7 give chemical formulae for some of the more commonly used epoxies, hardeners, and catalysts, which are used in numerous different combinations. Whereas most hardeners and catalysts are relatively pure materials, epoxy resins are not. They usually consist of a mixture of monomer, higher oligomers, and various by-products, and the composition of a given resin can vary from plant to plant or from batch to batch within the same plant. Hence the probability of variation in matrix chemistry is quite high. The chemistry of epoxy resins has been extensively studied [27] and will be discussed further later. The most widely used epoxy resin overall is DGEBA. In advanced composites, the most widely used is TGDDM, usually in conjunction with the hardener DDS. These acronyms are explained in Figures 4 and 5.

2.3 Physicochemical Characterization Methods

2.3.1 Liquid Chromatography (LC):

Liquid chromatography [36,37] is generally considered the most sensitive technique for detecting variations in matrix chemistry. It involves the separation of a mixture into its components by introducing it into a liquid mobile phase which passes through a stationary phase consisting of solid particles, usually packed in a column. Different components of the mixture interact with the phases in different ways. Depending on the relative strengths of interaction with the solid phase and the mobile phase, certain components of the mixture will take longer to pass through the stationary phase than others. Thus a separation is effected and the various components can be detected and quantitatively measured.

Most liquid chromatography performed today is done using high pressure to speed up the analysis and is known as HPLC, for "high performance liquid chromatography". For analysis of epoxies [38, 76-78], three different modes of separation are commonly used: normal-phase HPLC (NPLC), reverse-phase HPLC (RPLC), and size exclusion chromatography (SEC).

In normal-phase HPLC, a tubular column is packed with fine particles of a material such as silica, whose surface is covered with highly polar groups. The mobile phase is less polar and consists of one or more organic solvents. The sample to be analyzed is injected into the flowing mobile phase at the entrance to the column. The more polar

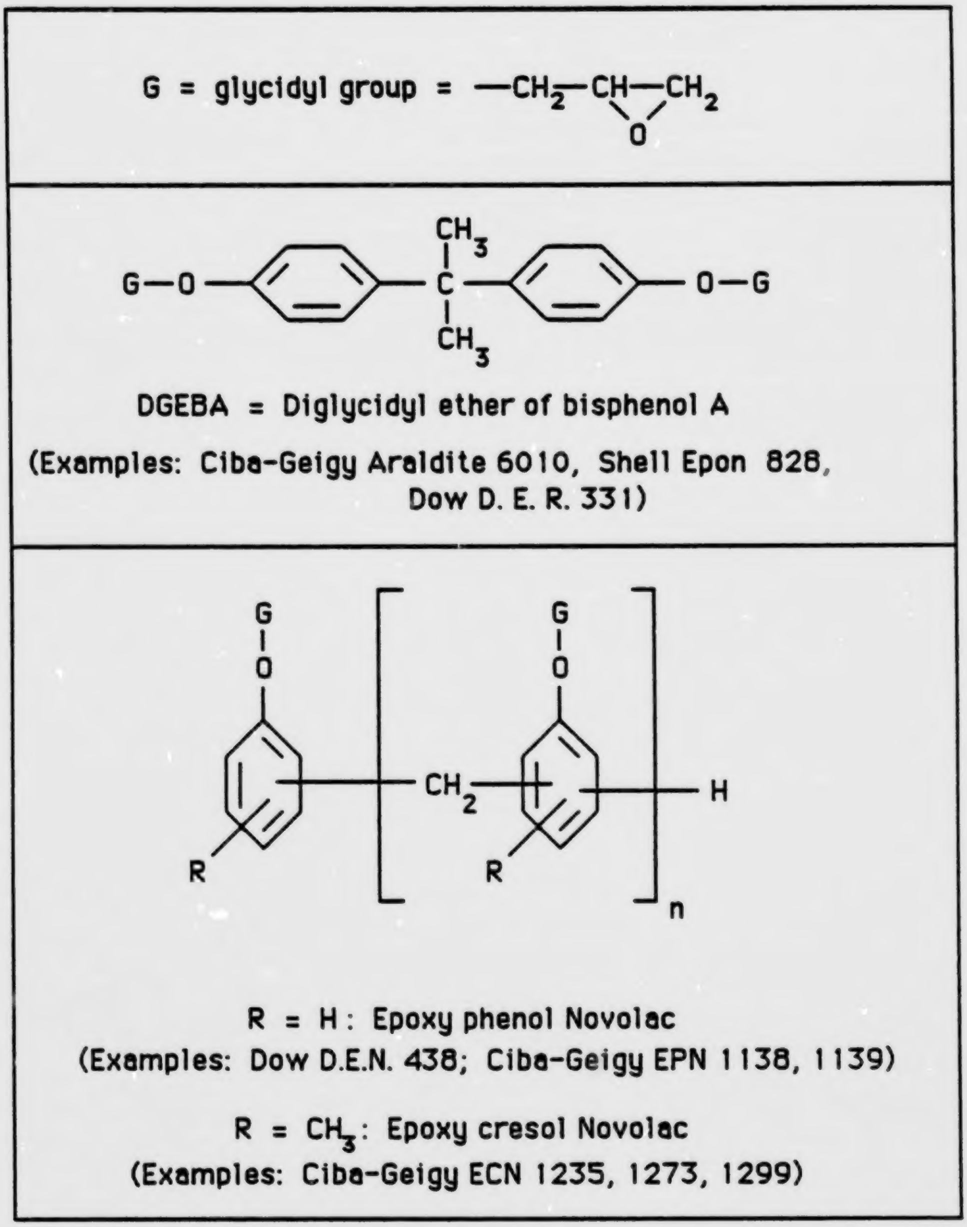

G = glycidyl group = —CH2—CH—CH2
O
CH3
G—O
C
O—G
CH3
G
O
CH2
H
R
n

DGEBA = Diglycidyl ether of bisphenol A

(Examples: Ciba-Geigy Araldite 6010, Shell Epon 828, Dow D. E. R. 331)

R = H : Epoxy phenol Novolac

(Examples: Dow D.E.N. 438; Ciba-Geigy EPN 1138, 1139)

R = CH_3: Epoxy cresol Novolac

(Examples: Ciba-Geigy ECN 1235, 1273, 1299)

Figure 4(a). Some typical epoxy resins.

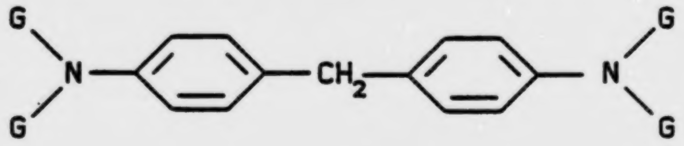

TGDDM = Tetraglycidyldiaminodiphenylmethane, or

TGMDA = Tetraglycidylmethylenedianiline

(Examples: Ciba-Geigy Araldite MY 720,
FIC Corp. Glyamine G-120)

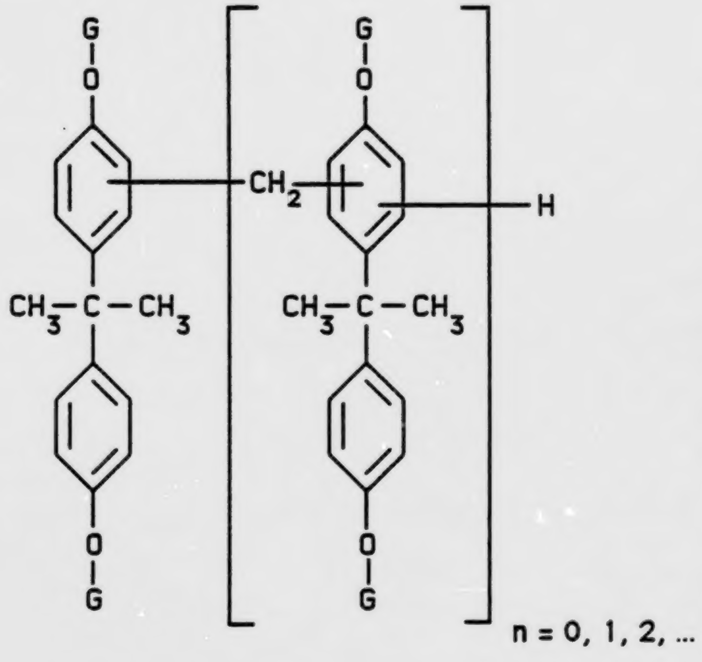
G
O
G
O
CH2
H
CH3 C CH3
CH3 C CH3
O
G
O
G
n = 0, 1, 2, ...

Bisphenol A Novolac epoxy

(Example: Celanese Epi-Rez SU-8)

Figure 4(b). Some typical epoxy resins (contd.).
G = glycidyl group, shown in Figure 4(a)

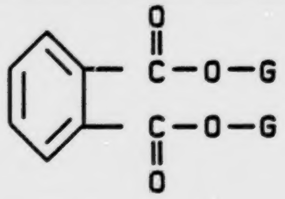

DGOP = Diglycidylorthophthalate
(Example: Celanese Glycel 100)

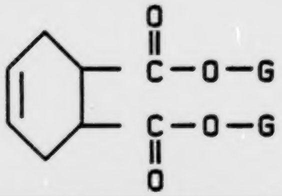

Diglycidyltetrahydrophthalate

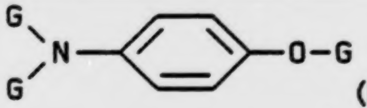

TGPAP = Triglycidyl-p-aminophenol
(Example: Ciba-Geigy ERL 0500, 0510)

C_4H_9-O-G

BGE = Butyl glycidyl ether (reactive diluent)
(Example: Ciba-Geigy Araldite RD-1)

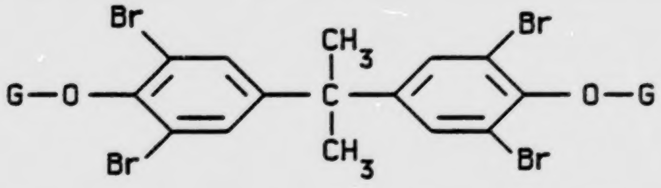

Diglycidyl ether of tetrabromobisphenol A

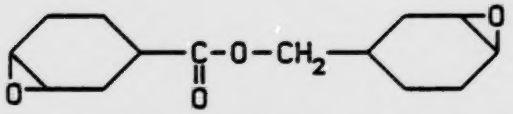

3,4-Epoxycyclohexylmethyl-3,4-epoxycyclohexanecarboxylate
(Examples: Union Carbide ERLA 4221, Ciba-Geigy CY 179)

Figure 4(c). Some typical epoxy resins (contd.).
G = glycidyl group, shown in Figure 4(a)

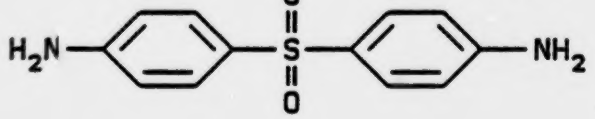

DDS = Diaminodiphenylsulphone ("Dapsone")
(Example: Ciba-Geigy Hardener HT 976, "Eporal")

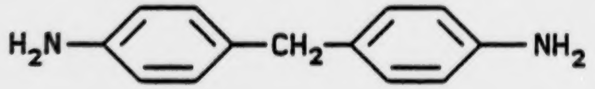

DDM = Diaminodiphenylmethane, or
MDA = Methylenedianiline

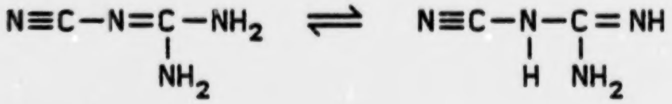

$$N{\equiv}C-N{=}\underset{NH_2}{\underset{|}{C}}-NH_2 \rightleftharpoons N{\equiv}C-\underset{H}{\underset{|}{N}}-\underset{NH_2}{\underset{|}{C}}{=}NH$$

DICY = dicyandiamide, or cyanoguanidine

$H_2N-CH_2CH_2-NH-CH_2CH_2-NH_2$

DETA = Diethylenetriamine
(Example: Dow D.E.H. 20)

$H_2N-CH_2CH_2-NH-CH_2CH_2-NH-CH_2CH_2-NH_2$

TETA = Triethylenetetramine
(Example: Dow D.E.H. 24)

Figure 5(a). Some typical amine hardeners.

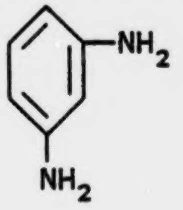

MPDA = meta-Phenylenediamine

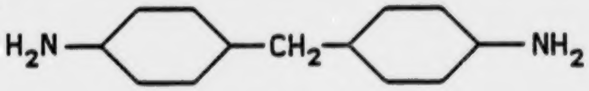

Bis(p-aminocyclohexyl)methane
(Example: DuPont PACM-20)

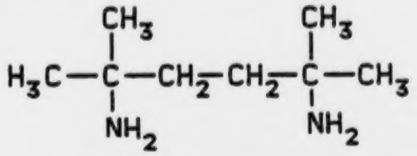

$$H_3C-\overset{CH_3}{\underset{NH_2}{C}}-CH_2-CH_2-\overset{CH_3}{\underset{NH_2}{C}}-CH_3$$

DMHDA = 2,5-dimethyl-2,5-hexanediamine

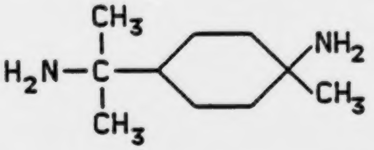
CH$_3$
H$_2$N
CH$_3$
NH$_2$
CH$_3$

MNDA = Menthanediamine

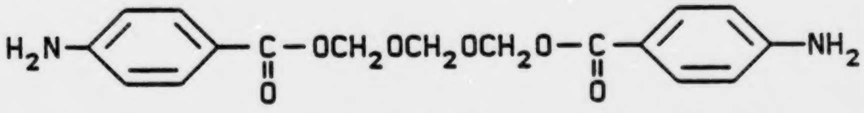
H$_2$N
C
O
OCH$_2$OCH$_2$OCH$_2$O
C
O
NH$_2$

TMAB = Trimethyleneglycol di-p-aminobenzoate

Figure 5(b). Some typical amine hardeners (contd.).

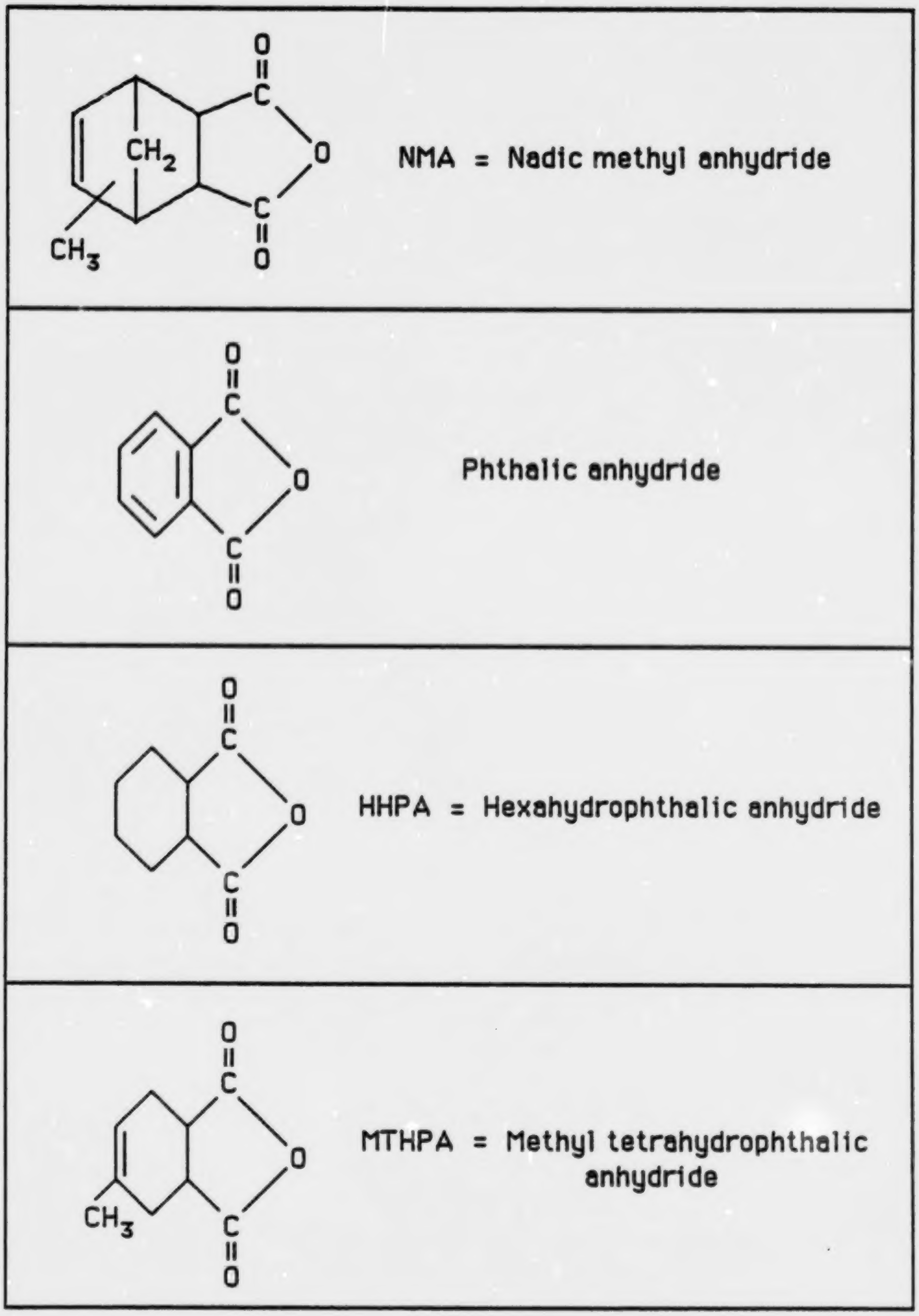
NMA = Nadic methyl anhydride
Phthalic anhydride
HHPA = Hexahydrophthalic anhydride
MTHPA = Methyl tetrahydrophthalic anhydride

Figure 6. Some typical anhydride hardeners.

$C_2H_5NH_2 \cdot BF_3$	Boron trifluoride monoethylamine (MEA) complex
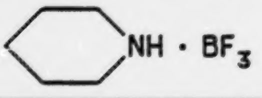	Boron trifluoride piperidine complex
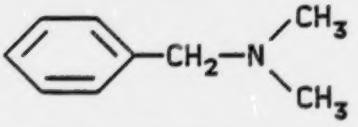	BDMA = Benzyl dimethyl amine
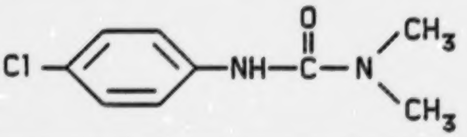	Chlorophenyl dimethyl urea (Monuron)
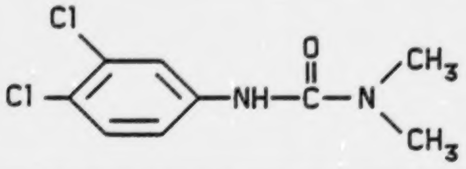	3,4-Dichlorophenyl-1,1-dimethyl urea (Diuron)
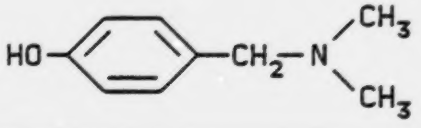	Dimethylaminomethylphenol (Example: Rohm and Haas DMP-10)
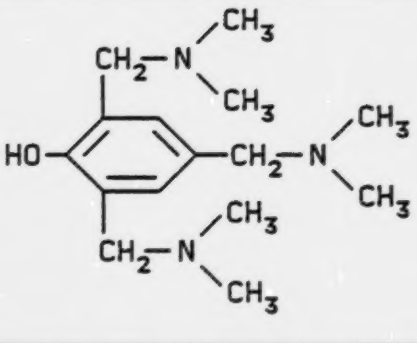	Tri(dimethylaminomethyl)-phenol (Example: Rohm and Haas DMP-30)

Figure 7. Some typical catalysts and accelerators for epoxy cure.

components will interact more strongly with the stationary phase and therefore require a longer time to elute from the column. As the various components elute they are quantitatively detected, usually by means of ultraviolet absorption or changes in refractive index. Unknown components can be isolated and identified by other techniques or by comparison of their retention times with those of standard samples.

Reverse-phase HPLC resembles normal-phase HPLC except that the mobile phase is more polar than the stationary phase. Silica-type stationary phases can be made non-polar (hydrophobic) by grafting long hydrocarbon chains to the surface. This makes it possible to use as a mobile phase highly polar solvents, including water. This is one of the reasons for which reverse-phase HPLC is now more widely used than normal-phase HPLC. Often gradient elution is used, in which the solvent composition is varied with time in order to achieve a more efficient separation. In this case, refractive index detection cannot be used.

Size exclusion chromatography (SEC), or gel permeation chromatography (GPC), differs from the preceding methods in that the separation is achieved not through differences in polarity but through differences in molecular size. The stationary phase consists of a porous material (usually a polymeric resin) with pores of a certain size. Larger molecules are excluded from the pores and move through the column more quickly than smaller ones, which are retained by the packing. Size exclusion chromatography is particularly valuable for determining molecular weight distributions, including those of polymers.

Another type of chromatography, thin layer chromatography or TLC [94], is a relatively simple technique using flat plates coated with the stationary phase, which may be hydrophilic or hydrophobic. A spot of sample is placed near the bottom of the plate and the lower edge is submerged in a solvent. As the solvent moves up the plate through capillary action it acts as the mobile phase and separates the initial spot into a series of spots corresponding to the different components. These are detected by fluorescence in UV light or by the formation of coloured complexes with certain chemicals. Quantitative measurements can be made but are more difficult than with HPLC. The technique is of value mainly as a simple, cheap, qualitative method.

2.3.2 Infrared Spectroscopy (IR):

This technique has a long tradition as one of the most widely used in materials characterization [39-43, 77, 78]. When matter is exposed to infrared radiation it absorbs energy at those frequencies which correspond to the characteristic frequencies of vibration of the atomic groups making up the material. A graph of the degree of absorption versus frequency is known as the infrared spectrum. Often it is quite detailed and serves as a unique "fingerprint" of the material, so IR spectroscopy is widely used for identifying unknown samples. In addition, since the absorption is directly related to the amount of material, it can be used as a quantitative analysis method. It is also used to study changes in molecular structure which occur as a result of chemical reaction. It can be applied to solids, liquids, and gases. In the case of composite matrices, it is used in a number of ways, for example: qualitative and quantitative analysis of the resin, study of the curing reaction, and study of environmental degradation.

The last ten years have seen a tremendous growth in the use of Fourier transform infrared (FTIR) spectrometers [42]. These instruments, which make use of interferometers rather than monochromators to analyze the frequency distribution of the radiation, are extremely powerful. Compared to conventional instruments they are much more sensitive, rapid, and precise, and their use of computers makes it possible to extract much more information from the spectrum. The high sensitivity makes it possible to successfully use a number of reflectance methods, thereby extending the range of applications to a greater number of materials. The possibilities of this technique have only just begun to be exploited.

2.3.3 Thermal Analysis:

This technique [44-46] measures the response of a material when it is subjected to well-defined temperature conditions. Usually this is either a constant temperature (isothermal conditions) or a program in which the temperature varies linearly with time. In thermogravimetric analysis (TGA), the sample's weight is monitored to detect changes which may occur, for example, as a result of decomposition. In differential thermal analysis (DTA), the sample's temperature is monitored and compared to that of an inert reference. This detects any changes in the sample which are accompanied by an absorption of heat (endotherm) or a release of heat (exotherm). Differential scanning calorimetry (DSC) resembles DTA except that the quantity of heat absorbed or released is accurately measured. In the case of epoxy matrices, DSC is widely used to study the kinetics of the curing reaction and to measure the heat of curing. The latter is directly related to the amount of uncured epoxy in the resin.

2.3.4 Gas Chromatography (GC):

Gas chromatography [47,48] is based on the same principles as liquid chromatography except that the mobile phase is a gas such as helium. This limits its use to samples which are volatile enough to become gases at reasonable temperatures (≤ 300°C). Detection is usually based on thermal conductivity or flame ionization. The best resolution is obtained using open tubular capillary columns whose walls are coated with the stationary phase.

Because of the volatility requirement, GC alone is not widely used for epoxy resins (except to determine volatile components). However it can be used to analyze high-molecular-weight resins and polymers if it is combined with pyrolysis [49]. If a sample is pyrolyzed under carefully controlled conditions it yields a mixture of characteristic decomposition products which can be quantitatively analyzed by GC. Hence pyrolysis gas chromatography (PGC) can be used for fingerprinting, for quantitative analysis, and for studying degradation mechanisms.

2.3.5 Nuclear Magnetic Resonance (NMR):

Nuclear magnetic resonance measures the absorption of radiofrequency energy by a sample placed in a strong magnetic field [50, 51]. This results from transitions between energy levels of atomic nuclei possessing magnetic moments, such as hydrogen and carbon-13. Like infrared spectroscopy, it is widely used for fingerprinting and quantitative analysis, but normally it is applied to organic materials and requires that the sample be in solution. In the case of composites, this limits its use to uncured resins, so it is less widely used than infrared spectroscopy. Recently new techniques have been developed to obtain high-resolution NMR spectra of solids such as polymers [52, 53], and these should prove useful for the study of cured resins. Also, NMR imaging techniques, of the type used in medical research, have potential for the nondestructive analysis of composites, such as the determination of moisture distribution [54]. However, both high-resolution solid-state NMR and NMR imaging are still expensive sophisticated research techniques which are unlikely to be used on a routine basis for some time.

2.3.6 Dynamic Mechanical Analysis (DMA):

In general terms, this technique [55] measures the mechanical response (deformation, strain) of a material to an applied stress. The ratio of stress to strain, or modulus, is a measure of the stiffness of the material. Measurements are usually made using a cyclical (sinusoidal) applied stress. The resulting deformation is also sinusoidal but may differ in phase because of a time lag required for molecular rearrangements occurring in response to the applied stress. In this case the modulus may be expressed in terms of a real part, the storage modulus, and an imaginary part, the loss modulus. The quantity tan δ, where δ is the phase angle, is known as the loss tangent, internal friction, or damping. It is related to the amount of energy dissipated as heat during the deformation. A plot of tan δ versus temperature often shows maxima which correspond to specific changes occurring in the sample at the molecular level, such as the glass transition. Dynamic mechanical analysis is very closely related to rheology. Depending on the nature of the sample, a number of different physical configurations are used [55], including the Rheovibron technique, the torsion pendulum, torsional braid analysis (TBA), dynamic spring analysis (DSA), the vibrating reed, and the rotational rheometer.

DMA is a valuable technique for studying both the rheological changes which occur during the processing of composites and the effect of temperature on the mechanical properties of cured composites.

2.3.7 Dynamic Dielectric Analysis (DDA):

DDA [56-58] is similar to DMA except that the applied stress is electrical rather than mechanical. The sample is placed between two electrodes and subjected to a sinusoidal electric field. In response, dipoles within the sample attempt to align with this field, and the ability to align depends on the molecular structure and mobility. The response is measured in terms of capacitance (energy stored) and dissipation factor (energy dissipated). The loss tangent tan δ depends on molecular mobility in much the same way as the tan δ measured by DMA, and yields much the same information when the sample is subjected to a temperature program. Since DDA is relatively simple to use, it can be used in actual process conditions to monitor the curing of a composite part.

2.3.8 Ultraviolet-Visible Spectroscopy (UV-VIS):

UV-visible spectroscopy resembles infrared spectroscopy except that the frequency of the radiation is higher and corresponds to electronic rather than vibrational transitions in the molecules. UV-visible spectra are usually much less detailed than IR spectra. The method has not been widely used in composites characterization [109, 110].

2.3.9 Other Techniques:

A number of other techniques are used in composites evaluation but are not discussed here because they do not directly concern the chemistry. They include, for example, nondestructive evaluation [59], infrared imaging techniques [60, 61], and acoustic emission [62].

3. LITERATURE REVIEW: SYSTEMS BASED ON TGDDM AND DDS

The literature concerning the characterization of matrix resins is extensive. This chapter is therefore limited to a fairly comprehensive, although not exhaustive, review of recent work involving systems based on TGDDM (tetraglycidyldiaminodiphenylmethane, Figure 4b) and DDS (diaminodiphenylsulphone, Figure 5). The TGDDM-DDS combination is the most widely used matrix in high-performance epoxy-based composites. It has proven to be quite durable and is expected to remain the "workhorse" matrix for some time [164], in spite of current work to develop new improved systems. Several commercial products are based on combinations of these two materials with smaller amounts of other epoxies and catalysts. The more common ones and their reported compositions are given in Table 1. It must be emphasized that although they all contain largely TGDDM and DDS, the differences in the minor components can result in very substantial differences in processing behaviour and ultimate properties. The various systems are by no means interchangeable.

3.1 Analysis of Chemical Composition

3.1.1 Analysis of TGDDM Epoxy Resins:

The epoxy resin TGDDM is sold commercially as Araldite MY 720 (Ciba-Geigy), Glyamine G-120 (FIC Corp.), Reichold 37-106, Epiclon 430, YH-434, and ELM-434. In a series of articles published by Ciba-Geigy [67-73], MY 720 has been characterized and compared to competitive products. As a result of the manufacturing process, commercial MY 720 contains only about 60% TGDDM monomer [67]. Another 35% consists of dimer and higher oligomers, both linear and cyclic, in which two nitrogen atoms are linked by a $-CH_2-CHOH-CH_2-$ group. The remaining 5% includes various by-products in which glycidyl groups are replaced by $-CH_2-CHOH-CH_2Cl$ (chlorhydrin) or $-CH_2-CHOH-CH_2OH$ (α-glycol). The presence of a number of components in the resin is not necessarily detrimental. However, it is important that the composition be consistent in order to assure reproducible processing behaviour and physical properties. Gel permeation chromatography (GPC) and reverse-phase HPLC with gradient elution were used to check batch consistency [67,68]. The HPLC chromatogram shows eleven important peaks falling in three groups: unreacted or partially reacted starting materials (high polarity),

Table 1. Reported compositions of some commercial TGDDM-DDS systems.

Rigidite 5208 (Narmco Materials, Inc.)

Component	Composition (% by weight) as reported by: Trujillo [144]	Carpenter [63,144]	May [136,144]	Cizmecioglu [66,165]
TGDDM epoxy resin	64.2	67.6	72.6	73.4
DDS amine hardener	23.6	23.0	19.4	20.6
Bisphenol A Novolac epoxy	10.1	9.5	8.1	6.0
Acetone	1.4			
Water	0.7			

Magnamite 3501 (Hercules, Inc.)

Component	Composition (% by weight) [63-65, 82, 160, 161]
TGDDM epoxy resin	56.5
DDS amine hardener	24.9
Epoxy No. 2 †	9.0
Epoxy No. 3 †	8.5
BF_3 amine catalyst ††	1.1

† Reference 65 reports the minor epoxies to be a cycloaliphatic epoxy ester (e.g. Ciba-Geigy CY 179) and an o-cresol Novolac.

†† Reference 65 reports the amine to be monoethylamine; references 160 and 161 report it to be piperidine.

Resin System 934 (Fiberite, Inc.)

Component	Composition (% by weight) [134, 160, 161]
TGDDM epoxy resin	63.2
DDS amine hardener	25.3
DGOP (diglycidylorthophthalate)	11.2
BF_3 ethylamine catalyst	0.4

monomer and related products (intermediate polarity), and higher-molecular-weight oligomers (low polarity). The GPC curve, which is based on molecular weight, shows only four peaks, corresponding to the monomer and three ranges of higher-molecular-weight materials. In general, GPC chromatograms are less detailed than HPLC curves. The variation of the chromatograms was measured for over 20 batches and found to be within reasonable limits. A definite correlation was observed between resin viscosity and the amount of higher-molecular-weight material as determined by HPLC or GPC. MY 720 is available with different viscosities. Four Japanese versions of TGDDM (Epiclon 430, Glyamine G-120, YH-434, ELM-434) were analyzed and compared to MY 720 [68, 69]. They all showed a higher content of polar material and a lower content of high-molecular-weight components. On the other hand, Reichold 37-106 was found to contain a very high proportion of high-molecular-weight material. Correlations were established between peaks in the HPLC and GPC curves.

The aging of neat MY 720 resin was monitored at three different temperatures (0°, 25°, and 50°C) using several techniques (HPLC, GPC, DSC, viscosity measurement, epoxy value determination) [70-72]. At 0° the changes were negligible, even after 90 days. At 25° and 50° they were negligible up to 30 days but after 60 days an increase in viscosity and a decrease in epoxy value were observed. However, only after the fairly drastic treatment of 50° for 120 days were the changes so large that they would be expected to affect the resin processing. Chromatography showed that the large increase in viscosity was related to a small increase in the amount of high-molecular-weight constituents. Although this can affect the processing, it was found to have no detectable effect on the overall reactivity of the resin or on the mechanical properties of cured specimens prepared from MY 720 and Hardener HT 976 (DDS). It should be noted that mechanical testing results usually show a large degree of scatter because they are very sensitive to sample preparation and testing techniques.

Hagnauer and others have done considerable work on epoxy systems using several techniques, notably liquid chromatography [74-90]. Early work [74] involved a "round robin" study of mixtures based on MY 720, DDS, and BF_3 catalyst. Techniques used were LC, FTIR, and DSC. Methods were developed to separate and quantitatively analyze the MY 720 and DDS by GPC, normal-phase HPLC, and reverse-phase HPLC. In HPLC, gradient elution was found to give better results than isocratic elution. In FTIR, differences between samples were more easily detected when the spectra were subtracted from each other to make the differences stand out. The DSC curves were found to be sensitive to the batch composition. Samples which had undergone a greater degree of reaction (higher resin "advancement") gave a lower heat of reaction as measured by the area under the exotherm peak. Also, the shape of the peak depended on the amount of catalyst present. However, DSC was not as sensitive as LC for detecting variations in the ratio of epoxy to hardener. More recent work [85, 86, 91] involved the isolation of pure TGDDM monomer by preparative LC, and comparison with the commercial mixture. It was found that MY 720 contains about 69% TGDDM and Glyamine G-120 about 78%.

Hydrolysis of TGDDM converts epoxy rings into dihydroxy (α-glycol) groups, and the products can be detected by LC. The pure TGDDM was found to be more stable than the commercial product with respect to hydrolysis at 60°C and 96% RH. It was also slower to react with DDS and produced a material with a higher glass transition temperature. These results confirm that the presence of impurities in the epoxy resin has a significant effect on curing behaviour and ultimate properties. It was also found that N-glycidyl aromatic amines such as TGDDM are more sensitive to moisture than glycidyl ethers such as DGEBA [91]. The manufacture of MY 720 and the question of impurities have also been discussed by Gosnell [92] and Morgan [163]. Gulino et al. [93] have measured the proton NMR spectra at 350 MHz of TGDDM monomer and impurities isolated from MY 720 by liquid chromatography.

3.1.2 Analysis of TGDDM-DDS Mixtures:

May and co-workers have described methods for the physicochemical characterization of prepreg systems based on TGDDM and DDS [95-99]. Thin layer chromatography produces good separation of the resin components and, together with infrared spectroscopy, is especially useful for qualitative identification of the different constituents. For quantitative analysis, HPLC and GPC are better than TLC. HPLC can determine the amounts of unreacted DDS and TGDDM monomer, while GPC is a good indicator of the degree of polymerisation (B-staging). The total amount of hardener present can be determined by elemental sulphur analysis or by infrared spectroscopy using the sulphone band at 1150 cm^{-1}. The content of unreacted epoxy groups can also be measured by IR. The presence of BF_3 accelerator can be detected by emission spectroscopy and by its effect on the shape of the DSC curing curve; the amount can be measured by atomic absorption. Other methods mentioned are dynamic dielectric analysis (DDA), FTIR for studying curing, oxidation, and degradation, and carbon-13 NMR for detecting subtle changes in chemical structure. The use of both proton and carbon-13 NMR to analyze TGDDM-DDS formulations has been reported [100, 101].

3.1.3 Analysis of Narmco Rigidite 5208:

Several analyses of the Narmco 5208 system have been reported (Table 1). It contains three main components: a TGDDM resin (the major epoxy), DDS, and a bisphenol A Novolac epoxy resin (the minor epoxy). Hinrichs and Thuen [30] have described the analysis of Narmco 5208, TGDDM, and other epoxies using reverse-phase HPLC, IR, thermal analysis, and rheological measurements. They concluded that the most sensitive technique for detecting batch variations is HPLC. Researchers at Lockheed [33, 102] have reported an IR method for analyzing DDS and a HPLC method for analyzing TGDDM monomer, DDS, DGEBA monomer (the principal component of bisphenol A Novolac epoxy), and the 1:1 reaction product of TGDDM and DDS. Absolute quantities were determined by calibration using pure standards isolated by chromatography and recrystallization. In a series of commercial batches, HPLC detected significant differences in the monomer/oligomer ratio of the TGDDM resin; a low oligomer content was associated with the appearance of voids in cured laminates. Also, a rapid increase in viscosity on curing appeared to be related to a high content of minor epoxy. Gosnell [92] discusses the manufacture and quality control of prepreg based on Narmco 5208. Carpenter [63] has reported IR, LC, and DSC results for this system. IR was used to determine DDS and epoxide equivalent, HPLC to determine the minor epoxy. DSC gives a curve with a single exotherm peak which is somewhat sensitive to the DDS content. In batches made with a ±10% variation in the amount of DDS, the difference was accurately detected by IR. Cizmecioglu et al. have analyzed Narmco 5208 using LC and FTIR [66]. For DDS determination they used an IR method based on a band at 690 cm^{-1}. Chen and Hunter [103] have done an extensive study of the Narmco 5208 system using physical testing, HPLC, GPC, ion chromatography, DSC, IR, DMA, viscosity measurement, and mechanical testing. Again, HPLC was considered the most sensitive method for detecting variations. Numerous parameters affecting the analyses were investigated. In DSC, they observed an unexpectedly large variation when repeated measurements of the heat of polymerisation were made on the same batch. This was traced to the presence of various foreign particles ranging from wear metal to bits of wood and cotton. More reproducible results were obtained when the resin was extracted with acetone and the solution centrifuged to remove impurities. However, this procedure required that the resin be heated to 60°C for four hours to remove all the solvent. No significant changes were detected by IR or dielectric analysis, but HPLC showed some advancement. The curing of the resin was studied by FTIR while heating at 10°C per minute. Major changes occurred around 200°C, which corresponds to the DSC peak onset.

3.1.4 Analysis of Hercules Magnamite 3501:

Chen and Hunter [103] and Carpenter [63,64] also studied the Hercules 3501 system (Table 1). Although based on TGDDM and DDS, it is quite different from Narmco 5208. Instead of bisphenol A Novolac epoxy, it contains two other minor epoxies as well as a BF_3 amine catalyst. As mentioned previously, the latter can be analyzed by atomic absorption. One of the minor epoxies is an ester and can be detected by IR (carbonyl band near 1720 cm^{-1}). Both are volatile enough to be analyzed by gas chromatography. Unlike the case for Narmco 5208, the DSC curve shows an exotherm with two peaks. This is a result of the presence of BF_3 catalyst, which changes the cure kinetics. The ratio of the peak heights is related to the catalyst concentration. Because of this difference, a different cure procedure is recommended. Whereas Narmco 5208 requires a thermal dwell stage at 135°C (275°F) (Section 2.1), Hercules 3501 is heated directly to 177°C (350°F) [104]. Further methods for analyzing Hercules 3501 have been reported by Wickham et al. [105] and Sewell [106]. These involve wet chemistry, reverse-phase HPLC, GPC, IR, DSC, and atomic absorption.

3.1.5 Analysis of Fiberite Resin System 934:

This system has received less attention than the two previously described. It is reported to contain, in addition to TGDDM and DDS, one minor epoxy (diglycidylorthophthalate, DGOP) and BF_3-ethylamine catalyst [134, 160, 161]. The minor epoxy gives a strong ester carbonyl band at 1740 cm^{-1} in the IR spectrum, and the catalyst gives rise to multiple peaks in the DSC curve [31].

3.1.6 Other Analytical Work:

Kowalska and Wirsén [107] report data for a number of commercial prepregs, including the following based on TGDDM and DDS: Narmco 5208, Hercules 3501, Courtauld Grafil HC 3501, Fothergill & Harvey Carboform 69, 3M (Minnesota Mining and Manufacturing) SP 313, Fiberite Hy-E 1034E, Fiberite Hy-E 2034A, and Fiberite HMF-330C-34. They used GPC, NMR, and mass spectrometry. Carbon-13 NMR is useful for qualitative analysis and for quantitative determination of the TGDDM-to-DDS ratio. Mass spectra were measured for various components and used to identify fractions separated by GPC. Luoma [94] has applied TLC to several systems including MY 720, Narmco 5208, and Hercules 3501. The latter was shown to contain at least nineteen different components. Lindgren has used pyrolysis gas chromatography to determine the ratio of TGDDM to DDS in cured samples [108]. There have been two reports [109, 110] of the use of ultraviolet or UV derivative spectroscopy to do quantitative analysis of Hercules 3502 and Narmco 5208. Hercules 3502 is an uncatalyzed system resembling Narmco 5208.

3.2 Effects of Altering Composition

Roylance et al. [111] separated Glyamine G-120 into pure TGDDM monomer and high-molecular-weight components by preparative liquid chromatography. These were then reacted with DDS to form test pieces. Similar pieces were made from MY 720 and the following properties were studied: mechanical, dynamic mechanical, and moisture absorption. Little difference was observed among the different samples. The results were more sensitive to the thermal history or to the concentration of DDS.

Browning et al. [112] used dynamic mechanical shear behaviour to study the effects of altered composition in three different systems. The first consisted of TGDDM, DDS, and BF_3 catalyst. The others resembled Narmco 5208 and Hercules 3501. The only significant differences observed were in the first system, where variations in the viscosity of the base resin affected the results. However, absorption of moisture by the samples had a definite plasticizing effect.

Miller and Barbee [26] studied a system (possibly Narmco 5208) based on TGDDM, DDS, and a minor epoxy. The DDS concentration was varied from the normal level by ±25%. No correlation was found between ultimate fracture stress of cured samples and variation in composition. Fracture analysis showed that fracture initiation was due mainly to the presence of foreign particulate material, and that this masked any effects of composition. However, dynamic mechanical analysis showed up differences which agreed with the expected behaviour. Samples with a higher DDS content had a higher glass transition temperature, no doubt resulting from a higher degree of crosslinking. It was also shown that processing conditions are just as important as chemical composition in determining the dynamic mechanical behaviour.

Borstell [25] has examined the effects of composition variation in Hercules 3501. Eleven batches with controlled variations were prepared under production conditions and tested using various methods (mechanical testing, IR, LC, DSC, DDA). All variations could be detected by one or another of the analytical techniques. All the batches met practically all the Hercules shipping specifications for prepreg physical properties and laminate mechanical properties. The only exception observed was the "flow test" result. In order to see significant differences among the cured laminates, it was necessary to do static testing at 127°C (260°F) after humidity exposure and ambient fatigue testing. In this case, a batch made with 20% excess accelerator showed poor tensile properties and was considered unacceptable. Similarly, a "brittle" batch made with low viscosity resin, 10% less hardener, and 20% excess accelerator showed unacceptable in-plane shear properties. The remaining batches were acceptable.

Carpenter [64] also studied Hercules 3501, using sixteen batches made with controlled alterations of composition. The DSC curve could detect variations in DDS and BF_3 levels but was not so sensitive to variations in minor epoxy content or degree of advancement. Viscosity measurements were used to derive equations relating gel time to the heating conditions, and the gel time was found to vary significantly with altered composition. The glass transition temperature of cured resin was less sensitive to composition than expected; it increased slightly with the amount of hardener.

Results such as those described above indicate that short-term mechanical testing is not very sensitive to variations in batch composition and that other factors such as particulate impurities and processing conditions can be of considerable importance. However, in the longer term, corresponding to the expected service life of a typical composite part, it is believed that such variations are much more significant in view of the relationship between matrix chemistry and response to environmental exposure and service conditions. Little experimental data concerning this relationship has been reported to date because of the large amount of work and long time span involved. For the present, since mechanical testing is so insensitive, the safest approach to ensuring optimum long-term behaviour is to minimize batch variations by using accurate physicochemical characterization methods.

3.3 Effects of Prepreg Aging

The prepreg used to make composite parts contains both epoxy resin and hardener. To avoid premature reaction which could render it unusable, it must be stored at low temperature and protected from humidity. The effects of exposure to adverse conditions have been studied by several groups.

Crabtree and Hewitt [113] used reverse-phase HPLC and GPC to follow the aging of TGDDM-DDS mixtures. They observed a slight change after 46 days at 22°C and a substantial change after one year. At 0°C the changes were negligible, even after three years. Cured parts made from the latter material had the same strength as those made from fresh material. A later paper [114] reports more quantitative results for Narmco 5208 and Hercules 3501. The ratio of certain peaks in the GPC chromatogram varies linearly with aging time. In the case of Hercules 3501, a similar trend was found for the ratio of peak heights in the DSC curve. Narmco 5208 gives only one DSC peak so this analysis could not be applied.

Hinrichs and Thuen [115] studied Narmco 5208 using HPLC, moisture analysis, and rheological measurements. When prepreg is exposed to 50% or higher relative humidity, the moisture reaches a saturation level of about 0.7% in 5 hours. If the humidity is less than 35%, the prepreg loses moisture to a limiting level of about 0.1%, also in 5 hours. HPLC could detect no changes in prepreg exposed 5 days at 0% and 98% R.H. A high moisture content was found to increase the tackiness, to affect the viscosity profile during cure, and to produce porosity in the laminate. Fortunately, the moisture effects were found to be reversible. After humidity-exposed prepreg was dried in a desiccator, it behaved in the same way as it did before moisture absorption. The viscosity profile during cure was also found to be highly dependent on the degree of advancement, or B-staging, of the resin.

Lawless [104] used dynamic dielectric analysis to study the aging of Narmco 5208 and Hercules 3501. A typical DDA curve plots the dissipation factor or loss tangent tan δ versus time as the sample is subjected to a controlled temperature program. Resin systems such as the ones mentioned usually show two peaks related to molecular mobility. The first, known as the "flow" peak, corresponds to a drop in viscosity which occurs when the resin is first heated. The second, or "gel" peak, corresponds to the point at which the resin is crosslinked to the extent of forming a three-dimensional network or "gel". In a resin system with a high degree of advancement, these two peaks occur closer together and may even merge. Lawless exposed prepreg in both dry (0% R.H.) and wet (100% R.H.) conditions. In both cases, the Narmco prepreg became noticeably more rigid, or "boardy", after 2-3 weeks. After 6 weeks, both Narmco and Hercules prepregs lost essentially all tack and flow properties as compared to unexposed material. The DDA curves showed changes even after one day. Initially, the absorption of moisture has a plasticizing effect and moves the flow peak to lower temperature. After 1-2 weeks, resin advancement begins to dominate. The DDA curve begins to show distortion and after 6 weeks the flow peak has disappeared completely, but the cure peak remains. Similar results have been reported by May [183] for TGDDM-DDS mixtures.

Sanjana [116] studied the aging of Hercules 3501 prepreg under the following conditions: ambient (26°C & 62% R.H.), 49°C dry, 49°C & 95% R.H., 49°C & 80% R.H. intermittent. Changes were easily detected by DDA and DMA but not by DSC. The first noticeable physical change was loss of tack and drapability, which was considered to render the prepreg unusable. This occurred in two days at 49°C and in 3-4 weeks under ambient conditions. Laminate mechanical properties did not deteriorate until well beyond this point. The DMA curve measured for prepreg shows an initial damping peak associated with softening and flow of the resin, and the temperature at which this peak occurs increases linearly with the aging time. The same is true for the flow peak observed in DDA. Measurements of resin flow showed a corresponding gradual decrease. All these changes were correlated with readings given by a Time/Temperature Watch (TTW). This is a commercial device which indicates by a colour change the extent to which a material has been exposed to unfavourably high temperatures.

Hagnauer has also studied the aging of Hercules 3501 [81, 82] using GPC and normal-phase HPLC to determine the amounts of unreacted TGDDM monomer and DDS. He concluded that the prepreg becomes unacceptable for processing when these amounts drop from their initial values of 40% and 24% respectively to 28% and 16%. At 49°C this happens in two days, at 22° it takes over two weeks, and at -13° the prepreg is still good after one year. At 22° the drop in TGDDM and DDS is more rapid during the first week.

May [99] reports an HPLC analysis of a TGDDM-DDS formulation in which TGDDM and DDS were monitored as a function of aging time. The amounts decreased from 51% and 30% respectively to 44% and 22% over a period of 63 days. Similarly, Sewell [106] found that for Hercules 3501 after 40 days under dry ambient-temperature conditions the content of free DDS decreased by 35% and the amount of Novolac epoxy by 40%. Scola [65] used reverse-phase HPLC and IR to follow the aging of Hercules 3501 prepreg for up to 14 days at 25°C and relative humidities of 0, 31, 51, and 93%. He found that the prepreg absorbed about twice as much moisture from the atmosphere as did the neat resin. The BF_3-amine catalyst has a particularly high affinity for moisture. In HPLC the ratio of the TGDDM peak to the reaction product peak was found to decrease with aging time, the rate being higher at higher humidity levels. In IR the ratio of the epoxy peak at 910 cm^{-1} to the aromatic band at 1605 cm^{-1} was used as a measure of the amount of unreacted epoxy. The results were inconclusive because of substantial scatter. Physical and mechanical properties (void content, compressive strength, interlaminar shear strength) did not appear to be adversely affected by the aging.

3.4 Effect of Adverse Environment on Cured Composite

This is an important aspect of composites since in service they may be exposed to unfavourable conditions of moisture, high temperature, and radiation. Considerable work has been done in this field, of which a few examples are mentioned here.

The durability of epoxies has been reviewed by Morgan and O'Neal [152]. Unlike prepreg, finished composite parts are often likely to come into intimate contact with liquid water in addition to atmospheric water vapour. Under such circumstances, matrices such as those based on TGDDM and DDS can absorb a surprisingly high amount of water, of the order of 5% by weight based on neat resin or 2% based on a typical composite. The water acts as a plasticizer and lowers the glass transition temperature of the epoxy, causing it to "soften" at a lower temperature. The decrease in T_g can be as much as 80°C. The result is a decrease in mechanical properties, especially at higher temperatures. The plasticization is reversible, so drying often restores the original properties. However the water can also have irreversible effects. For example, it can cause swelling stresses which produce bond cleavage and weaken the network. On the other hand, by enhancing molecular mobility it can allow hitherto unreacted groups to react with each other and form crosslinks, thus strengthening the network. The overall effect depends on the particular circumstances.

Sandorff and Tajima [117, 118] have developed a technique for measuring the distribution of moisture within a laminate and have used it to determine the rate of diffusion of water into laminates made from Narmco 5208 and 5209. The moisture content at saturation is between 1 and 2%. Similar work has been reported by Loos and Springer [119] for the absorption of water, fuels, and oil by Narmco 5208, Hercules 3501, and Fiberite 1034. In Carpenter's study of Hercules 3501 batches of altered composition [64], moisture absorption remained relatively constant at 5-6%; it appeared to be higher for batches with higher amounts of BF_3. Ryan et al. [120] are using new techniques for studying the penetration of D_2O into resins such as Hercules 3501. These include laser pyrolysis gas chromatography mass spectroscopy, high resolution laser pyrolysis infrared spectroscopy, and infrared imaging photography. Ho [121] has reported on the effects of temperature and humidity on the mechanical properties of a composite based on Narmco 5208 and Kevlar 49. The effects of moisture on the DMA of Narmco 5208 have been studied by Seferis [140, 187] and Kaelble [188]. The former found that moisture changes the form of the DMA curve through plasticization and restriction of molecular chain movement; the latter observed irreversible reduction in shear strength.

Other studies of the TGDDM-DDS system include those of Morgan et al. [189], Moy and Karasz (broad line NMR) [190], and Apicella et al. [122-124, 275, 276]. The latter showed that moisture absorption lowers the T_g by varying amounts depending on the DDS content. Two mechanisms were suggested: free volume and hydrogen bonding. The effects of mechanical stress, high temperature, and moisture on the matrix chemistry have been studied by Levy et al. [125] using internal reflectance FTIR spectroscopy and near-infrared spectroscopy. Certain irreversible changes were observed such as the disappearance of residual epoxy rings. Water had an important plasticizing effect which was related to hydrogen bonding with the oxygen atoms of the sulphone groups, based on changes observed in the IR spectrum. The fluorescence behaviour is also affected by moisture absorption [126]. Wolf, Fanter, and Grayson [129-132] have studied the microchemical changes occurring in the TGDDM-DDS system as a result of exposure to moisture, temperature, and stress. They used chemiluminescence, vaporization gas chromatography and mass spectrometry, precision abrasion mass spectrometry, and stress mass spectrometry. A correlation was found between chemiluminescence intensity and extent of aging. Thermal aging produced several volatile products, notably propenal (acrolein). Stress mass spectrometry showed that mechanical fracture produces chemical decomposition with sulphur dioxide as the principal product. Young et al. [133] used diffuse reflectance FTIR to monitor the thermal aging of Hercules 3501 and observed the formation of carbonyl groups through oxidation.

Kong et al. have published several papers [134-139, 277] on the "physical aging" of graphite-epoxy composites including Narmco 5208 and Fiberite 934. This is a specific term which refers to changes occurring when a matrix is annealed at a temperature somewhat below the glass transition temperature. The changes are related to free-volume collapse and enthalpy relaxation in the non-equilibrium glassy network. They are important because they affect the mechanical behaviour of the matrix, which as a consequence becomes dependent on the thermal history.

For applications in space, the effects of high-energy radiation on the composite must be considered. Netravali et al. [127] have studied this aspect, in addition to that of moisture, using DSC and IR spectroscopy. Both electron- and γ-radiation produce further crosslinking of the epoxy matrix. Moisture studies using D_2O showed that there is exchange of protons between the water molecules and OH groups present in the matrix. Giori and Yamauchi [128] subjected graphite-reinforced Narmco 5208 and Fiberite 934 to ultraviolet and electron radiation and analyzed the volatile decomposition products by gas chromatography and mass spectrometry. The samples were found to have high electron radiation stability but low UV stability.

3.5 Cure Kinetics and Matrix Morphology

One very important aspect of composites technology concerns the mechanism of the curing reaction and its effect on the matrix properties, including the morphology. A knowledge of the cure kinetics is necessary in order to set up a proper curing program. In spite of the work which has been done, this knowledge is limited at present because of the complexity of the curing reactions, but research is being performed with the aim of achieving a more complete understanding. This is making it possible to develop numerical models relating the chemistry and rheology to parameters such as time, temperature, and the geometry of the part being cured. Such models can be used by process engineers to monitor, control, and optimize the manufacturing of composite parts in industrial situations. This aspect of polymer processing is sometimes referred to as "chemorheology" or "processing science". It has been discussed by Halpin et al. [34] for a typical TGDDM-DDS system such as Narmco 5208. Other general articles have been published by May et al. [142, 185]. Among the groups making contributions to this field are those associated with Seferis [140-148, 278, 279], Apicella [149-151, 275], Morgan [152-164], and Cizmecioglu [165-167].

3.5.1 Matrix Morphology:

One of the interesting findings which has emerged from the research being done is that the matrix is not always entirely homogeneous. According to Morgan [156], depending on polymerization conditions (temperature, solvent, chemistry), phase separation due to "microgelation" can occur, giving rise to regions of high and low crosslink density in the cured matrix. Electron microscopy showed "nodules" of size 6-9 nm in a matrix made from DGEBA and DETA, but no evidence of heterogeneous crosslink distribution in TGDDM-DDS. However, in the latter system, if the concentration of DDS is sufficiently high, crystals of unreacted DDS can form. If the curing temperature exceeds the melting point of DDS (162°C), these can melt and flow, creating microvoids in the composite and lowering the mechanical strength and moisture resistance. Such voids were found in Narmco 5208 [155]. Comparison of Narmco 5208 with Fiberite 934 showed several differences attributed to the presence of BF_3 catalyst in Fiberite 934 [153]. For instance, the 934 shows birefringence (domains of about 1 mm), whereas the 5208 does not, and this was attributed to non-homogeneous BF_3 distribution. Also the 934 has a lower T_g and higher density than the 5208. Finally, IR spectroscopy showed that in 934 the epoxy groups disappear significantly faster than in 5208 on curing at 177°C. In general, these systems were considered to be not highly crosslinked, since they can undergo elongation of up to 15% before rupture. Seferis et al. [141, 148] used electron microscopy, DSC, DMA, and formic acid etching to study the morphology of a matrix (similar to Narmco 5208) based on TGDDM, DDS, and bisphenol A Novolac epoxy. They found that samples prepared by the standard melt-processing technique were heterogeneous with regions of high and low crosslink density. However, films prepared using a solution-processing method with N,N-dimethylacetamide as solvent were homogeneous. It is obvious from the results just described that the network structure depends on a number of factors involved in the preparation of the matrix.

3.5.2 The Curing Reaction:

The curing of the epoxy resin system involves a number of different reactions. In the case of an amine-cured system such as TGDDM-DDS, the first to occur is the reaction of epoxy rings (E) with primary amine groups of the hardener (PA), producing a link containing a secondary amine group (SA) and a hydroxyl group (OH):

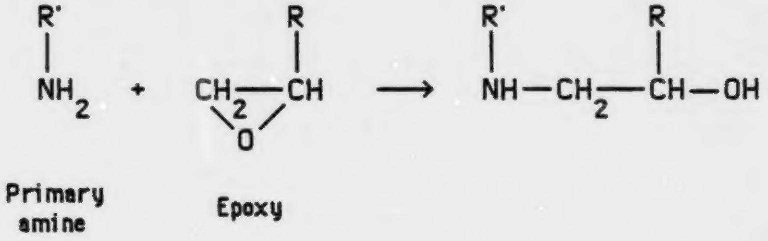

The ring opening can also take place on the opposite side, giving rise to a primary alcohol group rather than a secondary one, but the reaction shown is the predominant one. The hydroxyl group produced can react with an epoxy group to produce an ether link and another hydroxyl group, which is available for further reaction:

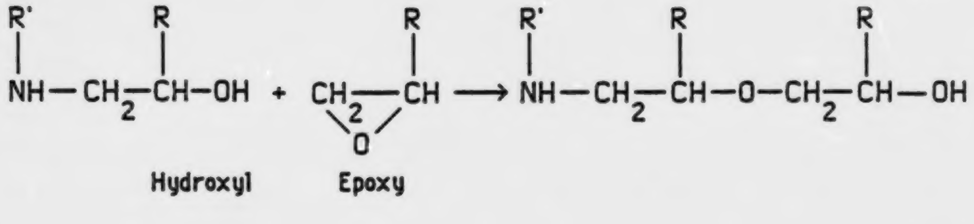

Hydroxyl-containing impurities in the resin, such as α-glycol, can also react in this manner. Similarly, the secondary amine group can react to produce a tertiary amine group and a hydroxyl group:

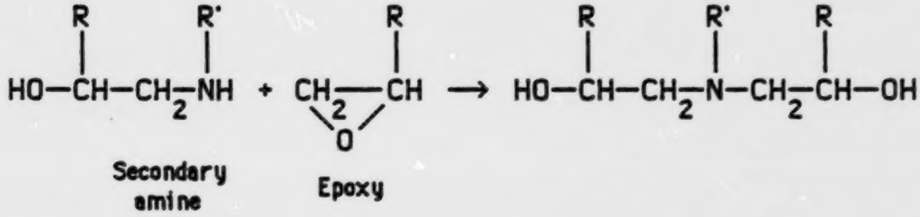

Another reaction which can occur, even in the absence of amine hardener, is epoxy homopolymerisation, a reaction accelerated by the presence of BF_3 catalyst and hydroxyl- or amine-containing impurity:

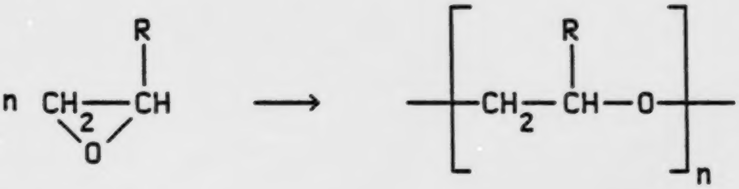

If such homopolymerization involves two epoxy groups in the same TGDDM molecule it can produce a cyclic morpholine-type structure:

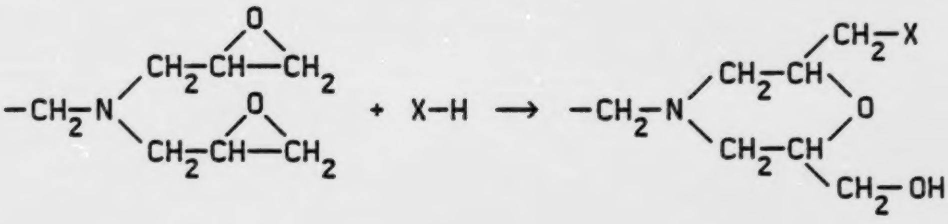

This very brief description of the curing mechanism serves to illustrate the complexity of the situation and the difficulties involved in developing a numerical model to describe it.

3.5.3 Cure Kinetics:

The kinetics and mechanism of the curing reaction are best studied by DSC and IR spectroscopy. The application of DSC has been reviewed by several authors [46, 280, 281]. Experiments have been done in both isothermal (constant temperature) and dynamic (temperature increasing linearly with time) modes, and the results have been interpreted using various mathematical treatments. Cizmecioglu and Gupta [165] have analyzed the kinetics of reaction of epoxy groups in Narmco 5208 using a very simple model, namely a general nth-order Arrhenius-type equation with a single rate constant. They obtained an activation energy E_a of 107 kJ/mol (25.6 kcal/mol) but found that the apparent reaction order n depended on the heating rate. This is probably a consequence of the over-simplification of the analysis. Not only are various different reactions involved, but Narmco 5208 contains two different epoxy resins which can behave quite differently. Later work by the same group [166, 167] involved DSC, FTIR, and ESR (electron spin resonance) studies of the isothermal cure of TGDDM-DDS mixtures at 177°C. They concluded that the first stage of the cure (up to about one hour) involves mainly the highly exothermic PA-E reaction with a rate constant of $5.5 \times 10^{-4}\ s^{-1}$ and a heat of reaction ΔH of 1200 J/g. The second stage is dominated by the OH-E reaction, which has a rate constant an order of magnitude smaller ($4.8 \times 10^{-5}\ s^{-1}$) and is much less exothermic ($\Delta H = 150$ J/g). However, this reaction is expected to have a lower activation energy than the PA-E reaction, so at lower temperatures it could become the dominant one. The SA-E reaction appears to be much less important than the OH-E one, and this is attributed to restricted diffusional transport in the partially-cured matrix and to steric hindrance by the aromatic ring adjacent to the NH group. When TGDDM was cured with N,N'-dimethyldiaminodiphenylsulphone (DMDDS) the heat of reaction was much the same as with DDS, which suggests that in both cases only one hydrogen atom reacts per amine group.

Morgan et al. [157-163] reached similar conclusions from their IR and DSC work. They compared the reactivity (with DDS) of pure TGDDM monomer, commercial MY 720, and MY 720 with added DGOP and/or BF_3 catalyst. The MY 720 reacts faster than the pure monomer, apparently because of the presence of catalyzing impurities such as the α-glycol. The catalyzing effect of hydroxy compounds on the epoxy-amine reaction has been pointed out by King and Bell [168]. With added BF_3 the reaction rate is higher still, and the DSC curve shows extra peaks. The four principal reactions (PA-E, OH-E, SA-E, and homopolymerization E-E) were estimated to have relative rate constants of 1 : 0.1 : 0.1 : 0.005. Thus they attribute equal importance to the SA-E and OH-E reactions, which is somewhat different from the conclusion of Cizmecioglu et al. They also found that there is significant intramolecular ring formation in addition to the formation of intermolecular linkages. The BF_3-amine catalysts in Hercules 3501 and Fiberite 934 were characterized in detail by NMR [163, 169].

Seferis et al. have studied the cure process using DSC, DMA, and rheological measurements [141-147, 278]. They found that even for simple TGDDM-DDS mixtures the shape of the DSC curve and the kinetic parameters calculated therefrom change with heating rate, and they interpreted this in terms of a change in the relative importance of two reactions with different activation energies, such as PA-E and OH-E. This also has an effect on the final structure of the cured material. The DMA curve shows three main peaks, one of which is sensitive to the heating rate. A second peak is sensitive to the degree of cure and disappears completely when the resin is fully cured. The third peak corresponds to the normal glass transition. From the DSC results it was concluded that multiple reactions occur, the system is autocatalysed, and analysis using a simple Arrhenius equation is not valid. The kinetics were analysed in terms of two reaction regimes, the first corresponding to the PA-E reaction (E_a = 16.7 kcal/mol or 70 kJ/mol) and the second to a combination of the OH-E, SA-E, and E-E reactions (E_a about 42.3 kcal/mol or 177 kJ/mol). Because of the higher activation energy, the second regime becomes important only at higher temperatures. This interpretation is different from that of Cizmecioglu et al. Inclusion of bisphenol A Novolac epoxy in the system complicates the situation further [144, 145]. Apparently the Novolac reacts with DDS much faster than does TGDDM, so in a mixture containing both, the Novolac will react almost completely before the TGDDM begins to react to a significant extent. The highly functional Novolac acts as a chain concentrator and gives rise to domains of higher crosslink density. Furthermore, the presence of Novolac appears to facilitate the subsequent OH-E reaction and increase the overall extent of cure. A probabilistic model was developed [143, 145] to provide a quantitative description of the network structure in terms of parameters such as the molecular weight between crosslinks. This required certain simplifying assumptions, for example, that only the PA-E and SA-E reactions are significant, and that the first proceeds to completion before the second takes place. Seferis et al. have also used DDA and dynamic viscosity measurements to study this system [147] and obtained E_a values similar to that obtained by DSC (12 to 17 kcal/mol, 50 to 71 kJ/mol). When a BF_3-amine catalyst is added to the system, it significantly affects the network structure, as shown by DMA measurements [278]. Apicella et al. [149-151] used HPLC in addition to DSC and viscosity measurements to characterize the TGDDM-DDS cure. Again, they analysed the data in terms of a two-stage mechanism involving the PA-E reaction (E_a = 16.6 kcal/mol or 69.5 kJ/mol) and the etherification reaction (E_a = 41.0 kcal/mol or 172 kJ/mol).

Mijovic et al. [282] have pointed out the discrepancies among published interpretations of the TGDDM-DDS kinetics and the need for further research. Their own work involved isothermal DSC analysis of mixtures of MY 720 and HT 976. The results were interpreted in terms of an autocatalytic mechanism using a rate equation involving two rate constants and an overall reaction order of 2. Good agreement was observed up to about 40% degree of conversion, but beyond this point deviations occurred. This was attributed to a decline in importance of the initial reaction regime and the appearance of a new exothermic reaction. The initial autocatalytic reaction was found to have an activation energy of 50-67 kJ/mol or 12-16 kcal/mol. The same group has also studied the cure of Hercules 3501 using different heating rates between the initial and final stages of cure [290]. They found that a faster heating rate gives a lower extent of conversion and a lower T_g, but that post-curing at 207°C for four hours eliminates the differences.

Lee et al. [174] studied Hercules 3501 using DSC and viscosity measurements and developed a two-stage model to describe the cure, based on equations proposed by Sourour and Kamal [175] and Prime [176]. For less than 30% conversion, they use an autocatalytic-type equation involving two rate constants, which were found to have activation energies of 80.7 and 77.8 kJ/mol. Beyond 30% conversion, a simple first-order equation applies, and the activation energy is 56.6 kJ/mol.

Several other groups have also studied the cure of TGDDM-DDS systems. Hagnauer and Pearce [88] used size exclusion chromatography to study the kinetics of the initial stages of the TGDDM-DDS reaction. They confirmed that the PA-E reaction is predominant and has an activation energy of 16.6 kcal/mol (69.5 kJ/mol). Dynes and Kaelble [31, 188] have compared the different DSC curves obtained for Narmco 5208, Fiberite 934, and Hercules 3501 with those of pure TGDDM and a TGDDM-DDS mixture. As mentioned previously, Carpenter [64] has measured DSC and viscosity data for Hercules 3501 batches of varying composition. Schneider and Gillham [171] used torsional braid analysis to determine the points of gelation and vitrification during cure of Fiberite 934 and Hercules 3501. Zukas, MacKnight, and Schneider [172] similarly examined Narmco 5208 using dynamic spring analysis and dielectric relaxation in addition to TBA. They calculated activation energies for the initial stage of cure ranging from 15.0 to 17.5 kcal/mol (62.8 to 73.2 kJ/mol). The origin of the peaks in the dielectric analysis curve is not as clear as in the DMA methods. Nevertheless, it can be a very useful tool, as pointed out by May [183-185]. One advantage is that the electrical properties correlate reasonably well with viscosity measurements, as demonstrated for Narmco 5208 by

Tajima [173], but they are easier to measure and can be determined for actual parts during the manufacturing process. DDA is capable of detecting variations such as those due to prepreg aging [104, 183, 185] or the effects of BF_3 catalyst [183-186].

Other papers of interest include: a general discussion [43] of the curing process and analytical techniques (including Raman spectroscopy); a general discussion of the network formation process [177]; a study of TGDDM-DDS sustems of varying crosslink density [180]; the in-situ analysis of the cure of Narmco 5208 prepreg by diffuse reflectance FTIR [181]; the low-temperature curing of Hexcel F263 [182]; the microwave curing of composites [283]; and the effects of using salicylic acid as a catalyst in the TGDDM-DDS system [170]. Equipment for producing prepreg on a laboratory scale has been developed by the Seferis [279] and Mijovic [291, 292] groups.

3.5.4 Rheological Studies:

The viscosity of the resin is an extremely important variable in the cure cycle. It determines whether or not there is proper consolidation of the various prepreg layers, and it determines to what extent excess resin flows into the bleeder material. Considerable attention has been devoted to viscosity measurements of epoxy systems during cure. The viscosity and the degree of cure are intimately related. A complete model of the cure process should allow one to calculate both the degree of cure and the viscosity as a function of time and temperature throughout the cure cycle. This then makes it possible to predict the outcome for any specified conditions of temperature, pressure, and part geometry.

In conjunction with their kinetics studies on Hercules 3501, Springer et al. [174] performed viscosity measurements and developed an equation relating viscosity to temperature and degree of cure. The same authors have published other articles on modelling of the curing process [179, 284, 285]. Hinrichs et al. [178, 286, 287] have discussed rheological measurements and have shown that the viscosity profile of Narmco 5208 during cure is affected by moisture absorption and by the degree of advancement of the resin. Apicella et al. [149-151, 275] performed measurements on TGDDM-DDS mixtures and demonstrated that, at least under the conditions used (low degree of cure), the results could be fitted by the William-Landel-Ferry (WLF) equation. The same equation has been applied to a system resembling Narmco 5208 [288, 289]. Seferis et al. [142] studied TGDDM-DDS mixtures with and without BF_3 catalyst and developed a six-parameter mathematical model to predict the viscosity as a function of the time-temperature heat history.

Viscosity measurement is not without experimental difficulties. It is easier to perform measurements on neat resin than on prepreg, but this requires separation of the resin from the fibres. If a solvent is used, traces remaining in the resin can alter the rheological behaviour. However, heating to remove all the solvent can cause advancement of the resin. Methods have been developed to extract the resin by applying pressure under conditions which avoid significant resin advancement [293, 294]. However, it has been demonstrated that the presence of fibres in the resin can significantly change the curing and flow behaviour; consequently attention has been given to developing methods to do rheology measurements directly on prepreg [295-297].

4. LITERATURE REVIEW: SYSTEMS OTHER THAN TGDDM-DDS

Extensive work similar to that described above has been done on systems other than those based on TGDDM and DDS. These include, for example, matrices based on TGDDM and DICY, and numerous mixtures based on DGEBA resins in various combinations with other products. In addition, research is being done on thermoset systems other than epoxies, such as polyimides. These are used primarily because of their stability at high temperatures. Their chemistry is different from that of the epoxy systems. There is also increasing interest in high-performance thermoplastic matrices, such as polyphenylenesulphide (PPS) and polyetheretherketone (PEEK). Although such systems involve no curing, close control of the manufacturing process is necessary to assure the proper degree of crystallinity, which affects the mechanical properties.

The literature on these systems will not be described here. Tables 2 to 4 list a number of relevant references which should prove a useful starting point for those interested in obtaining further information. The tables give the system studied, the type of study (compositional analysis, curing behaviour, etc.), and the techniques used.

Table 2. References concerning epoxy systems other than TGDDM-DDS (†)

System	Description	References
Reliable Manufacturing RAC 7250 (TGDDM, DICY, ECN, Diuron)	Analysis, HPLC, IR Analysis, HPLC, GPC, FTIR, moisture Curing, IR	77 191 78, 192
TGDDM + DICY + Diuron	Analysis, HPLC, GPC, FTIR	75, 76
TGDDM + DICY + accelerator	Curing, DMA, TBA	193
TGDDM + DICY + DGEBA + Novolac	Curing, DSC, TBA	194
American Cyanamid FM300K (TGDDM + DICY etc.)	Analysis, HPLC, IR, DSC, TMA, moisture	195
3M Scotchply 1009 (Epon 828, DEN 438, BF_3)	Curing, IR, DMA Curing, degradation, FTIR Photochemical degradation, IR, UV Weathering, IR	78 77 196 197

3M SP250 (Epon 828 + ECN 1273 + DICY + Monuron + flexibilizer)	Analysis, HPLC, GPC	76, 83
	Analysis, HPLC, GPC, FTIR, moisture	77, 191
	Quantitative analysis, FTIR	198
	Cure kinetics, DSC, HPLC	87
	Curing, FTIR, DC resistance	62
	Curing, TBA	171
	Curing, IR	78, 192
DGEBA + DICY etc.	Analysis, IR, DSC, LC, DDA	199
	Analysis, HPLC	84
	Analysis, LC, FTIR	75
	Aging, HPLC, TLC, IR	91
	Curing, DSC, TBA	194
	Curing, DMA	193
DGEBA resins	Analysis, various techniques	24
	Analysis, HPLC, GPC	30, 76, 79, 80, 200-203
	Analysis, TLC	94
	Hydroxyl analysis, IR	204
	Analysis & curing, near-IR	205, 206
	Analysis, C-13 NMR	51, 207
DGEBA + Versamid	Analysis, IR	99
	Curing, DSC, IR	176, 224
DGEBA + polyamide	Curing, morphology	212
DGEBA + amine	Cure kinetics, DSC	208
	Curing, IR	209
DGEBA + EDA, DETA, TETA	Environmental degradation	123, 210
DGEBA + DETA	DMA, morphology	211
DGEBA + TETA	Degradation, DMA	140
	Curing, DSC	230
DGEBA + Jeffamine T-403, DETA, DMHDA	Curing, morphology, IR, DMA	152, 156 216, 217
DGEBA + MDA (DDM)	Analysis, HPLC, GPC, TLC	222
	Cure kinetics, DSC	213
	Cure kinetics, DMA, IR, viscosity	214, 215
	Curing, IR	218-221
DGEBA + MPDA	Cure kinetics, DSC, IR	223
	Curing, DSC, IR	176
	Cure kinetics, DSC	175, 225
	Moisture, NMR	229
	Cure kinetics, HPLC, NMR	231
	Morphology, electron microscopy	306
DGEBA + ECN + DMHDA	Cure kinetics, TBA, TPA, FTIR	226, 227

DGEBA + MNDA	Curing, DSC, FTIR, TBA	228
DGEBA + DDS	Curing, DDA	232
	Cure kinetics, DSC	233
	Cure kinetics, DMA, IR, viscosity	214, 215
	Curing, DSC, DDA	184
DGEBA + piperidine	Cure kinetics, C-13 NMR	234
DGEBA + BDMA	Curing, C-13 magic angle NMR	53
DGEBA + anhydride	Analysis, IR	235
DGEBA + anhydride + catalyst	Curing, GPC	236
DGEBA + NMA	Moisture, NMR	229
DGEBA + NMA + BDMA	Analysis, FTIR	237
	Moisture effects, FTIR	238, 239
	Cure kinetics, FTIR, NMR	240, 241
	Silane coupling agents, FTIR	242
	Curing, IR	218-221
	Curing, IR	243
DGEBA + HHPA + BDMA	Curing, IR	243
DGEBA + HHPA + DMP-30	Cure kinetics, DSC	246
DGEBA + phthalic anhydride + imidazole	Curing, DSC, IR	245
Araldite F + MTHPA + BDMA	Curing, DSC, TMA, TGA	247
DGEBA + trimethoxyboroxine	Degradation, FTIR	244, 248
DGEBA + epoxy rubber + imidazole	QC adhesives, IR, GPC	249
DGEBA resin system + fibreglass	Moisture, NMR	54
DGEBA + PACM-20, TMAB	Cure kinetics, DMA, IR, viscosity	214, 215
American Cyanamid BP-927 (TGPAP + brominated DGEBA + DDS)	Composition, aging	250
TGPAP	Analysis, HPLC	30
	Aging, HPLC, TLC, IR	91
	Analysis, TLC	94
AVCO 5505-4	Analysis, LC, etc.	25
DGEBF (†), DGEPP (†) + trimethoxyboroxine	Degradation, FTIR	244, 248

Dow 7818 + Epon Z	Analysis, GPC, DTA	113
Celanese SU-8	Analysis, LC	251
Ciba-Geigy ERE 1359, Heloxy 69 (Resorcinol epoxies)	Analysis, HPLC	30, 201
Ciba-Geigy CY207-HT903 & CT200-HT901	Cure kinetics, IR	252
Ciba-Geigy ECN 1139	Analysis, TLC	94
Novolacs + DICY	Curing, DDA	183
CE339, X-30, Narmco 5209	Degradation, mechanical tests	253
Ciba-Geigy Reliabond RB398 & Narmco MB329-7 Adhesives	Analysis, HPLC, FTIR	254
Hysol Epoxy Adhesives	Analysis, HPLC Analysis, TLC	255, 256 94
American Cyanamid FM400 Adhesive	Analysis, IR, DSC, etc.	63
Narmco 5216 & other adhesives	Curing, DTA	257
Various adhesives	Curing, DDA	57
Epoxy-anhydride	Glass transition temp., IR	258
Epoxy-glass prepregs	Curing, DSC	259, 260
Epoxy powder coatings	Curing, DSC	261
Circuit board resins	Analysis, HPLC, GPC, DMA, DSC	307
Release agents on composite surfaces	Analysis, FTIR	262
Simple epoxy molecules	Analysis, near-IR	263
Epoxy model compounds	Cure mechanism, HPLC, IR	89, 90
Amine hardeners	Amine content, GPC	264

(†) DGEBF = Diglycidyl ether of 9,9-bis(4-hydroxyphenyl)fluorene

DGEPP = Diglycidyl ether of phenolphthalein

Other abbreviations: See Figures 4 to 7

Table 3. References concerning polyimide systems

System	Description	References
Polyimides	Curing, DDA, DSC	184
	Curing, diff. refl. FTIR	265
LARC-160 polyimide	Curing	185
	Aging, HPLC, MS, TMA	266
	Analysis & aging, IR, DSC, LC, DDA, viscosity	267
PMR polyimide resins	Analysis, aging, NMR	268
	Moisture absorption	120
Skybond 703 polyimide	Curing, IR	269
Skybond 710 polyimide	Degradation, diff. refl. FTIR	133
Kerimid 601 polyimide	Curing, DSC	260
Hexcel F-178 polyimide	Aging, NMR	270
NR-150 polyimide	QC analysis, HPLC	271
K-II polyimide	Curing, TGA-IR	272
Polyimide blends	Curing, DSC, DMA	273
XU 292 polyimide	Analysis, DSC, GPC	274
LARC-TPI	Curing, TGA, DSC	308

Table 4. References concerning thermoplastic matrix systems

System	Description	References
PEEK, PPS	Crystallinity, FTIR, DSC, X-ray	298
PEEK	Crystallinity, solvent resistance, DMA, DSC	299
PEEK	Crystallinity, DSC	300
PEEK	Crystallinity, DSC, DMA	301
PEEK	General	302
PEEK	Crystallinity, IR, X-ray, DSC	303-305

GLOSSARY

DDA	Dynamic dielectric analysis
DDS	Diaminodiphenylsulphone [Figure 5(a)]
DGEBA	Diglycidyl ether of bisphenol A [Figure 4(a)]
DGOP	Diglycidyl orthophthalate [Figure 4(c)]
DICY	Dicyandiamide [Figure 5(a)]
DMA	Dynamic mechanical analysis
DSA	Dynamic spring analysis
DSC	Differential scanning calorimetry
DTA	Differential thermal analysis
FTIR	Fourier transform infrared (spectroscopy)
GC	Gas chromatography
GPC	Gel permeation chromatography
HPLC	High performance liquid chromatography
IMRI	Industrial Materials Research Institute
IR	Infrared (spectroscopy)
LC	Liquid chromatography
NMR	Nuclear magnetic resonance
NPLC	Normal-phase liquid chromatography
NRCC	National Research Council Canada
PEEK	Polyetheretherketone
PGC	Pyrolysis gas chromatography
PPS	Polyphenylenesulphide
RPLC	Reverse-phase liquid chromatography
SEC	Size exclusion chromatography
TBA	Torsional braid analysis
TGA	Thermogravimetric analysis
TGDDM	Tetraglycidyldiaminodiphenylmethane [Figure 4(b)]
TLC	Thin layer chromatography
UV-VIS	Ultraviolet-visible (spectroscopy)

BIBLIOGRAPHY

1. J. Delmonte
Technology of Carbon and Graphite Fiber Composites
Van Nostrand Reinhold, 1981

2. J. Weiss, C. Bord
Les matériaux composites. I. Structure, constituants, fabrication. II. Calculs, essais et contrôles, conception.
Editions de l'Usine nouvelle, Paris, 1983

3. M. M. Schwartz
Composite Materials Handbook
McGraw-Hill, 1984

4. N. L. Hancox (Ed.)
Fibre Composite Hybrid Materials
Applied Science Publishers, 1981

5. M. R. Piggott
Load Bearing Fibre Composites
Pergamon Press, 1980

6. R. M. Christensen
Mechanics of Composite Materials
Wiley-Interscience, 1979

7. G. S. Springer (Ed.)
Environmental Effects on Composite Materials, Vols. 1 & 2
Technomic Publ. Co., 1981

8. SAMPE J., May/June 1985, p. 51

9. SAMPE J., July/August 1985, pp. 89-90

10. J. R. Soderquist (Federal Aviation Administration)
Society of Automotive Engineers Technical Paper Series No. 811061
Certification of civil composite aircraft structure.

11. D. K. Unsworth, J. G. Sutton (Sikorsky Aircraft)
Proc. 40th Annual Forum American Helicopter Society, Arlington, VA, May 1984, pp. 253-261
An assessment of the impact of technology on VTOL weight prediction.

12. D. T. Lovell (Boeing Co.)
The Role of the Polymeric Matrix in the Processing and Structural Properties of Composite Materials, J. C. Seferis & L. Nicolais (Eds.), Plenum Press, 1983, pp. 19-31
Composites in commercial aircraft.

13. R. L. Coggeshall (Boeing Co.)
Nat. SAMPE Tech. Conf. 15: 310-320 (1983)
Service experience with composites on Boeing commercial aircraft.

14. R. H. Stone (Lockheed Co.)
Nat. SAMPE Tech. Conf. 15: 277-287 (1983)
Composite flight service experience at Lockheed California Company.

15. H. Zinberg (Bell Helicopter Textron)
Nat. SAMPE Tech. Conf. 15: 263-276 (1983)
Flight service experience with composite helicopter components.

16. B. Rupe, B. J. Hunter (Bell Helicopter Textron)
Proc. 40th Annual Forum American Helicopter Society, Arlington, VA, May 1984, pp. 273-284
Advanced methodology for quality control of composite rotor blades at Bell Helicopter Textron.

17. M. J. Rich, D. W. Lowry (Sikorsky Aircraft)
Nat. SAMPE Tech. Conf. 15: 299-309 (1983)
Flight service evaluation of composite helicopter components.

18. C. Y. Kam, J. Gaidulis (McDonnell Douglas)
Nat. SAMPE Tech. Conf. 15: 251-262 (1983)
Flight service of composite structures on McDonnell Douglas commercial airplanes.

19. M. G. Hammond (Boeing Canada), K. Farrell (Spar Technology)
Proc. 2nd Intl. Conf. on Composite Materials, Metallurgical Society of AIME, Toronto, 1978, pp. 1392-1404
Graphite epoxy composite material components for communications satellites.

20. D. R. Dunbar, A. R. Robertson, R. Kerrison (General Dynamics and Spar)
Proc. 2nd Intl. Conf. on Composite Materials, Metallurgical Society of AIME, Toronto, 1978, pp. 1360-1376
Graphite/epoxy booms for the space shuttle remote manipulator.

21. R. J. Hébert (Canadair)
Canadian Aeronautics and Space Journal 28: 159-164 (1982)
The Canadair Challenger advanced composite material program.

22. Boeing Material Specification BMS 8-212

23. K. Schmidtke (MBB Central Laboratories)
Progress in Advanced Materials and Processes: Durability, Reliability, and Quality Control, G. Bartelds & R. J. Schliekelmann (Eds.), Elsevier, 1985, pp. 95-102
Experience with chemical control for quality assurance of epoxy matrix systems.

24. W. W. Wright
British Polymer J. 15: 224-242 (1983)
Characterisation of a bisphenol A epoxy resin. A collaborative study carried out by technical panel PTP3 of the technical cooperation programme.

25. H. Borstell
Nat. SAMPE Symp. Exhib. [Proc.] 24: 422-445 (1979)
The structural effects and detection of variations in Hercules 3501-5A and AVCO 5505 resin systems.

26. A. G. Miller, J. H. Barbee
Nat. SAMPE Symp. Exhib. [Proc.] 24: 1223-1235 (1979)
The correlation of chemical composition and mechanical properties of epoxy resins used in carbon/epoxy composites.

27. C. A. May, Y. Tanaka (Eds.)
Epoxy Resins, Chemistry and Technology
Marcel Dekker, 1973

28. U. S. Army Materials and Mechanics Research Center
Report AMMRC-MS-77-2, January 1977
Proceedings of the TTCP-3 Critical Review: Techniques for the Characterization of Polymeric Materials.

29. L. S. Penn
Composite Materials: Testing and Design (Fifth Conference), ASTM STP 674, S. W. Tsai (Ed.), American Society for Testing and Materials, 1979, pp. 519-532
Physicochemical characterization of composites and quality control of raw materials.

30. R. Hinrichs, J. Thuen (Narmco Materials Inc.)
Nat. SAMPE Symp. Exhib. [Proc.] 24: 404-421 (1979)
Advanced chemical characterization techniques applied to manufacturing process control.

31. P. J. Dynes, D. H. Kaelble
Composite Materials: Testing and Design (Fifth Conference), ASTM STP 674, S. W. Tsai (Ed.), American Society for Testing and Materials, 1979, pp. 566-577
Physicochemical analysis of graphite-epoxy composite systems.

32. A. B. Hunter
Nat. SAMPE Tech. Conf. 12: 394-400 (1980)
Chemical characterization of composites.

33. A. K. Rogers, Y. A. Tajima, R. C. Young
Nat. SAMPE Symp. Exhib. [Proc.] 27: 277-291 (1982)
and
Composite Materials: Quality Assurance and Processing, ASTM STP 797, C. E. Browning (Ed.), American Society for Testing and Materials, 1983, pp. 15-28
The development of a material specification for 177°C (350°F) curing graphite/epoxy composites.

34. J. C. Halpin, J. L. Kardos, M. P. Dudukovic
Pure & Appl. Chem. 55: 893-906 (1983)
Processing science: an approach for prepreg composite systems.

35. G. Bartelds, R. J. Schliekelmann (Eds.)
Progress in Advanced Materials and Processes: Durability, Reliability, and Quality Control; Materials Science Monographs, 29; Proc. 6th Intl. European Chapter Conf. of the Society for the Advancement of Material and Process Engineering, Scheveningen, The Netherlands, May 28-30, 1985
Elsevier, 1985

36. L. R. Snyder, J. J. Kirkland
Introduction to Modern Liquid Chromatography, 2nd Ed.
Wiley-Interscience, 1979

37. C. Horváth (Ed.)
High-Performance Liquid Chromatography. Advances and Perspectives, Vols. 1, 2, 3
Academic Press, 1980, 1983

38. S. A. Mestan, C. E. M. Morris
J. Macromol. Sci. Rev. Macromol. Chem. Phys. C24: 117-172 (1984)
Chromatography of epoxy resins.

39. A. L. Smith
Applied Infrared Spectroscopy: Fundamentals, Techniques, and Analytical Problem-Solving (Chemical Analysis, Vol. 54)
Wiley-Interscience, 1979

40. R. G. J. Miller & B. C. Stace (Eds.)
Laboratory Methods in Infrared Spectroscopy, 2nd Ed.
Heyden & Son, 1979

41. L. J. Bellamy
The Infra-red Spectra of Complex Molecules, 3rd Ed.
Chapman & Hall, 1975

42. P. R. Griffiths
Chemical Infrared Fourier Transform Spectroscopy (Chemical Analysis, Vol. 43)
Wiley-Interscience, 1975

43. Y. T. Liao, J. L. Koenig
Dev. Reinf. Plast. 4: 31-87 (1984)
Applications of Fourier transform infrared spectroscopy to the study of fiber-resin composites.

44. W. W. Wendlandt
Thermal Methods of Analysis, 2nd Ed. (Chemical Analysis, Vol. 19)
Wiley-Interscience, 1974

45. R. L. Hassel, R. L. Blaine
Nat. SAMPE Symp. Exhib. [Proc.] 24: 342-349 (1979)
Composite evaluation by thermal analysis.

46. J. Sickfeld, W. Mielke
Progr. Org. Coat. 12: 27-116 (1984)
Application of thermal analysis for the investigation of epoxy resins.

47. R. L. Grob (Ed.)
Modern Practice of Gas Chromatography
Wiley-Interscience, 1977

48. J. Tranchant et al.
Manuel pratique de chromatographie en phase gazeuse, 3^{e} édition
Masson, 1982

49. W. J. Irwin
Analytical Pyrolysis, A Comprehensive Guide
Marcel Dekker, 1982

50. E. D. Becker
High Resolution NMR: Theory and Chemical Applications, 2nd Ed.
Academic Press, 1980

51. C. F. Poranski, W. B. Moniz
J. Coatings Technol. 49 (632): 57-61 (1977)
Characterization of epoxy resin systems using carbon-13 Fourier transform NMR.

52. C. A. Fyfe
Solid State NMR for Chemists
C.F.C. Press, Guelph, Canada, 1983

53. A. Cholli, W. M. Ritchey, J. L. Koenig
ACS Symp. Ser. 243: 233-239 (1984)
Carbon-13 magic angle NMR spectroscopic studies of an epoxy resin network.

54. W. P. Rothwell, D. R. Holecek, J. A. Kershaw
J. Polym. Sci., Polym. Lett. Ed. 22: 241-247 (1984)
NMR imaging: study of fluid absorption by polymer composites.

55. T. Murayama
Dynamic Mechanical Analysis of Polymeric Material; Materials Science Monographs, 1
Elsevier, 1978

56. Tetrahedron Associates, Inc. (5060A Convoy Street, San Diego, CA 92111)
"The Audrey System" for dielectric analysis.

57. M. R. Mitchell
Nat. SAMPE Tech. Conf. 15: 465-477 (1983)
Cure monitoring of adhesives and prepregs.

58. Z. N. Sanjana, R. L. Selby
Nat. SAMPE Symp. Exhib. [Proc.] 29: 1233-1242 (1984)
Monitoring cure of epoxy resins using a microdielectrometer.

59. I. G. Scott, C. M. Scala
NDT International, April 1982, pp. 75-86
A review of non-destructive testing of composite materials.

60. R. Paulson, A. Aquino, H. Decker, T. Schapp
Proc. Soc. Photo-Opt. Instrum. Eng. 366: 88-95 (1983)
Infrared imaging techniques for flaw detection in composite materials.

61. C. W. Souder, G. E. Singleton
Proc. Soc. Photo-Opt. Instrum. Eng. 366: 80-87 (1983)
Thermographic technique for the nondestructive evaluation of graphite composite structures.

62. W. W. Houghton, R. J. Shuford, J. F. Sprouse
Nat. SAMPE Tech. Conf. 11: 131-150 (1979)
Acoustic emission as an aid for investigating composite manufacturing processes.

63. J. F. Carpenter (McDonnell Aircraft Co.)
Report prepared for Naval Air Systems Command, Contract No.
N00019-76-C-0138, July 1977; NTIS Document AD-A042853
Quality control of structural nonmetallics.

64. J. F. Carpenter
Nat. SAMPE Symp. Exhib. [Proc.} 24: 446-457 (1979)
Physicochemical testing of altered composition 3501-6 epoxy resin.

65. D. A. Scola
Nat. SAMPE Tech. Conf. 15: 9-20 (1983)
The effects of humidity exposure on AS/3501-6 prepreg material.

66. M. Cizmecioglu, S. D. Hong, J. Moacanin, A. Gupta
Polym. Preprints 22: 224-225 (1981)
Spectroscopic characterization of Narmco 5208 epoxy neat-resin formulations.

67. J. J. King, R. N. Castonguay, J. P. Zizzi
Nat. SAMPE Tech. Conf. 13: 53-63 (1981)
HPLC evaluation of MY 720.

68. J. J. King, R. N. Castonguay, J. P. Zizzi
Nat. SAMPE Symp. Exhib. [Proc.] 27: 163-177 (1982)
HPLC evaluation of MY 720. II.

69. C. A. Cobuzzi, J. J. King, R. N. Castonguay
Nat. SAMPE Symp. Exhib. [Proc.] 28: 877-892 (1983)
HPLC evaluation of MY 720. III.

70. M. Chaudhari, J. J. King
Nat. SAMPE Tech. Conf. 15: 676-687 (1983)
Characterization of MY 720. IV.

71. C. A. Cobuzzi, J. J. King, M. A. Chaudhari
Nat. SAMPE Symp. Exhib. [Proc.] 29: 1261-1276 (1984)
Characterization of MY 720. V.

72. M. A. Chaudhari, C. A. Cobuzzi, J. J. King
Nat. SAMPE Tech. Conf. 16: 565-576 (1984)
Characterization of MY 720. VI.

73. C. A. Cobuzzi, T. J. Galvin, M. A. Chaudhari
Nat. SAMPE Symp. Exhib. [Proc.] 30: 724-734 (1985)
Characterization of MY 720. VII.

74. G. L. Hagnauer, J. F. Sprouse, R. E. Sacher, I. Setton, M. Wood
U. S. Army Materials and Mechanics Research Center Report AMMRC TR 78-8
(1978), NTIS No. AD A054625
Evaluation of new techniques for the quality control of epoxy resin formulations.

75. G. L. Hagnauer, I. Setton
J. Liq. Chromatography 1: 55-73 (1978)
Compositional analysis of epoxy resin formulations.

76. G. L. Hagnauer, D. A. Dunn
Ind. Eng. Chem. Prod. Res. Dev. 21: 68-73 (1982)
High performance liquid chromatography. A reliable technique for epoxy resin prepreg analysis.

77. B. M. Halpin, J. F. Sprouse, G. L. Hagnauer
Proc. 33rd Ann. Tech. Conf. Reinforced Plastics/Composites Institute, Society of the Plastics Industry, 1978, Paper 15-G
Characterization of epoxy resins, prepregs, and composites using HPLC and FTS-IR.

78. G. R. Thomas, B. M. Halpin, J. F. Sprouse, G. L. Hagnauer, R. E. Sacher
Nat. SAMPE Symp. Exhib. [Proc.] 24: 458-505 (1979)
Characterization of epoxy resins, prepregs, and composites using HPLC, FTS-IR, and DSC.

79. G. L. Hagnauer
U. S. Army Materials and Mechanics Research Center Report AMMRC TR-79-59 (1979), NTIS No. AD A080221
HPLC and GPC analysis of Epon 828 epoxy resins.

80. G. L. Hagnauer
Ind. Res. Dev., April 1981, pp. 128-133
Analysis of commercial epoxies by HPLC and GPC.

81. G. L. Hagnauer, J. M. Murray, B. M. Bowse
U. S. Army Materials and Mechanics Research Center Report AMMRC TR-79-33 (1979), NTIS No. AD A072294
HPLC monitoring of graphite-epoxy prepreg aging.

82. G. L. Hagnauer
Polym. Compos. 1: 81-87 (1980)
Quality assurance of epoxy resin prepregs using liquid chromatography.

83. G. L. Hagnauer, D. A. Dunn
Nat. SAMPE Tech. Conf. 12: 648-655 (1980)
Quality assurance of an epoxy resin prepreg using HPLC.

84. G. L. Hagnauer, D. A. Dunn
J. Appl. Polym. Sci. 26: 1837-1846 (1981)
Dicyandiamide analysis and solubility in epoxy resins.

85. G. L. Hagnauer, P. J. Pearce
Org. Coat. Appl. Polym. Sci. Proc. 46: 580-584 (1982)
and
ACS Symp. Ser. 221: 193-209 (1983)
The effects of impurities on the hydrolytic stability and curing behaviour of an epoxy resin.

86. G. L. Hagnauer, P. J. Pearce, B. R. Laliberté, M. E. Roylance
Org. Coat. Appl. Polym. Sci. Proc. 47: 429 (1982)
and
ACS Symp. Ser. 227: 25-47 (1983)
Cure kinetics and mechanical properties of a resin matrix: effects of impurities and stoichiometry.

87. G. L. Hagnauer, B. R. Laliberté, D. A. Dunn
Org. Coat. Appl. Polym. Sci. Proc. 46: 646-650 (1982)
and
ACS Symp. Ser. 221: 229-244 (1983)
Isothermal cure kinetics of an epoxy resin prepreg.

88. G. L. Hagnauer, P. J. Pearce
ACS Symp. Ser. 245: 333-354 (1984)
Size exclusion chromatography analysis of epoxy resin cure kinetics.

89. C. A. Byrne, G. L. Hagnauer, N. S. Schneider, R. W. Lenz
Org. Coat. Plast. Chem. 41: 293-298 (1979)
and
Polym. Compos. 1: 71-76 (1980)
Model compound studies on the amine cure of epoxy resins.

90. C. A. Byrne, G. L. Hagnauer, N. S. Schneider
Polym. Compos. 4: 206-212 (1983)
Effects of variation in composition and temperature on the amine cure of an epoxy resin model system.

91. P. J. Pearce, R. G. Davidson, C. E. M. Morris
J. Appl. Polym. Sci. 26: 2363-2372 (1981)
Hydrolytic stability of some uncured epoxy resins.

92. R. B. Gosnell
Technical Report NASA-CR-145211 (1977), NTIS No. N78-13133
Technical assessment for quality control of resins.

93. D. Gulino, J. Galy, J. P. Pascault, Q. T. Pham
Makromol. Chem. 185: 297-316 (1984)
Etude du prépolymère époxyde par chromatographie et ^{1}H NMR à 350 MHz, 2.

94. G. A. Luoma
J. Chromatography 318: 75-84 (1985)
Fingerprinting epoxy resin systems using two-dimensional reversed-phase thin-layer chromatography.

95. C. A. May, T. E. Helminiak, H. A. Newey
Nat. SAMPE Tech. Conf. 8: 274-294 (1976)
Chemical characterization plan for advanced composite prepregs.

96. D. W. Hadad
Nat. SAMPE Symp. Exhib. [Proc.] 22: 301-311 (1977)
and
SAMPE J., July/August 1978, pp. 4-10
Chemical quality assurance of epoxy resin formulations by gel permeation, liquid, and thin layer chromatography.

97. C. A. May, D. K. Hadad, C. E. Browning
Proc. 33rd Ann. Tech. Conf. Reinforced Plastics/Composites Institute, Society of the Plastics Industry, 1978, Paper 15-D
and
Polymer Engineering and Science 19: 545-551 (1979)
Physicochemical quality assurance methods for composite matrix resins.

98. C. A. May
Nat. SAMPE Symp. Exhib. [Proc.] 24: 390-403 (1979)
Composite matrix quality assurance -- an art becomes a science.

99. C. A. May
Pure & Appl. Chem. 55: 811-818 (1983)
The chemical characterization and processing science of composites.

100. C. F. Poranski, W. B. Moniz
ASTM Special Technical Publication 674: 553-565 (1979)
Carbon-13 and proton nuclear magnetic resonance spectroscopy of thermosetting polymers; analysis of tetraglycidylmethylenedianiline/ diaminodiphenylsulfone formulations.

101. F. G. Herring, N. R. Jagannathan, G. Luoma
J. Polym. Sci. Polym. Chem. Ed. 23: 1649-1659 (1985)
The elucidation of the ^{1}H- and ^{13}C-NMR spectra of bis[N,N-di(2,3-epoxypropyl)-4-aminophenyl]methane (TGMDA) and composite with bis(4-aminophenyl)-sulfone (DDS) using two-dimensional Fourier transform techniques.

102. D. Crozier, G. Morse, Y. Tajima
SAMPE J., Sept./Oct. 1982, pp. 17-22
The development of improved chemical analysis methods for epoxy resins.

103. J. S. Chen, A. B. Hunter
Technical Report NASA-CR-3531 (1982), NTIS No. N82-22318
Development of quality assurance methods for epoxy graphite prepreg.

104. G. W. Lawless
Nat. SAMPE Symp. Exhib. [Proc.] 24: 979-989 (1979)
Room temperature moisture effects on uncured composite resins and prepregs.

105. A. A. Wickham, D. D. Rice, R. J. DuBois
Nat. SAMPE Symp. Exhib. [Proc.] 24: 506-521 (1979)
Chemical analysis of advanced composite prepregs and resins.

106. T. A. Sewell
ASTM Special Technical Publication 797: 3-14 (1983)
Quality assurance of graphite/epoxy by high-performance liquid chromatography.

107. M. Kowalska, A. Wirsén
Nat. SAMPE Symp. Exhib. [Proc.] 25: 389-402 (1980)
Chemical analysis of epoxy prepregs - market survey and batch control.

108. I. F. Lindgren
Nat. SAMPE Symp. Exhib. [Proc.] 29: 1395-1404 (1984)
Quantitative analysis of some cured epoxy composites.

109. I. Plavin, H. Rosenthal, U. Arnon
Nat. SAMPE Tech. Conf. 16: 696-704 (1984)
Chemical characterisation of graphite/epoxy matrix resins.

110. G. A. Morse
Nat. SAMPE Tech. Conf. 16: 721-732 (1984)
Derivative spectroscopy in polymer analysis: the chemical characterization of an epoxy resin.

111. M. E. Roylance, W. W. Houghton, S. R. Ghiorse
Nat. SAMPE Symp. Exhib. [Proc.] 28: 309-317 (1983)
The effect of epoxide purity and thermal history on the properties of a tetrafunctional epoxy resin.

112. M. von Kuzenko, C. E. Browning, C. F. Fowler
ACS Symp. Ser. 132: 275-292 (1980)
Dynamic mechanical characterization of advanced composite epoxy matrix resins of altered composition.

113. D. J. Crabtree, D. B. Hewitt
Chromatographic Science 8: 63-77 (1977)
Chromatographic analysis of epoxy resins.

114. D. J. Crabtree
ACS Symp. Ser. 132: 459-468 (1980)
Quantitative analysis of resin matrix aging by gel permeation chromatography and differential scanning calorimetry.

115. R. Hinrichs, J. Thuen
Nat. SAMPE Symp. Exhib. [Proc.] 24: 557-574 (1979)
Environmental effects on the control of advanced composite materials processing.

116. Z. N. Sanjana
Nat. SAMPE Symp. Exhib. [Proc.] 24: 330-341 (1979)
Overage indicators for prepreg products.

117. P. E. Sandorff, Y. A. Tajima
SAMPE Quarterly, January 1979, pp. 21-28
A practical method for determining moisture distribution, solubility, and diffusivity in composite laminates.

118. Y. A. Tajima
SAMPE Quarterly, July 1980, pp. 1-9
The diffusion of moisture in graphite fiber reinforced epoxy laminates.

119. A. C. Loos, G. S. Springer
J. Compos. Mater. 13: 131-147 (1979)
Moisture absorption of graphite-epoxy composites immersed in liquids and in humid air.

120. L. E. Ryan, M. P. Gardner, R. W. Vaughan
Proc. 33rd Ann. Tech. Conf., Reinforced Plastics/Composites Institute of The Society of the Plastics Industry, 1978, Paper 15-A
Determination of moisture in polymers and composites.

121. T. Ho
U. S. Army Materials and Mechanics Research Center Report AMMRC TR-82-11 (1982), NTIS No. AD A115292
The effect of environment on the mechanical behaviour of Kevlar/epoxy materials.

122. A. Apicella, L. Nicolais, C. Carfagna, C. de Notaristefani, C. Voto
Nat. SAMPE Symp. Exhib. [Proc.] 27: 753-762 (1982)
The effect of the prepolymer composition on the environmental aging of epoxy based resins.

123. A. Apicella, L. Nicolais
Ind. Eng. Chem. Prod. Res. Dev. 23: 288-297 (1984)
Role of processing on the durability of epoxy composites in humid environments.

124. A. Apicella, L. Nicolais, C. de Cataldis
Adv. Polym. Sci. 66: 189-207 (1985)
Characterization of the morphological fine structure of commercial thermosetting resins through hygrothermal experiments.

125. R. L. Levy, D. L. Fanter, C. J. Summers
J. Appl. Polym. Sci. 24: 1643-1664 (1979)
Spectroscopic evidence for mechanochemical effects of moisture in epoxy resins.

126. R. L. Levy, D. P. Ames
ACS Polym. Mater. Sci. Eng. 53: 176-179 (1985)
Effect of sorbed water on epoxy fluorescence.

127. A. N. Netravali, R. E. Fornes, R. D. Gilbert, J. D. Memory
J. Appl. Polym. Sci. 29: 311-318 (1984)
Investigations of water and high energy radiation interactions in an epoxy.

128. C. Giori, T. Yamauchi
J. Appl. Polym. Sci. 29: 237-249 (1984)
Effects of ultraviolet and electron radiations on graphite-reinforced polysulfone and epoxy resins.

129. C. J. Wolf, D. L. Fanter, M. A. Grayson
Report Number MDC Q0743, U. S. Naval Air Systems Command Contract N00019-80-C-0102 (1981)
Aging of polymers and composites.

130. C. J. Wolf, D. L. Fanter, M. A. Grayson
ACS Symp. Ser. 227: 121-139 (1983)
Chemiluminescence of thermosetting resins.

131. M. A. Grayson, C. J. Wolf
Polym. Preprints 25(1): 95-96 (1984)
Mechanochemistry of an epoxy resin system.

132. C. J. Wolf, D. L. Fanter, M. A. Grayson
Polym. Mater. Sci. Eng. 52: 509-514 (1985)
Simulated environmental aging of epoxy resins.

133. P. R. Young, B. A. Stein, A. C. Chang
Nat. SAMPE Symp. Exhib. [Proc.] 28: 824-837 (1983)
Resin characterization in cured graphite fiber reinforced composites using diffuse reflectance FTIR.

134. E. S. W. Kong
Composites Technol. Rev. 4: 97-100 (1982)
The effect of physical aging on the time-dependent properties of carbon-fiber-reinforced epoxy composites.

135. E. S. W. Kong
Org. Coat. Appl. Polym. Sci. Proc. 46: 568-573 (1982)
Physical aging and its effect on the mechanical and physical properties of graphite/epoxy composites.

136. E. S. W. Kong, S. M. Lee, H. G. Nelson
Polym. Compos. 3: 29-33 (1982)
Physical aging in graphite/epoxy composites.

137. E. S. W. Kong
Nat. SAMPE Symp. Exhib. [Proc.] 28: 838-850 (1983)
Physical aging in graphite/epoxy composites.

138. E. S. W. Kong
ACS Symp. Ser. 221: 171-191 (1983)
Influence of physical aging on the time-dependent properties of network epoxies and epoxy-matrix composites.

139. K. Heinemann, E. S. W. Kong
Technical Report NASA-CR-173870, NTIS No. N84-31289
Physical aging and its influence on the reliability of network epoxies and epoxy-matrix composites.

140. W. J. Mikols, J. C. Seferis
ACS Symp. Ser. 227: 95-112 (1983)
Moisture-temperature effects on the dynamic mechanical properties of epoxy polymers.

141. E. B. Stark, A. M. Ibrahim, J. C. Seferis
Nat. SAMPE Symp. Exhib. [Proc.] 28: 581-589 (1983)
Experimental analysis of the network structure for the high-performance TGDDM-Novolac-DDS epoxy matrix system.

142. M. R. Dusi, C. A. May, J. C. Seferis
ACS Symp. Ser. 227: 301-318 (1983)
Predictive models as aids to thermoset resin processing.

143. H. S. Chu, J. C. Seferis
Pp. 53-125 in "The Role of the Polymeric Matrix in the Processing and Structural Properties of Composite Materials", J. C. Seferis & L. Nicolais (Eds.), Plenum Press, 1983
Network structure description and analysis of amine-cured epoxy matrices.

144. H. S. Chu, J. C. Seferis
Polym. Compos. 5: 124-140 (1984)
Dynamic mechanical experiments for probing process-structure-property relations in amine-cured epoxies.

145. E. B. Stark, A. M. Ibrahim, J. C. Seferis
Pp. 23-41 in "Interrelations between Processing, Structure, and Properties of Polymeric Materials", J. C. Seferis & P. S. Theocaris (Eds.), Elsevier, 1984
The effect of bisphenol-A Novolac resin on high-performance epoxy formulations.

146. E. B. Stark, J. C. Seferis, A. Apicella, L. Nicolais
Thermochim. Acta 77: 19-33 (1984)
Stoichiometric and heating-rate effects on DSC-evaluated kinetics for a high-performance epoxy system.

147. E. B. Stark, J. C. Seferis
Polym. Preprints 26: 23-25 (1985)
Kinetic information from multiple thermal analysis techniques.

148. A. M. Ibrahim, J. C. Seferis
Pp. 325-341 in "Interrelations between Processing, Structure, and Properties of Polymeric Materials", J. C. Seferis & P. S. Theocaris (Eds.), Elsevier, 1984
Solution processing of epoxy resins.

149. A. Apicella, L. Nicolais, J. C. Halpin
Nat. SAMPE Symp. Exhib. [Proc.] 28: 518-527 (1983)
The role of the processing chemo-rheology on the ageing behaviour of high-performance epoxy matrices.

150. A. Apicella, L. Nicolais, M. Iannone, P. Passerini
J. Appl. Polym. Sci. 29: 2083-2096 (1984)
Thermokinetics and chemorheology of the cure reactions of the tetraglycidyldiaminodiphenylmethane-diaminodiphenylsulfone epoxy systems.

151. A. Apicella, P. Masi, L. Nicolais
Rheologica Acta 23: 291-296 (1984)
Rheological behaviour of a commercial TGDDM-DDS based epoxy matrix during the isothermal cure.

152. R. J. Morgan, J. E. O'Neal
Polym.-Plast. Technol. Eng. 10(1): 49-116 (1978)
The durability of epoxies.

153. R. J. Morgan, E. T. Mones
Compos. Technol. Rev. 1(4): 17-19 (1979)
Tetraglycidyl-4,4'-diaminodiphenylmethane (TGDDM) epoxies cured with diaminodiphenylsulfone (DDS).

154. R. J. Morgan, J. E. O'Neal, D. B. Miller
J. Mater. Sci. 14: 109-124 (1979)
The structure, modes of deformation and failure, and mechanical properties of diaminodiphenylsulphone-cured tetraglycidyl-4,4'-diamino-diphenylmethane epoxy.

155. R. J. Morgan, E. T. Mones
ACS Symp. Ser. 132: 233-245 (1980)
Structure-property relations of composite matrices.

156. R. J. Morgan
Chapter 7 (pp. 211-229) in "Developments in Reinforced Plastics. I. Resin Matrix Aspects", G. Pritchard (Ed.), Applied Science Publishers, 1980
Structure-property relationships and the environmental sensitivity of epoxies.

157. E. T. Mones, R. J. Morgan
Polym. Preprints 22: 249-250 (1981)
FTIR studies of the chemical structure of high-performance composite matrices.

158. E. T. Mones, C. M. Walkup, J. A. Happe, R. J. Morgan
Nat. SAMPE Tech. Conf. 14: 89-100 (1982)
The characterization of diaminodiphenylsulfone (DDS) cured tetraglycidyl-4,4'-diaminodiphenylmethane (TGDDM) epoxies.

159. R. J. Morgan, J. A. Happe, E. T. Mones
Nat. SAMPE Symp. Exhib. [Proc.] 28: 596-607 (1983)
The processing, cure reactions, network structure, and mechanical properties of TGDDM/DDS epoxies.

160. C. M. Walkup, R. J. Morgan, T. H. Hoheisel
Polym. Preprints 25: 187-188 (1984)
Systematic differential scanning calorimetry studies of the cure of carbon fiber epoxy composite prepregs.

161. R. J. Morgan, C. M. Walkup, T. H. Hoheisel
J. Appl. Polym. Sci. 30: 289-296 (1985)
Differential scanning calorimetry studies of the cure of carbon fiber epoxy composite prepregs.

162. E. T. Mones, R. J. Morgan
Proc. ACS Meeting, Div. Polymeric Materials 51: 430-434 (1984)
The cure reactions, network structure, and mechanical response of diaminodiphenylsulfone cured tetraglycidyl-4,4'-diaminodiphenylmethane epoxies.

163. R. J. Morgan
Adv. Polym. Sci. 72: 1-43 (1985)
Structure-property relations of epoxies used as composite matrices.

164. R. J. Morgan et al.
Polym. Preprints 26: 286-287 (1985)
Composite matrices -- their role in composite performance and durability.

165. M. Cizmecioglu, A. Gupta
Proc. 37th Ann. Conf., Reinforced Plastics/Composites Institute, Society of the Plastics Industry, January 11-15, 1982, Paper 20-E
and
SAMPE Quarterly, April 1982, pp. 16-20
Cure kinetics of epoxy matrix resin by differential scanning calorimetry.

166. J. Moacanin, M. Cizmecioglu, F. Tsay, A. Gupta
Org. Coat. Appl. Polym. Sci. Proc. 47: 587-591 (1982)
and
ACS Symp. Ser. 227: 83-94 (1983)
Mechanism and kinetics of the curing process in a resin system.

167. A. Gupta, M. Cizmecioglu, D. Coulter, R. H. Liang, A. Yavrouian, F. D. Tsay, J. Moacanin
J. Appl. Polym. Sci. 28: 1011-1024 (1983)
The mechanism of cure of tetraglycidyldiaminodiphenylmethane with diaminodiphenylsulfone.

168. J. J. King, J. P. Bell
ACS Symp. Ser. 114: 225-257 (1979)
Reactions in a typical epoxy-aliphatic diamine system.

169. J. A. Happe, R. J. Morgan, C. M. Walkup
Nat. SAMPE Symp. Exhib. [Proc.] 29: 921-933 (1984)
and
Preprint UCRL-89627, submitted for publication in "Polymer"
^{1}H, ^{19}F, and ^{11}B Nuclear magnetic resonance characterization of BF_3:amine catalysts used in the cure of C fiber-epoxy prepregs.

170. A. M. Ibrahim, J. C. Seferis
Nat. SAMPE Symp. Exhib. [Proc.] 29: 1405-1410 (1984)
and
Polym. Compos. 6: 47-53 (1985)
Salicylic acid modified high performance amine cured epoxy matrices.

171. N. S. Schneider, J. K. Gillham
Polym. Compos. 1(2): 97-102 (1980)
TBA studies of prepreg curing behaviour.

172. W. X. Zukas, W. J. MacKnight, N. S. Schneider
Org. Coat. Appl. Polym. Sci. Proc. 47: 425-428 (1982)
and
ACS Symp. Ser. 227: 223-250 (1983)
Dynamic mechanical and dielectric properties of an epoxy resin during cure.

173. Y. A. Tajima
Polym. Compos. 3(3): 162-169 (1982)
Monitoring cure viscosity of epoxy composite.

174. W. I. Lee, A. C. Loos, G. S. Springer
J. Compos. Mater. 16: 510-520 (1982)
Heat of reaction, degree of cure, and viscosity of Hercules 3501-6 resin.

175. S. Sourour, M. R. Kamal
Thermochim. Acta 14: 41-59 (1976)
Differential scanning calorimetry of epoxy cure: isothermal cure kinetics.

176. R. B. Prime
Polym. Eng. & Sci. 13: 365-371 (1973)
Differential scanning calorimetry of the epoxy cure reaction.

177. J. K. Gillham
Polym. Eng. & Sci. 19: 676-682 (1979)
Formation and properties of network polymeric materials.

178. R. J. Hinrichs
ACS Symp. Ser. 227: 187-199 (1983)
Rheological cure transformation diagrams for evaluating polymer cure dynamics.

179. G. S. Springer
J. Compos. Mater. 16: 400-410 (1982)
Resin flow during the cure of fiber reinforced composites.

180. D. Argyropoylos, K. A. Hodd, W. W. Wright
Proc. 7th Int. Conf. Thermal Analysis 2: 1099-1105 (1982)
The influence of crosslink density on thermal properties of some epoxy resins based on 4,4'-diaminophenylmethane.

181. P. R. Young, A. C. Chang
Nat. SAMPE Tech. Conf. 16: 136-147 (1984)
Prepreg cure monitoring using diffuse reflectance FTIR.

182. R. J. Milligan, C. L. Carpenter
Nat. SAMPE Symp. Exhib. [Proc.] 28: 318-333 (1983)
Properties of TGDDM/DDS resin systems cured at temperatures below 177°C (350°F).

183. C. A. May
Nat. SAMPE Symp. Exhib. [Proc.] 20: 108-116 (1975)
Dielectric measurements for composite cure control - two case studies.

184. C. A. May, D. K. Whearty, J. S. Fritzen
Nat. SAMPE Symp. Exhib. [Proc.] 21: 803-818 (1976)
Composite cure studies by dielectric and calorimetric analyses.

185. C. A. May, M. R. Dusi, J. S. Fritzen, D. K. Hadad, M. G. Maximovich, K. S. Thrasher
Org. Coat. Appl. Polym. Sci. Proc. 47: 419-423 (1982)
and
ACS Symp. Ser. 227: 1-24 (1983)
Process automation: a rheological and chemical overview of thermoset curing.

186. D. Kranbuehl, S. Delos, E. Yi, M. Hoff, M. Whitham, T. Hou
ACS Polym. Mater. Sci. Eng. 53: 191-195 (1985)
Analysis of the polymerization of amine-based epoxy resins by dynamic dielectric analysis.

187. J. D. Keenan, J. C. Seferis, J. T. Quinlivan
J. Appl. Polym. Sci. 24: 2375-2387 (1979)
Effects of moisture and stoichiometry on the dynamic mechanical properties of a high-performance structural epoxy.

188. D. H. Kaelble
ACS Symp. Ser. 132: 395-417 (1980)
Experimental analysis of hydrothermal aging in fiber-reinforced composites.

189. R. J. Morgan, J. E. O'Neal, D. L. Fanter
J. Mater. Sci. 15: 751-764 (1980)
The effect of moisture on the physical and mechanical integrity of epoxies.

190. P. Moy, F. E. Karasz
Polym. Eng. & Sci. 20(4): 315-319 (1980)
Epoxy-water interactions.

191. R. M. Lamothe, B. M. Halpin, D. Neal
U. S. Army Materials and Mechanics Research Center Report 81-0542
Design allowable determination on a fully characterized composite material.

192. J. F. Sprouse, B. M. Halpin, R. E. Sacher
U. S. Army Materials and Mechanics Research Center Report AMMRC TR-78-45 (1978), NTIS No. AD A067197
Cure analysis of epoxy composites using Fourier transform infrared spectroscopy.

193. G. A. Senich, W. J. MacKnight, N. S. Schneider
Polym. Eng. & Sci. 19(4): 313-318 (1979)
A dynamic mechanical study of the curing reaction of two epoxy resins.

194. N. S. Schneider, J. F. Sprouse, G. L. Hagnauer, J. K. Gillham
Polym. Eng. & Sci. 19(4): 304-312 (1979)
DSC and TBA studies of the curing behaviour of two DICY-containing epoxy resins.

195. D. A. Scola
Nat. SAMPE Tech. Conf. 16: 328-339 (1984)
Effects of humidity exposure on FM 300 K adhesive material and bond strength.

196. G. A. George, R. E. Sacher, J. F. Sprouse
J. Appl. Polym. Sci. 21: 2241-2251 (1977)
Photo-oxidation and photoprotection of the surface resin of a glass fiber epoxy composite.

197. J. F. Sprouse
U. S. Army Materials and Mechanics Research Center Report AMMRC MS-77-2 (1977), NTIS No. AD A036082, pp. 43-54
Fourier transform infrared spectroscopy as a method for studying weathering of glass fiber epoxy composites.

198. T. F. Saunders, M. Ciulla, S. Wehner, J. Brown
Proc. SPIE 289: 292-294 (1981)
Application of Fourier transform infrared spectroscopy for quality control analysis of epoxy resin prepregs used in helicopter rotor blades.

199. D. K. Hadad, A. Wereta, C. A. May
Nat. SAMPE Tech. Conf. 12: 585-601 (1980)
Chemical characterization of highly staged circuit board material.

200. E. Dan, M. B. Roller
J. Polym. Sci. Polym. Lett. Ed. 21: 875-879 (1983)
GPC calibration for epoxy resins.

201. D. W. Eggimann, J. C. Brand, C. K. Elliott
Nat. SAMPE Symp. Exhib. [Proc.] 26: 304-312 (1981)
The application of a reversed phase liquid chromatography separation method to selected epoxies, plasticizers, and halocarbon flotation fluids.

202. I. G. Hinton
British Polymer J. 15(1): 47-49 (1983)
Chromatographic studies of epoxy resins.

203. S. Shiono, I. Karino, A. Ishimura, J. Enomoto
J. Chromatography 193: 243-253 (1980)
Separation and characterization of by-product oligomers in epoxy resins by reversed-phase high-performance liquid chromatography.

204. M. R. Adams
Anal. Chem. 36: 1688-1689 (1964)
Infrared determination of hydroxyl content of epoxy resins.

205. H. Dannenberg
SPE Transactions, January 1963, pp. 78-88
Determination of functional groups in epoxy resins by near-infrared spectroscopy.

206. H. Dannenberg, W. R. Harp
Anal. Chem. 28: 86-90 (1956)
Determination of cure and analysis of cured epoxy resins.

207. W. W. Fleming
J. Appl. Polym. Sci. 30: 2853-2862 (1985)
Carbon-13 NMR characterization of DGEBPA epoxy resins.

208. H. E. Bair
Polym. Preprints 26(1): 10-11 (1985)
Curing behaviour of an epoxy resin above and below T_g.

209. C. E. Feazel, E. A. Verchot
J. Polym. Sci. 25: 351-353 (1957)
A simple technique for use with infrared spectroscopy to study the curing of epoxy resins.

210. A. Apicella, L. Nicolais
Ind. Eng. Chem. Prod. Res. Dev. 20: 138-144 (1981)
Environmental aging of epoxy resins: synergistic effect of sorbed moisture, temperature, and applied stress.

211. J. Mijovic, L. Tsay
Polymer 22: 902-906 (1981)
Correlations between dynamic mechanical properties and nodular morphology of cured epoxy resins.

212. R. J. Morgan, J. E. O'Neal
J. Macromol. Sci. - Phys. B15(1): 139-169 (1978)
Effect of epoxy monomer crystallization and cure conditions on physical structure, fracture topography, and mechanical response of polyamide-cured bisphenol-A diglycidyl ether epoxies.

213. J. M. Barton
Die Makromolekulare Chemie 171: 247-251 (1973)
Monitoring the curing reaction of an aromatic amine/epoxide resin system by differential scanning calorimetry (DSC): determination and significance of the activation energy.

214. J. B. Enns, J. K. Gillham
Org. Coat. Appl. Polym. Sci. Proc. 46: 592-598 (1982)
Molecular structure/macroscopic property relationships of epoxy/amine systems using time-temperature-transformation (TTT) cure diagrams.

215. J. B. Enns
Ph. D. Thesis, Princeton Univ., 1982; Univ. Microfilms 82-21568
The cure of thermosetting epoxy/amine systems.

216. F. M. Kong, C. M. Walkup, R. J. Morgan
ACS Symp. Ser. 221: 211-227 (1983)
and
Polymer 25: 375-386 (1984)
Structure-property relations of polyethertriamine-cured bisphenol-A diglycidyl ether epoxies.

217. R. J. Morgan, J. E. O'Neal
J. Mater. Sci. 12: 1966-1980 (1977)
The microscopic failure processes and their relation to the structure of amine-cured bisphenol-A diglycidyl ether epoxies.

218. A. Garton
J. Polym. Sci. Polym. Chem. Ed. 22: 1495-1506 (1984)
The crosslinking of epoxy resins at interfaces. I. Germanium, germanium dioxide, and silane-treated germanium.

219. A. Garton, J. H. Daly
National Research Council Canada Publication 23756 (1984)
Characterization of the aramid/epoxy and carbon/epoxy interphases.

220. A. Garton, J. H. Daly
J. Polym. Sci. Polym. Chem. Ed. 23: 1031-1041 (1985)
The crosslinking of epoxy resins at interfaces. II. At an aromatic polyamide surface.

221. A. Garton
Polym. Compos. 5(4): 258-263 (1984)
A novel technique for the study of coupling agent phenomena.

222. H. Tighzert, J. M. Lucas, B. Chabert, M. Marichy, G. Nemoz
Bull. Scient. Inst. Text. Fr. 11(42): 17-23 (1982)
Etude par des techniques chromatographiques (CCM; GPC; HPLC) de la polycondensation d'un système résine diépoxyde - diamine aromatique destiné à la préimpregnation de tissus de verre. A. Identification et caractérisation des produits de départ.

223. M. A. Acitelli, R. B. Prime, E. Sacher
Polymer 12: 335-343 (1971)
Kinetics of epoxy cure: (1) The system bisphenol-A diglycidyl ether / m-phenylenediamine.

224. R. B. Prime, E. Sacher
Polymer 13: 455-458 (1972)
Kinetics of epoxy cure: (2) The system bisphenol-A diglycidyl ether / polyamide.

225. M. E. Ryan, A. Dutta
Polymer 20: 203-206 (1979)
Kinetics of epoxy cure: a rapid technique for kinetic parameter estimation.

226. L. J. Buckley, D. K. Roylance
Proc. 37th Ann. Conf. Reinforced Plastics/Composites Institute of the Society of the Plastics Industry, January, 1982, Paper 8-B
Kinetics of a sterically hindered amine-cured resin system.

227. L. Buckley, D. Roylance
Polym. Eng. & Sci. 22(3): 166-171 (1982)
Kinetics of a sterically hindered amine-cured epoxy resin system.

228. T. Donnellan, D. Roylance
Polym. Eng. & Sci. 22(13): 821-825 (1982)
The curing of a bisphenol-A type epoxy resin with 1,8-diamino-p-menthane.

229. L. W. Jelinski, J. J. Dumais, A. L. Cholli, T. S. Ellis, F. E. Karasz
Macromolecules 18: 1091-1095 (1985)
Nature of the water-epoxy reaction.

230. N. Levy
ACS Symp. Ser. 197: 313-327 (1982)
Analysis of an epoxy curing reaction by differential scanning calorimetry.

231. M.-F. Grenier-Loustalot, P. Grenier
J. Polym. Sci. Polym. Chem. Ed. 22: 4011-4033 (1984)
Réaction époxy-amine: suivi du mecanisme réactionnel et de la cinétique par RMN ^{13}C, ^{15}N et HPLC.

232. N. F. Sheppard, M. C. W. Coln, S. D. Senturia
Nat. SAMPE Symp. Exhib. [Proc.] 29: 1243-1250 (1984)
A dielectric study of the time-temperature-transformation (TTT) diagram of DGEBA epoxy resins cured with DDS.

233. J. M. Barton
Polymer 21: 603-606 (1980)
Kinetics of cure of epoxy resin system bisphenol-A diglycidyl ether - di(4-aminophenyl)sulphone.

234. S. A. Sojka, W. B. Moniz
J. Appl. Polym. Sci. 20: 1977-1982 (1976)
The curing of an epoxy resin as followed by carbon-13 NMR spectroscopy.

235. T. Sugita, M. Iko
Bull. Chem. Soc. Japan 38(10): 1620-1627 (1965)
Studies of thermosetting resin. I. The infrared analysis of cured epoxy resins.

236. R. D. Nuss
Chromatographic Science 8: 79-91 (1977)
Effect of different catalysts on an identical thermosetting epoxy-anhydride resin system evaluated through the B-staged curing conditions by gel permeation chromatography.

237. M. K. Antoon, K. M. Starkey, J. L. Koenig
Proc. 33rd Ann. Tech. Conf. Reinforced Plastics/Composites Institute of the Society of the Plastics Industry, 1978, Paper 15-B
and
ASTM Special Technical Publication 674: 541-552 (1979)
Applications of Fourier transform infrared spectroscopy to quality control of the epoxy matrix.

238. M. K. Antoon, J. L. Koenig, T. Serafini
J. Polym. Sci. Polym. Phys. Ed. 19: 1567-1575 (1981)
Fourier transform infrared study of the reversible interaction of water and a crosslinked epoxy matrix.

239. M. K. Antoon, J. L. Koenig
J. Polym. Sci. Polym. Phys. Ed. 19: 197-212 (1981)
Irreversible effects of moisture on the epoxy matrix in glass-reinforced composites.

240. M. K. Antoon, J. L. Koenig
J. Polym. Sci. Polym. Chem. Ed. 19: 549-570 (1981)
Crosslinking mechanism of an anhydride-cured epoxy resin as studied by Fourier transform infrared spectroscopy.

241. M. K. Antoon, B. E. Zehner, J. L. Koenig
Polym. Compos. 2(2): 81-88 (1981)
Spectroscopic determination of the in-situ composition of epoxy matrices in glass fiber reinforced composites.

242. C. Chiang, J. L. Koenig
Proc. 36th Ann. Tech. Conf. Reinforced Plastics/Composites Institute of the Society of the Plastics Industry, February 1981, Paper 2-D
Comparison of primary and secondary aminosilane coupling agents in anhydride-cured epoxy fiberglass composites.

243. S. M. Lee, S. Brelant
Modern Plastics 44: 150-151 (1963)
Determination of cure of epoxy resins by infrared analysis.

244. C. S. Chen, B. J. Bulkin, E. M. Pearce
J. Appl. Polym. Sci. 28: 1077-1091 (1983)
New epoxy resins. III. Application of Fourier transform IR to degradation and interaction studies of epoxy resins and their copolymers.

245. E. W. Crandall, W. C. Mih
Org. Coat. Appl. Polym. Sci. Proc. 47: 592-594 (1982)
and
ACS Symp. Ser. 227: 113-119 (1983)
Crosslinking reaction of an epoxy resin with phthalic anhydride.

246. R. A. Fava
Polymer 9: 137-151 (1968)
Differential scanning calorimetry of epoxy resins.

247. R. Riesen, H. Sommerauer
American Laboratory 15(1): 30-37 (January 1983)
Curing of reaction molding resins studied by thermoanalytical methods.

248. S. C. Lin, B. J. Bulkin, E. M. Pearce
J. Polym. Sci. Polym. Chem. Ed. 17: 3121-3148 (1979)
Epoxy resins. III. Application of Fourier transform IR to degradation studies of epoxy systems.

249. T. E. Baker, G. L. Fix, J. S. Judge
Nat. SAMPE Symp. Exhib. [Proc.] 24: 1211-1222 (1979)
Control of adhesives through analytical characterization.

250. F. Larsson, A. Wirsén
Nat. SAMPE Tech. Conf. 10: 622-635 (1978)
Effect of long time freezer storage on an epoxy prepreg and its composites.

251. T. D. Zucconi
ASTM Special Technical Publication 674: 533-540 (1979)
Control and testing of epoxy resins used for printed circuit boards.

252. G. C. Stevens
J. Appl. Polym. Sci. 26: 4279-4297 (1981)
Cure kinetics of a high epoxide/hydroxyl group ratio bisphenol-A epoxy resin anhydride system by infrared absorption spectroscopy.

253. V. F. Mazzio, G. Huber
Nat. SAMPE Tech. Conf. 15: 234-250 (1983)
Effect of temperature, moisture, and radiation exposures on composite mechanical properties.

254. K. G. Kibler
SAMPE Quarterly, April 1982, pp. 39-45
Characterization of composition variations in a structural adhesive.

255. J. R. Woodlee, F. D. Medina, D. E. Jackson
Nat. SAMPE Symp. Exhib. [Proc.] 28: 862-876 (1983)
Chromatographic characterization of a toughened epoxy adhesive system.

256. J. R. Woodlee
Nat. SAMPE Symp. Exhib. [Proc.] 30: 471-478 (1985)
Optimization in reverse phase liquid chromatography as applied to an epoxy adhesive.

257. A. Schiraldi, P. Rossi
Proc. 7th Int. Conf. Thermal Analysis 2: 1151-1154 (1982)
Quantitative DTA of epoxy adhesives and prepregs.

258. P. Roush
Proc. SPIE 289: 124-126 (1981)
Use of heated attenuated total reflectance (ATR) to monitor polymer transitions.

259. L. T. Pappalardo
SPE Tech. Papers 20: 13-16 (1974)
DSC evaluation of B-stage epoxy-glass prepregs for multilayer boards.

260. L. T. Pappalardo
J. Appl. Polym. Sci. 21: 809-820 (1977)
DSC evaluation of epoxy and polyimide-impregnated laminates (prepregs).

261. T. R. Manley, G. Scurr
Proc. 7th Int. Conf. Thermal Analysis 2: 1380-1385 (1982)
Use of thermal analysis to study the degree of cure of epoxy resins.

262. R. H. Pater, D. A. Scola
Nat. SAMPE Tech. Conf. 11: 13-15 (1979)
Non-destructive analysis of composite surface contamination by Fourier transform infrared spectroscopy.

263. R. F. Goddu, D. A. Delker
Anal. Chem. 30: 2013-2016 (1958)
Determination of terminal epoxides by near-infrared spectrophotometry.

264. P. Bauer, M. Richter
Informations Chimie (242): 153-156 (1983)
Dosage de l'amine résiduelle dans les durcisseurs pour époxydes par chromatographie sur gel.

265. P. R. Young, A. C. Chang
Nat. SAMPE Symp. Exhib. [Proc.] 30: 889-902 (1985)
Polyimide analysis using diffuse reflectance FTIR.

266. P. R. Young, G. F. Sykes
ACS Symp. Ser. 132: 479-490 (1980)
Characterization of aging effects of LARC-160.

267. A. Wereta, D. K. Hadad
ACS Symp. Ser. 132: 215-232 (1980)
Analytical techniques applied to the optimization of LARC-160 composite lamination.

268. R. W. Lauver, R. D. Vanucci
Nat. SAMPE Symp. Exhib. [Proc.] 24: 522-532 (1979)
Characterization of PMR polyimides - correlation of ester impurities with composite properties.

269. R. Fountain, T. W. Hass
J. Appl. Polym. Sci. 19: 1767-1770 (1975)
Application of infrared spectroscopy to the cure of polyimide laminates.

270. H. C. Nash, C. F. Poranski, R. Y. Ting
ACS Symp. Ser. 132: 469-478 (1980)
Effect of room-temperature aging on graphite/polyimide prepreg materials.

271. E. F. Hoegger
Nat. SAMPE Symp. Exhib. [Proc.] 24: 533-552 (1979)
Chemical quality control of NR-150 polyimide precursor solutions.

272. H. H. Gibbs
SAMPE J., July/August 1985, pp. 22-27
Processing studies on K-polymer composite materials. Part I. Prepregs based on K-II polyimide.

273. Y. Yamamoto, S. Satoh, S. Etoh
SAMPE J., July/August 1985, pp. 6-10
Preparation and characterization of thermoplastic/thermosetting polyimide blends.

274. M. Chaudhari, T. Galvin, J. King
SAMPE J., July/August 1985, pp. 17-21
Characterization of bismaleimide system, XU 292.

275. A. Apicella, L. Nicolais, M. R. Nobile, M. A. Castiglione-Morelli
Composites Science and Technology 24: 101-121 (1985)
Effect of processing variables on the durability of epoxy resins for composite systems.

276. A. Apicella, L. Nicolais
Adv. Polym. Sci. 72: 69-77 (1985)
Effect of water on the properties of epoxy matrix and composite.

277. E. S.-W. Kong, M. Adamson, L. Meuller
Composites Technology Review 6(4): 170-173 (1984)
Moisture diffusion and solid-state NMR investigations on the physical aging processes in network epoxy glasses.

278. T. E. Munns, J. C. Seferis
J. Appl. Polym. Sci. 28: 2227-2233 (1983)
High performance epoxy resins cured in the presence of BF_3 catalyst.

279. W. J. Lee, J. C. Seferis, D. C. Bonner
SAMPE Quarterly 17(2): 58-68 (January 1986)
Prepreg processing science.

280. R. B. Prime
Chapter 5 (pp. 435-569) in Thermal Characterization of Polymeric Materials, E. Turi (Ed.), Academic Press, 1981
Thermosets.

281. J. M. Barton
Adv. Polym. Sci. 72: 111-154 (1985)
The application of differential scanning calorimetry (DSC) to the study of epoxy resin curing reactions.

282. J. Mijovic, J. Kim, J. Slaby
J. Appl. Polym. Sci. 29: 1449-1462 (1984)
Cure kinetics of epoxy formulations of the type used in advanced composites.

283. W. I. Lee, G. S. Springer
J. Compos. Mater. 18: 387-409 (1984)
Microwave curing of composites.

284. G. S. Springer
Proc. Int. Conf. Comp. Mater. (ICCM-IV), "Progress in Science and Engineering of Composites", T. Hayashi et al. (Eds.), Japan Soc. for Composite Materials, 1982, pp. 23-35
A model of the curing process of epoxy matrix composites.

285. A. C. Loos, G. S. Springer
ASTM Special Technical Publication No. 797, "Composite Materials: Quality Assurance and Processing", C. E. Browning (Ed.), 1983, pp. 110-118
Calculation of cure process variables during cure of graphite/epoxy composites.

286. R. Hinrichs, J. Thuen
SAMPE Journal 15(6): 12-21 (Nov./Dec. 1979)
Environmental effects on the control of advanced composite materials processing.

287. R. J. Hinrichs, J. M. Thuen
Composites Technology Review 2(3): 11-14 (1980)
Characterizing rheological cure behaviour of epoxy composite materials.

288. Y. A. Tajima, D. Crozier
Polym. Eng. & Sci. 23(4): 186-190 (1983)
Thermokinetic modeling of an epoxy resin. I. Chemoviscosity.

289. T. H. Hou
SPE Ann. Tech. Conf. 31: 1253-1255 (1985)
On the applications of WLF theory to thermosetting resins.

290. J. Mijovic
Polymer Communications 25: 271-273 (1984)
On processing-property relationships in graphite/epoxy composites.

291. J. Mijovic, H. T. Wang
Proc. 40th Ann. Conf., Reinforced Plastics/Composites Institute of the Society of the Plastics Industry, Jan. 28 - Feb. 1, 1985, Paper 20-D.
Processing-property relationships in autoclave-cured graphite/epoxy composites.

292. J. Mijovic, H. T. Wang
SPE Ann. Tech. Conf. 31: 1266-1268 (1985)
Processing-property relationships in autoclave-cured graphite/epoxy composites. Part I.

293. D. Crozier, F. Tervet
SAMPE Journal 18(6): 12-16 (Nov./Dec. 1982)
Rheological characterization of epoxy prepreg resins.

294. S. R. Farber
Nat. SAMPE Tech. Conf. 17: 512-523 (1985)
Resin extraction of epoxy composites.

295. M. G. Maximovich, R. M. Galeos
Nat. SAMPE Symp. Exhib. [Proc.] 28: 568-580 (1983)
Rheological characterization of advanced composite prepreg materials.

296. L. D. Lauer
SAMPE Quarterly 14(1): 31-35 (Oct. 1983)
Dynamic mechanical analysis of epoxy composite prepregs.

297. D. S. Lee, C. D. Han
SPE Ann. Tech. Conf. 31: 1212-1215 (1985)
Effects of particulate and fiber reinforcement on the curing behaviour of unsaturated polyester resin and epoxy resin.

298. A. O. Kays, J. D. Hunter
ASTM Special Technical Publication No. 797, "Composite Materials: Quality Assurance and Processing", C. E. Browning (Ed.), 1983, pp. 119-132
Characterization of some solvent-resistant thermoplastic matrix composites.

299. E. J. Stober, J. C. Seferis, J. D. Keenan
Polymer 25: 1845-1852 (1984)
Characterization and exposure of polyetheretherketone (PEEK) to fluid environments.

300. C. N. Velisaris, J. C. Seferis
SPE Ann. Tech. Conf. 31: 401-403 (1985)
Thermal processing and characterization of polyetheretherketone (PPEK) matrices.

301. W. J. Sichina, P. S. Gill
SPE Ann. Tech. Conf. 31: 293-295 (1985)
Characterization of PEEK/carbon fiber composites by thermal analysis.

302. G. R. Belbin
Proc. Instn. Mech. Engrs. 198B(6): 71-81 (1984)
Thermoplastic structural composites - a challenging opportunity.

303. J. M. Chalmers, W. F. Gaskin, M. W. Mackenzie
Polymer Bulletin 11: 433-435 (1984)
Crystallinity in poly(aryl-ether-ketone) plaques studied by multiple internal reflection spectroscopy.

304. D. J. Blundell, J. M. Chalmers, M. W. Mackenzie, W. F. Gaskin
SAMPE Quarterly 16(4): 22-30 (July 1985)
Crystalline morphology of the matrix of PEEK-carbon fiber aromatic polymer composites. I. Assessment of crystallinity.

305. D. J. Blundell, B. N. Osborn
SAMPE Quarterly 17(1): 1-6 (Oct. 1985)
Crystalline morphology of the matrix of PEEK-carbon fiber aromatic polymer composites. II. Crystallization behaviour.

306. V. B. Gupta, L. T. Drzal, W. W. Adams, R. Omlor
J. Mater. Sci. 20: 3439-3452 (1985)
An electron microscopic study of the morphology of cured epoxy resin.

307. C. M. Tung, P. J. Dynes
ASTM Special Technical Publication No. 797, "Composite Materials: Quality Assurance and Processing", C. E. Browning (Ed.), 1983, pp. 38-53
Chemorheological characterization of B-stage printed wiring board resins.

308. S.-Y. Chang, S. J. Huang, J. F. Johnson
SPE Ann. Tech. Conf. 31: 267-268 (1985)
Analytical instrumentation to study the curing mechanism of LARC-TPI high temperature adhesive.

IGM 86-101- 321
Etude n° 321
Dossier 8355-101

PHYSICOCHEMICAL CHARACTERIZATION OF HIGH-PERFORMANCE FIBRE-REINFORCED ORGANIC-MATRIX COMPOSITES

PART 2. APPLICATIONS OF INFRARED SPECTROSCOPY

by

K. C. Cole and D. Noël

Industrial Materials Research Institute
National Research Council Canada
75, boul. de Mortagne
Boucherville, Québec, Canada
J4B 6Y4

June 1986

CNRC 26034

TABLE OF CONTENTS

List of figures....iii
List of tables....v
Preface....vi
Acknowledgement....vii
Summary....viii
Résumé....ix

1. INTRODUCTION....1

2. EXPERIMENTAL....3

2.1 Materials....3
2.2 Instrumentation....5
2.3 Heatable IR Cell Procedure....5

3. THE TRANSMISSION METHOD....8

3.1 Description of the Method....8
3.2 Choice of a Solvent....9
3.3 The Infrared Spectrum of Narmco 5208 Resin....10
3.4 Quantitative Analysis....20
3.5 Comparison of Different Batches....29
3.6 Resin Cure....30
3.7 Near-Infrared Spectroscopy....39
3.8 Recommended Procedure for Quantitative Analysis of Narmco 5208 Prepreg by IR Transmission....42

4. THE INTERNAL REFLECTION METHOD....44

4.1 Description of the Method....44
4.2 The ATR Spectrum of Narmco 5208 Prepreg....46
4.3 Quantitative Analysis by ATR....49
4.4 Comparison of Different Batches....55
4.5 Recommended Procedure for Quantitative Analysis of Narmco 5208 Prepreg by IR Spectroscopy Using ATR....56

5. THE DIFFUSE REFLECTION METHOD....58

5.1 Description of the Method....58
5.2 The Diffuse Reflectance Spectrum of Narmco 5208 Prepreg....61
5.3 Importance of Fibre Orientation....64
5.4 Quantitative Analysis by Diffuse Reflection....69
5.5 Prepreg Cure....75
5.6 Microanalysis by Diffuse Reflection....76
5.7 Recommended Procedure for Measuring IR Spectra of Composites by Diffuse Reflection....84

6. CONCLUSIONS....86

BIBLIOGRAPHY....88

LIST OF FIGURES

Figure	Description	Page
1	Chemical structures of principal components of Narmco 5208 resin	4
2	Diagram of heatable IR transmission cell used to study epoxy cure	6
3	Transmission IR spectrum of Narmco 5208 resin Batch 1010 (uncured) in transmittance units	12
4	Transmission IR spectrum of Narmco 5208 resin Batch 1010 (uncured) in absorbance units	13
5	Transmission IR spectrum of Ciba-Geigy Araldite MY 720	14
6	Transmission IR spectrum of Ciba-Geigy Hardener HT 976	15
7	Transmission IR spectrum of Celanese Epi-Rez SU-8	16
8	Absorption bands used for quantitative analysis of Narmco 5208 resin	17
9	Transmission IR spectrum of Narmco 5208 resin Batch 1010 (cured)	19
10	Effect of sample thickness variation on measured absorbance	24
11	Transmission IR spectra of Narmco 5208 resin: Specimen #1 - film of uniform thickness; Specimen #4 - film of varying thickness	25
12	Relationship between peak absorbance values for spectra of Figure 11	26
13	Temperature program used for IR study of Narmco 5208 cure	31
14	Evolution of IR transmission spectrum during cure of Narmco 5208	33
15	Variation of "single sulphone" index as measured by IR transmission during cure of Narmco 5208 resin	34
16	Variation of "multiple sulphone" index as measured by IR transmission during cure of Narmco 5208 resin	35
17	Variation of "single epoxy" index as measured by IR transmission during cure of Narmco 5208 resin	36
18	Variation of "multiple epoxy" index as measured by IR transmission during cure of Narmco 5208 resin	37
19	Variation of "epoxy + aromatic" index as measured by IR transmission during cure of Narmco 5208 resin	38
20	Near-infrared transmission spectra of Narmco 5208 resin	41
21	Attenuated total reflectance IR spectrum of Narmco 5208/WC3000 prepreg Batch 1010 recorded using 45° KRS-5 prism	47

22 Attenuated total reflectance IR spectrum of woven graphite cloth recorded using 45° KRS-5 prism 48

23 ATR spectrum of Narmco 5208/WC3000 prepreg after baseline correction and normalization 50

24 Comparison of transmission and normalized ATR spectra of Narmco 5208 51

25 Diffuse reflectance IR spectrum of Narmco 5208/WC3000 prepreg Batch 1010, as recorded 62

26 Diffuse reflectance IR spectrum of woven graphite cloth 63

27 Diffuse reflectance IR spectrum of Narmco 5208/WC3000 prepreg after conversion to Kubelka-Munk units and baseline correction 65

28 Diffuse reflectance IR spectrum of Narmco 5208/WC3000 cured laminate, as recorded 66

29 Diffuse reflectance IR spectrum of Narmco 5208/WC3000 cured laminate, after conversion to Kubelka-Munk units and baseline correction 67

30 Effect of fibre orientation on diffuse reflectance IR spectrum of Narmco 5208/WC3000 prepreg and cured laminate 68

31 Comparison of transmission, specular reflectance, and diffuse reflectance spectra of Narmco 5208 resin and prepreg 71

32 Effect of covering with KBr on the diffuse reflectance IR spectrum of Narmco 5208/WC3000 prepreg 73

33 Effect of embedded KBr on the diffuse reflectance IR spectrum of Narmco 5208/WC3000 prepreg 74

34 Evolution of diffuse reflectance IR spectrum during cure of Narmco 5208/WC3000 prepreg 77

35 Variation of "single sulphone" index as measured by diffuse reflectance IR during cure of Narmco 5208/WC3000 prepreg 78

36 Variation of "multiple sulphone" index as measured by diffuse reflectance IR during cure of Narmco 5208/WC3000 prepreg 79

37 Variation of "single epoxy" index as measured by diffuse reflectance IR during cure of Narmco 5208/WC3000 prepreg 80

38 Variation of "multiple epoxy" index as measured by diffuse reflectance IR during cure of Narmco 5208/WC3000 prepreg 81

39 Diffuse reflectance IR spectrum of pure TGDDM monomer obtained by liquid chromatographic separation of MY 720 82

40 Diffuse reflectance IR spectrum of 1 μg of Narmco 5208 resin 83

LIST OF TABLES

Table	Description	Page
1	Narmco 5208 IR spectrum band assignments	11
2	Quantitative analysis of Narmco 5208/WC3000 prepreg Batch 1010 by IR transmission (first experiment)	21
3	Quantitative analysis of Narmco 5208/WC3000 prepreg Batch 1010 by IR transmission (second experiment)	27
4	Quantitative analysis of Narmco 5208/WC3000 prepreg Batch 1014 by IR transmission	28
5	Quantitative analysis of different batches of Narmco 5208 by IR transmission	29
6	Quantitative analysis of Narmco 5208/WC3000 prepreg Batch 1010 by attenuated total reflection IR	53
7	Comparison of IR transmission and ATR results for Narmco 5208/WC3000 prepreg Batch 1010	54
8	Quantitative analysis of different batches of Narmco 5208/WC3000 prepreg by attenuated total reflection IR	55
9	Quantitative analysis of Narmco 5208/WC3000 prepreg Batch 1010 by diffuse reflection IR	70
10	Quantitative analysis of Narmco 5208/WC3000 prepreg Batch 1014 by diffuse reflection IR	75

PREFACE

This report is the second of a series resulting from a cooperative effort involving the Industrial Materials Research Institute (IMRI) of the National Research Council Canada (NRCC) (Boucherville, Québec) and Canadair Limited (Montréal, Québec). The subject is one of growing importance in high-technology manufacturing, namely the physicochemical characterization of high-performance fibre-reinforced organic-matrix composites. The first report in the series contains a general discussion of the subject followed by a review of the recent literature. Subsequent reports describe the results of original research involving the application of various chromatographic and spectroscopic techniques to typical commercial composite systems, with particular attention given to the graphite-epoxy system Narmco Rigidite 5208/WC3000. This particular report deals with infrared spectroscopy. The titles of the complete series are as follows:

Part 1. General Discussion and Literature Review
Part 2. Applications of Infrared Spectroscopy
Part 3. Applications of Liquid Chromatography
Part 4. Applications of Pyrolysis Gas Chromatography and Thermal Analysis
Part 5. A Study of the Room-Temperature Aging of Narmco 5208/WC3000 Prepreg
Part 6. Methods for Quality Control of Matrix Chemistry

ACKNOWLEDGEMENT

Apart from the authors, the following people directly contributed to the research described in this series of reports:

H. Roberge	NRCC-IMRI
A. Pilon	NRCC-IMRI
J.-J. Hechler	NRCC-IMRI
J. Boulanger	NRCC-IMRI
K. C. Overbury	Canadair Ltd.
A. Chouliotis	Canadair Ltd.
S. Toy	Canadair Ltd.

SUMMARY

The report describes a systematic investigation of the application of infrared spectroscopy to the analysis of fibre-reinforced organic-matrix composites, using as a test case the graphite-epoxy system Rigidite 5208/WC3000 manufactured by Narmco Materials, Inc. Three methods of obtaining the IR spectrum (transmission, internal reflection, and diffuse reflection) have been studied and compared, and the advantages and disadvantages of each are discussed. Although it appears to be a widely accepted method for quantitative analysis of uncured resin, the transmission method is shown to be subject to considerable error due to nonuniform thickness of cast films. Very careful sample preparation is needed to give acceptable results. The internal reflection method is better for quantitative analysis because it gives more reproducible results and can be applied directly to prepreg. This avoids the problem of nonuniform thickness and also results in considerable time savings in sample preparation. The diffuse reflection method is not recommended for quantitative work with composites because it is subject to variations due to front-surface (Fresnel) reflection and scattering effects. However, it is an excellent method for qualitative work because it allows measurement of both uncured and cured samples with practically no sample preparation. It could be used as a nondestructive method for confirming completion of cure in finished parts. It is also a quite sensitive method for analysing small quantities of material such as fractions of samples separated by liquid chromatography. Although most IR work is done in the mid-infrared region (4000 - 400 cm^{-1}), the near-infrared region is also interesting for the study of Narmco 5208 since it provides information on the degree of cure and the moisture content.

RÉSUMÉ

Le rapport a pour sujet l'application de la spectroscopie infrarouge à l'analyse des composites à base de renforts fibreux et matrices organiques. Les différentes méthodes d'analyse ont été développées en utilisant le système graphite-époxyde Rigidite 5208/WC3000 fabriqué par Narmco Materials Inc. Trois méthodes pour obtenir le spectre infrarouge (transmission, réflexion interne, réflexion diffuse) ont été étudiées et comparées pour souligner leurs avantages et leurs inconvénients respectifs. Bien qu'elle soit couramment utilisée pour l'analyse de la résine non-durcie, la méthode de transmission est sujette à des erreurs importantes résultant de la non-uniformité de l'épaisseur du film déposé sur la fenêtre. Pour obtenir des résultats fiables, une préparation très soignée de l'échantillon est nécessaire. La méthode de réflexion interne est meilleure pour l'analyse quantitative parce qu'elle fournit des résultats plus reproductibles. De plus, le préimprégné peut être analysé sans extraction de la résine avec un solvant. Ainsi, cette méthode évite le problème d'épaisseur non-uniforme et permet des économies importantes en temps de préparation. La méthode de réflexion diffuse n'est pas recommandée pour l'analyse quantitative des composites parce que les spectres sont influencés par la réflexion Fresnel et par la diffusion du rayonnement infrarouge. Néanmoins, il s'agit d'une excellente méthode pour les mesures qualitatives puisqu'elle permet de mesurer les échantillons durcis et non-durcis avec très peu de préparation. Elle pourrait être utile comme méthode non-destructive pour confirmer l'achèvement du durcissement dans les pièces finies. C'est aussi une méthode très sensible pour l'analyse de petites quantités de produit telles les fractions séparées par la chromatographie liquide. Bien que la plupart des mesures dans l'infrarouge soient effectuées dans l'infrarouge moyen (4000 - 400 cm^{-1}), le proche infrarouge s'avère également intéressant pour l'étude du Narmco 5208, puisqu'il fournit des informations concernant le degré de durcissement et le taux d'humidité.

1. INTRODUCTION

This report is part of a series concerned with the application of physicochemical testing methods to high-performance composite materials consisting of high-strength reinforcing fibres (glass, carbon, graphite, Kevlar®) embedded in an organic polymer matrix (epoxy, polyimide, or polyester). As outlined in the first report [1], the objective of the research project was to develop improved methods for the rapid and accurate characterization of the chemical composition of the organic matrix materials. Such methods are being used more and more for quality control as composite materials are increasingly used in ever more critical applications, particularly in the aerospace industry. The first report also gives a general discussion of the subject and a comprehensive review of the recent literature including some 300 references.

This particular report is concerned with one particular technique, namely infrared spectroscopy. This technique [2-6] has a long tradition as one of the most extensively used for characterizing a wide range of materials, including composites [7-9]. When matter is exposed to infrared radiation it usually absorbs energy at specific frequencies which correspond to the characteristic frequencies of vibration of the atomic groups making up the material. A graph of the degree of absorption versus frequency is known as the infrared spectrum. Often it is quite detailed and serves as a unique "fingerprint" of the material, so IR spectroscopy is widely used for identifying unknown samples. In addition, since the absorption is directly related to the amount of material, it can be used as a quantitative analysis method. It is also used to study changes in molecular structure which occur as a result of chemical reaction. It can be applied to solids, liquids, and gases. In the case of composite matrices, it is used in a number of ways, for example: qualitative and quantitative analysis of the resin, study of the curing reaction, and study of environmental degradation. Several examples are cited in the literature review previously mentioned [1].

The last ten years have seen a tremendous growth in the use of Fourier transform infrared (FTIR) spectrometers [5,6]. These instruments, which make use of interferometers rather than monochromators to analyse the frequency distribution of the radiation, are extremely powerful. Compared to conventional instruments they are much more sensitive, rapid, and precise, and their use of computers makes it possible to extract much more information from the spectrum. The high sensitivity makes it possible to successfully use a number of reflectance methods, thereby extending the range of applications to a greater number of materials. The possibilities of this technique have only just begun to be exploited.

This report describes the results of research performed with the aim of better understanding the factors which influence the infrared spectra of composite materials, in order to develop more fully its potential. Three different methods of obtaining the spectrum were investigated: transmission, attenuated total reflection, and diffuse reflection. The advantages and disadvantages of all three are compared for both qualitative and quantitative analysis. Most of the results described herein were obtained for one particular composite system, Rigidite 5208/WC3000 from Narmco Materials, Inc. Applications of the method to other systems will be described in a subsequent report (Part 6 of this series).

2. EXPERIMENTAL

2.1 Materials

The composite system chosen for intensive study was the Rigidite 5208/WC3000 system sold by Narmco Materials, Inc. The reinforcement consists of Celion graphite fibres, 3000 fibres per yarn, woven in an 8-harness satin pattern (each warp yarn passing alternately over seven fill yarns and under one fill yarn). The woven fabric is impregnated with Narmco 5208 resin to a nominal resin content of 42% by weight and the prepreg is supplied on a plastic backing sheet in rolls. The recommended cure schedule consists of a one-hour dwell at 135°C (275°F) followed by a two-hour cure at 177°C (350°F).

It has been reported [10-14] that Narmco 5208 consists primarily of three components. The major epoxy, which accounts for about 70% by weight, is based on TGDDM (tetraglycidyldiaminodiphenylmethane). A common commercial product of this type is Ciba-Geigy Araldite MY 720. The second most important component (about 22% by weight) is the curing agent DDS (diaminodiphenylsulphone); an example of a commercial grade of this material is Ciba-Geigy Hardener HT 976. There is also a minor epoxy (about 8% by weight) which is of the bisphenol A Novolac type (for example, Celanese Epi-Rez SU-8). The chemical structures of these are given in Figure 1. The DDS is a relatively pure material, but the epoxy resins consist of a mixture of monomer, oligomers, and other products (starting materials and by-products). A more detailed discussion of the Narmco 5208 system, including composition, analysis, and the nature of the curing reaction, is given in an earlier report [1].

The following samples of the Narmco 5208 system were supplied by Canadair Ltd.:

Prepreg, Batch Number 1010
Prepreg, Batch Number 1014
Prepreg, Batch Number 1101
Prepreg, Batch Number 1103
Prepreg, Batch Number 1104
Neat resin on plastic backing sheet, Batch Number 1047
Neat resin in bulk form, Batch Number 1023.

Prepreg and reactive resin samples were stored in a freezer at all times except for sampling and performance of experiments. Samples of the following components were obtained from the respective companies:

Ciba-Geigy Araldite MY 720 epoxy resin (TGDDM), Lot Y5085
Ciba-Geigy Hardener HT 976 (DDS), Lot IL 2096
Celanese Epi-Rez SU-8 (bisphenol A Novolac epoxy), Lot L11-82182.

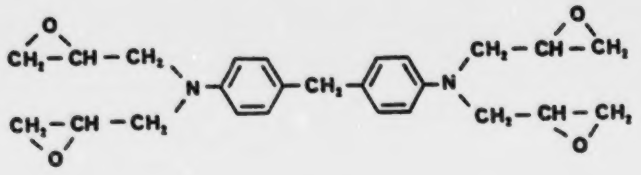

TGDDM

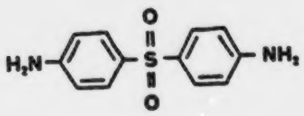

DDS

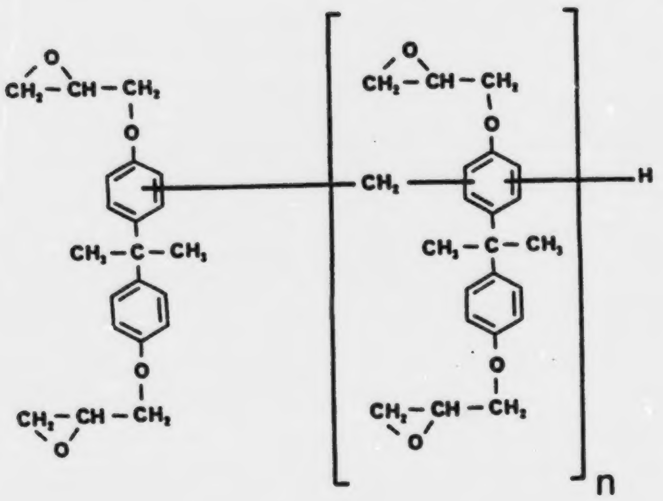

Bisphenol A Novolac Epoxy

Figure 1 - Chemical structures of principal components of Narmco 5208 resin.

These were stored in a refrigerator.

2.2 Instrumentation

Infrared spectra were recorded using a Nicolet Instruments Model 170SX Fourier transform infrared spectrometer equipped with a wide-range liquid-nitrogen-cooled mercury cadmium telluride detector. The following accessories from Harrick Scientific Corporation were also used:

(1) Twin Parallel Mirror Reflection Attachment (Variable Angle Manual) with Internal Reflection Accessory using single-pass parallelogram prisms (50 x 10 x 3 mm); for attenuated total reflectance measurements.

(2) Diffuse Reflection Attachment (Praying Mantis Model); for diffuse reflectance measurements.

(3) External Specular Reflection Attachment with angle of incidence 30°; for specular reflectance measurements.

(4) Temperature-Controlled Cell TFC-M25 with Automatic Temperature Controller ATC-10G.

Most infrared spectra were recorded using an accumulation of 128 scans with a resolution of 4 cm^{-1} and Happ-Genzel apodization. Further details are given in subsequent sections in the discussion of results.

2.3 Heatable IR Cell Procedure

The experimental setup used to study resin cure by IR transmission is shown in Figure 2. It includes a Model TFC-M25 heatable cell with two heating elements, manufactured by Harrick Scientific Corporation. Two potassium bromide disks of diameter 13 mm and thickness about 0.8 mm are made by pressing KBr powder in a typical KBr pellet die. Their spectra are recorded and epoxy resin is deposited from acetone solution on one of the disks to give a film of suitable thickness. A "sandwich" is then formed using the other disk and placed between two specially-made aluminium

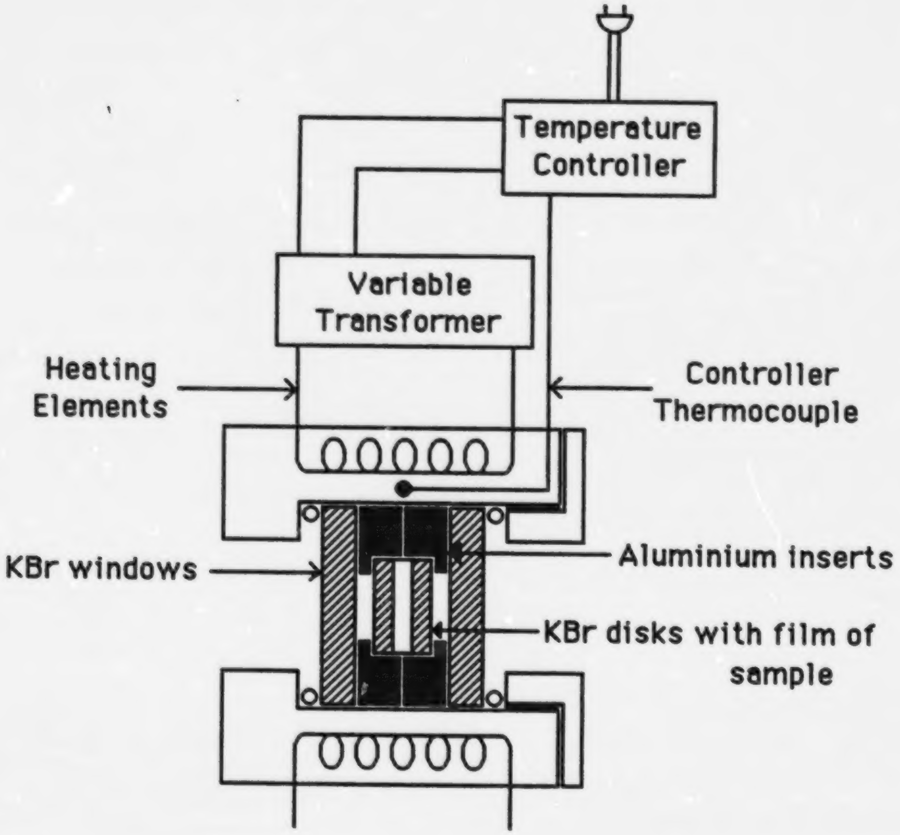
Temperature Controller
Variable Transformer
Heating Elements
Controller Thermocouple
KBr windows
Aluminium inserts
KBr disks with film of sample

Figure 2. Diagram of heatable IR transmission cell used to study epoxy cure.

inserts. These in turn are placed between two outer KBr windows (25 x 2 mm) to reduce heat losses. The desired sample temperature is determined by a proportional controller (Harrick Model ATC-10G) connected to an iron-constantan thermocouple embedded in the body of the cell. The time taken to achieve this temperature can be controlled to some extent by a variable transformer connected between the controller and the heating elements. Because of heat losses there is a temperature differential between the controller thermocouple and the centre of the sample. It is difficult to monitor the true sample temperature during spectral measurement because a thermocouple placed at the centre of the sample would interfere with the IR beam. Hence a "calibration" was performed without recording spectra by passing a second thermocouple through a small hole drilled in one of the outer windows and placing it in contact with the centre of the sample. Using the calibration curves, the controller and transformer settings can be chosen to give the desired sample temperature profile.

3. THE TRANSMISSION METHOD

3.1 Description of the Method

This is the traditional, most widely used method of measuring infrared spectra, particularly for quantitative analysis. An IR beam is allowed to pass through the sample and the intensity I of the transmitted radiation is divided by that of the incident radiation I_0 to obtain the transmittance T, which is a function of the frequency. The graph of T versus frequency is the IR spectrum. Frequency is usually expressed in terms of the wavenumber, or the reciprocal of the wavelength, with units of cm^{-1}.

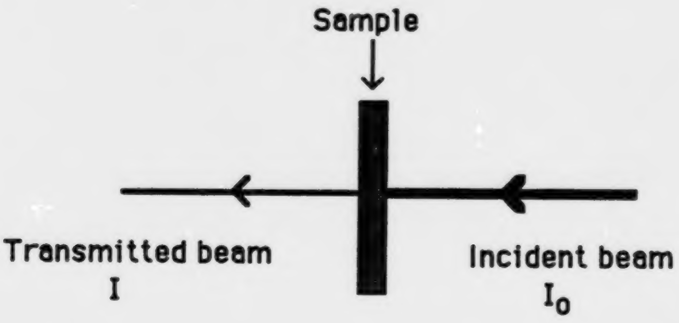

Often the sample consists of a solution contained between two transmitting windows. The Beer-Lambert law states that:

$$A = -\log_{10}T = abc$$

where A is known as the absorbance, a is the absorptivity (an intrinsic property of the absorbing species), b is the sample path length, and c is the concentration of the absorbing species. This equation makes it possible to perform quantitative analysis by using a cell of known path length and calibrating with solutions of known concentration. It has been used, for example, to analyse DDS in epoxy formulations using as solvents chloroform [10], dichloromethane [15], and acetonitrile [11,16]. Epoxy content has also been analysed in this way [10].

The solution method suffers from one important drawback. Most organic solvents absorb very strongly in the infrared region and will interfere with the absorption bands of the material to be analysed. The few solvents which transmit well in the IR, such as chloroform, carbon tetrachloride, dichloromethane, and carbon disulphide, are often toxic, unpleasant, or will not dissolve the compound to be analysed. In the case of epoxy formulations, it becomes increasingly difficult to find a good solvent as the resin becomes more polymerized. Hence the solution method is of limited usefulness.

In this work, the solution method was rejected in favour of the cast film technique. The resin is dissolved in a suitable solvent, a few drops are placed on an IR-transparent window, and the solvent is evaporated. This leaves a thin film of resin which is measured in transmission. This method is simpler and faster than the solution method, but has one disadvantage. Usually it is difficult to determine the thickness of the film, so the amount of sample absorbing is unknown. This problem is overcome by using one peak in the spectrum as an "internal standard" or reference to which other peaks are compared. Other complications involved in this method are discussed later.

3.2 Choice of a Solvent

The following solvents were tested as candidates for extraction of Narmco 5208 resin from prepreg and casting of films for IR spectroscopy: tetrahydrofuran, acetone, acetonitrile, dichloromethane, chloroform. Extractions were performed using 100 mL of solvent with a piece of prepreg measuring 5 cm x 5 cm. The best solvent in terms of solubility is tetrahydrofuran; it dissolves the resin even when it is significantly advanced beyond the usual B-stage. Although it is excellent for liquid chromatography work, it is unsuitable for IR work because it associates strongly with the resin and is very difficult to evaporate completely without heating. Traces left in the resin give peaks at 1070 and 925 cm^{-1} which interfere with the peaks used for quantitative analysis (discussed in Section 3.3). The association probably occurs through hydrogen bonding with the NH_2 groups of the DDS, because the N-H stretching peaks in the 3500-3200 cm^{-1} region are much broader than they are in the case of the other solvents mentioned. Further evidence of such association was obtained by size-exclusion chromatography, as discussed in a subsequent report (Part 3 of this series). The next best solvent to THF in terms of solubility, and the best for IR work, is acetone. It readily dissolves typical B-stage resin, it is easily removed by evaporation under vacuum, and even if traces remain, the major peaks do not coincide with the main peaks used for resin analysis. When acetonitrile is used to extract the resin, the solution is initially cloudy but clears after standing for about ten minutes. This indicates that the resin solubility is approaching the limit. Chloroform and dichloromethane are worse still, giving solutions which remain slightly cloudy permanently. Hence they are not recommended.

3.3 The Infrared Spectrum of Narmco 5208 Resin

Figure 3 shows the transmission infrared spectrum of a thin film of Narmco 5208 resin obtained by extracting prepreg Batch 1010 with acetone, casting on a potassium bromide window, and evaporating the acetone under vacuum. Figure 4 shows the same spectrum after conversion to absorbance units (Section 3.1) and correction of the baseline. Figures 5, 6, and 7 show the spectra of what are believed to be the main components of the system. Table 1 lists the major bands in the 5208 spectrum together with their assignment, where this is known [17, 18, 19]. The minor epoxy resin has strong bands at 1508, 1246, 1034, and 831 cm^{-1}; because the amount is small, only the 1034 cm^{-1} band appears as a distinct (but very weak) peak in the Narmco 5208 spectrum.

For quantitative analysis, either peak height or peak area can be used as a measure of intensity. With non-computerized instruments, peak heights are easier to determine. With computerized instruments, peak areas are easily calculated and are believed to be a better indicator of intensity because any variations in band width which may occur are expected to affect the peak area less than the peak height.

The bands of greatest interest for quantitative analysis are shown in detail in Figure 8. The first is the aromatic ring band at 1517 cm^{-1}, which arises mainly from the major epoxy; small contributions from the hardener and the minor epoxy are responsible for the shoulder around 1500 cm^{-1}. This band is the most suitable for use as an "internal standard". The second band of interest is really a group of bands at 1146, 1105, and 1073 cm^{-1} arising from the hardener. They are related to the sulphone group, which is not destroyed in the curing reaction, so they do not disappear on curing. The ratio of their area to that of the internal standard is thus an indicator of the total amount of hardener in the system, either free or crosslinked. The calculation can be done using either the 1146 cm^{-1} peak alone ("single sulphone") or a combination of all three ("multiple sulphone"). The third group of peaks of interest occurs between 1000 and 900 cm^{-1} and arises from unreacted epoxy rings. These peaks disappear when the epoxy rings react on curing, so they are an indicator of the amount of unreacted epoxy in the system. Peaks in this region have long been used to determine epoxy content or follow the cure [20-22]. In MY 720 a series of peaks is observed, with maxima at 906, 952, and 974 cm^{-1}, while in SU-8 there are only two peaks, at 914 and 972 cm^{-1}. For the 5208 resin, the calculation can be done using only the 906 cm^{-1} peak ("single epoxy") or the whole set ("multiple epoxy").

Table 1. Narmco 5208 IR spectrum band assignments

Frequency (cm^{-1})†	Origin†	Assignment
3466, 3368, 3239	H	N-H stretching
3045, 2996	E	Aliphatic C-H stretching (epoxide ring)
2920	E	Aliphatic C-H stretching
1626 (sh)	H	N-H deformation
1613	E	Benzene ring quadrant stretching
1595	H	" " " "
1517	E	Benzene ring symmetric stretching
1501 (sh)	H	" " " "
1384	E	
1335	E	
1293	H	Asymmetric SO_2 stretching
1256	E	
1234	E	
1190	E	
1146	H	Symmetric SO_2 stretching
1105	H	C-S stretching
1073	H	
1034	E'	
973, 952, 906	E	Epoxide ring vibrations
830	E, H	Benzene ring C-H wagging
806 (sh)	E	Epoxide ring vibration
754	E	
721	H	Benzene ring vibration
694	H	
554	H	

† E = major epoxy, H = hardener, E' = minor epoxy, sh = shoulder

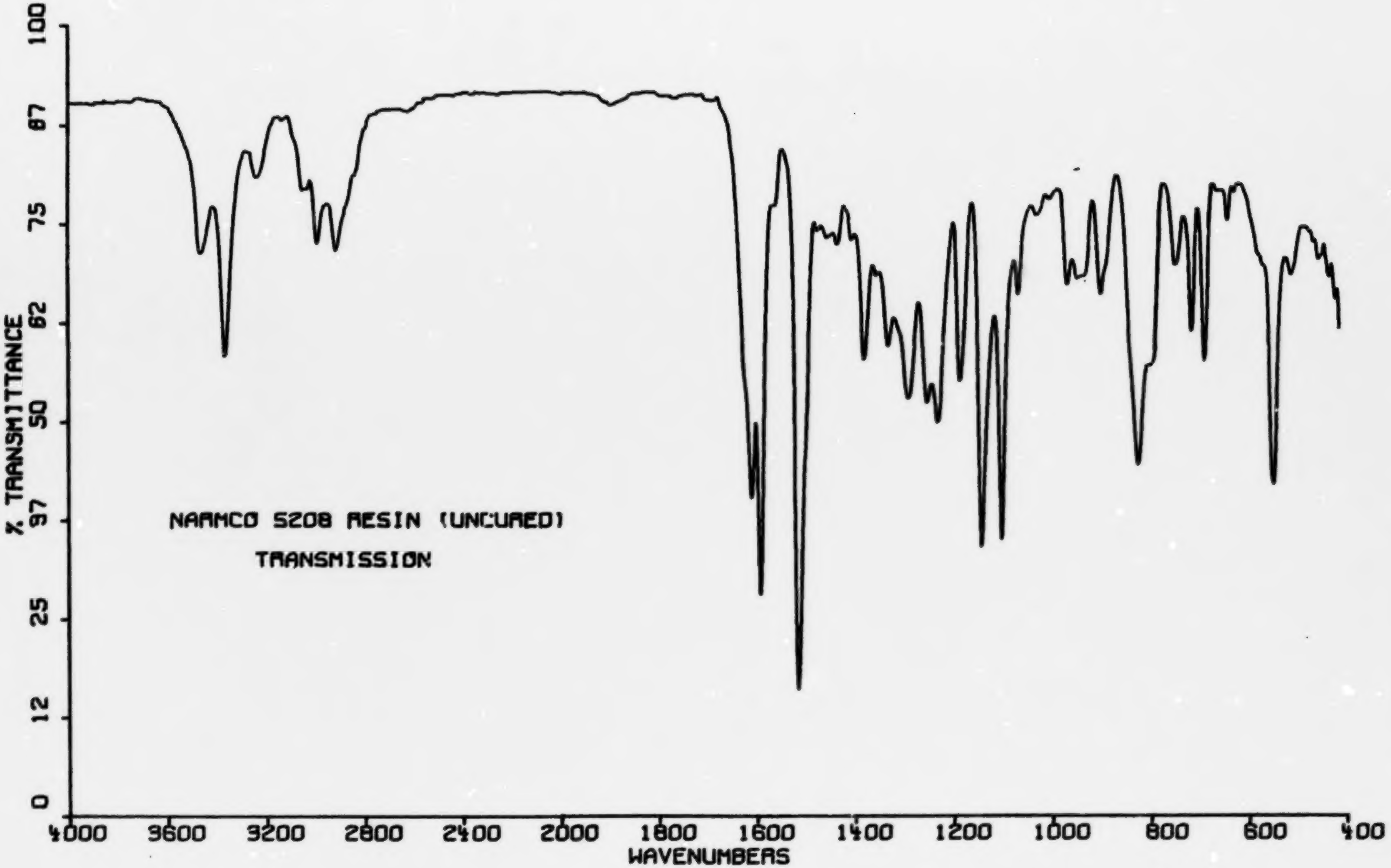

Figure 3 - Transmission IR spectrum of Narmco 5208 resin (Batch 1010, uncured). Thin film cast from acetone solution.

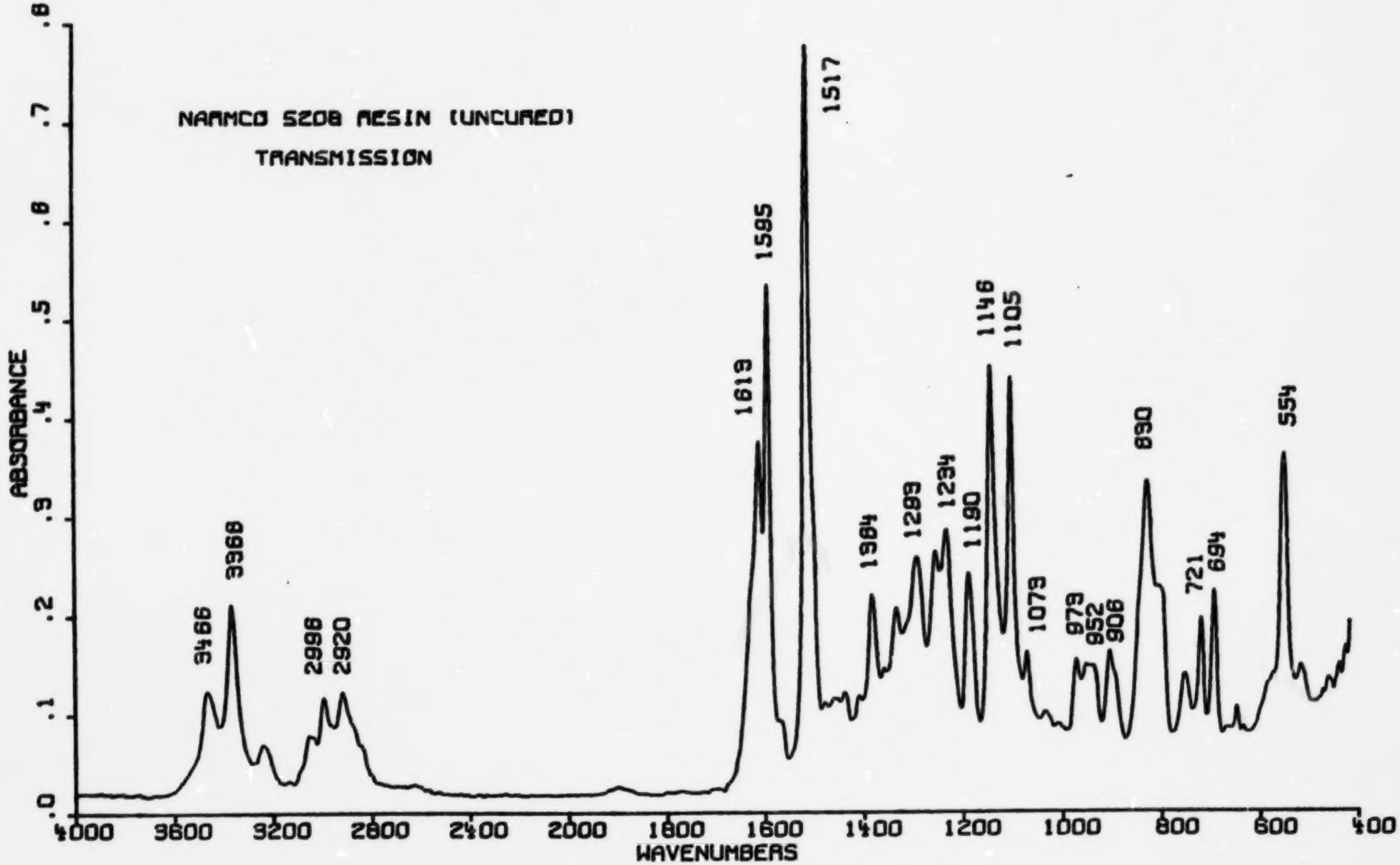

Figure 4 - Transmission IR spectrum of Narmco 5208 resin (Batch 1010) after conversion to absorbance units.

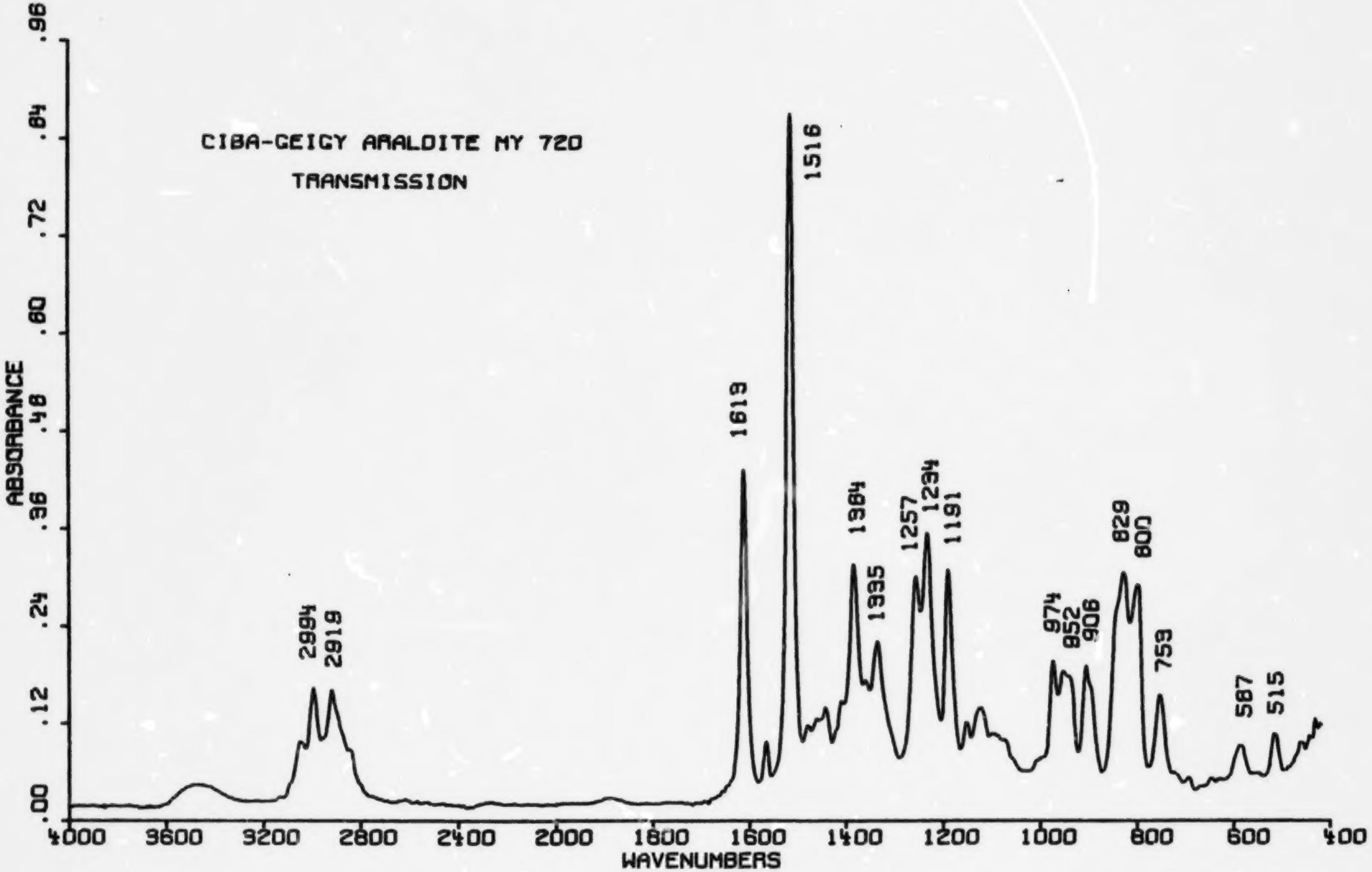

Figure 5 - Transmission IR spectrum of Ciba-Geigy Araldite MY 720 (TGDDM) epoxy resin. Thin film cast from acetone solution.

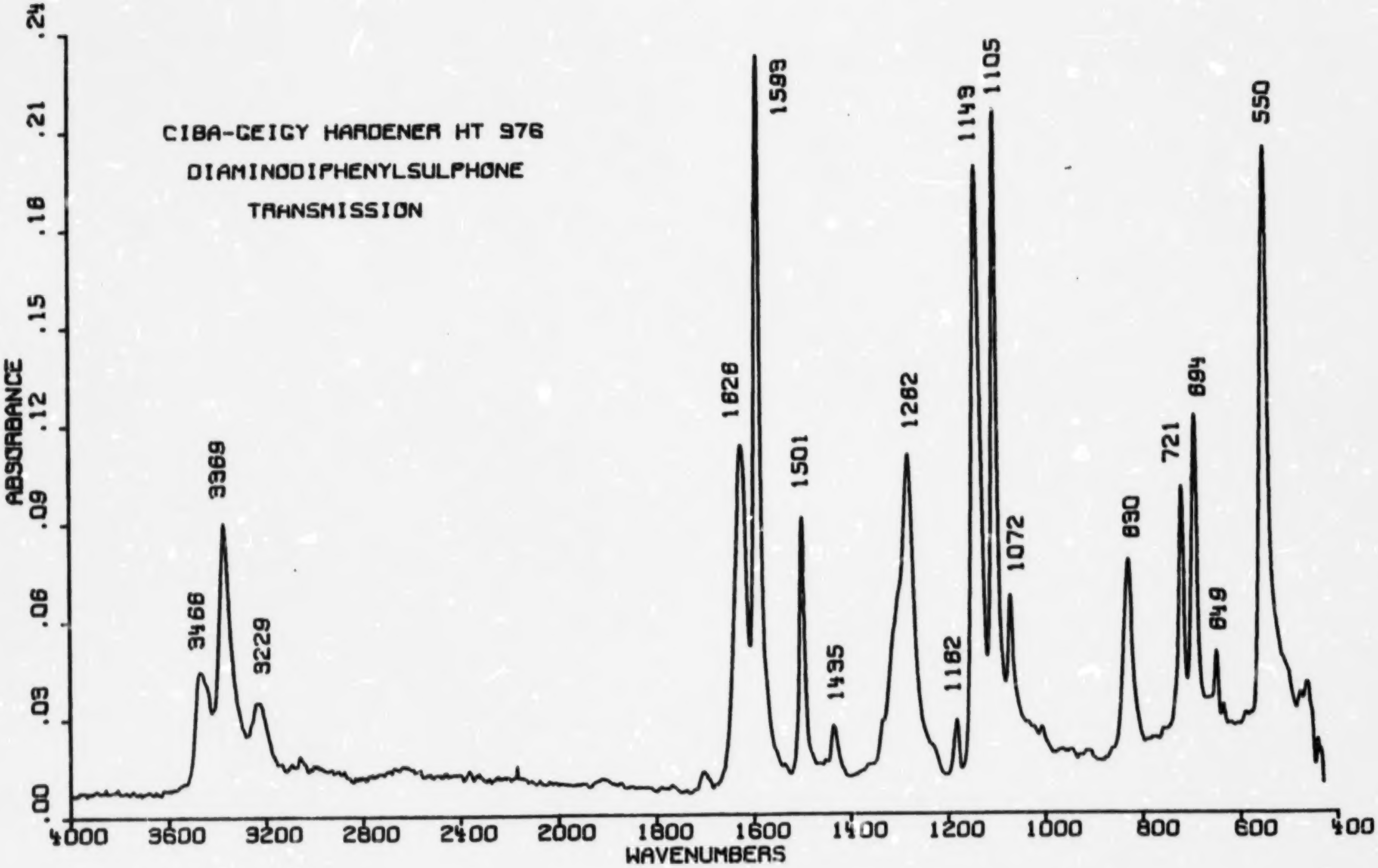

Figure 6 - Transmission IR spectrum of Ciba-Geigy Hardener HT 976 (DDS). Thin film cast from acetone solution.

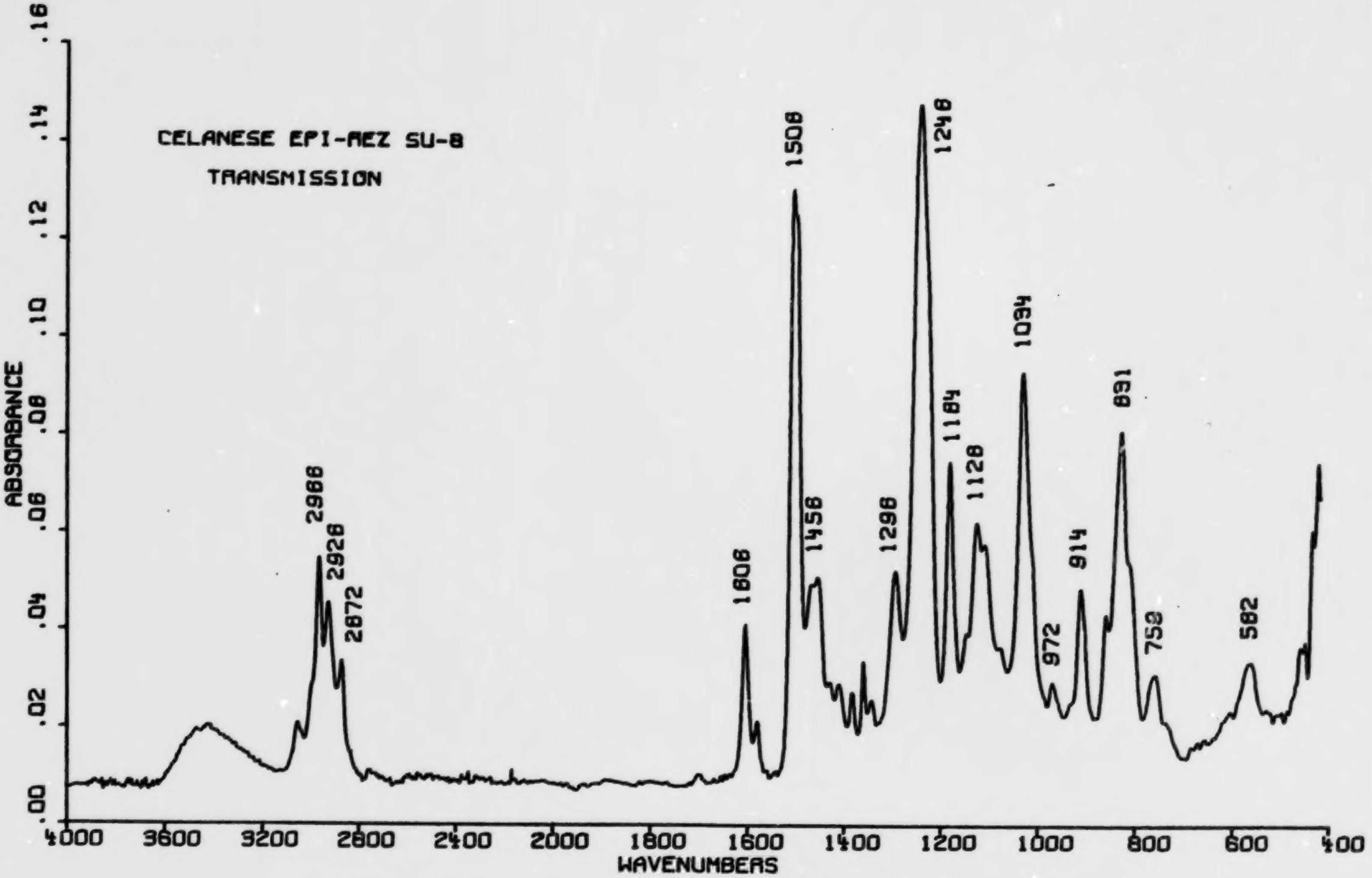

Figure 7 - Transmission IR spectrum of Celanese Epi-Rez SU-8 epoxy resin (bisphenol A Novolac epoxy).
Thin film cast from acetone solution.

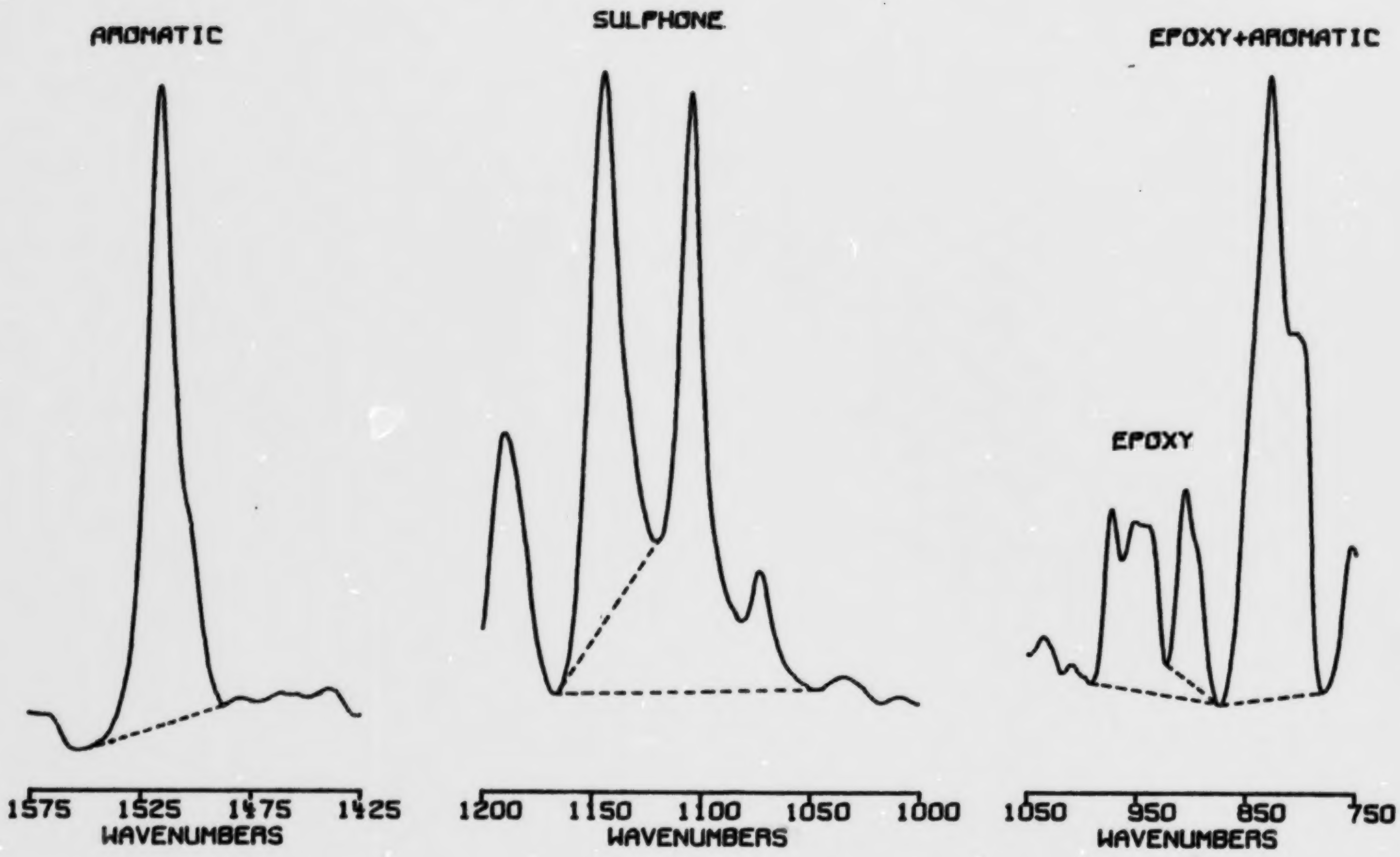

Figure 8 - Absorption bands used for quantitative analysis of Narmco 5208 resin.

Finally, there is a band at 830 cm^{-1} which is of lesser interest because it is a combination of several bands arising from aromatic ring C-H wagging and epoxide ring vibrations. All three components of the resin contribute to it.

The baselines used in calculating the peak areas are shown in Figure 8. The area under the peak and above the baseline was calculated using the Nicolet software. The quantities calculated by taking the ratio of the area (or height) of a given band against that of the "internal standard" aromatic band are henceforth referred to by the term "index" (single sulphone index, multiple sulphone index, etc.). It must be emphasized that these indices are somewhat empirical. Band shapes and intensities are affected to some extent by the molecular environment of the absorbing group. They may change, for instance, as the degree of advancement changes through aging or curing. Also, since the internal standard band contains contributions from all three components of the resin, it will be influenced to some extent by variations in composition. Thus the calculated indices are not an absolute measure of the quantity of material involved, that is, they are not necessarily directly proportional. Nevertheless, they are a very good indicator. Any increase in the amount of hardener at the expense of epoxy should result in an increase in the sulphone index. Likewise, any decrease in the number of free epoxy groups will be reflected in a decrease in the epoxy index.

The IR spectrum of the cured resin is shown in Figure 9. This was obtained using a thin film of resin (from prepreg Batch 1010) cured between two KBr disks for two hours at 135°C followed by three hours at 177°C. Comparison with Figure 4 shows several significant changes. The N-H stretching bands (3500-3200 cm^{-1}) have been largely replaced by a broad O-H band centred around 3400 cm^{-1}. In the C-H stretching region (3100-2800 cm^{-1}) the band shape has changed because of the disappearance of the epoxy peak at 2996 cm^{-1}. The epoxy peaks in the 1000-900 cm^{-1} region have also practically disappeared. The shoulder at 1626 cm^{-1} due to N-H deformation has vanished as a result of reaction of the N-H groups, and the peak at 1613 cm^{-1} has merged with the 1595 cm^{-1} band, increasing its apparent intensity. The "internal standard" aromatic ring band at 1517 cm^{-1} has shifted to slightly lower frequency (1514 cm^{-1}) and broadened somewhat, so that the shoulder at 1501 cm^{-1} (which can be seen in Figure 8) is no longer evident at all. The sulphone bands remain at much the same frequencies (1145 and 1106 cm^{-1}) but their relative intensities change. Gupta et al. [23] have related this to the transformation of the primary amine groups into secondary ones. The combination "epoxy + aromatic" band has changed shape due to the loss of epoxy groups and its maximum has shifted from 830 to 820 cm^{-1}. Other changes in the spectrum include the appearance of two new peaks at 1722 and 1666 cm^{-1}. These are due to carbonyl groups formed through oxidation of the resin.

As a consequence of the above, it can be seen that the infrared spectrum readily

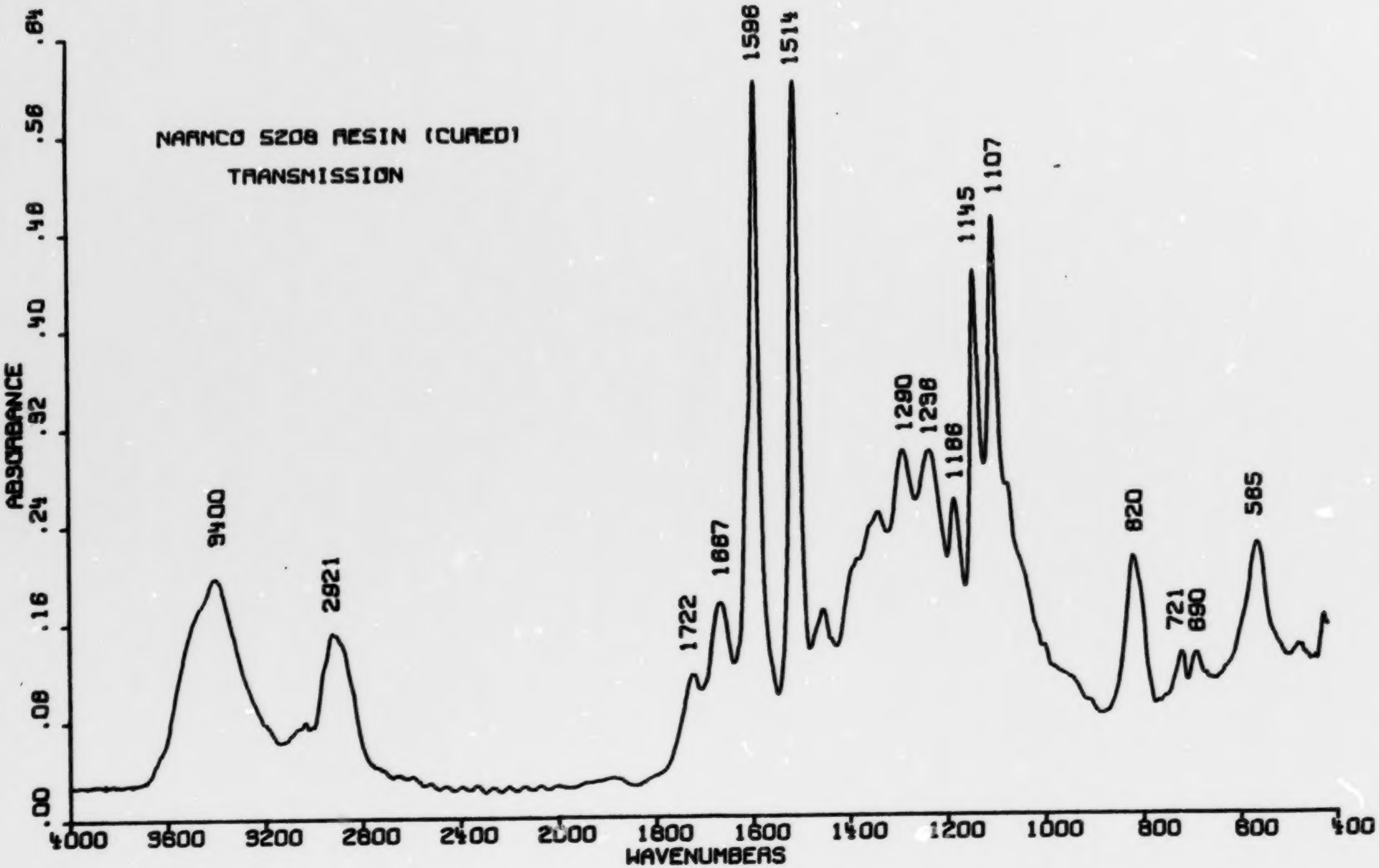

Figure 9 - Transmission IR spectrum of Narmco 5208 resin Batch 1010 (cured).

serves four useful purposes:

(a) As a "fingerprint" of the resin it can be used to detect contamination (new peaks) or significant changes in the resin composition.

(b) The sulphone bands at 1146 and 1105 cm^{-1} can be used to quantify the total hardener content of the resin.

(c) The epoxy bands in the 1000-900 cm^{-1} region can be used to quantify the content of unreacted epoxy, to follow the curing of the resin, and to confirm completeness of cure.

(d) The appearance of carbonyl bands near 1722 and 1666 cm^{-1} can be used to detect degradation due to oxidation.

3.4 Quantitative Analysis

An experiment was performed to evaluate the precision of the quantitative method outlined in the previous section. A square of prepreg from Batch 1010 measuring approximately 5 cm by 5 cm was extracted with 20 mL of acetone in two stages (15 mL + 5 mL). This gives a solution with a resin concentration of about 30 mg/mL. Ten different specimens were prepared by depositing a few drops of the solution on a KBr window, blowing with a stream of air from a rubber bulb to remove most of the solvent, and drying under vacuum (without heat) to remove the remainder of the solvent. The IR spectra were recorded and converted to absorbance. The areas of the five most useful bands shown in Figure 8 were calculated using Nicolet software with the following integration limits:

Aromatic ring (reference)	1550 - 1485 cm^{-1}
Single sulphone	1166 - 1120 cm^{-1}
Multiple sulphone	1166 - 1048 cm^{-1}
Single epoxy	923 - 875 cm^{-1}
Multiple epoxy	993 - 875 cm^{-1}.

To eliminate the effect of the sample thickness, the areas of the sulphone and epoxy bands were divided by the area of the aromatic ring reference band. This gives ratios which are indicators of the amounts of sulphone and epoxy respectively. The results are summarized in Table 2. Surprisingly, an enormous variation is observed, with standard deviations of 10% for the sulphone bands and 28% for the epoxy bands. This is obviously unacceptable for the present application and is much higher than expected considering the photometric accuracy of modern IR instruments.

Table 2. Quantitative analysis of Narmco 5208/WC3000 prepreg Batch 1010 by IR transmission (first experiment)

Specimen	Index = Band area divided by area of aromatic reference band			
	Single sulphone	Multiple sulphone	Single epoxy	Multiple epoxy
1	0.437	1.105	0.144	0.439
2	0.451	1.233	0.142	0.435
3	0.458	1.247	0.150	0.452
4	0.474	1.449	0.275	0.838
5	0.510	1.417	0.221	0.671
6	0.507	1.465	0.256	0.783
7	0.484	1.252	0.177	0.536
8	0.426	1.254	0.252	0.772
9	0.488	1.455	0.274	0.833
10	0.475	1.506	0.309	0.945
Average	0.471	1.338	0.220	0.670
Standard deviation	0.028 (5.9%)	0.135 (10.1%)	0.062 (28.3%)	0.191 (28.5%)

A number of factors were investigated as possible causes of the variation. These included:

(i) Choice of solvent. The experiment was repeated using chloroform and dichloromethane, but the same variation was observed. In addition, the resin solubility in these solvents is limited, and the rapid evaporation of dichloromethane sometimes cools the sample to the point of causing condensation of atmospheric moisture.

(ii) Presence of residual solvent. No correlation was observed between the variation of the results and the presence of weak residual solvent peaks in the spectra. This was true for the chlorinated solvents as well as acetone. Also, the presence of traces of moisture in the samples prepared using dichloromethane had little effect on the results.

(iii) Method of calculation. When band ratios were calculated using peak heights instead of areas, no improvement was observed. In fact, the variation was greater.

(iv) Sample inhomogeneity. The possibility of inhomogeneity resulting from separation of resin components (for example, epoxy and hardener) during solvent evaporation was considered. However, this is unlikely since specimens which show a high epoxy index also show a high sulphone index. Also, there was no visual evidence of separation.

(v) Overall spectral intensity. A very weak correlation was observed between the calculated indices and the overall intensity of the spectrum, which is related to the sample thickness. However, this is believed to be a secondary effect related to the true reason for the variation.

(vi) Nonuniform sample thickness. As explained in the next paragraph, this was found to be the main reason for the variation of the results. The weak correlation mentioned in (v) is a consequence of the fact that with thicker samples the effect is more pronounced.

The problem of nonuniform sample thickness has been discussed by Koenig [24] and Hirschfeld [25, 26]. It is sometimes referred to as the "wedging effect" since it occurs in liquid cells in which the windows are not parallel and the sample takes the shape of a wedge. As pointed out in Section 3.1, for a sample of uniform thickness b, the "internal transmittance", or the transmittance of the sample itself neglecting reflection effects at the boundary surfaces, is given by the Beer-Lambert law:

$$T = 10^{-abc} = e^{-kb}.$$

where k, known as the absorption coefficient, is related to a and c by the relation $k = ac \ln 10$. If, however, the sample thickness within the area covered by the IR beam varies uniformly over a range δ (i.e. from $b - 1/2\ \delta$ to $b + 1/2\ \delta$), it can be shown [24-26] that the apparent transmittance T' will be given by:

$$T' = e^{-kb} \times \frac{e^{\frac{1}{2}k\delta} - e^{-\frac{1}{2}k\delta}}{k\delta}$$

where b is now the average thickness. The apparent absorbance A' may be expressed in terms of the "true" absorbance A by the following equation:

$$A' = A - \log_{10}\left\{\frac{10^{\frac{1}{2}\frac{\delta}{b}A} - 10^{-\frac{1}{2}\frac{\delta}{b}A}}{\frac{\delta}{b}A \ln 10}\right\}$$

The effect is shown graphically in Figure 10. The apparent absorbance is always lower than the true absorbance and the deviation is greatest when the absorbance is high (i.e. for strongly absorbing bands and for thick samples) or when the thickness variation is high. The effect on the appearance of the spectrum is to produce an apparent suppression of the stronger bands. This is illustrated in Figure 11, which shows two spectra from the series used to calculate the results given in Table 2. The lower spectrum (from specimen 1) is one for which the thickness variation is believed to be low, whereas the upper one (from specimen 4) shows evidence of a substantial variation, which may be seen by looking at the aromatic ring band at 1517 cm^{-1}. In the upper spectrum, this band appears relatively less intense when compared to weaker bands such as the epoxy bands at 1000-900 cm^{-1}, due to the "suppression" mentioned above. In Figure 12, the absorbance at the band maximum in the spectrum of specimen 4 is plotted against the corresponding absorbance for specimen 1 for most of the bands in the spectrum. If both specimens were of uniform thickness, the two spectra would be identical in appearance (although not in absolute intensity), and the plot would be a straight line with slope equal to the ratio of the two thicknesses. Instead, a smooth curve is obtained whose form resembles that of the curves shown in Figure 10. This provides strong evidence that the deviations in the spectra are the result of a variation in sample thickness.

Since the degree of suppression is related to the band intensity, stronger bands such as the aromatic ring band will be affected more than weaker ones such as the sulphone and epoxy bands. As a result, the calculated indices given in Table 2 will always be artificially high if there is a thickness variation effect. The most reliable results in Table 2 are therefore those with the lowest values, namely specimens 1, 2, 3, and 7.

This also explains why a greater standard deviation is observed when peak heights

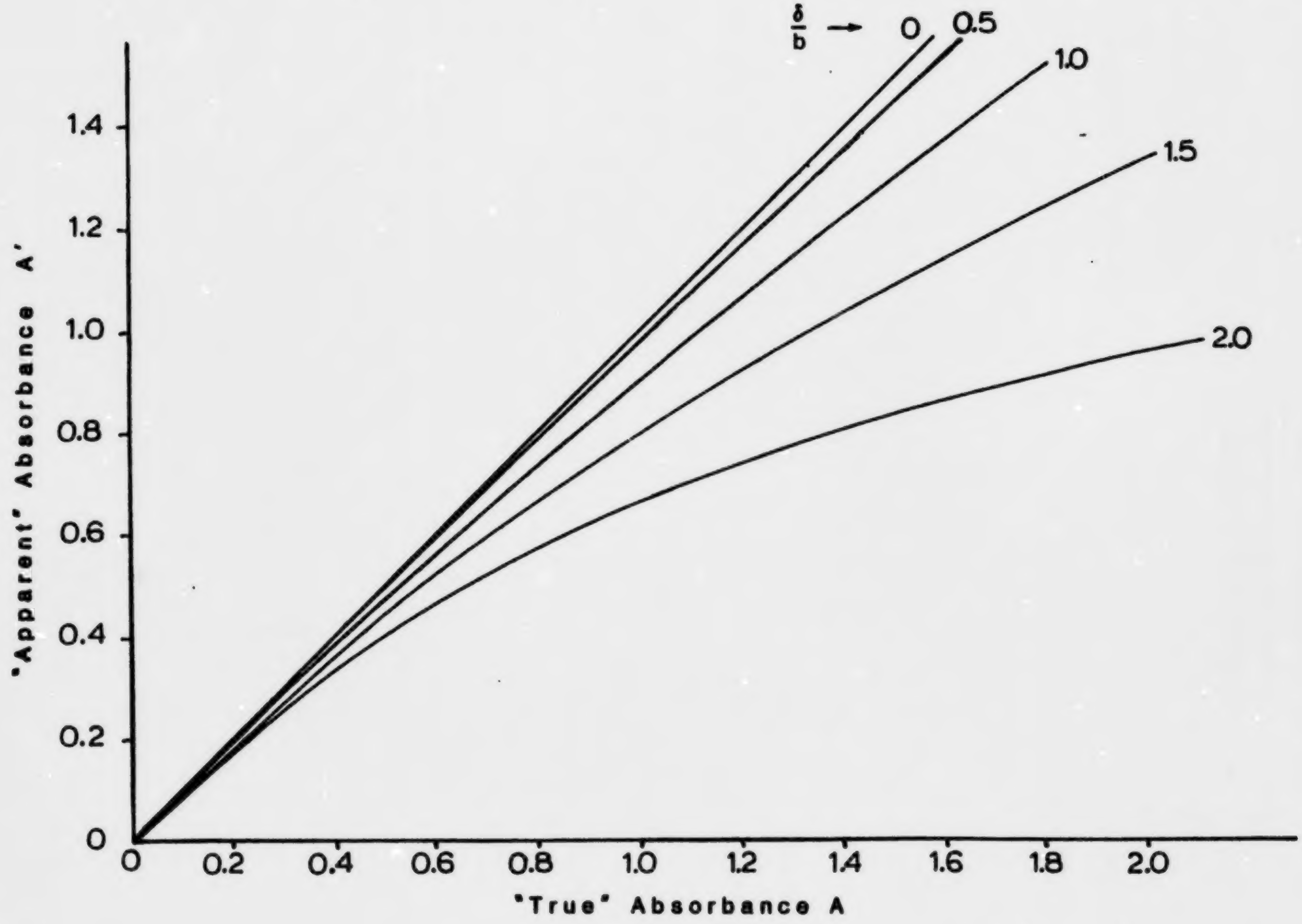

Figure 10 - Effect of sample thickness variation on measured absorbance.

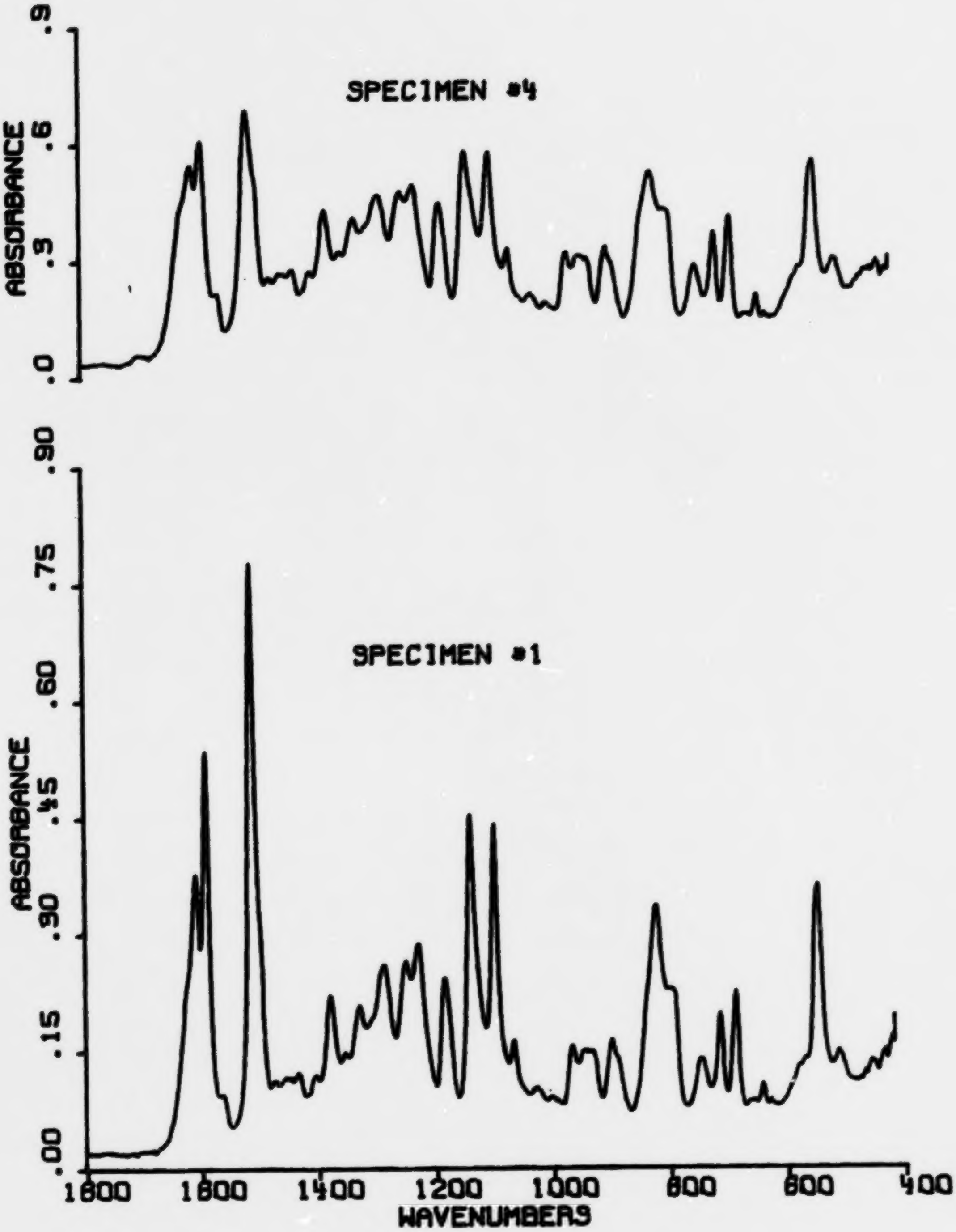

Figure 11 - Transmission IR spectrum of Narmco 5208 resin:
Specimen # 1 - film of uniform thickness;
Specimen # 4 - film of varying thickness.

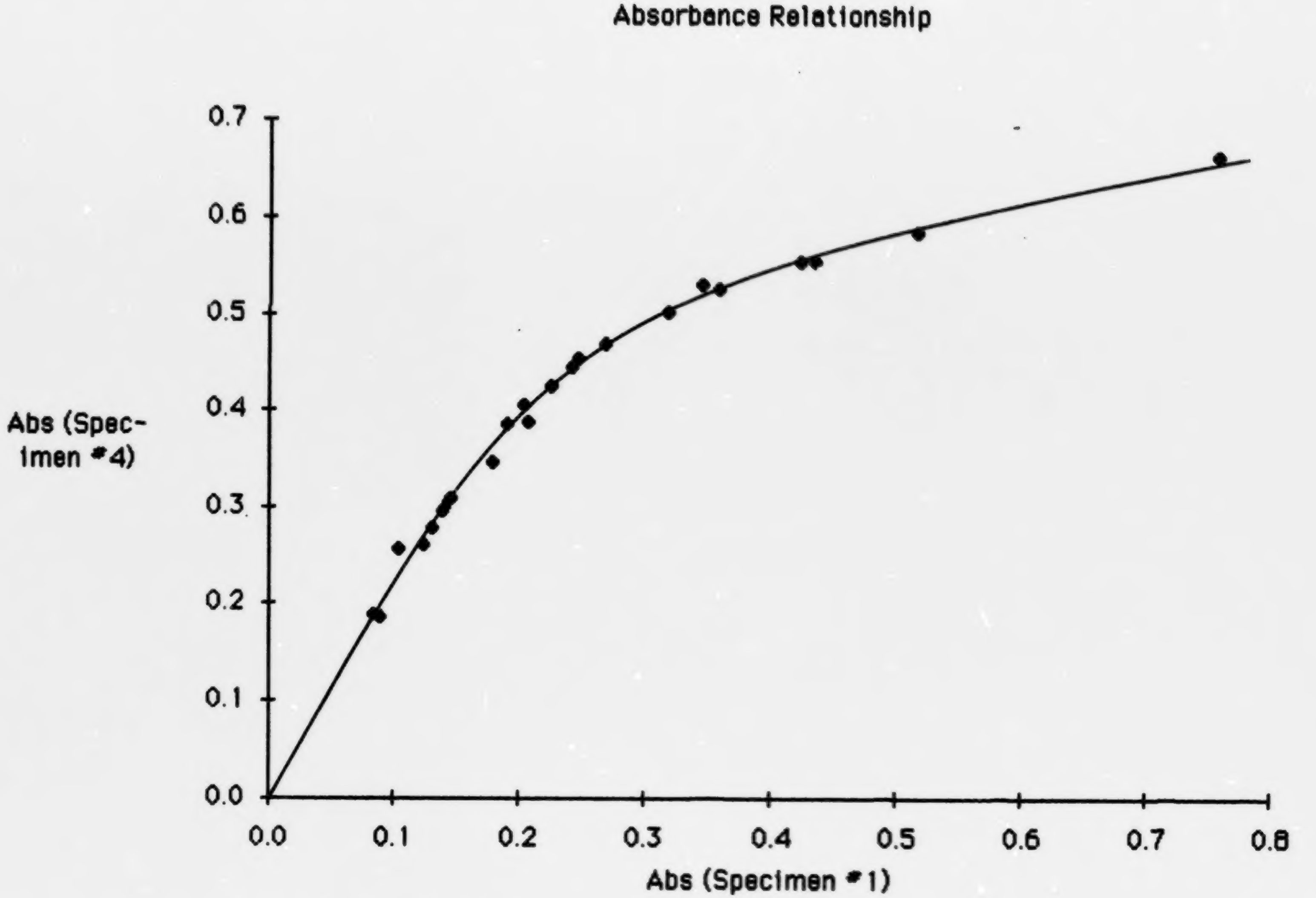

Figure 12 - Relationship between peak absorbance values for specimens # 4 and # 1 (see Figure 11).

are used for the calculation instead of peak areas. Peak heights are calculated on the basis of only one point, the point of maximum intensity, which is also the point where the deviation due to the thickness variation is at a maximum.

In an attempt to overcome the problem of thickness variation, the initial experiment was repeated using greater care in sample preparation. For example, the bulk of the solvent was left to evaporate by itself rather than subjected to a stream of air. Five specimens were measured and the results are summarized in Table 3. The reproducibility is much better than in the initial experiment. Specimen 2 gives significantly higher results than the four others, indicating a thickness variation effect. If this sample is eliminated from the averaging, the standard deviations drop to 2.5% or less.

Table 3. Quantitative analysis of Narmco 5208/WC3000 prepreg Batch 1010 by IR transmission (second experiment)

Specimen	Index = Band area divided by area of aromatic reference band			
	Single sulphone	Multiple sulphone	Single epoxy	Multiple epoxy
1	0.433	1.078	0.131	0.404
2	0.445	1.197	0.153	0.476
3	0.438	1.107	0.134	0.415
4	0.416	1.045	0.129	0.393
5	0.426	1.059	0.129	0.397
Average (all five)	0.432	1.097	0.135	0.417
Standard deviation	0.011 (2.6%)	0.060 (5.5%)	0.010 (7.5%)	0.034 (8.2%)
Average (without no. 2)	0.428	1.072	0.131	0.402
Standard deviation	0.010 (2.2%)	0.027 (2.5%)	0.002 (1.8%)	0.010 (2.4%)

A third experiment was subsequently done using Batch 1014 instead of Batch 1010. In addition to five carefully prepared specimens, two were prepared with use of an air stream from a rubber bulb to evaporate the solvent. The results are given in Table 4. For the carefully prepared samples, the reproducibility is about 2%, but the specimens prepared with blowing show deviations of greater than 60%.

Table 4. Quantitative analysis of Narmco 5208/WC3000 prepreg Batch 1014 by IR transmission

Specimen	Index = Band area divided by area of aromatic reference band			
	Single sulphone	Multiple sulphone	Single epoxy	Multiple epoxy
1	0.452	1.098	0.141	0.423
2	0.439	1.056	0.135	0.408
3	0.440	1.062	0.134	0.405
4	0.440	1.057	0.135	0.411
5	0.441	1.092	0.138	0.418
6†	0.482	1.328	0.224	0.678
7†	0.500	1.292	0.188	0.567
Average (1-5 only)	0.442	1.073	0.137	0.413
Standard deviation	0.005 (1.2%)	0.020 (1.9%)	0.003 (2.1%)	0.007 (1.8%)

†Specimens prepared with blowing to evaporate the solvent.

In conclusion, the transmission method with cast films is acceptable for IR quantitative analysis of Narmco 5208 prepreg provided care is taken to prepare films of uniform thickness. With good technique, a precision of 2% is obtainable. The recommended procedure is described in detail in Section 3.8. The importance of uniform sample thickness does not appear to have been recognized in previous work on analysis of epoxy resins. This may explain why in some cases a high degree of scatter has been observed [27], and why some workers feel that infrared spectroscopy is of value only as a qualitative tool [28]. The results shown here demonstrate that this is not the case.

3.5 Comparison of Different Batches

The seven different batches of Narmco 5208 resin described in Section 2.1 were analysed using the procedure developed as outlined above. The results obtained are given in Table 5.

Table 5. Quantitative analysis of different batches of Narmco 5208 by IR transmission spectroscopy

Batch No.	Index = Band area divided by area of aromatic reference band			
	Single sulphone	Multiple sulphone	Single epoxy	Multiple epoxy
1010	0.426 (0.004)	1.047 (0.011)	0.130 (0.001)	0.391 (0.005)
1014	0.436 (0.002)	1.052 (0.005)	0.136 (0.001)	0.408 (0.002)
1101	0.424 (0.002)	1.022 (0.007)	0.134 (0.001)	0.395 (0.002)
1103	0.424 (0.001)	1.045 (0.007)	0.127 (0.001)	0.375 (0.001)
1104	0.429 (0.003)	1.037 (0.008)	0.129 (0.001)	0.380 (0.002)
1047	0.448 (0.005)	1.087 (0.015)	0.136 (0.003)	0.411 (0.007)
1023	0.427 (0.004)	1.099 (0.012)	0.123 (0.001)	0.370 (0.004)

Each result is an average over five specimens with the standard deviation shown in parentheses. In most cases the deviation is under 1%. Comparison of the different batches shows no particularly large variations. The "multiple sulphone" indices are all within ±4% of the mean (1.056), and the "multiple epoxy" indices are all within ±6% of the mean (0.390). Nevertheless, in many cases the differences can be considered statistically significant. For the conditions used (five specimens per sample), it can be shown using standard statistical theory [29] that two indices X_1 and X_2 with respective unbiased standard deviations of S_1 and S_2 can be considered to be significantly different with a confidence level of 95% if the difference between them $|X_1-X_2|$ exceeds $1.03\sqrt{S_1^2 + S_2^2}$, or 1.46 S if $S_1 = S_2 = S$. Using this criterion and the multiple epoxy index, the batches can be arranged in order of free epoxy content as follows: 1047 ≈ 1014 > 1101 ≈ 1010 > 1104 > 1103 > 1023. The single epoxy index gives much the same result. The batch with the highest epoxy content (Batch 1047) consists of neat resin coated on a plastic sheet without graphite cloth; it is probably less highly advanced than the usual prepreg samples. Surprisingly, the batch with the lowest epoxy content also consists of neat resin, this time in bulk form. It is believed that this sample was heated to reduce its viscosity for transfer to the can in which it was shipped, and that this caused significant advancement of the resin. The sulphone indices are more difficult to interpret, since the overall variation is lower and the single and multiple indices do not follow the same order. This may be due to the fact that the sulphone bands are sensitive to effects such as hydrogen bonding and moisture absorption [17].

Transmission spectra were also recorded for cured films prepared as described in Section 3.3. All seven batches gave spectra very similar to Figure 9. No significant differences were observed.

3.6 Resin Cure

The changes occurring in the IR transmission spectrum during the cure cycle of the Narmco 5208 resin were studied using the setup described in Section 2.3. Controller and transformer settings were chosen to give a sample temperature profile which matched as closely as possible the recommended program for cure of Narmco 5208. The result is shown in Figure 13. The sample is heated to 135°C (275°F) within a one-hour period, maintained at this level for one hour, heated to 177°C (350°F) within half an hour, maintained at this level for two hours, then left to cool to room temperature.

With the cell and sample installed in the FTIR spectrometer, the heating program was begun and spectra were recorded at intervals of approximately 15 minutes using an accumulation of 32 scans (total collection time about 20 seconds). Upon completion of the experiment, the stored spectra were converted to absorbance and "corrected" by subtracting

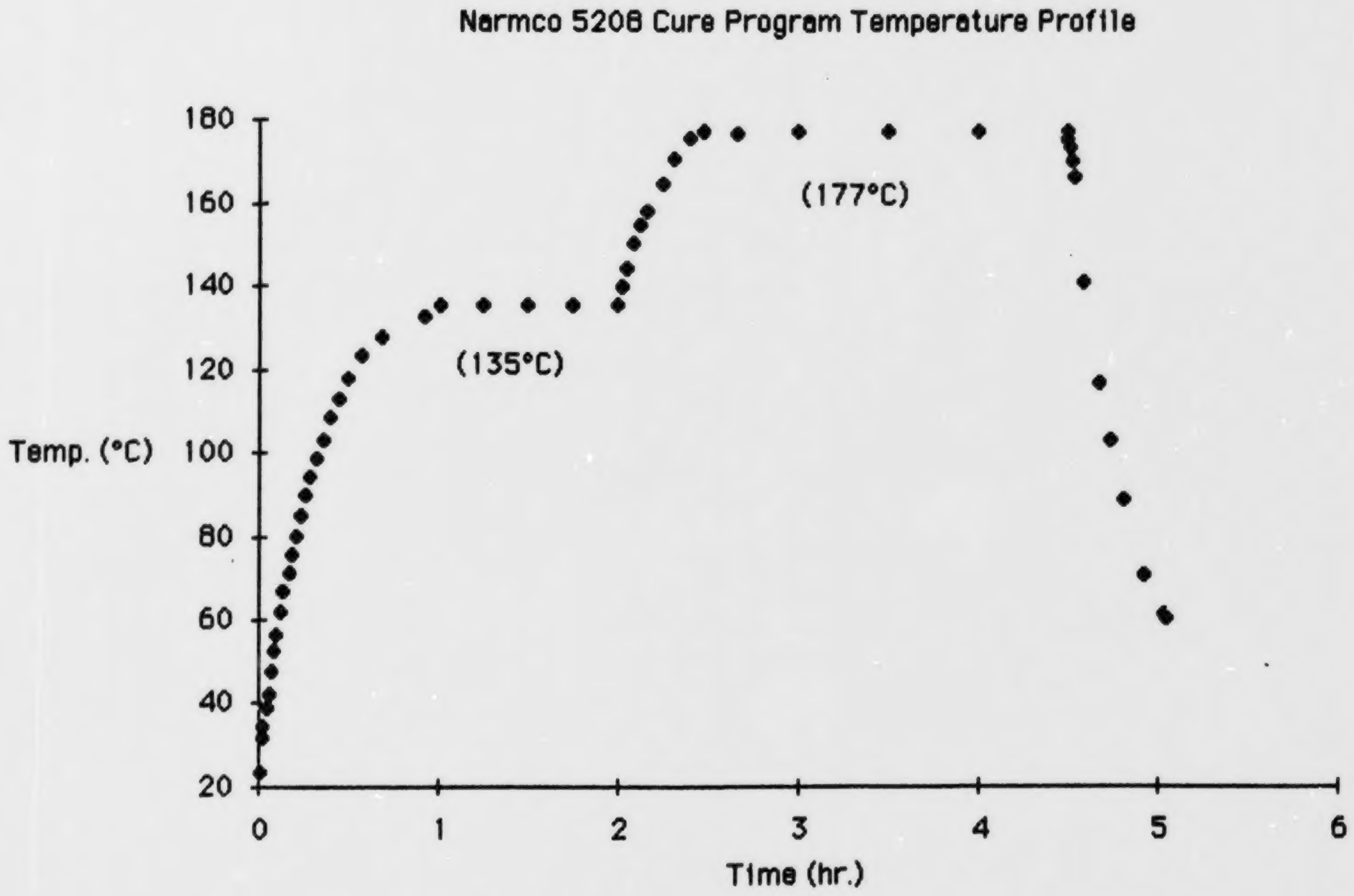

Figure 13 - Temperature program used for IR study of Narmco 5208 cure.

the spectra of the KBr windows, as well as those of any traces of water vapour or CO_2, and adjusting the baseline. The areas of the bands of interest were then calculated as described in Section 3.4. Where necessary, the limits of integration were changed slightly from those given in the recommended method to take account of changes in band shapes occurring as a result of the heating and curing. Sulphone and epoxy indices were calculated as described in Section 3.4 by taking the ratio of the appropriate band area with respect to that of the aromatic ring band at about 1517 cm^{-1}. In addition to the sulphone and epoxy bands, the combination "epoxy + aromatic" band at about 830 cm^{-1} (shown in Figure 8) was also analysed.

Two different batches of Narmco 5208 prepreg were studied: Batch 1014 and Batch 1103. Figure 14 shows the evolution of the IR spectrum during the cure of Batch 1014, and Figures 15 to 19 show the changes in the calculated indices. Although the general behaviour is the same for both batches, certain differences are apparent, for which the reasons are not clear. They may be related to the importance of uniform sample thickness, since the experiment involving Batch 1103 was done before this was discovered. For this reason, the curves for Batch 1014 are believed to be more reliable.

The sulphone indices show some variation with cure, probably related to the structural and temperature changes taking place. It has been shown that the sulphone band intensities are affected by the transformation from primary amine to secondary amine during cure [23, 30], as well as by the presence of moisture [17]. Intensities can also be affected by glass transitions [31]. The "single sulphone" index (Figure 15) appears to be more sensitive than the "multiple sulphone" index (Figure 16), which remains reasonably constant overall. Similar behaviour was observed in the aging study to be described in a later report (Part 5 of this series). The multiple sulphone index is therefore considered a better indicator of the total sulphone content.

The epoxy indices show interesting behaviour. They show that even during the first stage of the cure cycle there is significant reaction; by the end of the second hour about one-third of the epoxy groups have reacted. When the temperature is increased to 177°C, reaction occurs more rapidly, and by the end of the third hour only about 15% of the epoxy groups remain. Over the next two hours, there is further gradual reaction, but at the end of the recommended cure cycle (5 hours) there are still some unreacted epoxy groups (about 7% of the initial number). Comparison of the "single epoxy" and "multiple epoxy" curves (Figures 17 and 18) shows an interesting difference in shape at the beginning of the cure. The "single epoxy" index drops more rapidly than the "multiple epoxy" index. The reason is not obvious at this point. One possibility is that heating the resin brings about structural changes which influence the band intensities. A second possibility is a difference in

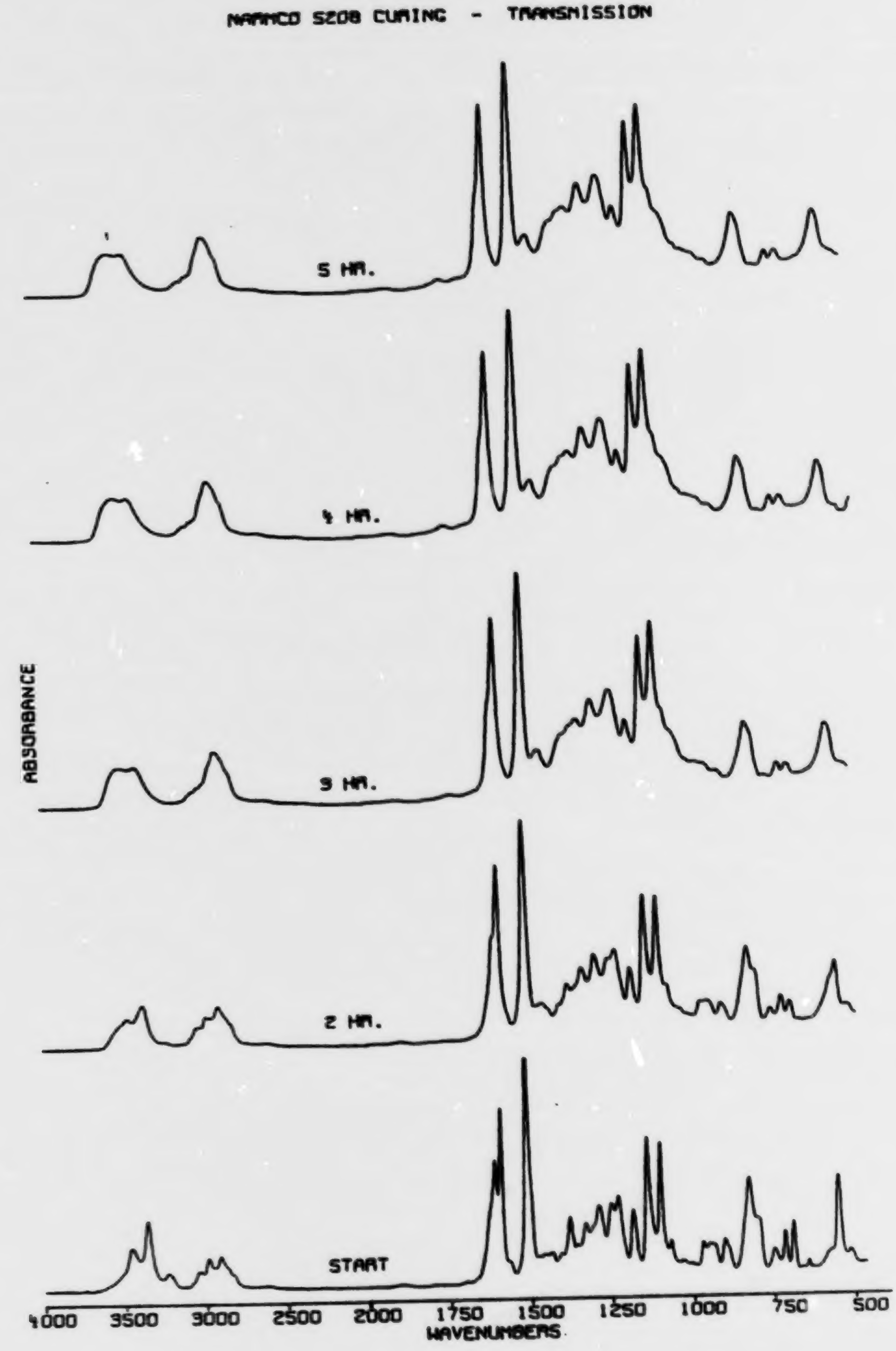

Figure 14 - Evolution of IR transmission spectrum during cure of Narmco 5208

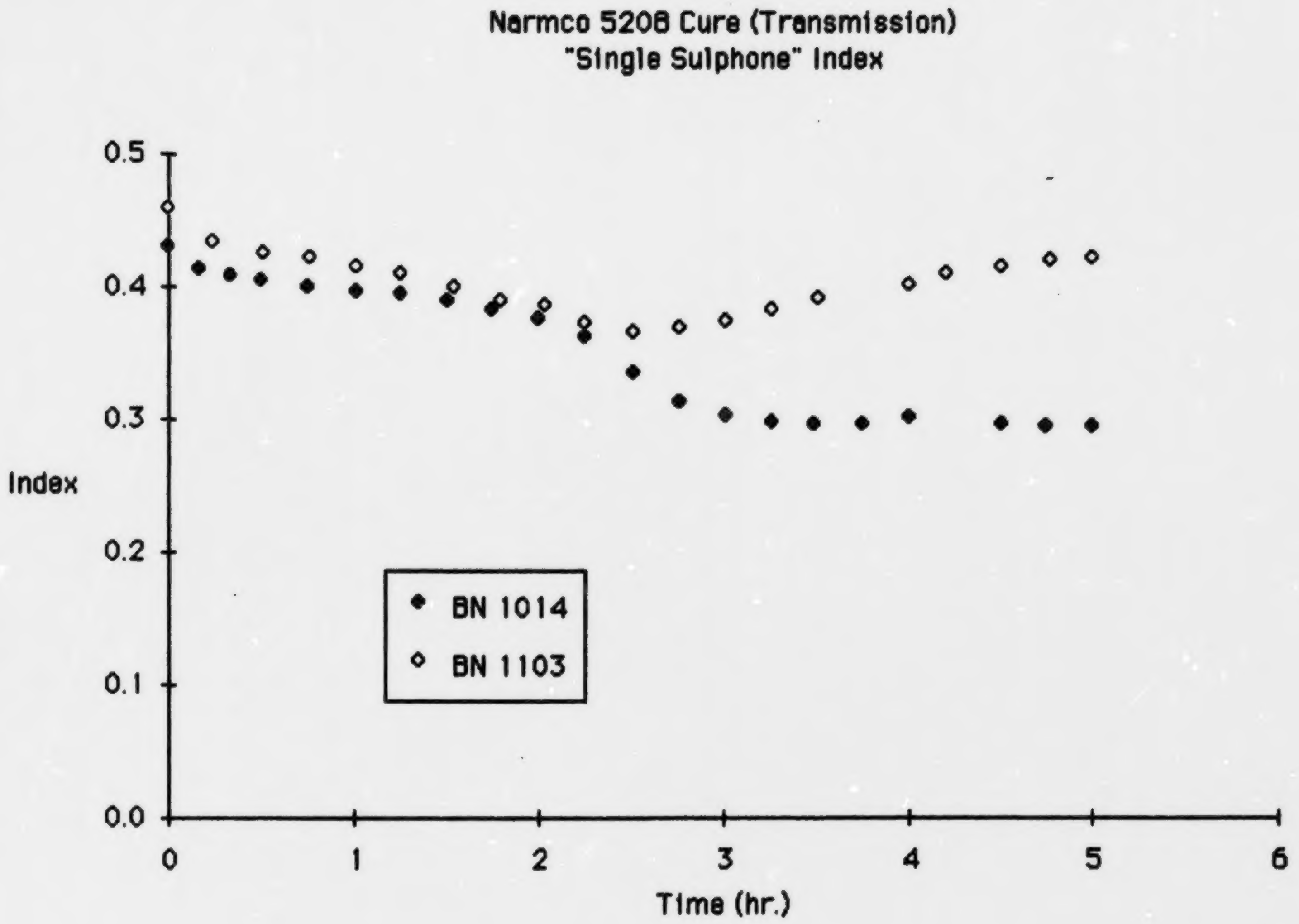

Figure 15 - Variation of "single sulphone" index as measured by IR transmission during cure of Narmco 5208 resin.

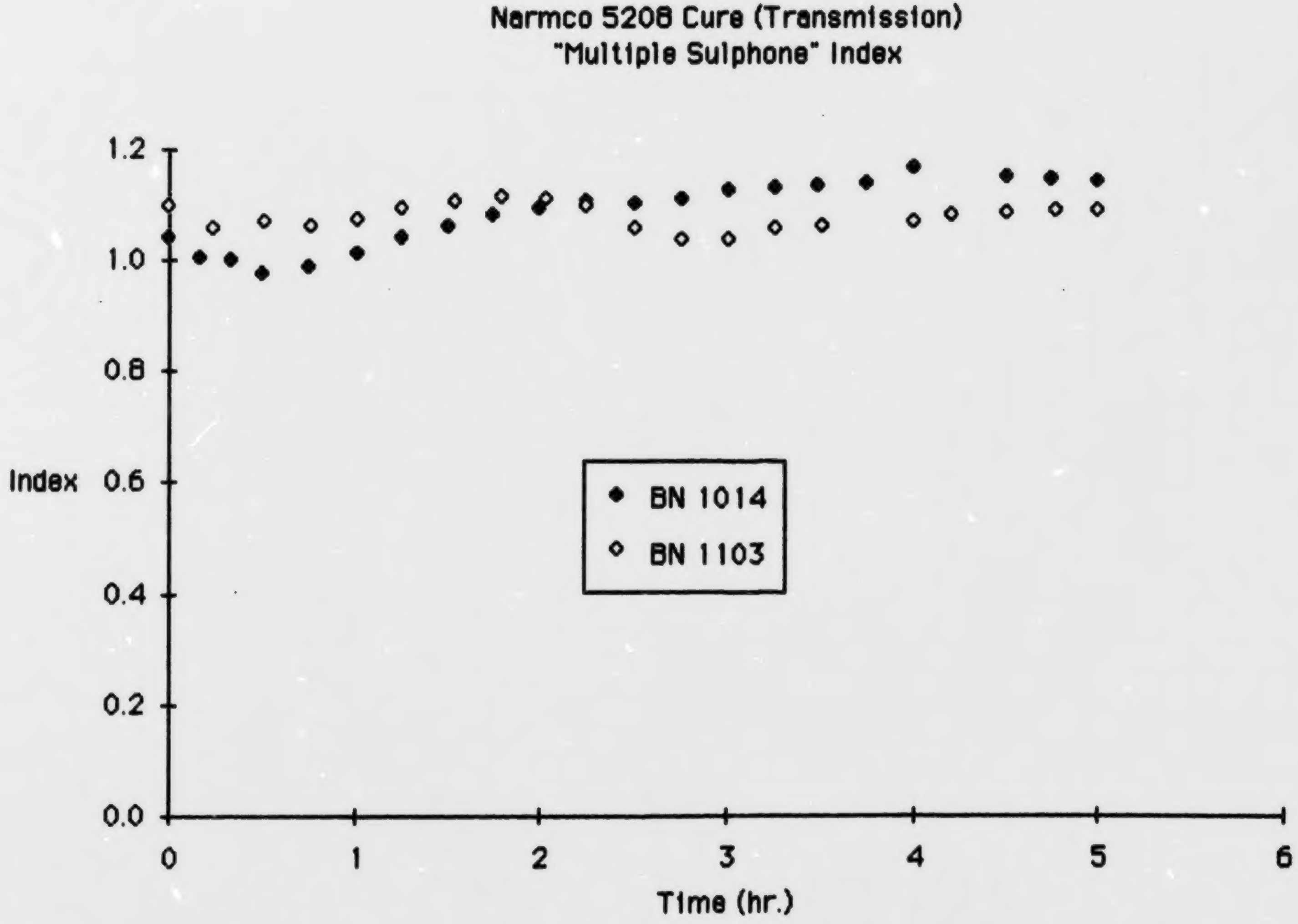

Figure 16 - Variation of "multiple sulphone" index as measured by IR transmission during cure of Narmco 5208 resin.

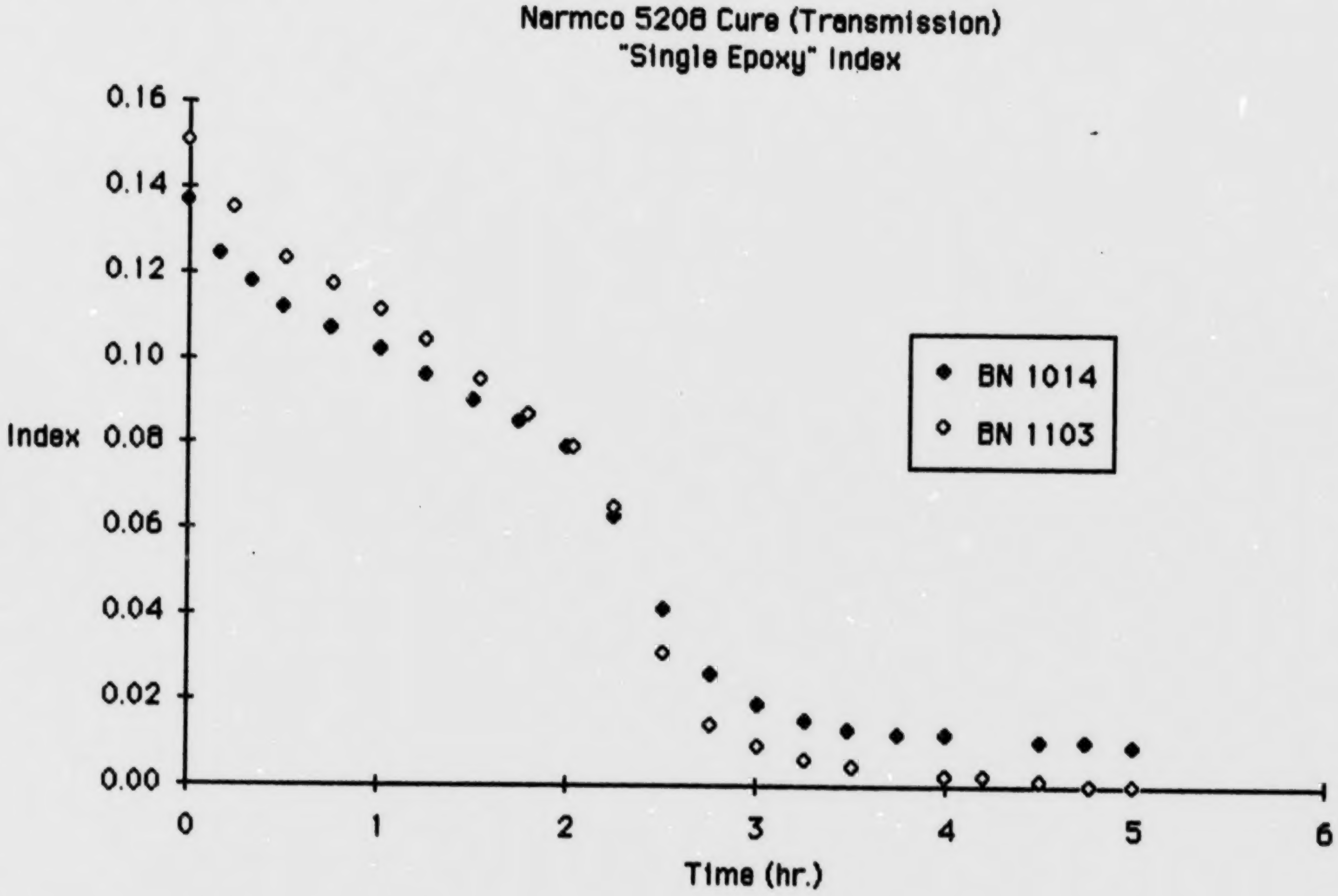

Figure 17 - Variation of "single epoxy" index as measured by IR transmission during cure of Narmco 5208 resin.

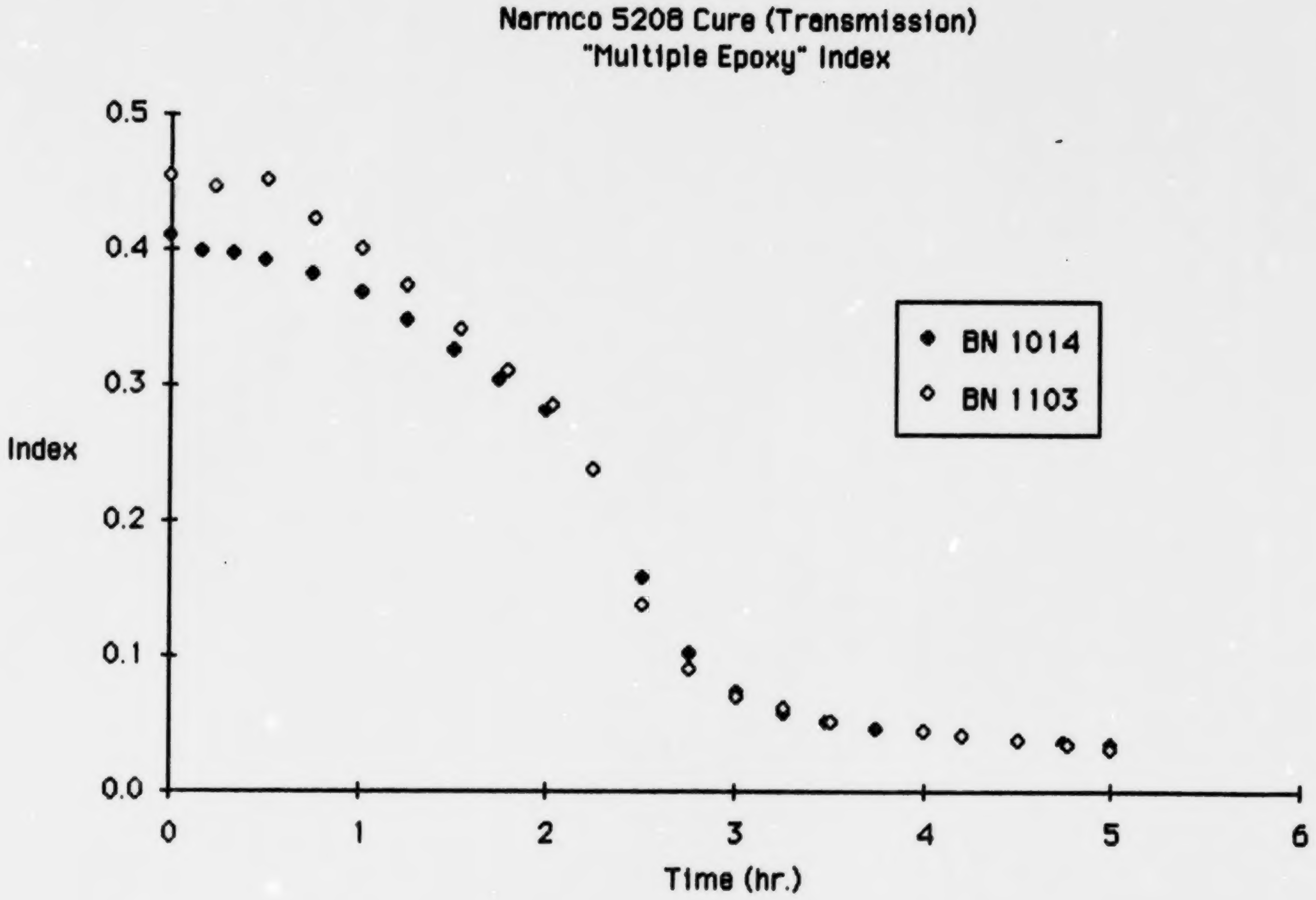

Figure 18 - Variation of "multiple epoxy" index as measured by IR transmission during cure of Narmco 5208 resin.

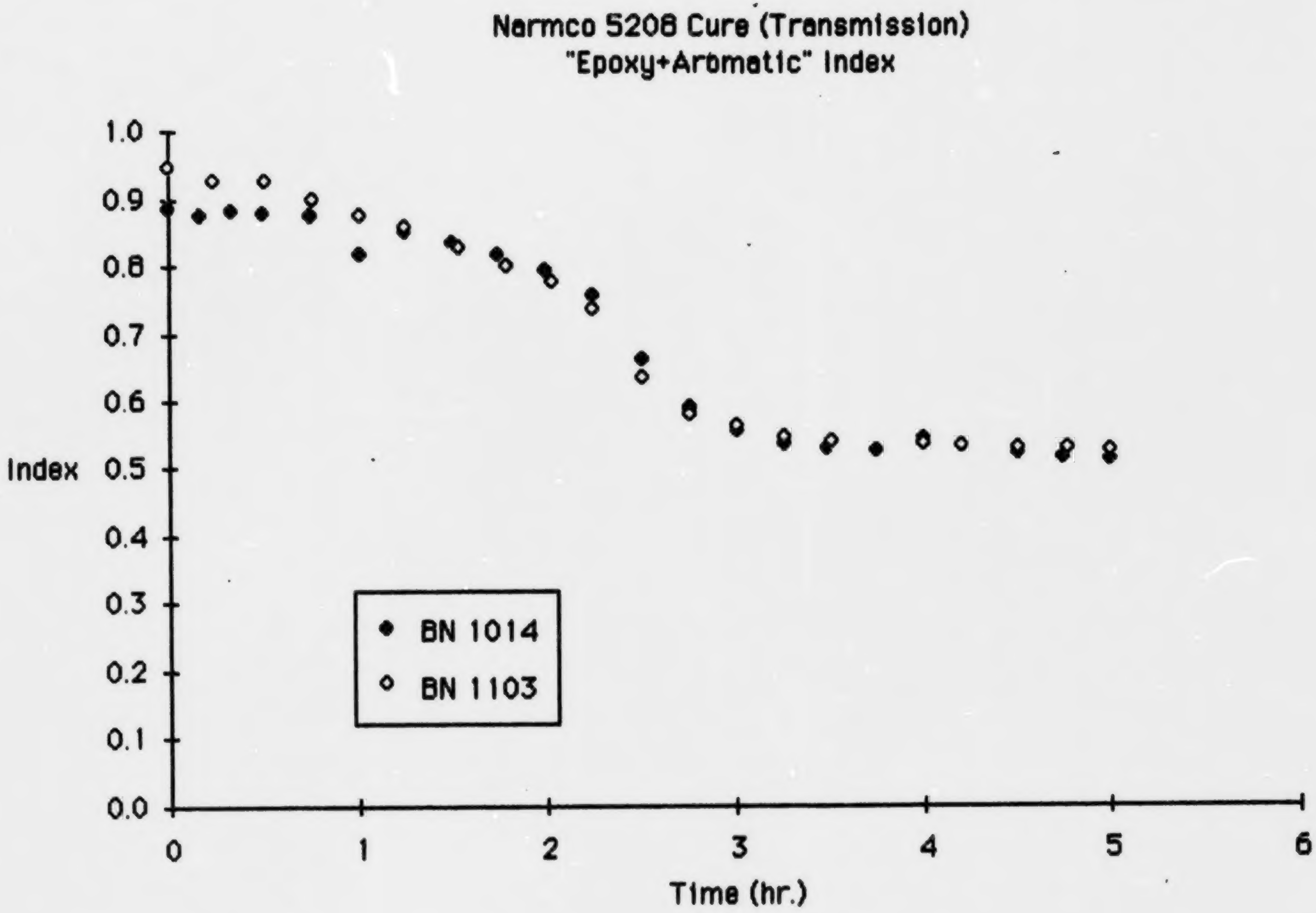

Figure 19 - Variation of "epoxy + aromatic" (band near 830 cm^{-1}) index as measured by IR transmission during cure of Narmco 5208 resin.

behaviour between the minor epoxy resin, which contributes only to the 906 cm^{-1} (single epoxy) band, and the major epoxy resin, which contributes to all three. (It has been shown [14] that the bisphenol A Novolac epoxy reacts with DDS much faster than does the TGDDM.) Whatever the explanation, the "multiple epoxy" index is considered to be a better indicator of the total free epoxy content, since it comprises all the peaks and its behaviour in the initial stages of cure (a gradual drop) is more in keeping with the behaviour expected at such low temperatures. Finally, Figure 19 shows the variation of the band near 830 cm^{-1}, which is generally considered to be an aromatic ring C-H wagging band and has been used as an internal reference instead of the 1517 cm^{-1} band to follow epoxy cure [32]. During the cure, the area of this band decreases in the same way as the epoxy bands, except that the ultimate value is not zero. This is because this band is actually a composite. The peak at 830 cm^{-1} is due to aromatic C-H wagging and appears in both Araldite MY 720 (Figure 5) and Hardener HT 976 (Figure 6). The shoulder at around 800 cm^{-1} is due mainly to epoxy rings [19] of the MY 720. The minor epoxy also contributes somewhat to both bands (Figure 7). In the Narmco 5208, the shoulder at 800 cm^{-1}, which accounts for about 44% of the band area in the two samples studied, disappears when the resin is cured and the epoxy groups react. The phenyl ring absorption remains. Because of this, this band is not really suitable for use as an "internal standard".

3.7 Near-infrared Spectroscopy

The near-IR region, located between the mid-IR and the visible, can also be used to characterize epoxy resins. Absorption coefficients tend to be much weaker than in the mid-IR, so thicker samples must be used. One advantage of this region is the low absorption of glass, which can be used as a cell material or sample support. Results have been reported for quantitative analysis of epoxy content [33, 34], the study of cure kinetics [35-37], and the analysis of moisture [17]. These analyses depend on two distinct bands, one at 4524 cm^{-1} (2.210 μm) arising from epoxy rings, and one at 5213 cm^{-1} (1.918 μm) arising from water. The 4524 cm^{-1} band is especially useful for quantitative analysis when the band near 900 cm^{-1} in the mid-infrared is subject to interference from other bands.

This region is currently of particular interest because it affords the possibility of embedding optical fibres in the organic matrix and using them as waveguides to pass a near-IR beam and probe the interior of the part. In this way, it should be possible to detect moisture penetration within the matrix, as well as monitor the extent of curing and the chemical composition in general. The method is based on the principle of internal reflection, or evanescent wave spectroscopy, which is discussed in Section 4.

To measure the near-IR spectrum of Narmco 5208 resin, a sample of prepreg Batch 1010 was extracted with acetone and a film about 0.2 mm thick was deposited on a glass microscope slide. This was then heated for 5 minutes at 110°C to remove residual acetone and give a more uniform film. The transmission spectrum was measured and the spectrum of the microscope slide subtracted to give the absorption spectrum of the uncured resin. The film was then cured by heating in an oven for 3 hours at 177°C, and the spectrum of the cured resin was measured in the same manner. The sample was then immersed in boiling water for five hours to saturate the cured resin with moisture. In the course of this treatment the film became detached from the slide. It was removed from the water, quickly wiped to remove surface moisture, rapidly weighed, and inserted in the spectrometer, where the spectrum was measured immediately. Finally, the sample was dried at 110°C for 3.5 hours and weighed again to determine the moisture content, which was found to be 5.0%.

The three spectra, measured using the Nicolet FTIR, are shown in Figure 20. The uncured resin shows a strong epoxy peak at 4524 cm^{-1}, as well as a second strong peak at 4054 cm^{-1}. In the cured resin, the epoxy band is much less intense but is still present, indicating that there are still some unreacted epoxy groups. (Further curing for 2 hours at 200°C reduced the intensity of this peak but it still did not disappear.) The 4054 cm^{-1} peak remains strong in the cured resin and could be used as a reference peak. The moisture-saturated cured resin gives essentially the same spectrum as the dry cured resin except for a very obvious water peak at 5213 cm^{-1}. When the sample was redried, this band disappeared completely.

Spectra were also recorded on a Cary 17 spectrometer, which covers the complete near-IR region from 0.7 to 2.5 μm (14300-4000 cm^{-1}). These did not provide any significant new information. They are given, together with further details on the near-IR spectra, in IMRI Internal Report No. 84-101-002.

In conclusion, the near-IR spectra of Narmco 5208 resin show distinct peaks which could be used to monitor the amount of unreacted epoxy and moisture in the resin.

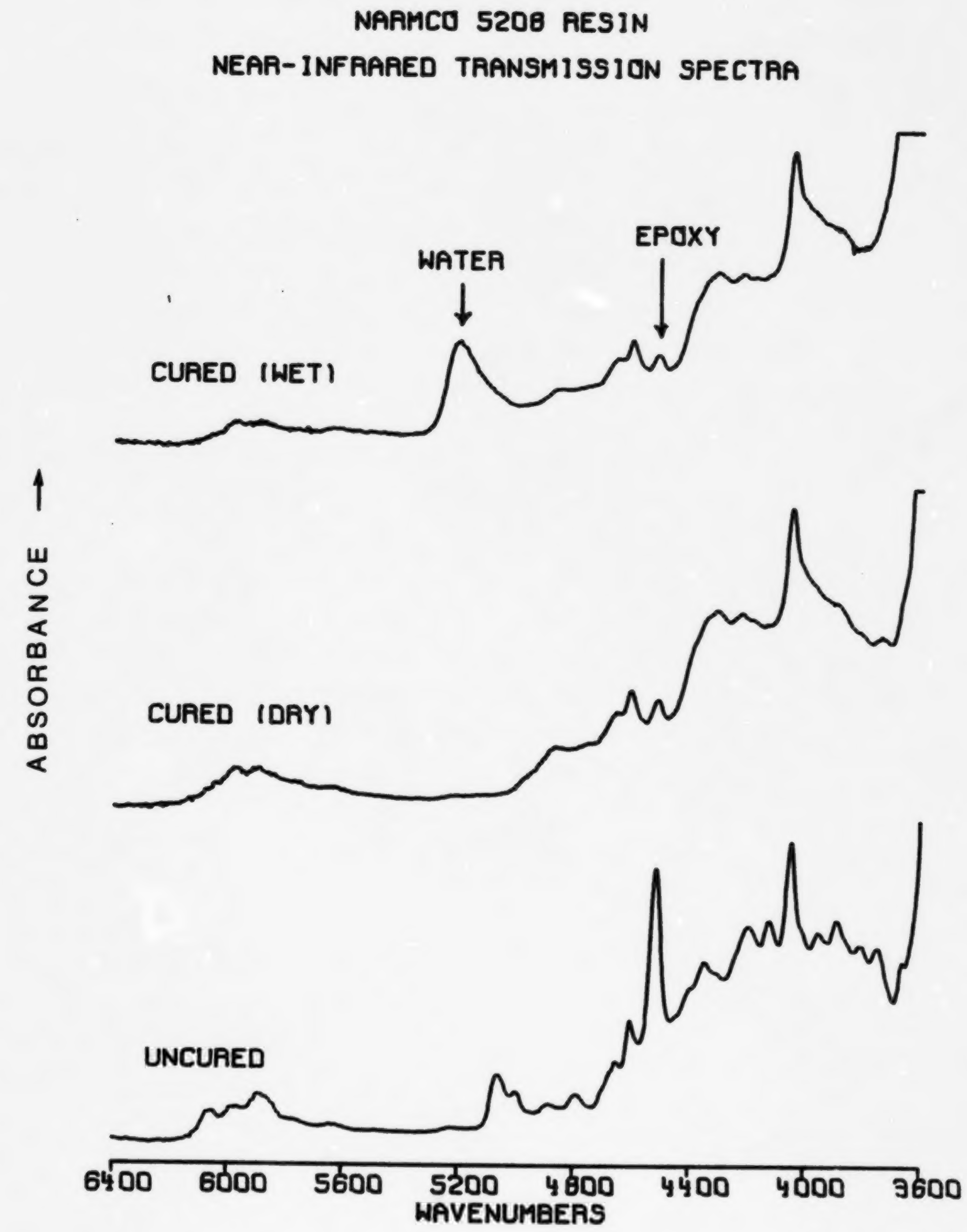

Figure 20 - Near-infrared transmission spectra of Narmco 5208 resin

3.8 Recommended Procedure for Quantitative Analysis of Narmco 5208 Prepreg by IR Transmission

(1) With clean scissors, and wearing gloves, cut a representative square of prepreg about 5 cm by 5 cm.

(2) With tweezers, carefully separate the prepreg from the plastic backing sheet and place it in a clean dry 250 mL Erlenmeyer flask.

(3) Add 25 mL of reagent grade acetone, stopper, and agitate gently for 15 minutes.

(4) Remove the graphite fibres with clean tweezers. The remaining solution contains about 25 mg/mL of resin.

(5) Prepare at least three (preferably five) clean windows of sodium chloride or potassium bromide. These should be of good quality with flat, highly polished surfaces. Repolish if necessary.

(6) In a location well protected from air currents, carefully deposit about 150 µL of resin solution in the centre of each window. A microsyringe can be used to control the amount. Stepwise addition is recommended to avoid having the solution flow over the edge. After each addition, let stand for a short time until the solvent evaporates. Do not blow with air and do not heat. Place the specimens under vacuum (without heating) for 15-30 minutes to remove residual solvent.

(7) Measure the infrared transmission spectra and convert to absorbance units. The strongest peak (1517 cm^{-1}) should have a maximum absorbance between 0.2 and 1.0, and there should be no obvious water vapour peaks in this region. If there are, they should be eliminated either by subtracting a reference spectrum of water vapour or by repeating the spectrum.

(8) Visually compare the spectrum with a reference spectrum of a typical batch and check for any unusual features.

(9) Calculate the areas of the peaks of interest using the available software with baselines drawn between the appropriate valleys. The following limits are suggested but

may be modified if necessary:

Aromatic ring (reference)	1545 - 1485 cm^{-1}
Single sulphone	1166 - 1119 cm^{-1}
Multiple sulphone	1166 - 1046 cm^{-1}
Single epoxy	923 - 875 cm^{-1}
Multiple epoxy	992 - 875 cm^{-1}
Epoxy + aromatic	874 - 779 cm^{-1}.

(10) Calculate "indices" by dividing the peak areas by the area of the aromatic ring reference peak. For routine analyses, the following two indices are considered sufficient: "multiple sulphone" and "multiple epoxy".

(11) The indices obtained for different specimens of the same prepreg sample should normally agree within about 2%. Specimens whose thickness is not uniform will give artificially high values. Specimens which give an index more than 5% higher than the lowest value should be rejected and repeated if necessary in order to give at least three good results for averaging.

(12) Compare the average values to the specifications to determine whether the batch is acceptable.

(13) Clean windows, syringes, etc. with acetone or a 50:50 mixture of acetone and toluene as soon as possible after use.

Note:

This method is suitable for typical B-stage resin. For more advanced prepreg, where the resin is less soluble, it is recommended to do a three-stage extraction using 50, 30, and 20 mL of acetone, followed by concentration of the combined extracts to a volume of about 25 mL on a rotary evaporator. A cloudy solution indicates a high degree of advancement and the results may be unreliable.

4. THE INTERNAL REFLECTION METHOD

4.1 Description of the Method

The technique of internal reflection spectroscopy, also known as attenuated total reflection (ATR) and multiple internal reflection (MIR), has been described in depth by Harrick [38]. A shorter description of the theory, together with some polymer applications, has been given by Knutson and Lyman [39]. The method is widely used for studying the surface of solid samples, and is also being used more and more for highly absorbing liquids and for "on-line" measurement in industrial processes. The principle is illustrated in the following diagram:

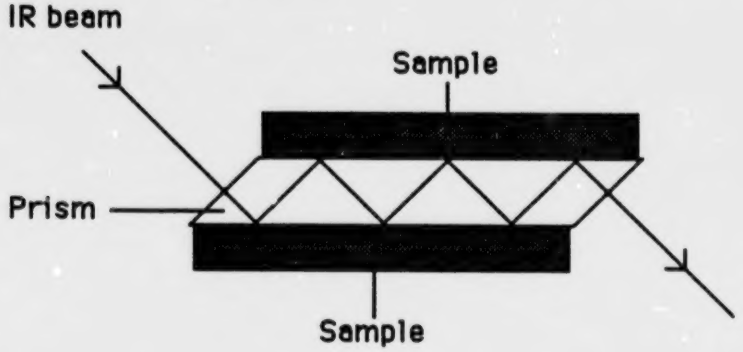

The sample is placed in intimate contact (using pressure if necessary) with an infrared-transmitting prism whose index of refraction is higher than that of the sample. Commonly used prism materials are KRS-5 (thallium bromoiodide) and germanium. In order for total internal reflection to occur, the geometry must be such that the angle of incidence is greater than a certain critical angle given by:

$$\sin \theta_c = n_s/n_p$$

where n_s and n_p are the refractive indices of the sample and prism respectively. Prisms with an angle of incidence of 45° or 60° are generally used. When an absorbing sample is in contact with the prism, the IR beam is "attenuated" by a partial absorption of the evanescent wave existing at the prism/sample interface. Before applying the sample to the prism, a "background" spectrum is recorded for the prism alone. The spectrum is then measured with the sample present and ratioed against this background to give the spectrum of the sample. The exact nature of this spectrum depends on a number of factors such as angle of incidence, indices of refraction of both prism and sample, number of reflections occurring in the prism, and degree of contact between sample and prism. As a result, there are two important differences between ATR and transmission spectra. Firstly, whereas the transmission spectrum of a sample is determined almost exclusively by the absorption coefficient k (Section 3.4), in ATR the index of refraction n can also play an important role. Like k, n also varies with the frequency of the radiation, but in a different manner, as shown qualitatively in the diagram below. The absorption coefficient k is zero except in the vicinity of an absorption band, which usually has a Lorentzian shape. The refractive index n, on the other hand, is approximately constant at frequencies where there is no absorption, but when there is absorption it shows a dispersion-type variation. In ATR, the reflectance at the prism-sample interface is determined by the optical constants (n and k) of both the prism and the sample, as well as by the angle of incidence and the polarisation of the radiation. The exact relationship, which is rather complicated, is given by Fresnel's equations [38]. Generally speaking, when the angle of incidence is much larger than the critical angle, the refractive index contribution is negligible and the ATR spectrum resembles a transmission spectrum. If the angle of incidence is near the critical angle, the refractive index contribution becomes more important and "distorts" the spectrum by introducing some dispersion (derivative) character into the usual Lorentzian-type peak. Refractive index effects can therefore be minimized either by increasing the angle of incidence or by decreasing the critical angle (for example, by using a prism of higher refractive index).

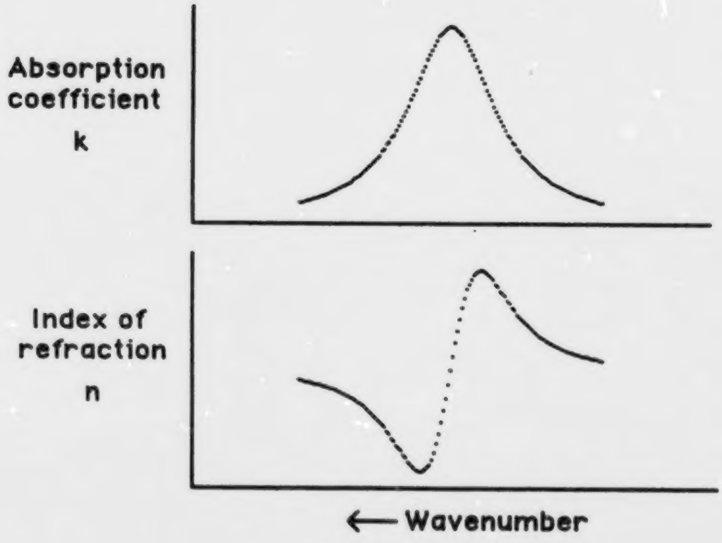

The second difference between ATR and transmission spectra is that, even if refractive index effects are negligible, in ATR the effective sample penetration depth is proportional to the IR wavelength. As a result, ATR spectra appear "skewed" when compared to transmission spectra, with peaks at shorter wavelength (higher wavenumber) appearing less intense. This can be corrected mathematically. Under typical conditions, the effective penetration depth, as defined by Harrick [38], is of the order of magnitude of one micrometre.

4.2 The ATR Spectrum of Narmco 5208 Prepreg

The ATR method is particularly interesting for prepreg analysis because it is possible to measure the IR spectrum directly from the prepreg, without performing the solvent extraction step needed for transmission analysis. The prepreg is simply cut with scissors to give two strips of the appropriate size (about 5 x 1 cm), which are placed in contact with the prism in the ATR accessory. Finger pressure is usually sufficient to give good enough contact to obtain a suitable spectrum of the layer of resin on the surface. Unfortunately, cured composites are difficult to measure in this way because in order to achieve good contact, considerable pressure must be applied, and this can ruin the prism. Some work has been done on cured material [17, 40], but it required the preparation of samples with a very flat surface.

Figure 21 shows the ATR spectrum recorded for a sample of Narmco 5208/WC3000 prepreg (Batch 1010) using a 45° KRS-5 prism (single pass parallelogram, 50 x 10 x 3 mm). Comparison with the transmission spectrum of Figure 3 shows the two to be very similar but not identical. Firstly, the ATR spectrum shows a small peak at 1708 cm^{-1} which does not appear in the transmission spectrum. This was found to be due to a volatile product which was identified from its IR spectrum as acetone, apparently residual solvent from the prepreg manufacturing process. It is not seen in transmission because acetone is used to extract the resin from the prepreg and is then evaporated, together with any other volatiles present, before the spectrum is recorded. Secondly, the ATR spectrum shows an underlying background absorption, particularly at lower wavenumbers, which is due to the graphite fibres. The effect is more pronounced at low wavenumber because this corresponds to longer wavelength. The beam penetrates the surface layer of resin to a greater depth and is absorbed to a greater extent by the graphite cloth, which absorbs at all frequencies without distinctive peaks, as shown by the ATR spectrum of Figure 22. The importance of the graphite absorption will vary depending on the thickness of the surface layer of resin.

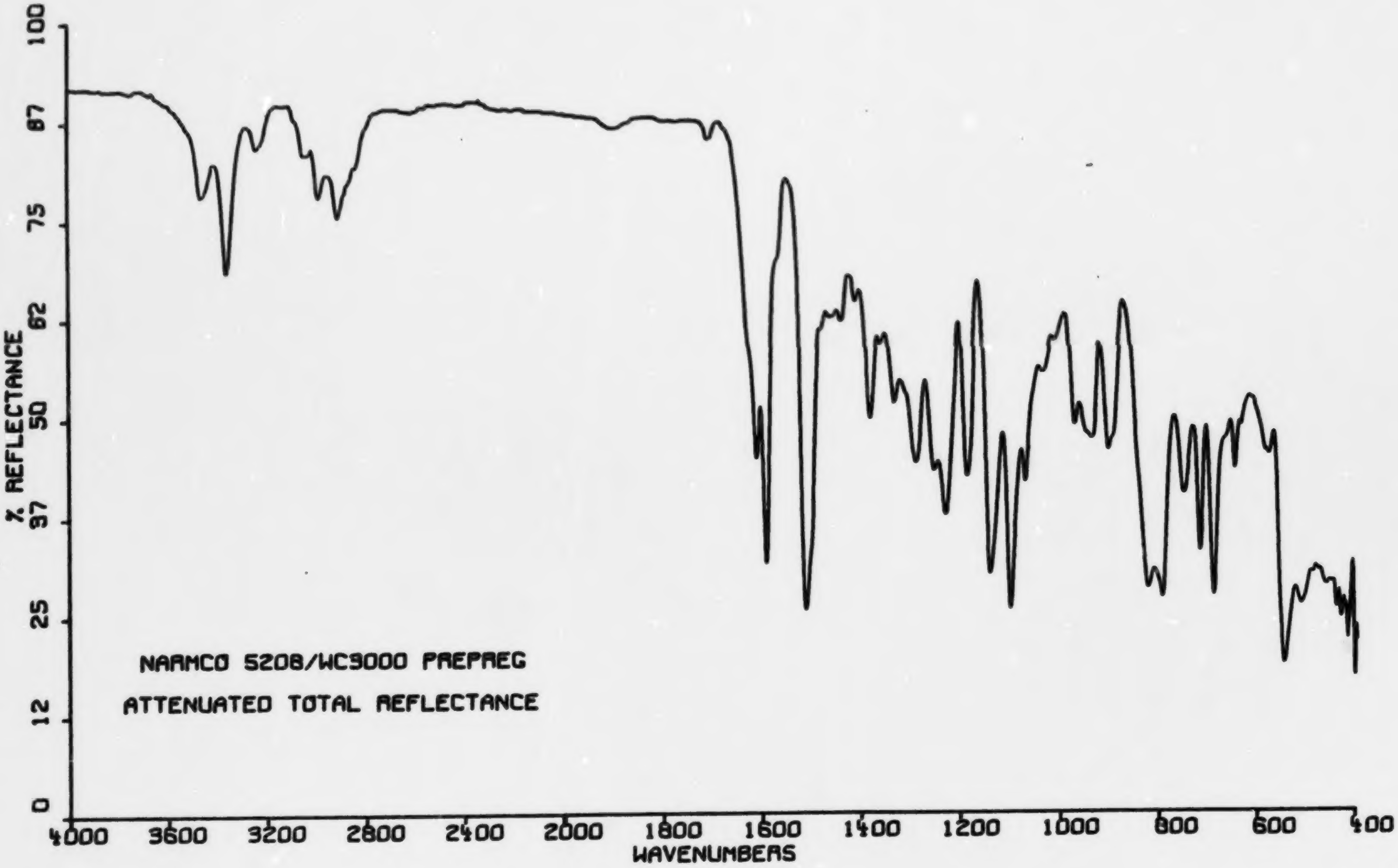

Figure 21 - Attenuated total reflectance IR spectrum of Narmco 5208/WC3000 prepreg Batch 1010 recorded using KRS-5 45° prism.

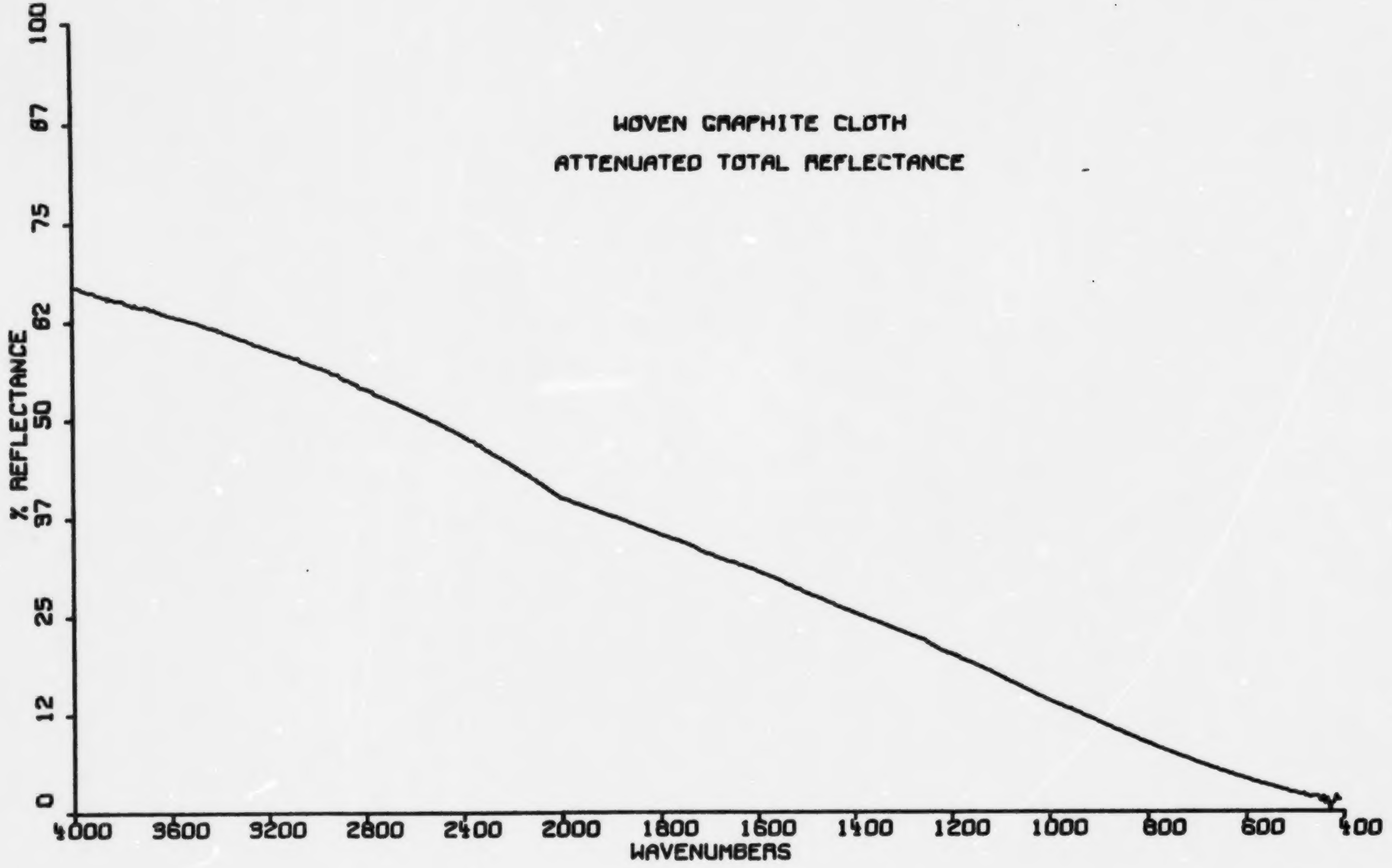

Figure 22 - Attenuated total reflectance IR spectrum of woven graphite cloth (KRS-5 prism, 45°)

The ATR spectrum can be better compared to the transmission spectrum if it is suitably transformed, as shown in Figure 23. This was done by converting to absorbance units, correcting the baseline, and then "normalizing" by multiplying by $\overline{\nu}/1000$, where $\overline{\nu}$ is the frequency in wavenumbers. The latter step corrects to a large extent for the variation of penetration depth with wavelength. However, when the resulting spectrum is compared to the absorbance spectrum measured in transmission (Figure 4) certain differences are still apparent in the form of variations in band shape which result in slight shifts of the peak maxima. These are most obvious in the case of the stronger peaks such as the aromatic ring band at 1517 cm^{-1}, the sulphone bands at 1146 and 1105 cm^{-1}, the aromatic/epoxy peak at 830 cm^{-1}, and the peak at 554 cm^{-1}. (The quoted frequencies correspond to the transmission spectrum of Figure 4.) The reason for this lies in refractive index effects. In regions of strong absorption, the refractive index of the resin increases and becomes closer to that of the prism. The critical angle, which is related to the difference in refractive index, increases and approaches the angle of incidence, with the result that the refractive index has a greater effect on the spectrum.

These effects can be reduced by using a larger angle of incidence or a prism of higher refractive index. This was checked by running ATR spectra using two other prisms, one of KRS-5 ($n = 2.37$) with an angle of 60°, and one of germanium ($n = 4.0$) with an angle of 45°. In Figure 24 these are compared (after the appropriate transformation) with the spectra just described. The KRS-5 60° prism gives some improvement over the KRS-5 45° one, but it is the Ge 45° prism which gives the spectrum most closely resembling the transmission spectrum. The differences are best seen by looking at the band near 830 cm^{-1}. One disadvantage of the Ge prism is that the spectrum ends at 700 cm^{-1} because Ge absorbs strongly beyond this point. A possible advantage of Ge is that the penetration depth is about four times lower than with KRS-5, so the effects of the graphite are less apparent.

4.3 Quantitative Analysis by ATR

A set of experiments was performed to investigate the feasibility of using the ATR method for quantitative analysis of the prepreg. The effects of several parameters were studied, namely:

(i) The type of prism. Three different prisms were used: KRS-5 (45°), KRS-5 (60°), and Ge (45°).

(ii) The presence or absence of prepreg. Spectra were recorded both with the

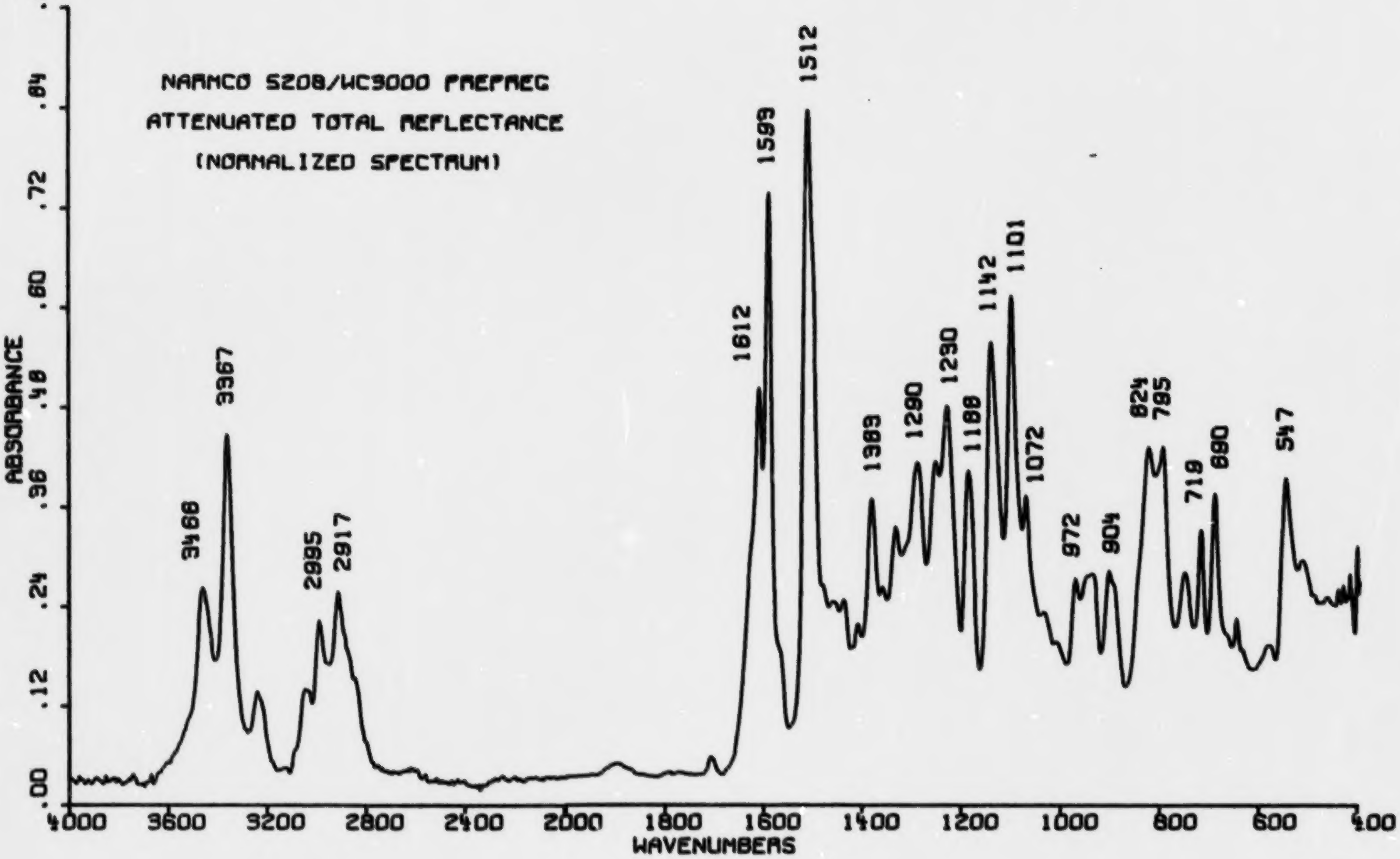

Figure 23 - ATR spectrum of Narmco 5208/WC3000 prepreg, after baseline correction and normalization.

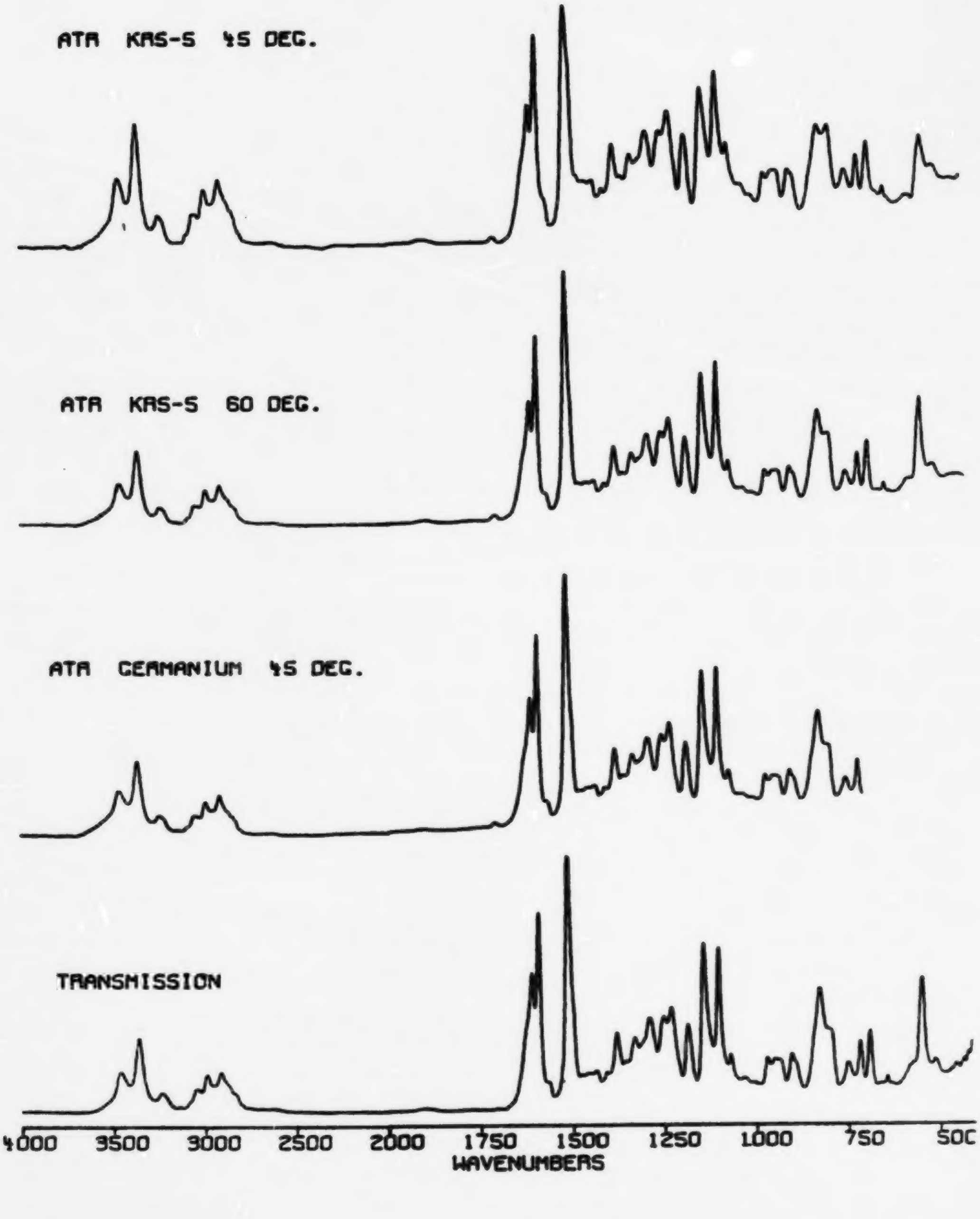

Figure 24 - Comparison of transmission and normalized ATR spectra of Narmo 5208 resin.

prepreg in contact with the prism and after removal of the prepreg. Sufficient resin is left behind on the prism to allow recording of the spectrum without interference from the graphite fibres. The two types of spectrum are labelled "prepreg" and "residue" respectively.

(iii) The fibre orientation. As a result of the 8-harness satin weave pattern used for the graphite cloth, on any given prepreg surface seven-eighths of the fibres are aligned in one direction (labelled the "principal fibre direction") while one-eighth are aligned in a direction perpendicular to this. (This is illustrated in Section 5.3.) Spectra were recorded with the principal fibre direction both parallel to the length of the prism and perpendicular to it.

Batch number 1010 of the Narmco 5208/WC3000 prepreg was selected for study. For each particular set of circumstances, five spectra were measured using fresh specimens for each spectrum. The prism was cleaned with solvent (50:50 acetone/toluene) after each specimen. The spectra were converted to absorbance and treated in the same way as the transmission spectra (Section 3.4). They were not normalized by multiplying by $\bar{\nu}/1000$ since this is an extra step which would not contribute anything to the results. It is necessary only when the spectra are to be directly compared with transmission spectra. When the calculated peak area ratios were examined, the fibre orientation was found to have no observable effect, so the figures for different orientations were combined, giving a total of ten results for averaging. These averages and their standard deviations (both absolute and relative) are shown in Table 6. Spectra measured for the case of the 45° KRS-5 prism with prepreg were not analysed because some bands were overly intense, due to the high effective penetration depth occurring under these circumstances. Examination of the results leads to the following comments:

(1) The reproducibility of the results appears to be lower in the case of the 45° KRS-5 prism, probably due to the greater "distortion" of peaks by refractive index effects, as discussed in Section 4.2. This would also explain why the ratios obtained with this prism are substantially different from those obtained with the others.

(2) The ratios obtained with "residue" spectra are somewhat lower than those obtained with "prepreg" spectra on the same prism. Since the precision is similar in both cases, and the "residue" spectra are not affected by graphite absorption, it might be expected that the "residue" spectra would be preferred. However, this is not the case, as there is another factor which must be considered, namely the thickness of the layer of residue. As pointed out previously, the beam penetration into the sample is proportional to wavelength (inversely proportional to wavenumber). If the layer of resin is sufficiently thin, the beam penetration may exceed the layer thickness at lower wavenumbers, causing

an apparent decrease in absorption intensity. This is the most probable explanation for the deviations observed in the present case. Because the sulphone and epoxy peaks occur at lower wavenumber than the aromatic reference band, they are more affected and the ratio with respect to the aromatic peak is lower than it is in the case of the "prepreg" spectra, where the effective resin layer is much thicker. The fact that the deviation is greater for the epoxy peaks than for the sulphone peaks offers further evidence, since the epoxy peaks occur at lower wavenumber. In the present case, the good reproducibility observed for the "residue" spectra indicates that the thickness of the residual layer is reasonably reproducible. However, a different batch of prepreg, with more viscous (more advanced) resin might leave a much thinner layer. To avoid possible problems related to such variation, it is recommended to record the spectra with the prepreg present.

Table 6. Quantitative analysis of Narmco 5208/WC3000 prepreg Batch 1010 by attenuated total reflection IR

Conditions	Index = Band area divided by area of aromatic reference band			
	Single sulphone	Multiple sulphone	Single epoxy	Multiple epoxy
KRS-5 (45°) Residue	0.595 (0.005, 0.9%)	1.836 (0.035, 1.9%)	0.311 (0.012, 4.0%)	0.938 (0.037, 4.0%)
KRS-5 (60°) Residue	0.562 (0.003, 0.5%)	1.523 (0.008, 0.6%)	0.234 (0.002, 0.9%)	0.698 (0.006, 0.8%)
KRS-5 (60°) Prepreg	0.573 (0.002, 0.3%)	1.561 (0.007, 0.4%)	0.246 (0.002, 0.8%)	0.729 (0.006, 0.8%)
Ge (45°) Residue	0.543 (0.003, 0.5%)	1.403 (0.006, 0.5%)	0.209 (0.002, 1.0%)	0.636 (0.008, 1.2%)
Ge (45°) Prepreg	0.554 (0.001, 0.2%)	1.436 (0.007, 0.5%)	0.220 (0.003, 1.3%)	0.669 (0.008, 1.2%)

(3) Although there is not a lot of difference between the KRS-5 (60°) and Ge (45°) results, the Ge (45°) prism is preferred since refractive index effects are less important and the spectrum better resembles the transmission spectrum. The ratios given in Table 6 are considerably different from those obtained in transmission (Table 3) because the ATR spectra were not normalized. However, the results can be compared if the ATR indices are "corrected" for beam penetration effects by multiplying by $\bar{\nu}$(peak)/$\bar{\nu}$(reference), where $\bar{\nu}$(peak) is the wavenumber corresponding to the centre of the peaks in question, and $\bar{\nu}$(reference) is the wavenumber of the aromatic reference peak. This gives the results shown in Table 7. The ATR ratios are now very close to those obtained in transmission.

Table 7. Comparison of IR transmission and ATR results for Narmco 5208/WC3000 prepreg Batch 1010

Conditions	Index = Band area divided by area of aromatic reference band			
	Single sulphone	Multiple sulphone	Single epoxy	Multiple epoxy
Ge (45°) Prepreg Normalized	0.418	1.065	0.131	0.410
Transmission	0.428	1.072	0.131	0.402

In view of the results just described, the ATR method is recommended over the transmission method for the quantitative analysis of uncured prepreg based on epoxy resins and graphite fibres. Not only is sample preparation faster and simpler, but the results are just as reproducible, if not more, since the problem of variation in sample thickness associated with the transmission method is avoided. A further advantage of the ATR method is that it gives the spectrum of the prepreg as received, whereas the transmission method requires more extensive sample preparation which can change the resin composition. Thus ATR can detect volatile materials such as acetone, which are not detected by the transmission method (Section 4.2).

A detailed description of the recommended ATR method is given in Section 4.5.

4.4 Comparison of Different Batches

Six of the seven batches of Narmco 5208 analysed by IR transmission (Section 3.5) were also analysed by the recommended ATR method. Batch Number 1023 was excluded because it consisted of neat resin rather than prepreg. The results are summarized in Table 8. Each result is an average over five specimens with the standard deviation shown in parentheses. In most cases the deviation is less than 1%, so the reproducibility appears to be as good as in transmission. The calculated indices differ from those obtained in transmission because they are not corrected for the frequency dependence of the sample penetration. As in transmission, comparison of the different batches shows no substantial variations. All multiple sulphone ratios lie within ±2% of the mean (1.481), and all multiple epoxy ratios lie within ±3% of the mean (0.677). These ranges are only about half as wide as observed in transmission, and the reason is not obvious. However, the general trends are much the same. Using the multiple epoxy index, the batches can be arranged in order of free epoxy content as follows: 1047 > 1101 > 1014 ≈ 1010 > 1104 > 1103. Except for 1101 and 1014, this is the same order found by transmission. The sulphone results are more difficult to interpret, as was the case in transmission, because of the low overall variation. About the only reasonably definite conclusion which can be drawn, based on the multiple sulphone indices observed in ATR and transmission, is that BN 1101 appears to have a slightly low hardener content.

Table 8. Quantitative analysis of different batches of Narmco 5208/WC3000 prepreg by attenuated total reflection IR

Batch No.	Index = Band area divided by area of aromatic reference band			
	Single sulphone	Multiple sulphone	Single epoxy	Multiple epoxy
1010	0.558 (0.002)	1.482 (0.006)	0.231 (0.002)	0.677 (0.008)
1014	0.552 (0.003)	1.486 (0.009)	0.234 (0.002)	0.676 (0.006)
1101	0.565 (0.002)	1.457 (0.005)	0.239 (0.002)	0.688 (0.004)
1103	0.582 (0.001)	1.509 (0.004)	0.228 (0.001)	0.656 (0.005)
1104	0.565 (0.005)	1.468 (0.012)	0.230 (0.004)	0.668 (0.015)
1047	0.568 (0.001)	1.484 (0.002)	0.237 (0.001)	0.694 (0.003)

4.5 Recommended Procedure for Quantitative Analysis of Narmco 5208 Prepreg by IR Spectroscopy Using ATR

(1) Make sure that the internal reflection accessory is installed in the spectrometer and properly aligned. A 45° germanium prism of length 50 mm is recommended.

(2) With clean scissors, and wearing gloves, cut two strips of prepreg of approximately the same size as the prism surface.

(3) Record the "background" spectrum using the clean prism only, accumulating as many scans as necessary to give an acceptable noise level (at least 100).

(4) With tweezers, carefully remove the plastic backing sheet from the prepreg samples and place the freshly exposed surfaces in contact with the prism, one on each side. Press with the fingers to ensure good contact. If the prepreg has lost its tack and flexibility, it may be necessary to use pressure clamps to achieve sufficient contact.

(5) Record the spectrum with the prepreg in place and ratio against the background spectrum.

(6) Convert the spectrum to absorbance and check the intensity. The strongest peak (1517 cm^{-1}) should have a maximum absorbance between 0.2 and 1.0, and there should be no obvious water vapour peaks in this region. If there are, they should be eliminated either by subtracting a reference spectrum of water vapour or by repeating the spectrum.

(7) Visually compare the spectrum with a reference spectrum of a typical batch and check for any unusual features.

(8) Calculate the areas of the peaks of interest using the available software with baselines drawn between the appropriate valleys. The following limits are suggested but may be modified if necessary:

Aromatic ring (reference)	1545 - 1485 cm^{-1}
Single sulphone	1163 - 1120 cm^{-1}
Multiple sulphone	1163 - 1043 cm^{-1}

Single epoxy	921 - 872 cm^{-1}
Multiple epoxy	992 - 872 cm^{-1}.

(9) Calculate "indices" by dividing the peak areas by the area of the aromatic ring reference peak. For routine analyses, the following two indices are considered sufficient: "multiple sulphone" and "multiple epoxy".

(10) Measure at least three different specimens of a given prepreg sample. The spread between the lowest and highest values of a given index should not exceed 5%. If so, more specimens should be measured in order to obtain at least three good results for averaging.

(11) Compare the average values to the specifications to determine whether the batch is acceptable.

(12) After each specimen, the prism should be cleaned with solvent (acetone or 50:50 acetone-toluene) and thoroughly dried. Cotton wool swabs are recommended for wiping the prism.

5. THE DIFFUSE REFLECTION METHOD

5.1 Description of the Method

Although diffuse reflection (DR) spectroscopy has been known and studied for a long time, it did not come into widespread use in infrared spectroscopy until the highly sensitive FTIR instruments were developed. Since then it has proved extremely useful in a number of applications [41-44]. It is sometimes referred to as DRIFT (Diffuse Reflectance Infrared Fourier Transform). The following diagram illustrates the principle:

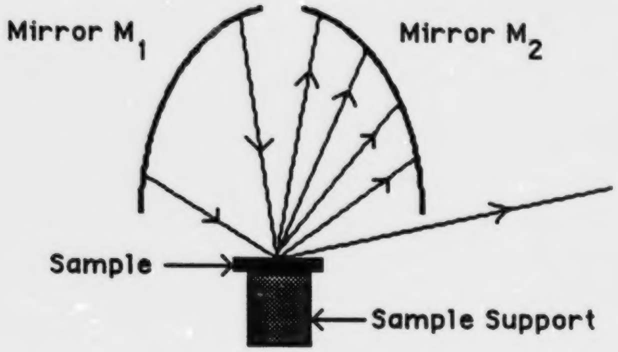

An elliptical mirror (M_1) focuses the infrared beam onto the surface of the sample, which may be a powder or a rough surface. Part of it is absorbed and the rest is reflected in all directions. A second elliptical mirror (M_2) captures some of this scattered (diffuse) radiation and focuses it toward the infrared detector for analysis. The resulting spectrum is compared to that of a non-absorbing reference such as powdered potassium bromide in order to determine the absorption properties of the sample.

Although generally applied to powders, diffuse reflection can be applied to any matte surface which reflects diffusely. As a result, it is particularly interesting for the study of composites, because it can be used not only for prepreg but also for cured parts. The spectrum can be obtained directly from the surface with no sample preparation other than cutting a piece small enough to fit inside the reflectance accessory. With certain types of accessory ("upward-looking" models) even this is not necessary, and actual parts can be examined in a non-destructive manner. Recently Young et al. [45, 46] have reported use of the method to study curing and degradation in composites.

Unfortunately, diffuse reflection suffers from one important complication, namely front-surface reflection [47]. This is illustrated below for the case of a fibre-reinforced epoxy-matrix composite.

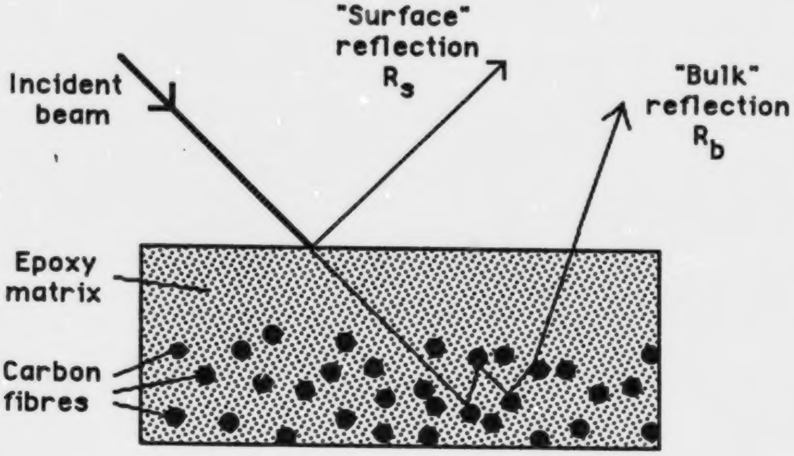

When the incident infrared beam impinges on the sample surface, part of it is reflected immediately before it ever enters the sample ("surface" reflection R_s). This reflection is governed by the laws of Fresnel, and depends on the angle of incidence, the polarisation of the beam, the index of refraction n of the sample, and the absorption coefficient k. The general relationship is quite complex, but for the special case of normal incidence it reduces to:

$$R = \frac{(n-1)^2 + \left(\frac{k}{4\pi\bar{\nu}}\right)^2}{(n+1)^2 + \left(\frac{k}{4\pi\bar{\nu}}\right)^2}$$

where $\bar{\nu}$ is the frequency in wavenumbers. As discussed in Section 4.1, both k and n vary with frequency. In regions where there is no absorption ($k = 0$), n is approximately constant, and for a typical organic material ($n \approx 1.5$), R is of the order of 4%. In the region of an absorption band, k passes through a maximum while n varies according to a dispersion-type curve. The net result is that the reflectivity varies with frequency and, paradoxically, can increase substantially at frequencies where the sample strongly absorbs. This is known as the reststrahlen effect. In the limiting case of very large k, R becomes equal to 1, or 100%.

That part of the beam which enters the sample undergoes absorption according to the Beer-Lambert law:

$$I = I_0 \exp(-kb)$$

where I_0 is the intensity of the entering beam, and I is the intensity after it has travelled a distance b within the sample. Eventually, it encounters a fibre-epoxy interface, where partial reflection occurs. After one or more such reflections, it can leave the sample again as R_b (for "bulk" reflection). The frequency dependence of this beam can be quite different from that of R_s because it depends primarily on k rather than on n. It more closely resembles that of a normal transmission spectrum. Both R_s and R_b are detected by the infrared detector, and the form of the resulting spectrum depends on the relative contributions of the two, which in turn depend on the nature of the sample. In some cases (for example, organic powders dispersed in KBr powder), R_s is negligible and the spectrum is similar to the transmission spectrum. In other cases (for example, highly absorbing materials or inorganic materials with a high index of refraction) R_s can dominate the spectrum to the point where it is almost unrecognizable compared to the transmission spectrum.

Even when front-surface reflection is negligible, the diffuse reflectance spectrum differs somewhat from the transmission spectrum, as a result of the physical differences involved. Absorption bands occur at much the same frequencies, but their relative intensities are different, since the Beer-Lambert law is not directly applicable. Instead, the following equation, which was developed by Kubelka and Munk, is widely used:

$$F(R_\infty) = (1 - R_\infty)^2 / 2 R_\infty = k/s$$

In this equation, R_∞ is the diffuse reflectance of the sample, which is assumed to be "infinitely thick", k is the absorption coefficent, and s is a scattering coefficient. The equation may be compared with the Beer-Lambert law for transmission:

$$A = -\log_{10}T = 0.4343\,kb$$

where A is the absorbance, T is the transmittance, and b is the sample thickness. Both the Kubelka-Munk function $F(R_\infty)$ and the absorbance A are related to the absorption coefficient k, but whereas b is a constant, the scattering coefficient s varies with frequency. Usually, however, the variation is gradual, and a diffuse reflectance spectrum converted to Kubelka-Munk units is very similar, although not identical, to a transmission spectrum converted to absorbance units. Although the Kubelka-Munk equation was derived for the case of a powdered sample, it is sometimes applied to other types of sample for which an appropriate model is lacking.

5.2 The Diffuse Reflectance Spectrum of Narmco 5208 Prepreg

Figure 25 shows the diffuse reflectance spectrum, as measured, of Narmco 5208/WC3000 prepreg (Batch 1010). To obtain this spectrum, a small square of prepreg (about 1 cm x 1 cm) was cut with scissors and mounted with double-sided adhesive tape on a flat horizontal support whose height could be adjusted to optimize the energy throughput in the diffuse reflectance accessory. The support was obtained from Harrick Scientific Corp. and is normally supplied with a mirror for checking the performance of the DR accessory. The sample height adjustment was found to be quite critical. As discussed in the next section, fibre orientation was also found to be important; the spectrum shown was obtained using the optimum orientation. All diffuse reflectance spectra discussed in this report were measured using as a "background" powdered infrared-grade potassium bromide placed in the standard sampling cup (14 mm diameter) and compacted with a spatula to give a smooth level surface. Spectra were generally recorded using 128 scans.

The most striking feature of the spectrum is the strong background absorption, which prevents the overall reflectance from exceeding about 40%. This is due largely to absorption by the graphite fibres, and is more pronounced than in the ATR spectra because the beam penetrates further into the prepreg and interacts with the graphite to a greater extent. The DR spectrum of graphite cloth is shown in Figure 26; as in ATR (Figure 22), there are no distinctive peaks. In the ATR spectrum the reflectance decreases at lower wavenumber because the effective penetration depth, and hence the absorption, increases with wavelength. In the DR spectrum, this is not the case. Instead the reflectance decreases somewhat toward higher wavenumber, probably because of increased scattering losses, which affect the shorter wavelengths to a greater extent. All the peaks seen in

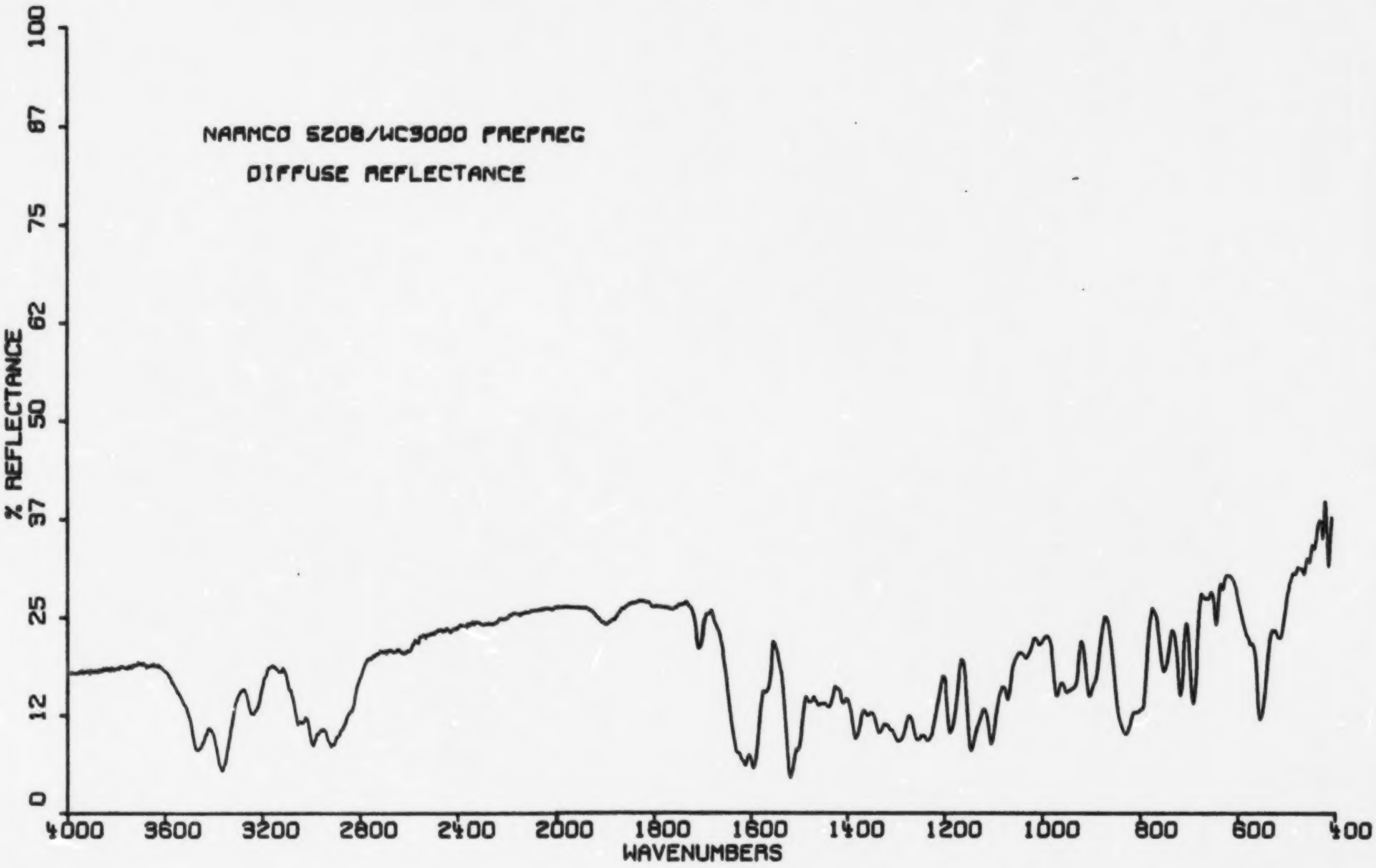

Figure 25 - Diffuse reflectance IR spectrum of Narmco 5208/WC3000 prepreg Batch 1010, as recorded.

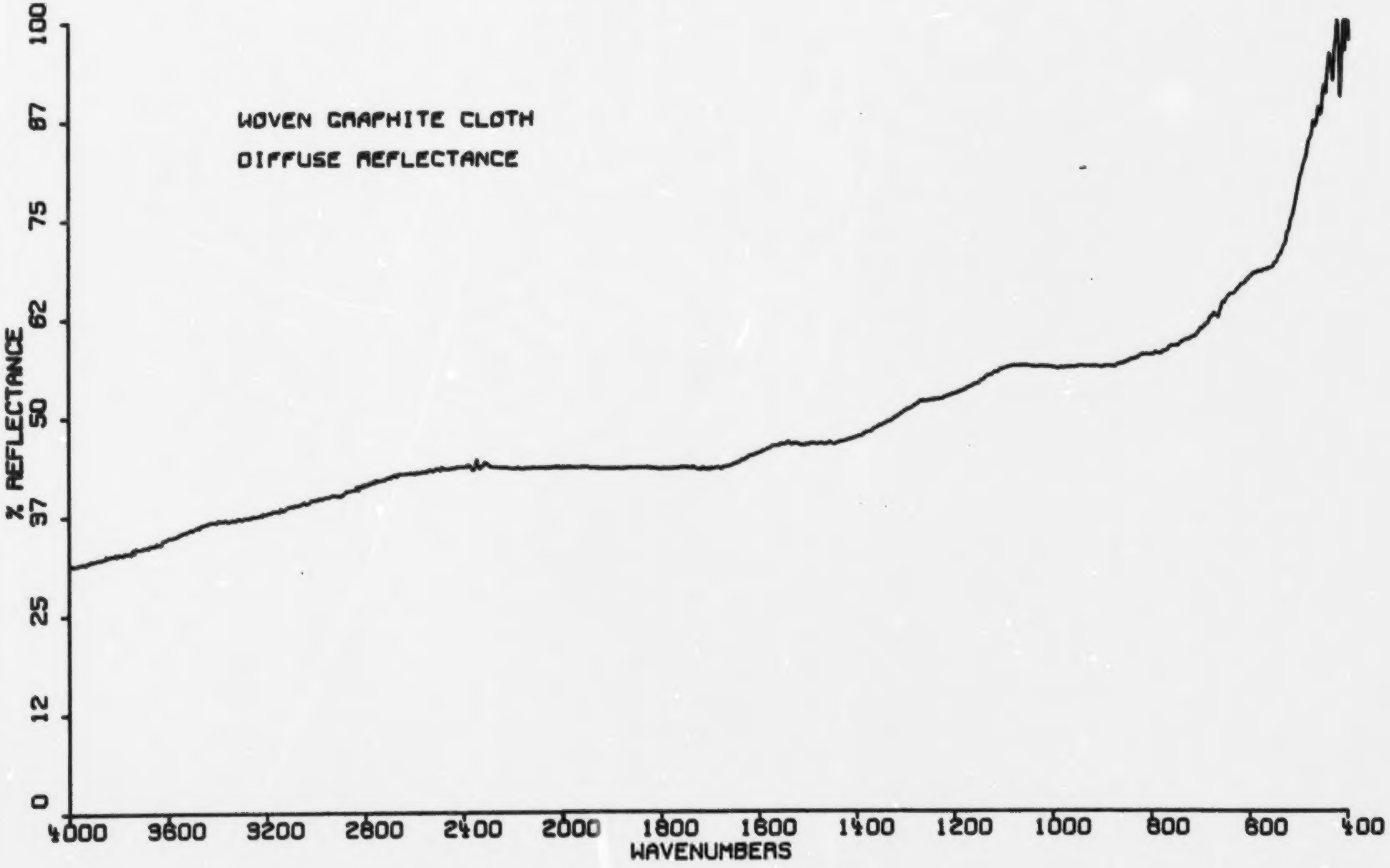

Figure 26 - Diffuse reflectance IR spectrum of woven graphite cloth.

Figure 25 correspond to those observed in transmission (Figure 3), except for the peak at 1708 cm^{-1}, which is due to residual acetone left in the prepreg by the solvent impregnation process. This peak is also observed in ATR (Section 4.2). Figure 27 shows the prepreg spectrum of Figure 25 after conversion to Kubelka-Munk units and correction of the baseline to remove the graphite absorption. When this is compared to the transmission spectrum in absorbance units (Figure 4), it is seen to be very similar, although there are slight differences in peak positions, band shape, and relative peak intensities. However, there is no loss of detail in the diffuse reflectance spectrum.

Figure 28 shows the DR spectrum of a cured test panel made from four plies of Narmco 5208/WC3000 prepreg (Batch 1014). This was measured in the same way as for the prepreg using a small square cut with a jigsaw and attached to the sample support using two-sided adhesive tape. As in the case of the prepreg, the graphite absorption is important, but when converted to Kubelka-Munk units and baseline-corrected, the spectrum (Figure 29) bears a close resemblance to the transmission spectrum (Figure 9). Since the test panel was cured under vacuum, there are no oxidation peaks at 1722 and 1667 cm^{-1}. The weak but definite peaks in the 1000-900 cm^{-1} region show that this particular panel contains a significant number of unreacted epoxy groups. This spectrum is of excellent quality and illustrates very well the usefulness of diffuse reflectance FTIR as a non-destructive method for monitoring the cure and composition of graphite-epoxy composites. (For the method to be truly non-destructive, it would be necessary to use a different sampling configuration which would not require cutting a piece of the sample.)

5.3 Importance of Fibre Orientation

As mentioned in Section 4.3, the prepreg used in this work involved graphite cloth based on an 8-harness satin weave pattern, which is illustrated in the diagram following this paragraph. Each fill yarn passes alternately over seven warp yarns and under one. Consequently, on a given prepreg surface, seven-eighths of the total area is covered by fibres aligned in one particular direction, which will be called the "principal fibre direction". To check the importance of sample orientation, spectra were measured for a given sample in the Harrick "praying mantis" accessory using two different orientations of the principal fibre direction with respect to the beam propagation direction of the instrument, i.e. "parallel" and "perpendicular". The results are shown in Figure 30. It is immediately obvious that the "parallel" orientation gives much better spectra, both for uncured prepreg and cured panels. The overall energy throughput is two to four times higher and the spectral contrast is much enhanced. All subsequent DR spectra were

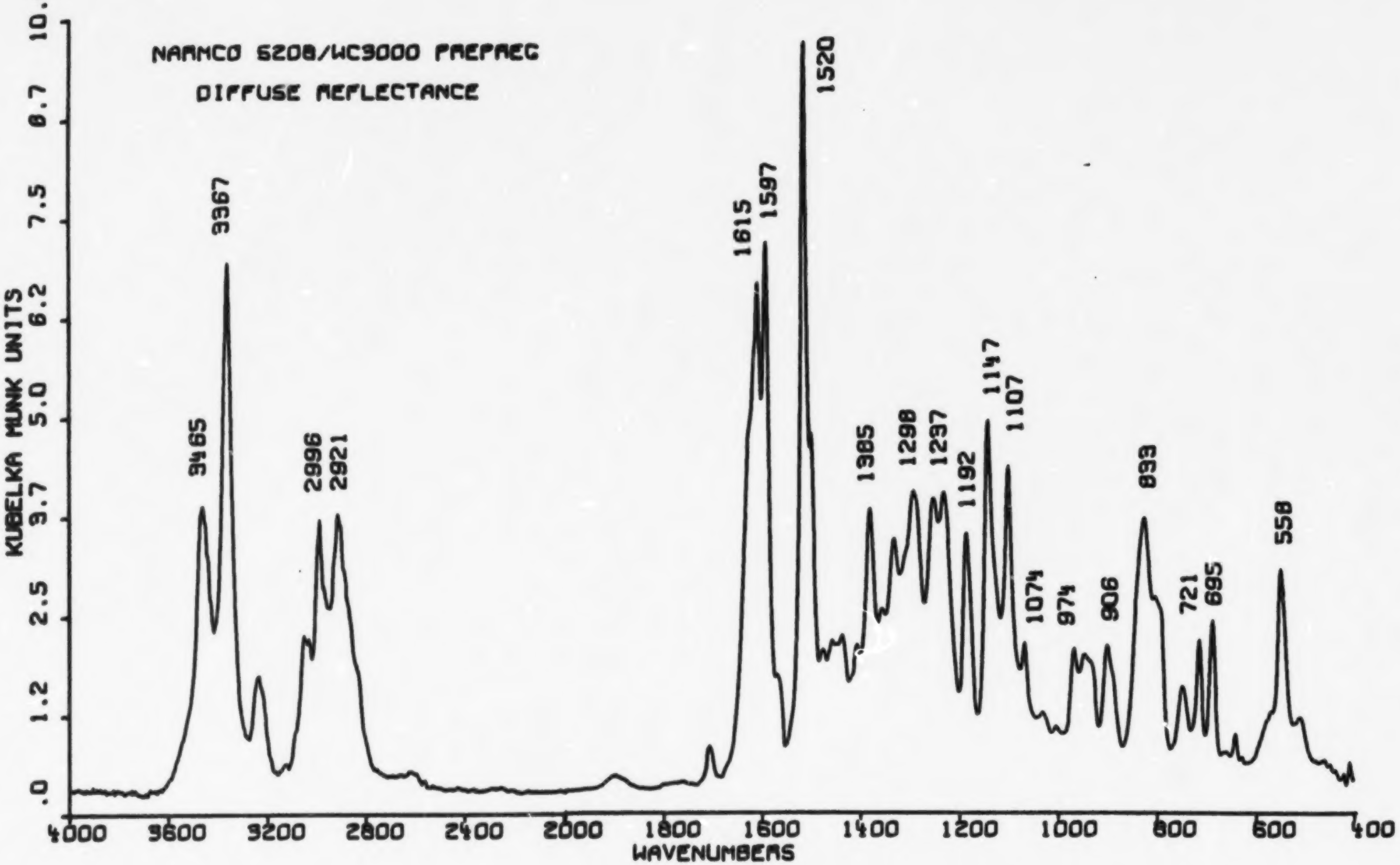

Figure 27 - Diffuse reflectance IR spectrum of Narmco 5208/WC3000 prepreg, after conversion to Kubelka-Munk units and baseline correction.

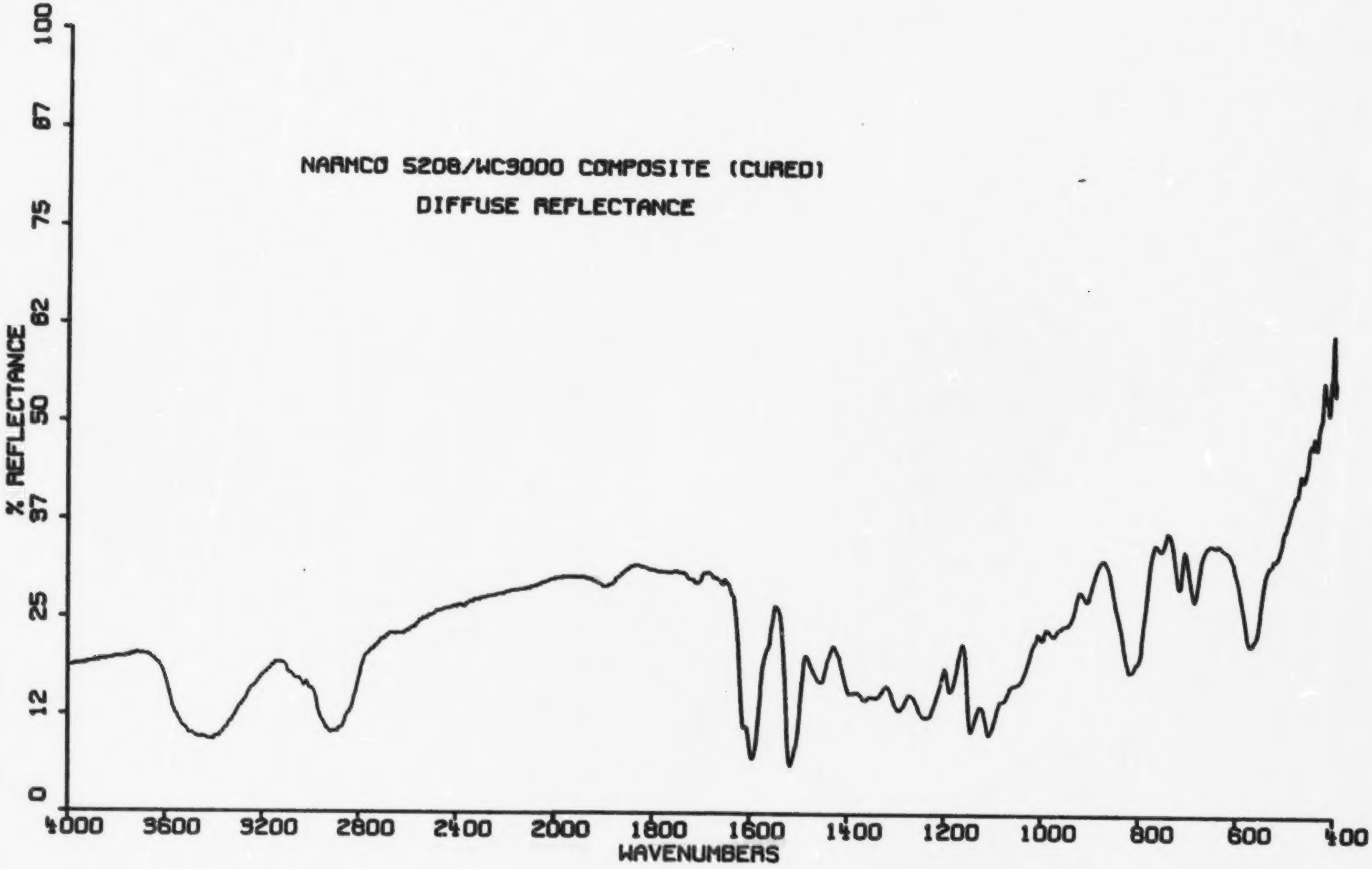

Figure 28 - Diffuse reflectance IR spectrum of cured laminate made from Narmco 5208/WC3000 prepreg.

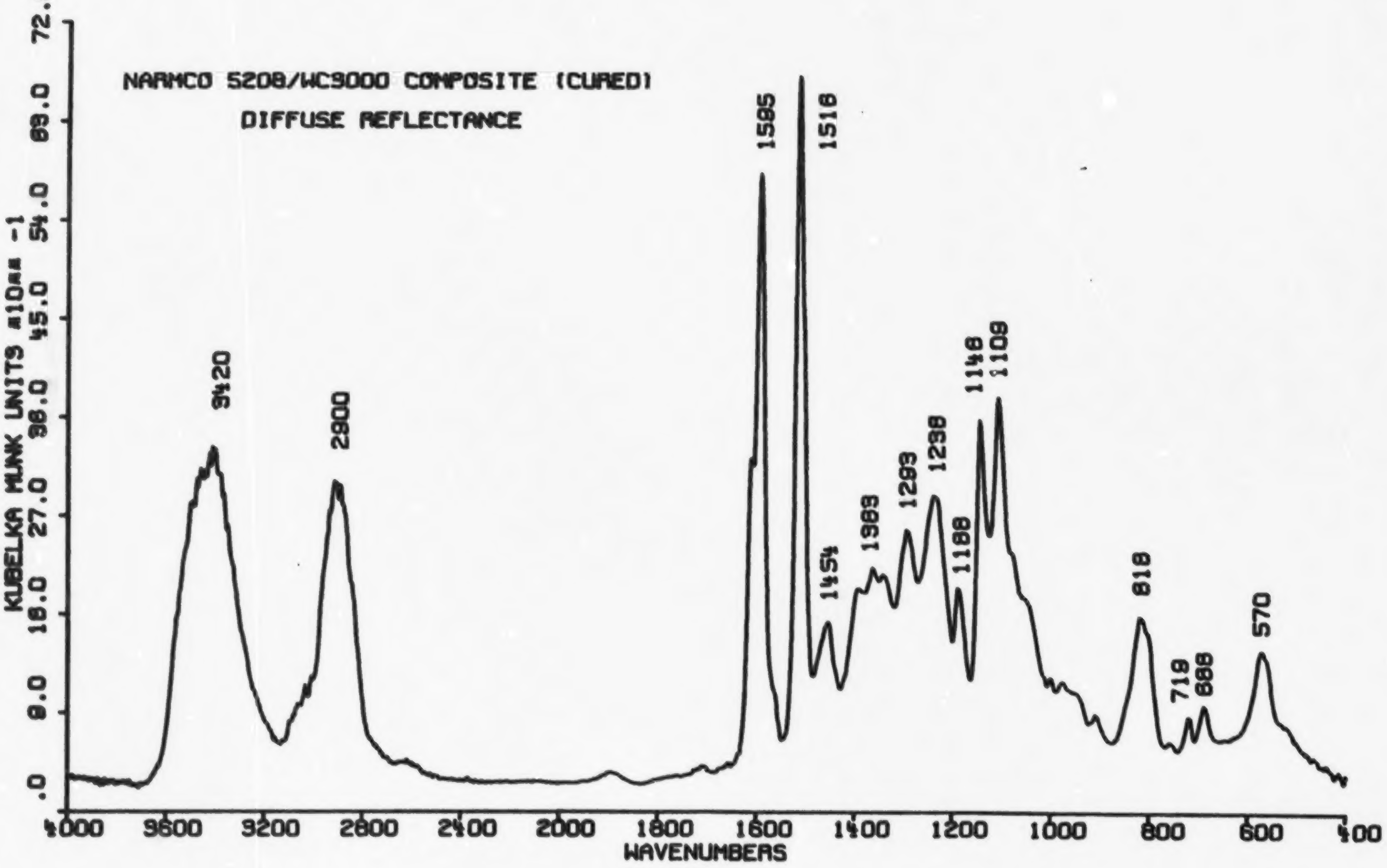

Figure 29 - Diffuse reflectance IR spectrum of cured laminate made from Narmco 5208/WC3000 prepreg, after conversion to Kubelka-Munk units and baseline correction.

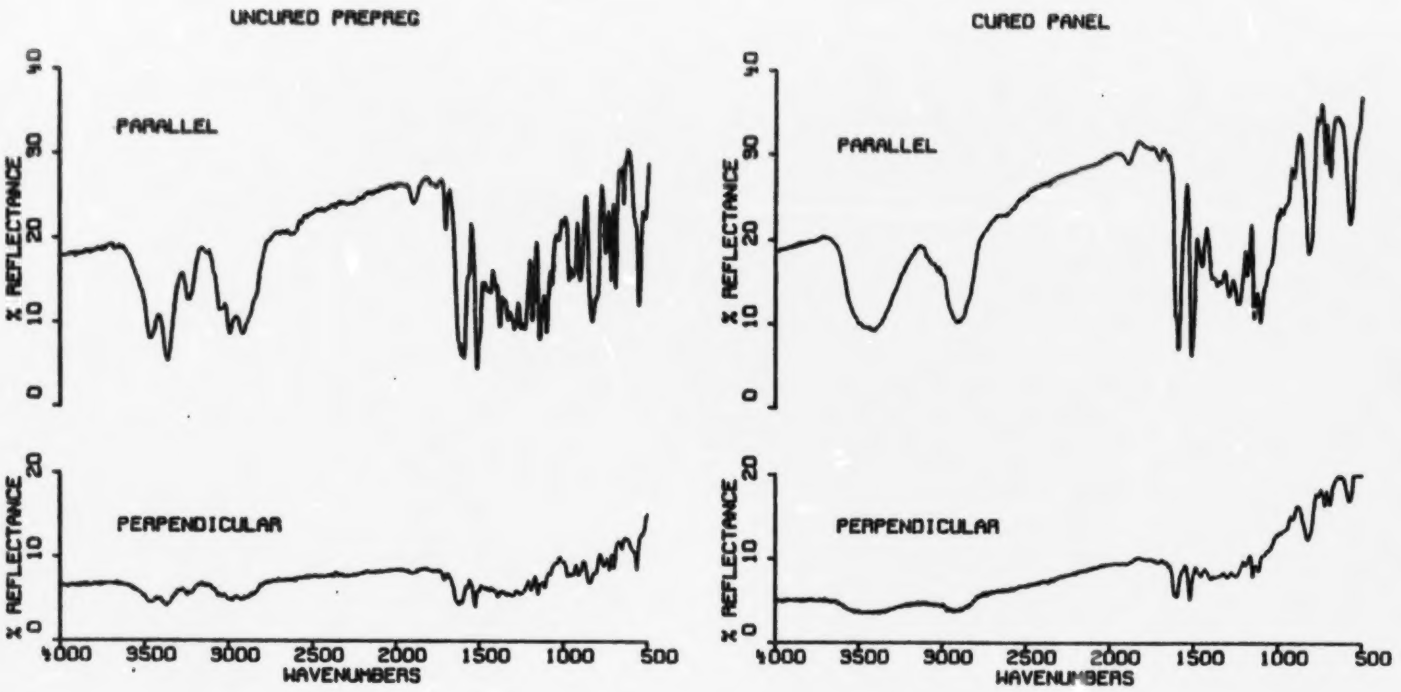

Figure 30 - Effect of fibre orientation direction on diffuse reflectance IR spectrum of Narmco 5208/WC3000 prepreg and cured laminate.

measured using the "parallel" orientation. This effect would be expected to be even more important for materials based on unidirectional tape, but would not be significant for those based on a regular two-dimensional weave pattern.

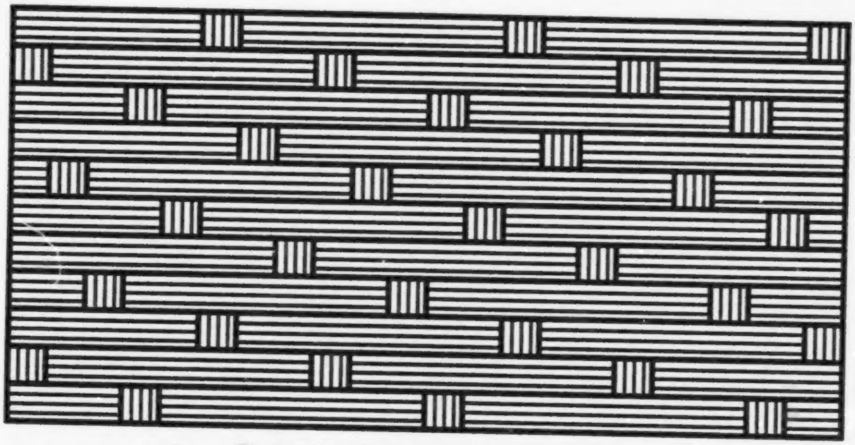

8-harness satin weave pattern

5.4 Quantitative Analysis by Diffuse Reflection

As in the case of transmission and ATR, an experiment was done to evaluate the feasibility of using diffuse reflectance for quantitative analysis of the prepreg. Although there are complications associated with the technique, it was felt that these might be reproducible enough so that it could still be used, if only in a somewhat more empirical manner than the other methods. If so, it would offer two important advantages: negligible sample preparation and the fact that it can be applied to composites at all stages of cure.

The prepreg used was Narmco 5208/WC3000, Batch 1010. A total of eighteen specimens were cut and measured using the optimized procedure outlined in Section 5.7. Spectra were converted to both Kubelka-Munk and absorbance units and peak areas and ratios were calculated in the same way as for transmission and ATR. The results are summarized in Table 9. The reproducibility is unacceptably poor, with standard deviations up to 16%. The results obtained using absorbance units are somewhat more reproducible, even though conversion to absorbance is less "correct" and the spectra do not resemble the true absorbance spectra as well as those expressed in Kubelka-Munk units. Nevertheless, the variation is still unacceptably high for routine quantitative analysis.

Table 9. Quantitative analysis of Narmco 5208/WC3000 prepreg Batch 1010 by diffuse reflection IR

Units used	Index = Band area divided by area of aromatic reference band			
	Single sulphone	Multiple sulphone	Single epoxy	Multiple epoxy
Kubelka-Munk units	0.408 (0.044, 10.8%)	1.118 (0.127, 11.4%)	0.179 (0.028, 15.6%)	0.567 (0.085, 15.0%)
Absorbance units	0.489 (0.028, 5.7%)	1.486 (0.097, 6.5%)	0.314 (0.029, 9.2%)	0.986 (0.088, 8.9%)

Close examination of the set of spectra obtained showed a variation in the shapes of certain bands. For instance, the aromatic ring reference band near 1520 cm^{-1} is particularly affected and the shoulder near 1500 cm^{-1} varies dramatically in prominence. The reason for this is believed to be primarily a variation of the thickness of the surface layer of resin on the prepreg, which gives rise to a variation in the relative importance of front-surface reflection effects. When the layer is thicker, the part of the beam which penetrates the resin is highly absorbed, so the component R_b is diminished and R_s dominates the spectrum. The effect is illustrated in Figure 31, which compares four different spectra of Narmco 5208. On the top left is the true transmission spectrum. On the top right is a true front-surface reflection spectrum, measured with a Harrick External Specular Reflection Attachment (30°) on a thick layer of 5208 resin deposited on a transparent KBr window. It is quite different from the transmission spectrum; the "dispersion-like" distortion caused by the refractive index variation is very evident. Below these spectra are two diffuse reflectance spectra measured on prepreg. One ("resin-poor") was measured for a specimen bearing a thin layer of resin on the surface. It resembles the transmission spectrum fairly well. The other ("resin-rich") was obtained for a specimen where the layer of resin was obviously thicker. Compared to the "resin-poor" spectrum, the band shapes are distorted and approach those of the front-surface reflection spectrum, thus confirming the postulated

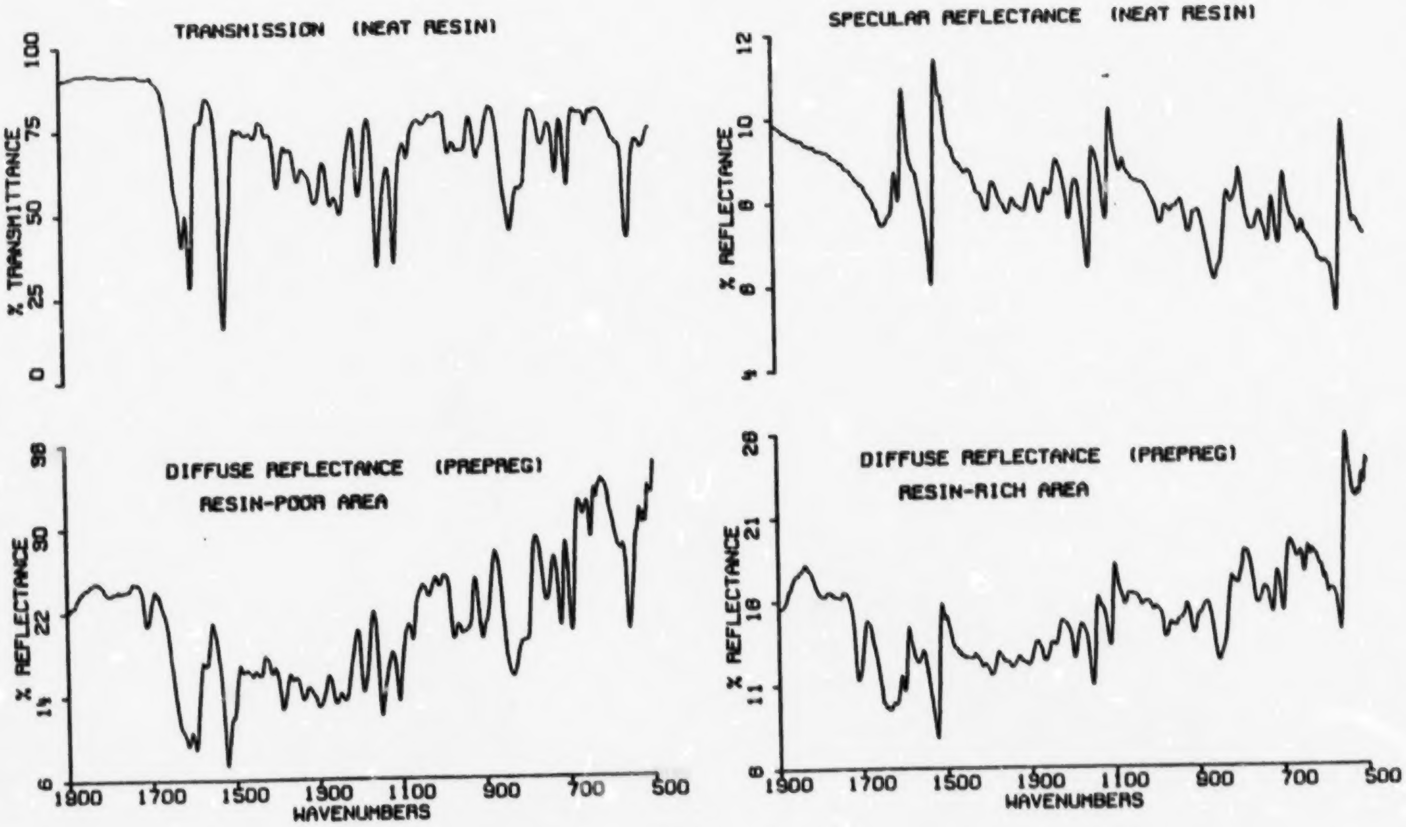

Figure 31 - Comparison of transmission, specular reflectance, and diffuse reflectance IR spectra of Narmco 5208 resin and prepreg.

reason for the variation in the diffuse reflectance spectra.

It has been demonstrated [48-50] that the effects of fibre orientation and front-surface reflection can be reduced if the sample is covered with a layer of powdered KBr. This approach was tried with the Narmco prepreg. In one case, the prepreg was covered with KBr which was then shaken off to leave a light sprinkling on the surface. In the second, a layer of KBr just sufficient to hide the surface was left in place. These two spectra are compared to the spectrum obtained without KBr in Figure 32. They are of rather poor quality because the overlayer of KBr reduces the spectral contrast considerably, especially when a thicker layer is used. The contrast is rather low to begin with, because of the graphite absorption.

Another approach was also tried. The prepreg was fully covered with powdered KBr, a piece of aluminium foil was placed on top, and the KBr was pressed into the resin using finger pressure. The sample was then inverted and tapped to shake off excess KBr, and the spectrum measured in the usual way. Although the resulting spectra are of lower contrast than those obtained without KBr, they are much more reproducible with respect to band shape, and the fibre orientation is found to have little or no effect on the quality, as shown in Figure 33. However, the band shapes are still somewhat different from those obtained in transmission. This suggests that front-surface reflection effects have not been eliminated, although they are more reproducible.

To check the effects of these treatments on the quantitative analysis, seven specimens from Batch 1014 were measured for each of the three conditions: no KBr, sprinkled with KBr, and KBr embedded. The spectra were treated as described above, using both Kubelka-Munk and absorbance units. Table 10 gives the results. Unfortunately, they show that sprinkling with KBr or embedding KBr in the prepreg do not improve the poor precision to any significant extent. Also, the ratios obtained with KBr present are substantially higher than those obtained without KBr, which are closer to those obtained in transmission. It appears that diffuse reflectance is of very limited use as a quantitative method for prepreg analysis, apparently because of front-surface reflection and scattering effects. Nevertheless, it can be of great value as a qualitative method for samples such as cured composites, which are difficult to measure by other means. In such cases it may also be of some use as a quantitative method if samples of significantly different composition are to be compared. Such is the case for the curing study described in the next section.

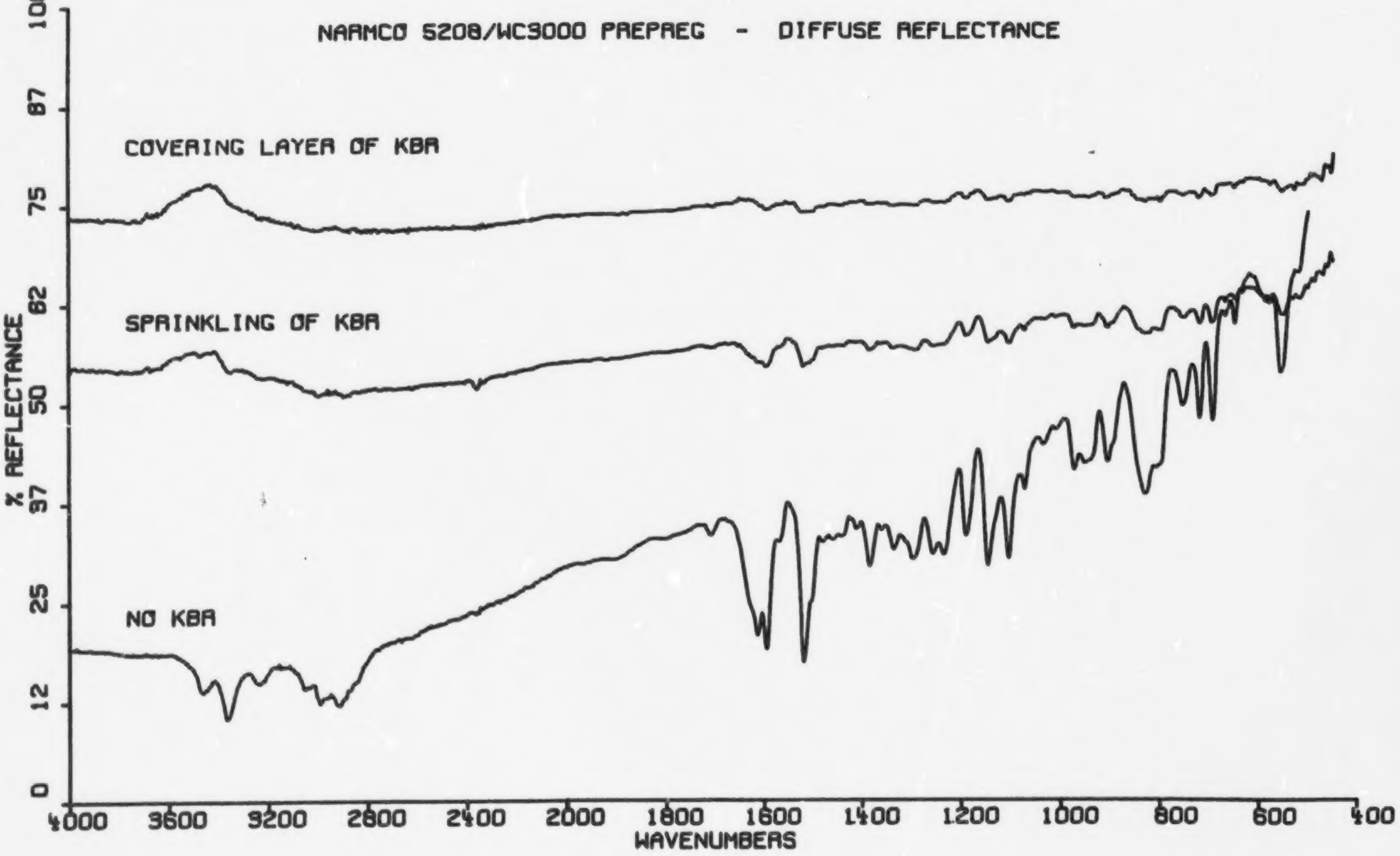

Figure 32 - Effect of covering with KBr on the diffuse reflectance IR spectrum of Narmco 5208/WC3000 prepreg.

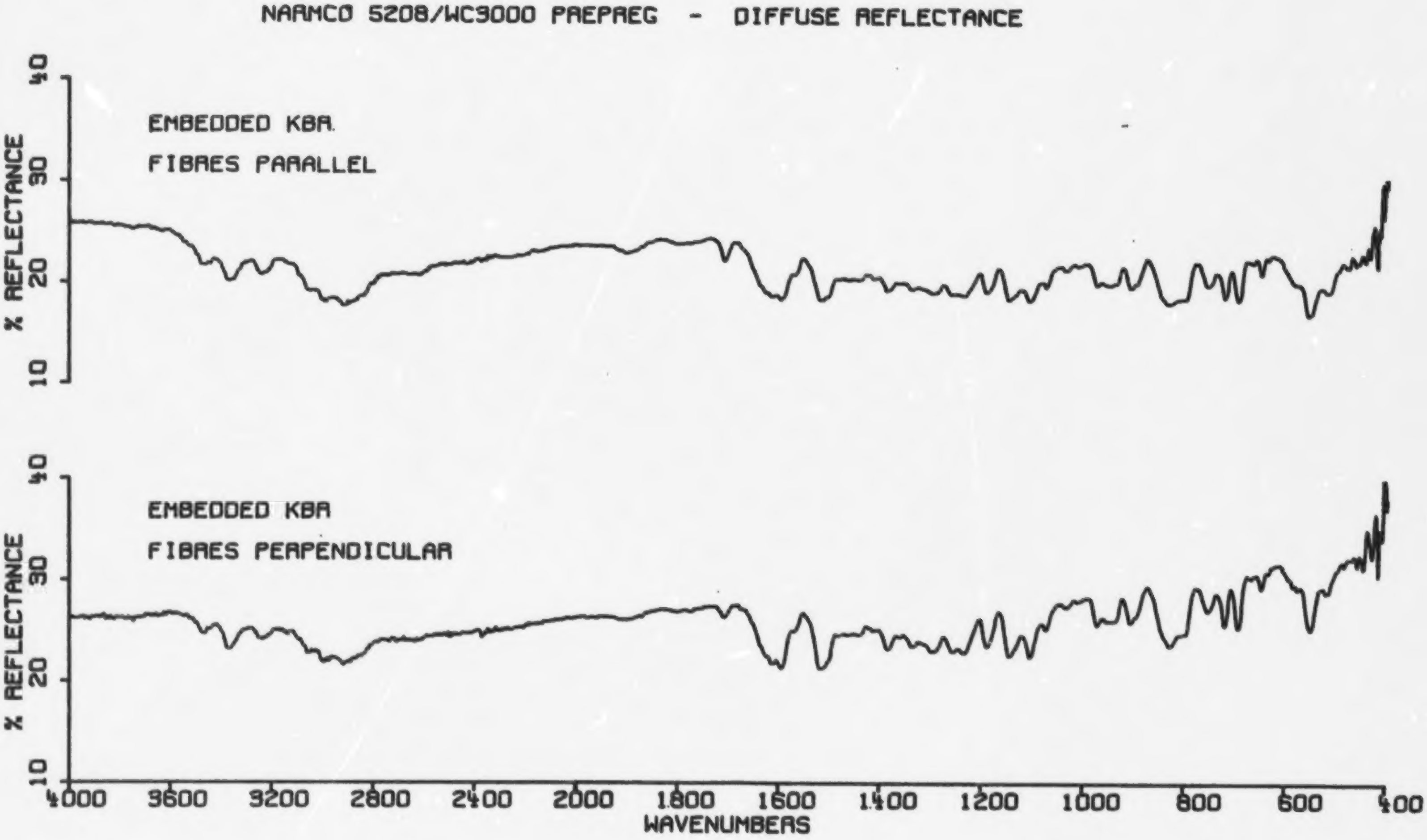

Figure 33 - Effect of embedded KBr on the diffuse reflectance IR spectrum of Narmco 5208/WC3000 prepreg.

Table 10. Quantitative analysis of Narmco 5208/WC3000 prepreg Batch 1014 by diffuse reflection IR

Conditions	Index = Band area divided by area of aromatic reference band			
	Single sulphone	Multiple sulphone	Single epoxy	Multiple epoxy
No KBr K-M units	0.323 (0.028, 8.6%)	0.855 (0.064, 7.4%)	0.167 (0.048, 28.9%)	0.541 (0.153, 28.1%)
No KBr Absorbance	0.438 (0.021, 4.7%)	1.272 (0.053, 4.1%)	0.314 (0.060, 19.2%)	1.005 (0.194, 19.3%)
KBr sprinkled K-M units	0.499 (0.045, 9.1%)	1.758 (0.084, 4.8%)	0.498 (0.134, 26.9%)	1.552 (0.397, 25.6%)
KBr sprinkled Absorbance	0.526 (0.064, 12.1%)	1.893 (0.135, 7.1%)	0.550 (0.118, 21.4%)	1.721 (0.345, 20.1%)
KBr embedded K-M units	0.501 (0.037, 7.5%)	1.863 (0.137, 7.4%)	0.483 (0.119, 24.7%)	1.484 (0.345, 23.2%)
KBr embedded Absorbance	0.508 (0.046, 9.1%)	1.934 (0.089, 4.6%)	0.527 (0.091, 17.2%)	1.622 (0.262, 16.2%)

5.5 Prepreg Cure

To demonstrate the usefulness of diffuse reflectance for studying actual composites, a study of the prepreg curing was performed using Batch 1014. A number of small squares of prepreg (about 1 cm x 1 cm) were cut and, after removal of the plastic backing sheet, were placed in sets of three between strips of Teflon-coated glass cloth. These were then put on a tray in an air-circulating oven, initially at room temperature. The oven was then turned on and set for 135°C. Two hours later the temperature was increased to 177°C and kept there for a further four hours. This cure programme is similar to the one used for the IR transmission curing study described previously (Section 3.6), except that the heat-up rate is not controlled. At half-hour intervals, one set of three squares was quickly removed from the oven and cooled to room temperature. The three specimens were then measured in diffuse reflectance in the usual way. After conversion of the spectra to Kubelka-Munk units, followed by baseline correction, peak areas and ratios were calculated in the same way as in the transmission study. The limits of integration were adjusted as necessary to account for changes in the spectrum with cure. The evolution of the spectrum is illustrated in Figure 34, which may be directly compared with the transmission spectra of Figure 14; the similarities are obvious. The disappearance of the epoxy peaks at 1000-900 cm^{-1} is just as evident in the DR spectra as in transmission. Two features distinguish the DR spectra from the transmission ones. The first is the small acetone peak at 1708 cm^{-1} in the initial DR spectrum. The second is the appearance of carbonyl peaks at 1724 and 1668 cm^{-1} in the later DR spectra. These are due to oxidation and are not observed in the transmission study because curing was done inside the FTIR spectrometer, which is purged with dry nitrogen. The results of the peak area ratio calculations are shown in Figures 35 to 38. In the case of the epoxy indices, the curves have the same general shape as in the transmission study (Figures 17 and 18), but details are less apparent because of the high degree of scatter. In the case of the sulphone indices, there is an apparent gradual decrease over the period of the cure. In transmission, a decrease was observed for the single sulphone index but not for the multiple sulphone index. The reasons for this are not understood at present.

5.6 Microanalysis by Diffuse Reflection

Diffuse reflection is very useful for measuring the spectrum of a small quantity of sample. Two spectra are reported here to illustrate the high sensitivity.

The first (Figure 39) is that of pure TGDDM monomer, obtained by reverse-phase liquid chromatographic separation of MY 720 resin. A fraction of the eluting solution corresponding to the main peak of the chromatogram was collected at the detector outlet and the solvent (acetonitrile/water) was removed by passing a stream of nitrogen over the surface, followed by vacuum drying. The residue was dissolved in a few drops of acetone. A diffuse reflectance microsampling cup (3 mm diameter) from Harrick Scientific Corp. was filled with powdered KBr and the surface compacted and levelled with a spatula. The solution was deposited on the surface a drop or two at a time, allowing the solvent to evaporate after each addition. This was followed by vacuum drying for 15 to 30 minutes at room temperature to remove all the acetone. The spectrum was then recorded

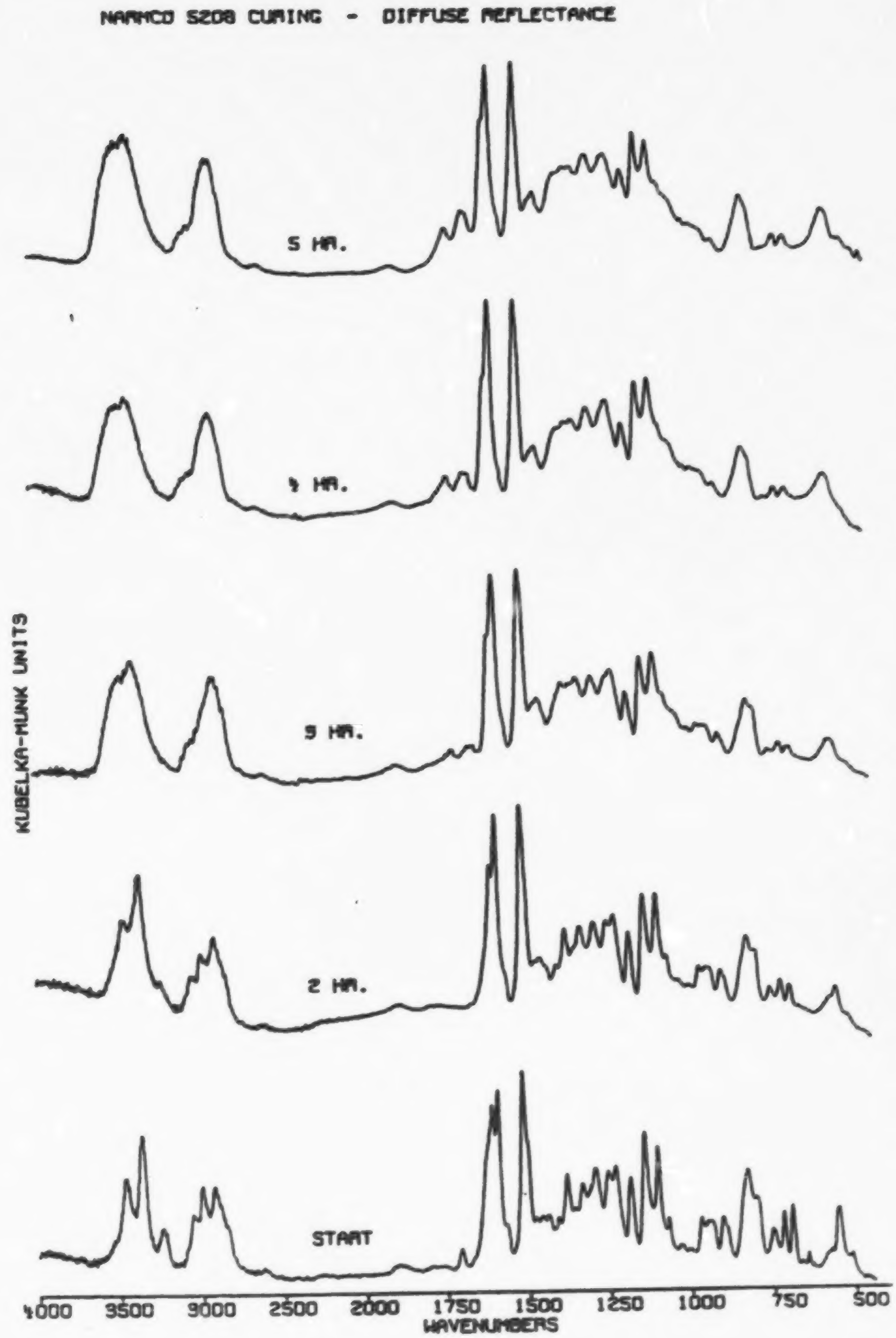

Figure 34 - Evolution of diffuse reflectance IR spectrum during cure of Narmco 5208/WC3000 prepreg.

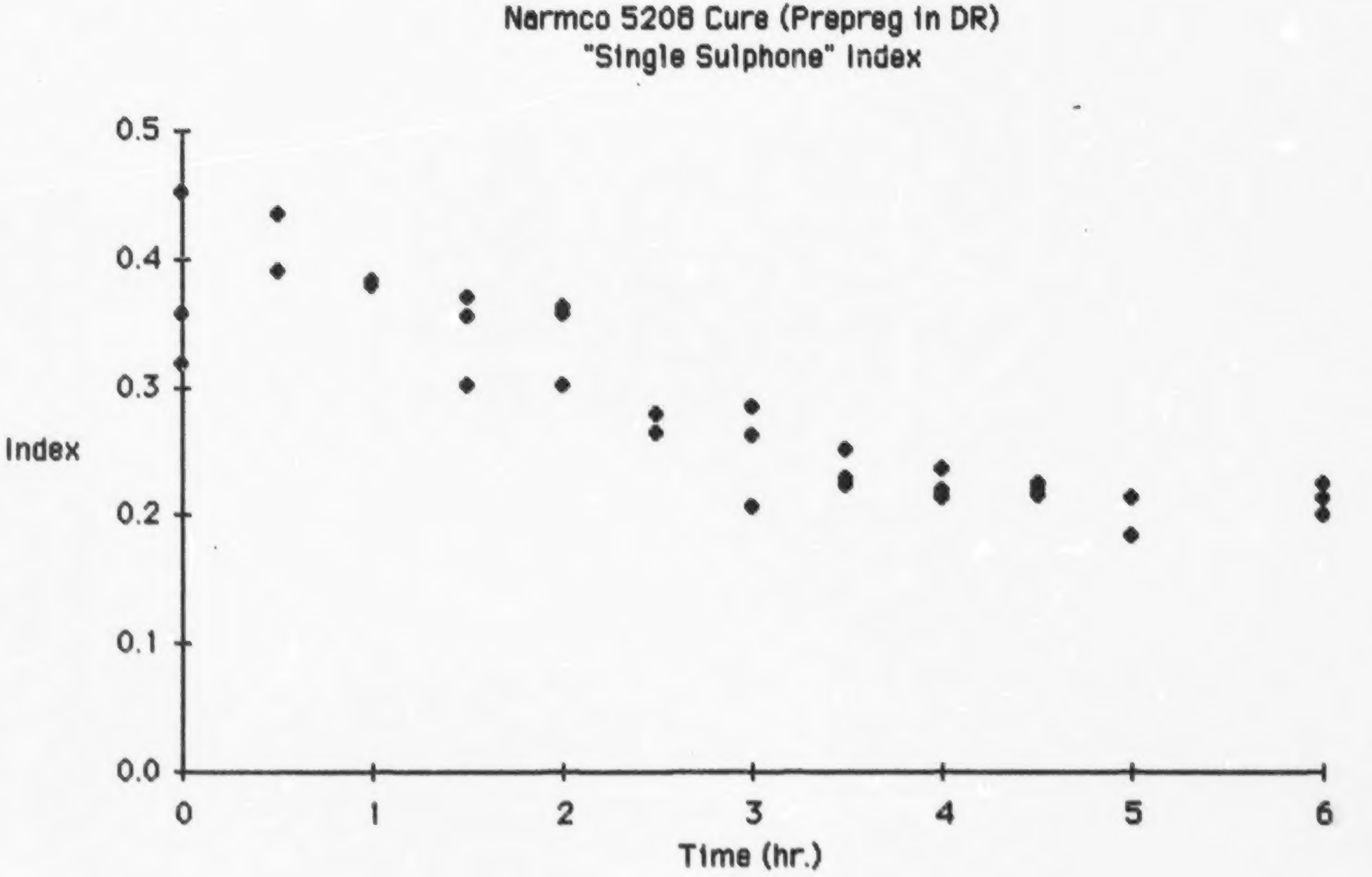

Figure 35 - Variation of "single sulphone" index as measured by diffuse reflectance IR during cure of Narmco 5208/WC3000 prepreg.

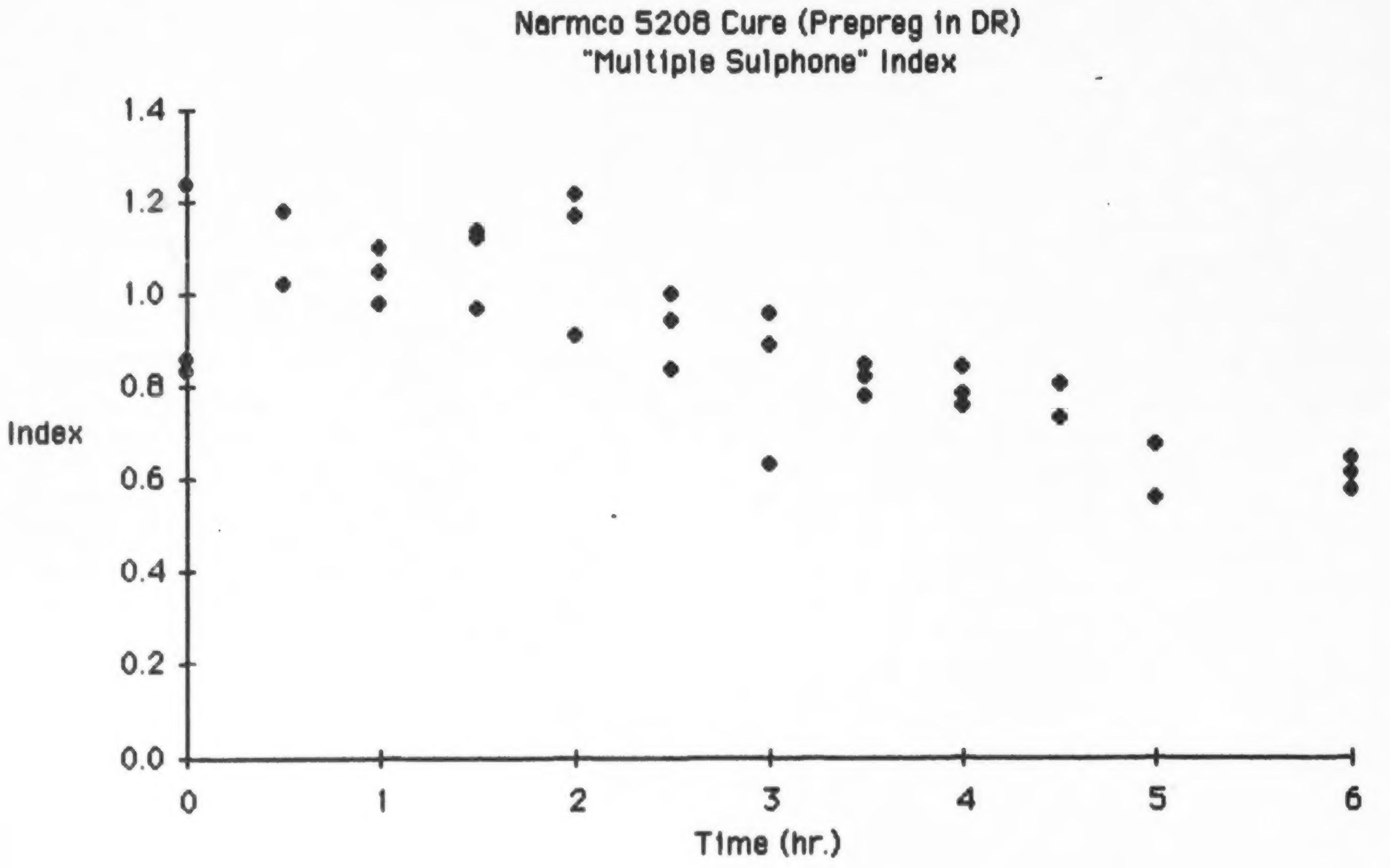

Figure 36 - Variation of "multiple sulphone" index as measured by diffuse reflectance IR during cure of Narmco 5208/WC3000 prepreg.

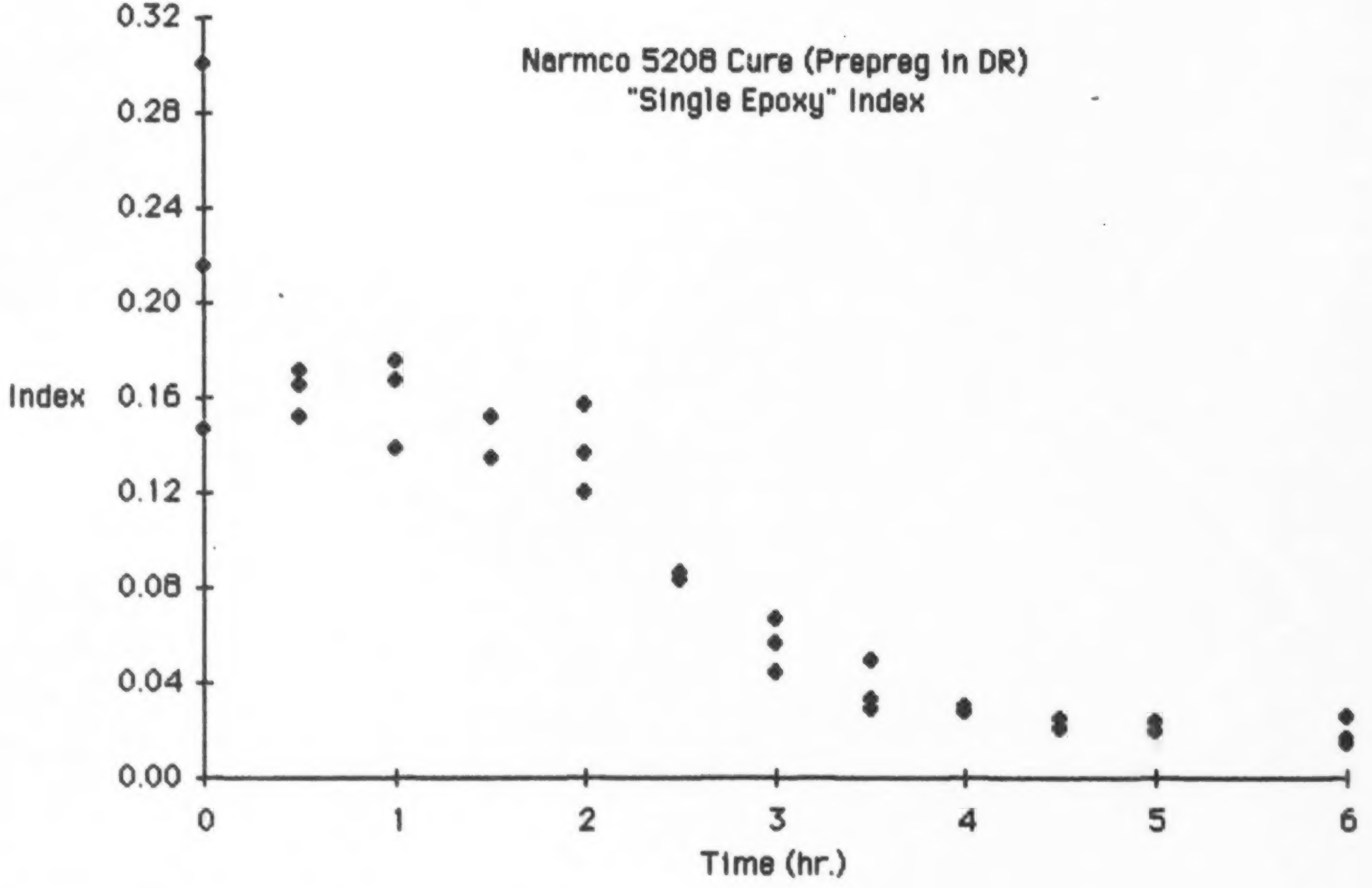

Figure 37 - Variation of "single epoxy" index as measured by diffuse reflectance IR during cure of Narmco 5208/WC3000 prepreg.

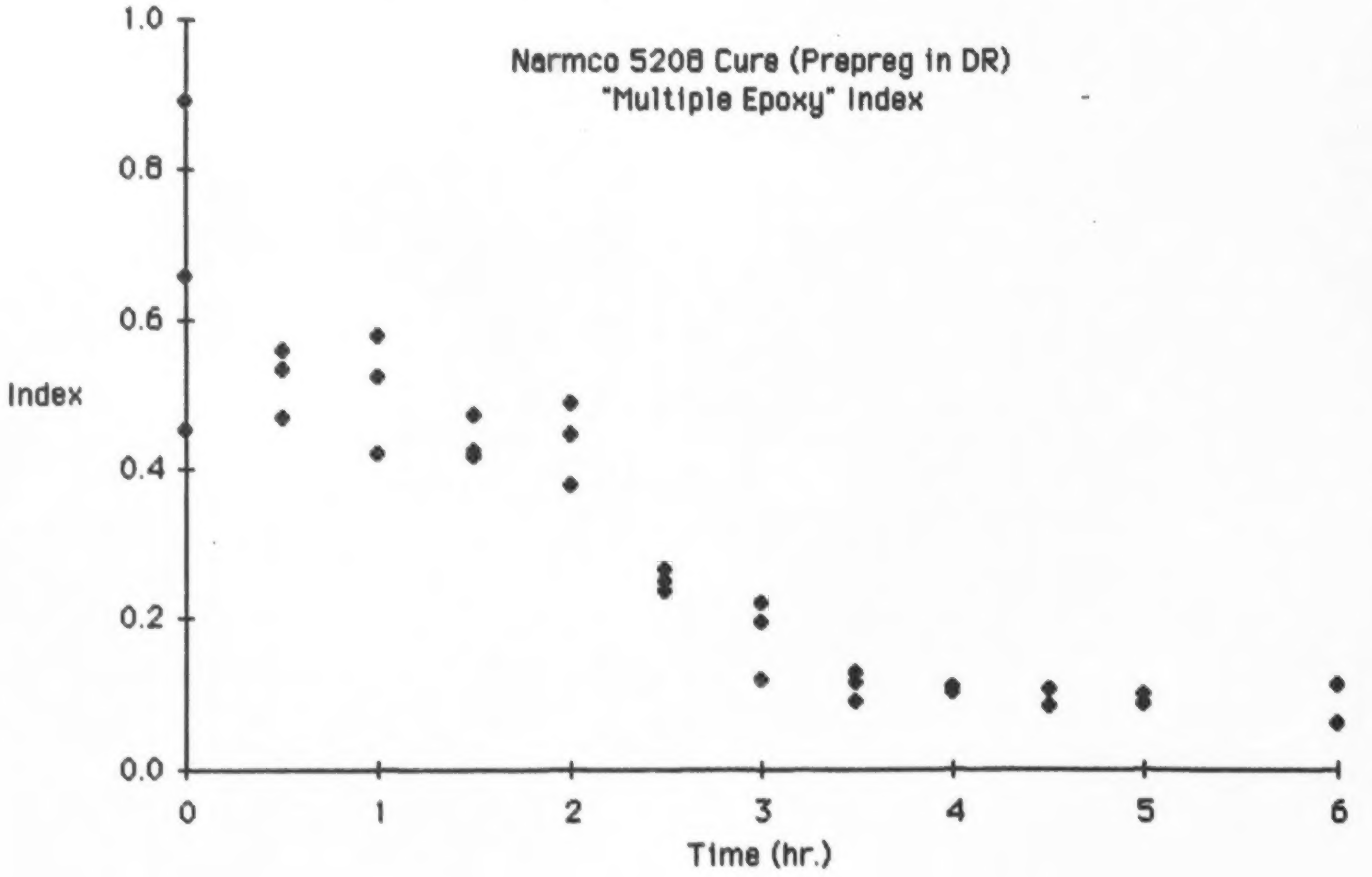

Figure 38 - Variation of "multiple epoxy" index as measured by diffuse reflectance IR during cure of Narmco 5208/WC3000 prepreg.

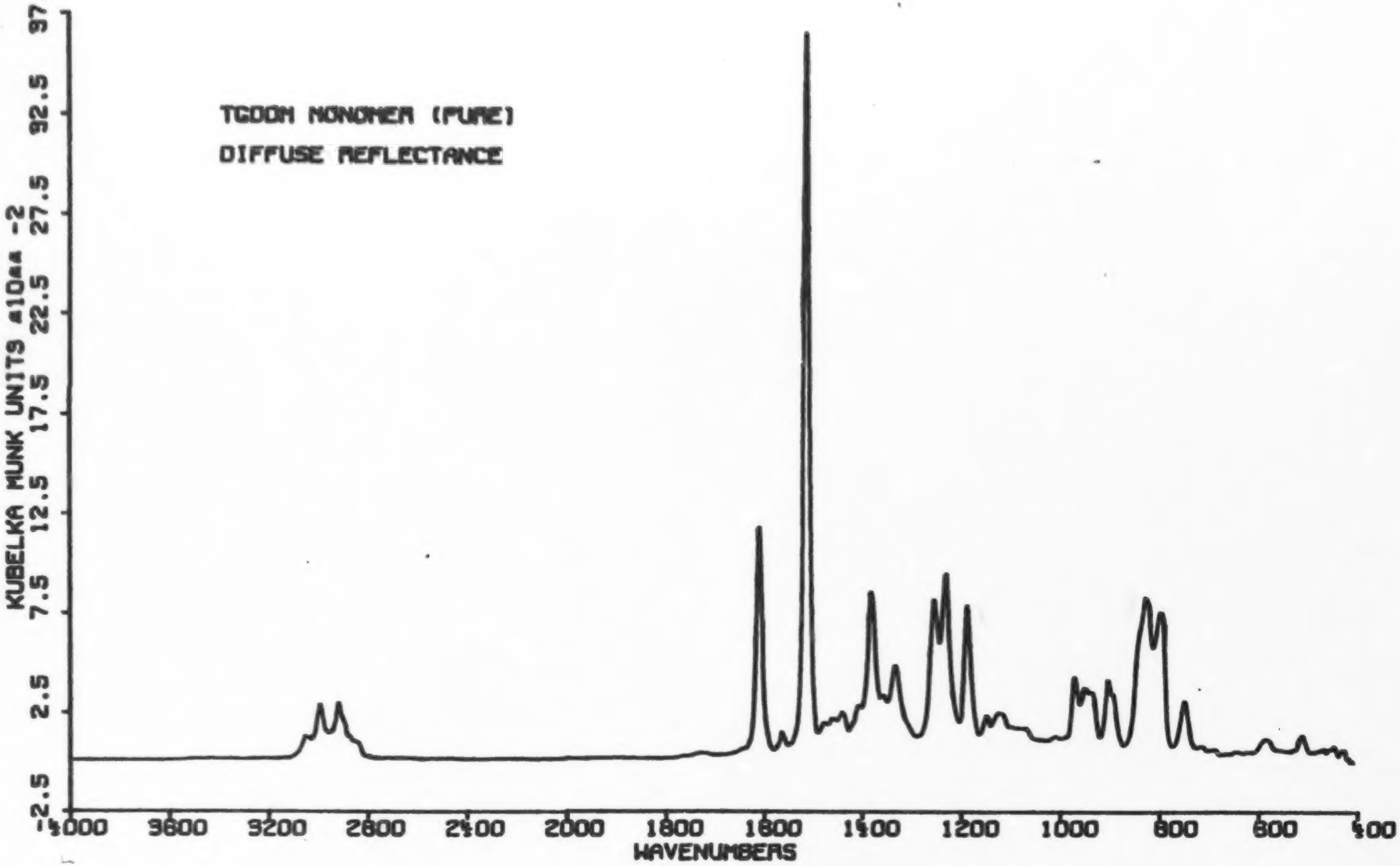

Figure 39 - Diffuse reflectance IR spectrum of pure TGDDM monomer obtained by liquid chromatographic separation of MY 720.

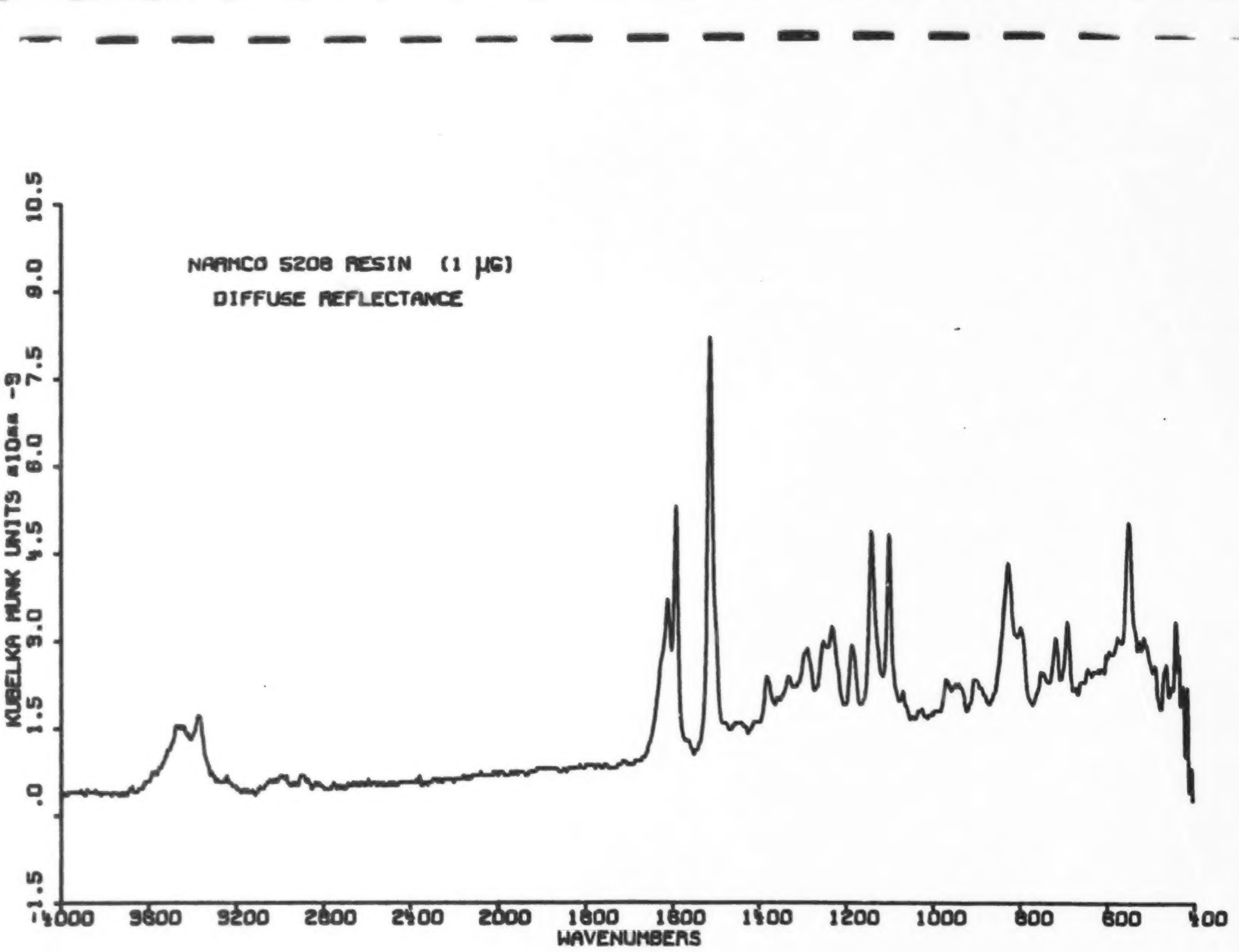

Figure 40 - Diffuse reflectance IR spectrum of 1 μg of Narmco 5208 resin.

using as a reference pure KBr. It closely resembles that of MY 720 (Figure 5), except for the absence of an OH band near 3500 cm^{-1}. This is because the monomer has no OH groups; they are present, however, in higher oligomers and in α-glycol by-products [51].

To check the sensitivity of the method, a solution of Narmco 5208 resin (Batch 1014) in acetone was prepared with a concentration of 0.1 g/L and a sample was prepared as described above using 10 μL of this solution. This corresponds to 1 μg of resin deposited on the KBr. The resulting spectrum (Figure 40) was measured using 512 scans. It is of good quality and is certainly sufficient to identify the resin.

5.7 Recommended Procedure for Measuring IR Spectra of Composites by Diffuse Reflection

(1) Make sure that the diffuse reflectance accessory is installed in the spectrometer and properly aligned.

(2) Prepare a potassium bromide reference sample by filling the appropriate sampling cup with ground KBr and compacting with a clean spatula to give a smooth surface.

(3) Prepreg and cured laminate samples are measured using a horizontal support of adjustable height, so that the sample surface can be adjusted to the same height as the potassium bromide reference sample. Preliminary trials should be done to find the optimum height adjustment (maximum energy throughput).

(4) Cut samples about 1 cm x 1 cm using scissors (for prepreg) or a jigsaw (for cured laminate).

(5) Affix the sample to the support. Prepreg is usually tacky enough to adhere by itself when pressed in place. This can be done with the fingers if the plastic backing sheet is left in place; the plastic is then carefully removed to record the spectrum of the freshly exposed surface. For cured samples, double-sided adhesive tape can be used. Avoid touching the surface to be measured with the fingers.

(6) If the fibre reinforcement does not have a plain weave pattern, the quality of the spectrum may depend on the orientation of the sample. In the Harrick "praying mantis"

accessory, best results are obtained if the principal fibre direction is parallel to the beam direction.

(7) Record spectra for both the KBr reference and the sample and take the ratio. It is recommended to accumulate at least 100 scans to obtain a good signal-to-noise ratio.

(8) If the spectrum is to be compared with transmission spectra, convert it to Kubelka-Munk units and do a baseline correction. This can then be compared to a transmission spectrum in absorbance units.

(9) Quantitative measurements are not recommended for diffuse reflectance spectra of this type of sample.

6. CONCLUSIONS

(1) Infrared spectroscopy, particularly Fourier transform infrared spectroscopy, is a very useful method for qualitative and quantitative analysis of high-performance composite systems. Spectra can be obtained by various methods (transmission, internal reflection, diffuse reflection), each of which has particular advantages and disadvantages.

(2) Quantitative analysis can be done based on the intensities of certain characteristic peaks in the spectrum. In the case of the Narmco 5208 epoxy resin system, these are the sulphone bands in the 1200-1100 cm^{-1} region arising from the DDS hardener and the bands at 1000-900 cm^{-1} arising from unreacted epoxide rings. The aromatic ring peak at 1517 cm^{-1} can be used as an internal reference. The peak at 830 cm^{-1} should not be used as a reference because it contains a shoulder at 800 cm^{-1} which is due to the epoxy groups. Better results are obtained if the sulphone and epoxy analysis is done using the area under multiple peaks rather than a single peak.

(3) The commonly used method for recording the spectrum, transmission through a thin film, requires separation of the resin from the fibre reinforcement. Sample preparation involves extraction of the resin from the prepreg with an organic solvent, followed by casting of a thin film on a transparent window. In quantitative analysis, substantial error can be produced if the film is not of uniform thickness. Good precision (a standard deviation of 2% or less) can only be achieved with very careful sample preparation. Acetone is recommended as solvent.

(4) The attenuated total reflection method can be used to obtain good spectra from uncured prepreg as is, thus avoiding solvent extraction and casting of a film. For quantitative analysis, the problem of nonuniform thickness associated with the transmission method does not exist, and good precision can be readily obtained (standard deviation under 2%). Better results are obtained using a germanium prism than with KRS-5. ATR is the recommended method for quantitative analysis of prepreg. It also allows detection of volatile components which are not detected by the transmission method.

(5) The diffuse reflection method also gives very good spectra and can be applied to both uncured prepreg and cured laminate. It is a rapid and "nondestructive" method. Although it gives excellent qualitative spectra, it is subject to effects arising from front-surface reflection and scattering which cause some variation in band shapes and

intensities. This severely limits its usefulness for quantitative analysis.

(6) The near-infrared region is also of interest for composite analysis. In the case of Narmco 5208, well-defined peaks appear in this region for unreacted epoxy groups and absorbed moisture.

(7) The curing of Narmco 5208 can be followed by infrared spectroscopy by means of the epoxy bands in the 1000-900 cm^{-1} region. Diffuse reflection can be used to confirm completion of cure in finished parts. It can also detect surface oxidation resulting in carbonyl peaks in the 1700 cm^{-1} region.

BIBLIOGRAPHY

1. K. C. Cole, D. Noël
Report IGM 86-101-307, National Research Council Canada Publication 25839, May 1986
Physicochemical characterization of high-performance fibre-reinforced organic-matrix composites. Part 1. General discussion and literature review.

2. A. L. Smith
Applied Infrared Spectroscopy: Fundamentals, Techniques, and Analytical Problem-Solving (Chemical Analysis, Vol. 54)
Wiley-Interscience, 1979

3. R. G. J. Miller, B. C. Stace (Eds.)
Laboratory Methods in Infrared Spectroscopy, 2nd Ed.
Heyden & Son, 1979

4. L. J. Bellamy
The Infra-red Spectra of Complex Molecules, 3rd Ed.
Chapman & Hall, 1975

5. P. R. Griffiths
Chemical Infrared Fourier Transform Spectroscopy (Chemical Analysis, Vol. 43)
Wiley-Interscience, 1975

6. J. R. Ferraro, L. J. Basile (Eds.)
Fourier Transform Infrared Spectroscopy: Applications to Chemical Systems (Vols. 1-4)
Academic Press, 1978-

7. Y. T. Liao, J. L. Koenig
Dev. Reinf. Plast. 4: 31-87 (1984)
Applications of Fourier transform infrared spectroscopy to the study of fiber-resin composites.

8. B. M. Halpin, J. F. Sprouse, G. L. Hagnauer
Proc. 33rd Ann. Tech. Conf. Reinforced Plastics/Composites Institute, Society of the Plastics Industry, 1978, Paper 15-G
Characterization of epoxy resins, prepregs, and composites using HPLC and FTS-IR.

9. G. R. Thomas, B. M. Halpin, J. F. Sprouse, G. L. Hagnauer, R. E. Sacher
Nat. SAMPE Symp. Exhib. [Proc.] 24: 458-505 (1979)
Characterization of epoxy resins, prepregs, and composites using HPLC, FTS-IR, and DSC.

10. J. F. Carpenter
Report prepared for Naval Air Systems Command, Contract No. N00019-76-C-0138, July 1977; NTIS Document AD-A042853
Quality control of structural nonmetallics.

11. M. Cizmecioglu, S. D. Hong, J. Moacanin, A. Gupta
Polym. Preprints 22: 224-225 (1981)
Spectroscopic characterization of Narmco 5208 epoxy neat-resin formulations.

12. M. Cizmecioglu, A. Gupta
Proc. 37th Ann. Conf., Reinforced Plastics/Composites Institute, Society of the Plastics Industry, January 11-15, 1982, Paper 20-E
and
SAMPE Quarterly, April 1982, pp. 16-20
Cure kinetics of epoxy matrix resin by differential scanning calorimetry.

13. E. S. W. Kong, S. M. Lee, H. G. Nelson
Polym. Compos. 3: 29-33 (1982)
Physical aging in graphite/epoxy composites.

14. H. S. Chu, J. C. Seferis
Polym. Compos. 5: 124-140 (1984)
Dynamic mechanical experiments for probing process-structure-property relations in amine-cured epoxies.

15. D. Crozier, G. Morse, Y. Tajima
SAMPE J., Sept./Oct. 1982, pp. 17-22
The development of improved chemical analysis methods for epoxy resins.

16. C. A. May, D. K. Hadad, C. E. Browning
Proc. 33rd Ann. Tech. Conf. Reinforced Plastics/Composites Institute, Society of the Plastics Industry, 1978, Paper 15-D
and
Polymer Engineering and Science 19: 545-551 (1979)
Physicochemical quality assurance methods for composite matrix resins.

17. R. L. Levy, D. L. Fanter, C. J. Summers
J. Appl. Polym. Sci. 24: 1643-1664 (1979)
Spectroscopic evidence for mechanochemical effects of moisture in epoxy resins.

18. J. B. Enns
Ph. D. Thesis, Princeton Univ., 1982; Univ. Microfilms 82-21568
The cure of thermosetting epoxy/amine systems.

19. R. A. Nyquist
Appl. Spectrosc. 40: 275-278 (1986)
Infrared group frequency data for 1,2-epoxyalkanes.

20. H. Dannenberg, W. R. Harp
Anal. Chem. 28: 86-90 (1956)
Determination of cure and analysis of cured epoxy resins.

21. C. E. Feazel, E. A. Verchot
J. Polym. Sci. 25: 351-353 (1957)
A simple technique for use with infrared spectroscopy to study the curing of epoxy resins.

22. H. Dannenberg, J. W. Forbes, A. C. Jones
Anal. Chem. 32: 365-370 (1960)
Infrared spectroscopy of surface coatings in reflected light.

23. A. Gupta, M. Cizmecioglu, D. Coulter, R. H. Liang, A. Yavrouian, F. D. Tsay, J. Moacanin
J. Appl. Polym. Sci. 28: 1011-1024 (1983)
The mechanism of cure of tetraglycidyldiaminodiphenylmethane with diaminodiphenylsulphone.

24. J. L. Koenig
Anal. Chem. 36: 1045-1046 (1964)
Effect of nonuniform distribution of absorbing material on the quantitative measurement of infrared band intensities.

25. T. Hirschfeld
Anal. Chem. 51: 495-499 (1979)
Diagnosis and correction of wedging errors in absorbance subtract Fourier transform infrared spectroscopy.

26. T. Hirschfeld
Chapter 6 in Fourier Transform Infrared Spectroscopy: Application to Chemical Systems, Vol. 2, J. R. Ferraro and L. J. Basile (Eds.), Academic Press, 1979, pp. 193-242
Quantitative FT-IR: A detailed look at the problems involved.

27. D. A. Scola
Nat. SAMPE Tech. Conf. 15: 9-20 (1983)
The effects of humidity exposure on AS/3501-6 prepreg material.

28. R. B. Gosnell
Technical Report NASA-CR-145211 (1977), NTIS No. N78-13133
Technical assessment for quality control of resins.

29. C. A. Bennett, N. L. Franklin
Statistical Analysis in Chemistry and the Chemical Industry
John Wiley & Sons, 1954

30. J. Moacanin, M. Cizmecioglu, F. Tsay, A. Gupta
Org. Coat. Appl. Polym. Sci. Proc. 47: 587-591 (1982)
and
ACS Symp. Ser. 227: 83-94 (1983)
Mechanism and kinetics of the curing process in a resin system.

31. P. Roush
Proc. Soc. Photo-Opt. Instrum. Eng. 289: 124-126 (1981)
Use of heated attenuated total reflectance (ATR) to monitor polymer transitions.

32. R. J. Morgan, E. T. Mones
Compos. Technol. Rev. 1: 17-19 (1979)
Tetraglycidyl-4,4'-diaminodiphenylmethane (TGDDM) epoxies cured with diaminodiphenylsulfone (DDS).

33. H. Dannenberg
SPE Transactions, January 1963, pp. 78-88
Determination of functional groups in epoxy resins by near-infrared spectroscopy.

34. R. F. Goddu, D. A. Delker
Anal. Chem. 30: 2013-2016 (1958)
Determination of terminal epoxides by near-infrared spectrophotometry.

35. T. E. Baker, G. L. Fix, J. S. Judge
Nat. SAMPE Symp. Exhib. [Proc.] 24: 1211-1222 (1979)
Control of adhesives through analytical characterization.

36. F. M. Kong, C. M. Walkup, R. J. Morgan
ACS Symp. Ser. 221: 211-217 (1983)
and
Polymer 25: 375-386 (1984)
Structure-property relations of polyethertriamine-cured bisphenol-A diglycidyl ether epoxies.

37. E. W. Crandall, W. C. Mih
Org. Coat. Appl. Polym. Sci. Proc. 47: 592-594 (1982)
and
ACS Symp. Ser. 227: 113-119 (1983)
Crosslinking reaction of an epoxy resin with phthalic anhydride.

38. N. J. Harrick
Internal Reflection Spectroscopy
Harrick Scientific Corp., Ossining NY, 1967.

39. K. Knutson, D. J. Lyman
Chapter 6 (pp. 197-247) in Surface and Interfacial Aspects of Biomedical Polymers, Vol. 1. Surface Chemistry and Physics, J. D. Andrade (Ed.), Plenum Press, 1985
Surface infrared spectroscopy.

40. W. W. Houghton, R. J. Shuford, J. F. Sprouse
Nat. SAMPE Tech. Conf. 11: 131-150 (1979)
Acoustic emission as an aid for investigating composite manufacturing processes.

41. M. P. Fuller, P. Griffiths
Anal. Chem. 50: 1906-1910 (1978)
Diffuse reflectance measurements by infrared Fourier transform spectroscopy.

42. P. R. Griffiths, M. P. Fuller
Adv. Infrared Raman Spectrosc. 9: 63-129 (1982)
Mid-infrared spectrometry of powdered samples.

43. J. M. Chalmers, M. W. Mackenzie
Appl. Spectrosc. 39: 634-641 (1985)
Some industrial applications of FT-IR diffuse reflectance spectroscopy.

44. G. Kortüm
Reflectance Spectroscopy: Principles, Methods, Applications
Springer-Verlag, 1969.

45. P. R. Young, B. A. Stein, A. C. Chang
Nat. SAMPE Symp./Exhib. 28: 824-837 (1983)
Resin characterization in cured graphite fiber reinforced composites using diffuse reflectance FTIR.

46. P. R. Young, A. C. Chang
Nat. SAMPE Tech. Conf. 16: 136-147 (1984)
Prepreg cure monitoring using diffuse reflectance FTIR.

47. P. J. Brimmer, P. R. Griffiths, N. J. Harrick
Appl. Spectrosc. 40: 258-265 (1986)
Angular dependence of diffuse reflectance infrared spectra. Part I. FT-IR spectrogoniophotometer.

48. M. T. McKenzie, S. R. Culler, J. L. Koenig
Appl. Spectrosc. 38: 786-790 (1984)
Applications of diffuse reflectance FT-IR to the characterization of an E-glass fiber/γ-APS coupling agent system.

49. S. R. Culler, M. T. McKenzie, L. J. Fina, H. Ishida, J. L. Koenig
Appl. Spectrosc. 38: 791-795 (1984)
Fourier transform diffuse reflectance infrared study of polymer films and coatings: a method for studying polymer surfaces.

50. M. T. McKenzie, J. L. Koenig
Appl. Spectrosc. 39: 408-412 (1985)
Further developments in the methodology of surface analysis by FT-IR: quantitative aspects of diffuse reflectance methods.

51. G. L. Hagnauer, P. J. Pearce
ACS Symp. Ser. 221: 193-209 (1983)
Effects of impurities on hydrolytic stability and curing behaviour.